

**Analysis of System Wide Distortion in an Integrated Power System
Utilizing a High Voltage DC Bus and Silicon Carbide Power Devices**
by

William F. Fallier

B.S. Electrical Engineering
The Citadel, 1999

Submitted to the Department of Mechanical Engineering and the Department of Electrical Engineering and Computer Science in Partial Fulfillment of the Requirements for the Degrees of

Naval Engineer

and

Master of Science in Electrical Engineering and Computer Science

at the
Massachusetts Institute of Technology
June 2007

© William F. Fallier, 2007. All rights reserved.

The author hereby grants MIT and the U.S. Government permission to reproduce and to distribute publicly paper and electronic copies of this thesis document in whole or in part.

Signature of Author:
Department of Mechanical Engineering and the
Department of Electrical Engineering and Computer Science
May 9, 2007

Certified by:
James L. Kirtley, Jr., Professor of Electrical Engineering
Department of Electrical Engineering and Computer Science
Thesis Supervisor

Certified by:
Joel P. Harbour, Associate Professor of the Practice of Naval Construction and Engineering
Department of Mechanical Engineering
Thesis Reader

Accepted by:
Professor Lallit Anand, Professor of Mechanical Engineering
Chair, Departmental Committee on Graduate Students
Department of Mechanical Engineering

Accepted by:
Arthur C. Smith, Professor of Electrical Engineering
Chair, Departmental Committee on Graduate Students
Department of Electrical Engineering and Computer Science

REPORT DOCUMENTATION PAGE

Form Approved
OMB No. 0704-0188

Public reporting burden for this collection of information is estimated to average 1 hour per response, including the time for reviewing instructions, searching existing data sources, gathering and maintaining the data needed, and completing and reviewing this collection of information. Send comments regarding this burden estimate or any other aspect of this collection of information, including suggestions for reducing this burden to Department of Defense, Washington Headquarters Services, Directorate for Information Operations and Reports (0704-0188), 1215 Jefferson Davis Highway, Suite 1204, Arlington, VA 22202-4302. Respondents should be aware that notwithstanding any other provision of law, no person shall be subject to any penalty for failing to comply with a collection of information if it does not display a currently valid OMB control number. **PLEASE DO NOT RETURN YOUR FORM TO THE ABOVE ADDRESS.**

1. REPORT DATE (DD-MM-YYYY) XX-06-2007		2. REPORT TYPE Master's Thesis		3. DATES COVERED (From - To) JAN-JUN 2007	
4. TITLE AND SUBTITLE Analysis of System Wide Distortion in an Integrated Power System Utilizing a High Voltage DC Bus and Silicon Carbide Power Devices				5a. CONTRACT NUMBER N62271-97-G-0026	
				5b. GRANT NUMBER	
				5c. PROGRAM ELEMENT NUMBER	
6. AUTHOR(S) William F. Fallier				5d. PROJECT NUMBER	
				5e. TASK NUMBER	
				5f. WORK UNIT NUMBER	
7. PERFORMING ORGANIZATION NAME(S) AND ADDRESS(ES) Massachusetts Institute of Technology				8. PERFORMING ORGANIZATION REPORT NUMBER	
9. SPONSORING / MONITORING AGENCY NAME(S) AND ADDRESS(ES) Naval Postgraduate School Monterey, Ca 93943				10. SPONSOR/MONITOR'S ACRONYM(S) NPS	
				11. SPONSOR/MONITOR'S REPORT NUMBER(S)	
12. DISTRIBUTION / AVAILABILITY STATEMENT 1. DISTRIBUTION STATEMENT A. Approved for public release; distribution is unlimited.					
13. SUPPLEMENTARY NOTES					
14. ABSTRACT This research investigates the distortion on the electrical distribution system for a high voltage DC Integrated Power System (IPS). The analysis was concentrated on the power supplied to a propulsion motor driven by an inverter with simulated silicon carbide switches. Theoretically, silicon carbide switches have the advantage of being able to withstand a very large blocking voltage and carry very large forward currents. Silicon carbide switches are also very efficient due to their quick rise and fall times. Since silicon carbide switches can withstand high voltage differentials and switch faster than silicon switches, the switching effects on the electrical distribution system were investigated. The current state of silicon carbide power electronics was also investigated. This research quantifies the current and voltage distortion over various operating conditions. A system model was developed using Matlab, Simulink, and SimPowerSystems. The model consisted of a synchronous generator supplying a rectifier and inverter set driving an induction motor. This induction motor simulates the propulsion motor for a Navy ship. This model had a DC link voltage of 10 kV in order to simulate future Navy IPS systems. The current and voltage distortion were compared to MIL STD 1399 and IEEE STD 519 and 45.					
15. SUBJECT TERMS					
16. SECURITY CLASSIFICATION OF:			17. LIMITATION OF ABSTRACT UU	18. NUMBER OF PAGES 172	19a. NAME OF RESPONSIBLE PERSON Sean Tibbitts, Educational Technician
a. REPORT	b. ABSTRACT	c. THIS PAGE			19b. TELEPHONE NUMBER (include area code) (831) 656-2319 civins@nps.edu

Page Intentionally Left Blank

**Analysis of System Wide Distortion in an Integrated Power System
Utilizing a High Voltage DC Bus and Silicon Carbide Power Devices**

by

William F. Fallier

Submitted to the Department of Ocean Engineering and the Department of Electrical Engineering and Computer Science in Partial Fulfillment of the Requirements for the Degrees of
Naval Engineer
and
Master of Science in Electrical Engineering and Computer Science

ABSTRACT

This research investigates the distortion on the electrical distribution system for a high voltage DC Integrated Power System (IPS). The analysis was concentrated on the power supplied to a propulsion motor driven by an inverter with simulated silicon carbide switches. Theoretically, silicon carbide switches have the advantage of being able to withstand a very large blocking voltage and carry very large forward currents. Silicon carbide switches are also very efficient due to their quick rise and fall times. Since silicon carbide switches can withstand high voltage differentials and switch faster than silicon switches, the switching effects on the electrical distribution system were investigated. The current state of silicon carbide power electronics was also investigated.

This research quantifies the current and voltage distortion over various operating conditions. A system model was developed using Matlab, Simulink, and SimPowerSystems. The model consisted of a synchronous generator supplying a rectifier and inverter set driving an induction motor. This induction motor simulates the propulsion motor for a Navy ship. This model had a DC link voltage of 10 kV in order to simulate future Navy IPS systems. The current and voltage distortion were compared to MIL STD 1399 and IEEE STD 519 and 45.

Thesis Supervisor: James L. Kirtley, Jr.
Title: Professor of Electrical Engineering

Thesis Reader: Joel P. Harbour
Title: Associate Professor of the Practice of Naval Construction and Engineering

Page Intentionally Left Blank

TABLE OF CONTENTS

ABSTRACT	3
TABLE OF CONTENTS	5
LIST OF FIGURES	7
LIST OF TABLES	8
LIST OF TABLES	8
CHAPTER 1: INTRODUCTION	9
BACKGROUND.....	9
SCOPE	11
CHAPTER 2: IPS BASIC PRINCIPLES	13
TRADITIONAL (NON-IPS) SHIPS.....	13
IPS SHIPS.....	15
ZONAL DISTRIBUTION AND TERMINOLOGY	17
CHAPTER 3: SILICON CARBIDE POWER ELECTRONICS	23
SiC BACKGROUND.....	24
SiC ADVANTAGES	25
SiC DISADVANTAGES	27
CURRENT SiC POWER ELECTRONIC DEVICES AND APPLICATIONS	27
FUTURE OF SiC DEVICES	29
SiC CONCLUSION.....	30
CHAPTER 4: SYSTEM MODEL	33
INTRODUCTION	33
POWER SUPPLY	33
RECTIFIER.....	34
DC LINK FILTER	35
INVERTER	36
INDUCTION MOTOR.....	37
MEASUREMENTS.....	39
MISCELLANEOUS CONTROL BLOCKS	39
VALIDATION	40
CHAPTER 5: SIMULATION RESULTS	43
SIMULINK SETUP.....	43
DISTORTION LIMITS	44
SIMULATION OUTPUTS.....	46
SIMULATION 1: IDEAL STEADY STATE UNFILTERED RESULTS	47
SIMULATION 2: IDEAL STEADY STATE FILTERED RESULTS	50
SIMULATION 3: IDEAL TRANSIENT UNFILTERED RESULTS	54
SIMULATION 4: IDEAL TRANSIENT FILTERED RESULTS.....	56

RECAP OF SIMULATIONS 1 – 4.....	59
SIMULATION 5: SIMULATED SiC STEADY STATE UNFILTERED RESULTS	60
SIMULATION 6: SIMULATED SiC STEADY STATE FILTERED RESULTS	64
SIMULATION 7: SIMULATED SiC TRANSIENT UNFILTERED RESULTS	67
SIMULATION 8: SIMULATED SiC TRANSIENT FILTERED RESULTS	69
RECAP OF SIMULATIONS 5 – 8.....	71
SIMULATION 9: SIMULATED SiC STEADY STATE AND TRANSIENT FILTERED RESULTS.....	71
CHAPTER 6: CONCLUSIONS AND FUTURE WORK.....	77
MODEL TESTING	77
MITIGATION TECHNIQUES.....	77
FUTURE WORK	78
CONCLUSIONS.....	79
REFERENCE LIST	81
APPENDICES.....	83
APPENDIX A: HARDWARE TRL DEFINITIONS [14]	84
APPENDIX B: MATLAB SYSTEM MODEL	86
APPENDIX C: MATLAB SIMULATION 1 OUTPUT.....	93
APPENDIX D: MATLAB SIMULATION 2 OUTPUT.....	105
APPENDIX E: MATLAB SIMULATION 3 OUTPUT	115
APPENDIX F: MATLAB SIMULATION 4 OUTPUT	120
APPENDIX G: MATLAB SIMULATION 5 OUTPUT	126
APPENDIX H: MATLAB SIMULATION 6 OUTPUT	135
APPENDIX I: MATLAB SIMULATION 7 OUTPUT	144
APPENDIX J: MATLAB SIMULATION 8 OUTPUT	151
APPENDIX K: MATLAB SIMULATION 9 OUTPUT	158

LIST OF FIGURES

Figure 1: Traditional Propulsion System [3]	15
Figure 2: Traditional Ring Electrical Bus [3]	15
Figure 3: IPS Configuration [3]	17
Figure 4: AC ZED System (DDG-79 and LPD-17) [3]	18
Figure 5: AC ZED System [5]	18
Figure 6: DC ZED System [5]	20
Figure 7: Technology Readiness Levels [7]	23
Figure 8: System Model Power Supply	34
Figure 9: Rectifier and DC Regulator	35
Figure 10: DC Link Filter	36
Figure 11: Inverter and Vector Control	37
Figure 12: Induction Motor.....	38
Figure 13: Advanced Induction Motor Configuration [17]	39
Figure 14: Transient Analysis Blocks.....	40
Figure 15: Complete System Model	41
Figure 16: Simulation 1 Individual Current Harmonic Distortion.....	47
Figure 17: Simulation 1 Individual Voltage Harmonic Distortion	48
Figure 18: Simulation 1 Voltage Waveform and FFT	49
Figure 19: Simulation 1 Current Waveform and FFT	50
Figure 20: Simulation 2 Individual Current Harmonic Distortion.....	51
Figure 21: Simulation 2 Individual Voltage Harmonic Distortion	52
Figure 22: Simulation 2 Voltage Waveform and FFT	53
Figure 23: Simulation 2 Current Waveform and FFT	53
Figure 24: Simulation 3 Individual Current Harmonic Distortion.....	54
Figure 25: Simulation 3 Individual Voltage Harmonic Distortion	55
Figure 26: Simulation 3 Voltage Waveform and FFT	56
Figure 27: Simulation 4 Individual Current Harmonic Distortion.....	57
Figure 28: Simulation 4 Individual Voltage Harmonic Distortion	58
Figure 29: Simulation 4 Voltage Waveform and FFT	59
Figure 30: Simulation 5 Individual Current Harmonic Distortion.....	61
Figure 31: Simulation 5 Individual Voltage Harmonic Distortion	62
Figure 32: Simulation 5 Voltage Waveform and FFT	63
Figure 33: Simulation 5 Current Waveform and FFT	63
Figure 34: Simulation 6 Individual Current Harmonic Distortion.....	64
Figure 35: Simulation 6 Individual Voltage Harmonic Distortion	65
Figure 36: Simulation 6 Voltage Waveform and FFT	66
Figure 37: Simulation 6 Current Waveform and FFT	66
Figure 38: Simulation 7 Voltage Waveform and FFT	68
Figure 39: Simulation 7 Current Waveform and FFT	68
Figure 40: Simulation 8 Voltage Waveform and FFT	70
Figure 41: Simulation 8 Current Waveform and FFT	70
Figure 42: Simulation 9 Individual Current Harmonic Distortion.....	73
Figure 43: Simulation 9 Individual Voltage Harmonic Distortion	74
Figure 44: Simulation 9 Voltage Waveform and FFT	75

LIST OF TABLES

Table 1: Total Installed Power on Selected Ship Classes [2]	14
Table 2: Harmonic Distortion Limits.....	46
Table 3: Recap of Simulations 1-4.....	59
Table 4: Recap of Simulations 5-8.....	71
Table 5: Simulation 9 Results	72

CHAPTER 1: INTRODUCTION

The purpose of this thesis is to investigate the system wide issues in the electrical distribution system with having a high voltage DC distribution bus (10 KV), coupled with a silicon carbide (SiC) based inverter for the electric propulsion motor. A model of a straight-line electrical distribution system was developed from the power generation to the propulsion motor. This model was analyzed in order to determine system wide issues to using an electrical distribution system of this type.

Background

The United States Navy is moving in the direction of utilizing more electrical applications in the ships of the future. One of the biggest examples is the integrated power system (IPS), whereby the propulsion system is powered by electric motors, unlike the current propulsion systems that utilize a direct mechanical link from the engine to the propeller. Combat systems and weapons of the future will require even greater amounts of power than today while more equipment is being converted from mechanical (hydraulic, for example) to electrical applications.

Current ships have over ninety percent of their total power reserved exclusively for the use by the propulsion system, with only a small percentage of installed power devoted to electrical power generation. Future ships that utilize an IPS system will be required to produce approximately 80 MW of power in an electrically usable form in order to propel the ship and to power the advanced weapon systems. Due to the high power demand of new electronic weapons, the ship will not be able to power all systems and weapons and maintain a high speed at the same time, since these systems will obtain their power from the same IPS system.

The IPS arrangement on future ship classes has the following advantages [1]:

- Increased fuel economy due to more efficient operation of the prime mover
- Arrangement flexibility due to the elimination of large mechanical shaft components and the reduction of total prime movers
- Availability of a large amount of electrical power for non-propulsion use
- Ability to accommodate the electrical power needs of future military systems
- Reduced manning requirements due to high levels of automation and control

This thesis will investigate the proposed use of using SiC switches in the power electronic converters within the power distribution system. Although only the effects of an electric propulsion motor was analyzed, this work can be used in order to assess the issues that will arise when using the same SiC devices for the combat system and other power systems throughout the ship.

SiC power electronics devices will be able to convert high voltage AC power directly into high voltage DC power. This is due to SiC's ability to block high voltages. SiC may also be able to eliminate electromechanical devices completely from the shipboard electrical distribution system. The elimination of electromechanical devices would be able to greatly reduce the weight of the electrical distribution system onboard Navy ships. The application of high voltage DC power would also be able to reduce the size and weight of the distribution system cabling.

Scope

The utilization of power electronic components for the transformation of power will have negative effects on the quality of the electrical distribution system. Due to the switching of the SiC switches in the power electronic components, the primary distribution bus will be affected due to the loads not drawing sinusoidal current. The power supplied to the power conversion components will be analyzed for distortion and recommendations made in order to reduce the distortion on the supply bus.

Page Intentionally Left Blank

CHAPTER 2: IPS BASIC PRINCIPLES

Traditional (Non-IPS) Ships

Traditional ships do not have integrated power systems. The electric power system on traditional ships consists only of the ship service electrical distribution system, which accounts for only a small percent of the total installed power. The remaining installed power is for the exclusive use of the propulsion system, which is a mechanical system that cannot be utilized for electrical power generation. Traditional systems have completely separate systems for propulsion and electric generation.

Table 1 lists a number of ship classes and the percent of power that is available to the electrical distribution system. This shows that an overwhelming majority of installed power is fixed to the propulsion system. One exception here is the new amphibious transport dock ship, LPD-17. Since this ship is new, a higher amount of electrical power was installed onboard in order to power newer equipment that has higher power demands than older electronic equipment. This installed power is also to ensure adequate power to the numerous electronic systems currently installed and to be installed in the future. Installing a surplus of power is referred to as electrical margin for future growth. Also, being an amphibious ship, the speed requirements of this ship are smaller than those of a combatant ship, therefore the percent of usable electrical power for the LPD-17 is significantly higher than the other examples in Table 1.

Ship Class	Ship Service (MW)	Propulsion (MW)	Total Installed Power (MW)	Percent Usable As Electrical Power
DDG-51, CG-47	7.5 (2.5 x3)	100 (LM2500 x4)	107.5	6.98%
DDG-79	9.0	100	109	8.26%
FFG-47	4 (1.0 x4)	50 (LM2500 x2)	54	7.41%
SSN 688	6	26	32	18.75%
SSBN 726	8	45	53	15.1%
LPD-17	12.5 (2.5 x5)	31 (7.755 x4)	43.5	28.7%

Table 1: Total Installed Power on Selected Ship Classes [2]

The typical installation for a traditional ship consists of the propulsion engines connected mechanically, sometimes through a reduction gear (depending on the speed of the engine), to the propulsion shaft and propeller. Most military instances have two engines connected to a single reduction gear driving a single shaft. This configuration is for redundancy. Figure 1 shows a typical propulsion system installation with two shafts and four propulsion engines. One of the issues that are readily apparent from Figure 1 is the restriction placed upon the location of the engines. This layout is for survivability, but due to the longitudinal separation, a long shaft is required.

The ship service electrical distribution system consists of three or more generators connected in a ring bus. Figure 2 shows the typical ring electrical distribution bus with three ship service generators. One advantage of the ship service system compared to the mechanically connected propulsion system is that the location of the ship service generators can be placed at different locations throughout the ship.

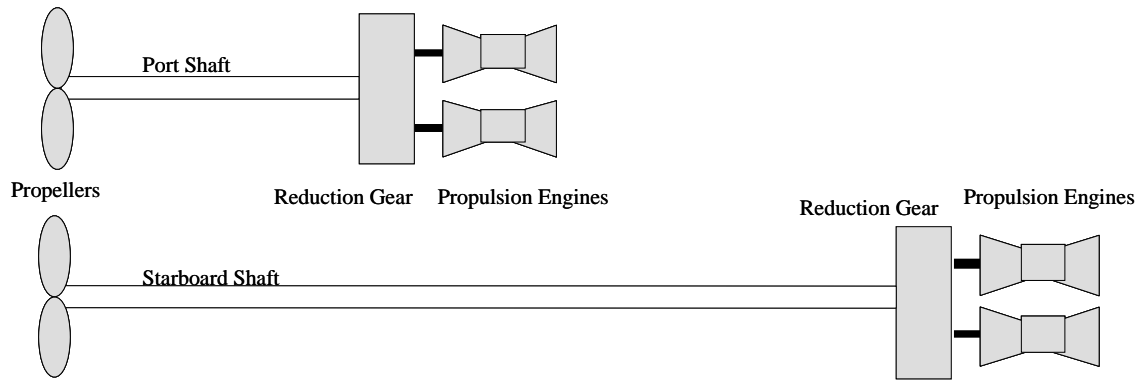


Figure 1: Traditional Propulsion System [3]

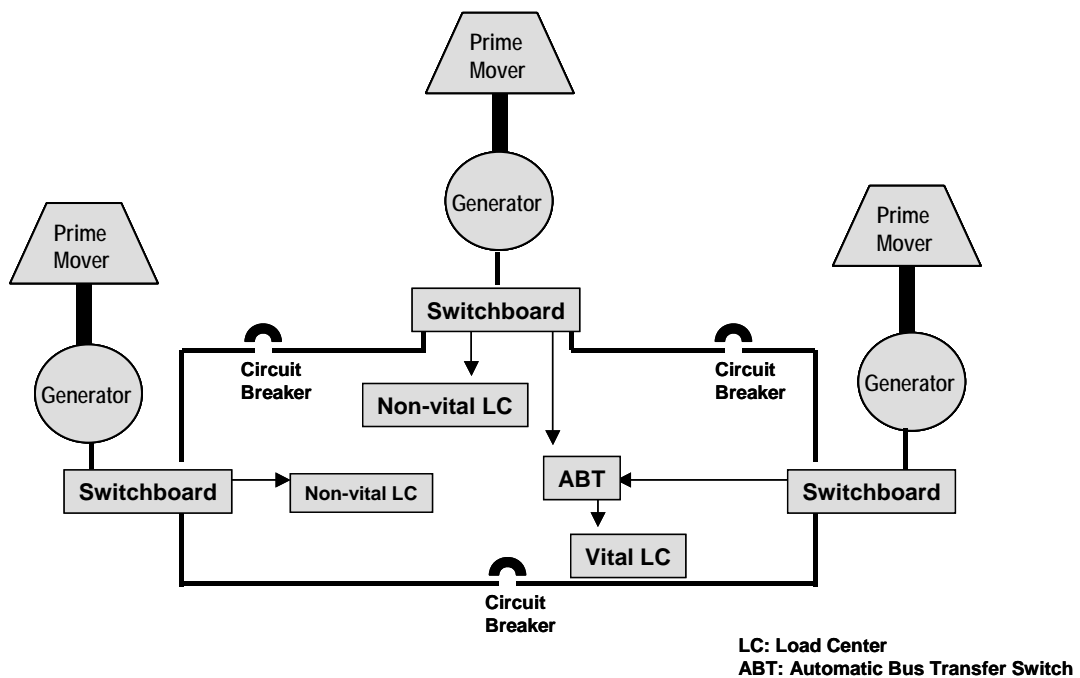


Figure 2: Traditional Ring Electrical Bus [3]

IPS Ships

A ship that has an integrated power system is different from the traditional configuration. An IPS ship has a combination of the propulsion system and electrical distribution system. This is accomplished with the use of electric drive propulsion motors, compared to mechanically

connected propulsion engines. For an IPS system, the propulsion and ship service distribution loads can be powered from any of the installed engines.

There are numerous advantages to using an IPS system. Some of the advantages with respect to the naval architecture layout are the following [4]:

- Vertical Stacking of Propulsion Components
- Pods
- Athwart ship Engine Mounting
- Horizontal Engine Foundation
- Engines in Superstructure
- Distributed Propulsion
- Small Engineering Spaces

As was seen in Figure 1, the layout of traditional mechanical drive propulsion systems was based on shaft alignment to the propellers and survivability. With an IPS system, the alignment of the shaft with the propellers is not a primary concern and the engines can be placed almost anywhere on the ship, while also taking ship survivability into account.

Figure 3 shows an IPS configuration. This shows that there is not a 'per se' propulsion engine or ship service engine. All of the engines can power everything that is connected to the electrical service bus. An electric drive motor is utilized for the propulsion of the ship, thereby allowing the propulsion to be powered by any of the installed engines. This specific IPS configuration has four electrical generating sets, two 30 MW and two 10 MW. This would provide the ship with 80 MW of total power, approximately the amount of power required to power ships in the near future.

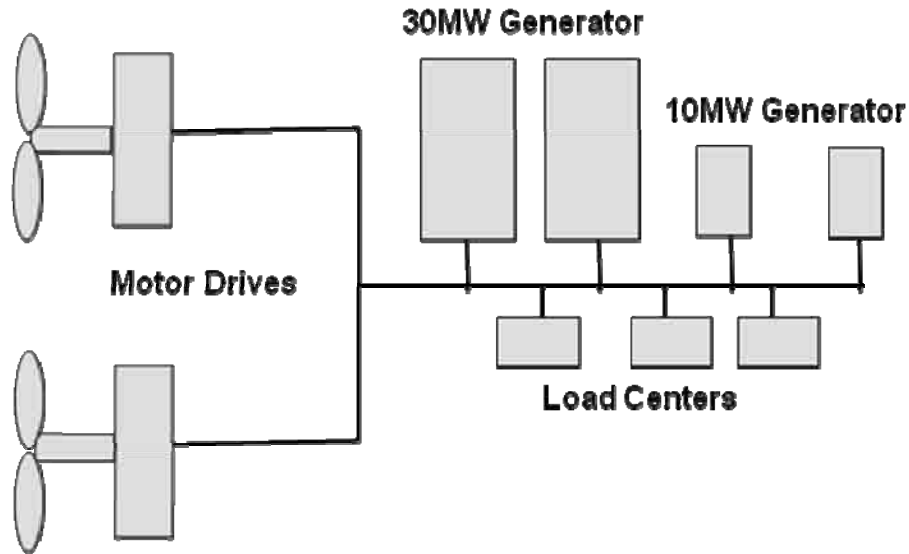


Figure 3: IPS Configuration [3]

Zonal Distribution and Terminology

A ZED system divides the electrical distribution system into ‘zones’ in order to maximize survivability. There are three types of topologies for electrical distribution systems [3]: AC radial (traditional ship type, see Figure 2), AC zonal, and DC zonal. A ship that utilizes an IPS with SiC switches would most likely be a DC zonal type system, although an AC zonal could also be used.

Figure 4 shows an AC zonal electrical distribution system [3]. This type of AC ZED is installed on the DDG-79 (and newer DDG-51 ships) and LPD-17 class ships. Figure 5 shows another type of AC ZED system [5]. In this configuration, unlike an AC radial distribution, two main power buses are utilized and the electrical distribution is divided up into a number of zones [5]. These main buses (port and starboard) have a two-deck vertical separation with one bus above the water line in order to maximize survivability. The two main buses are connected to all zones and the load centers are connected to each main bus. Therefore, if power to one zone or one main bus is lost, then power can be drawn from the other main bus in order to maintain power to the load center.

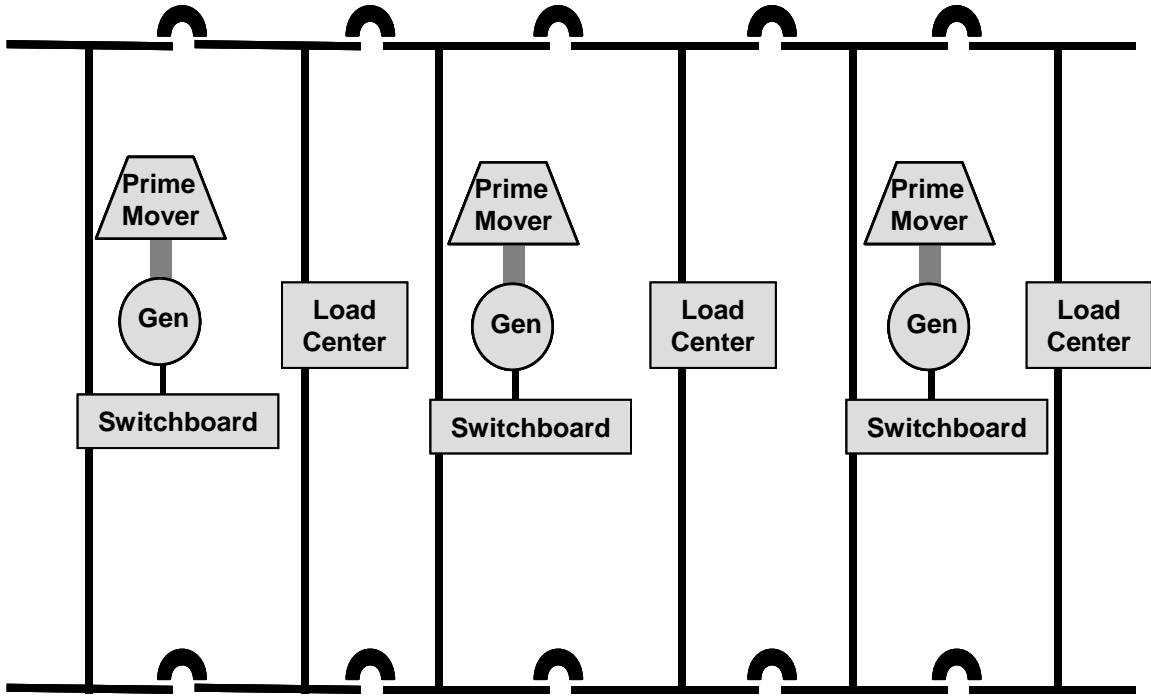


Figure 4: AC ZED System (DDG-79 and LPD-17) [3]

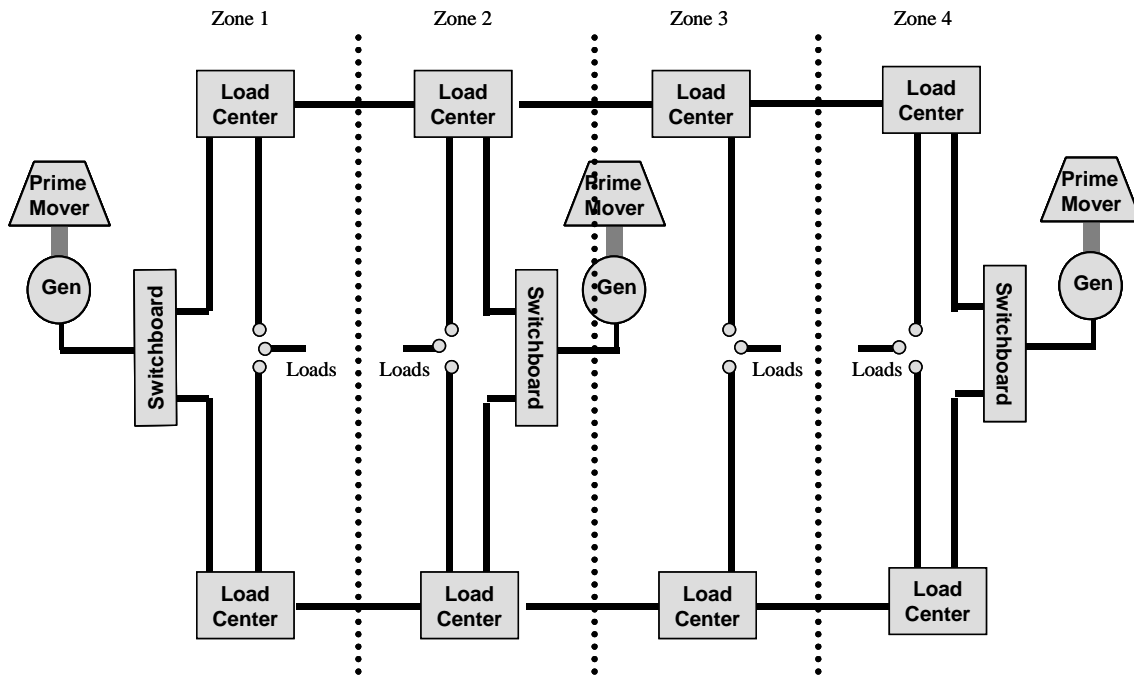


Figure 5: AC ZED System [5]

Figure 6 shows a DC ZED system [5]. This system is similar to the AC ZED system, with the exception that the two main buses have DC power instead of AC power. One advantage over the AC ZED system is the removal of the large electromechanical switchgear that is required in an AC system [5]. This results in a cost savings of the DC ZED over the AC ZED. Instead of using switchgear in order to limit current during casualties, power electronics can be utilized. In this DC ZED system, each PCM-1 (Power Conversion Module) reacts to maintain the voltage at the appropriate level with respect to the other zones on the bus. This allows the system to have integrated fight through power (IFTP) [5]. This functionality is applicable to AC and DC systems.

An IFTP system is utilized in order to maximize survivability. For instance, one of the two main power buses (port or starboard) will be entirely above the waterline. Therefore, if the ship is damaged and partially flooded, one of the main buses will be able to continue to provide power to the vital equipment on the ship. All of the load centers are connected to both main buses and will be able to pull power from either bus, thereby decreasing the probability that vital equipment will lose power during a casualty.

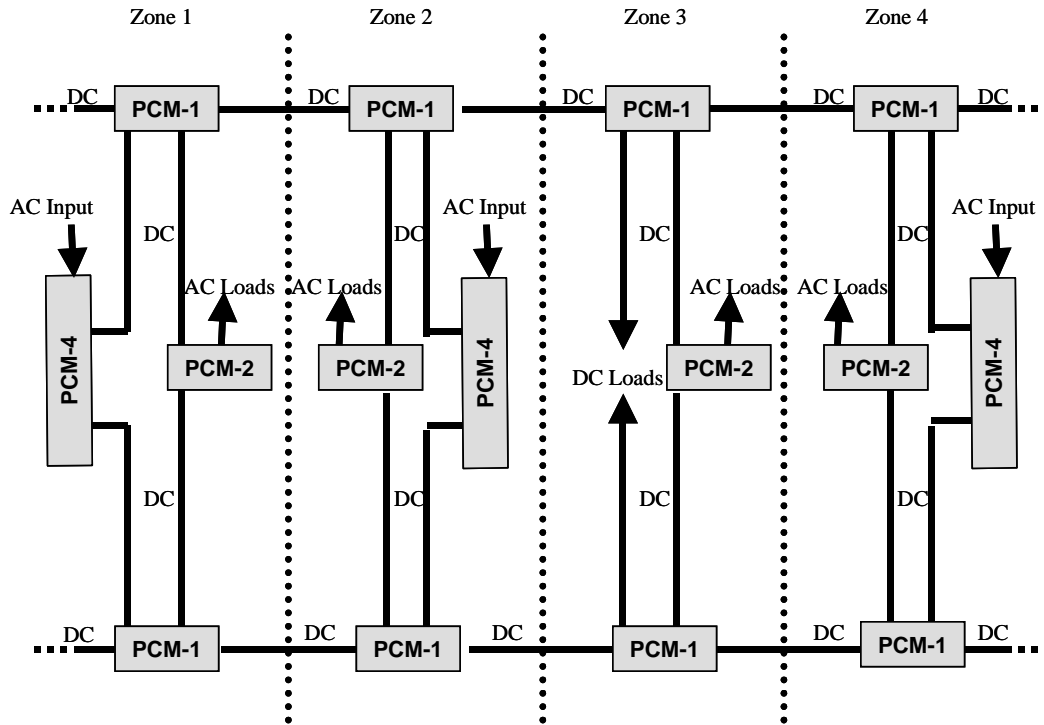


Figure 6: DC ZED System [5]

Although both IPS and IFTP relate to the electrical distribution system, their functions are completely different. An IPS system utilizes power from the electrical distribution system in order to provide propulsion to the ship by means of an electric motor. An IFTP system divides the electrical distribution system into zones for the purpose of survivability. IFTP allows redundant power to be supplied to ship load centers from each main bus. This will insure that power is maintained to the loads when one main bus losses power in a casualty.

Figure 6 introduced the PCM-1 with respect to the DC ZED system. This also shows numerous other modules that pertain to the electrical distribution system. The following are other modules pertaining to an IPS and ZED system and their descriptions [5]:

- Power Generation Module (PGM) – Prime mover and AC power generation
- Power Distribution Module (PDM) – Electrical distribution
- Power Conversion Module (PCM) [6]
 - PCM -4 AC/DC (medium voltage AC to 1000 VDC)
 - PCM -1 DC/DC (1000 VDC to 375-800 VDC)
 - PCM -2 DC/AC (800 VDC to 450 VAC)
- PLM – Power Load Module
 - Propulsion Motor Module (PMM) – Subset of the PLM, the electric motor and associated power electronics
- Power Control (PCON)
- Energy Storage Module (ESM)

Page Intentionally Left Blank

CHAPTER 3: SILICON CARBIDE POWER ELECTRONICS

In a report published six years ago (2001) about future shipboard power systems [7], the possibility of having a high voltage DC bus (10-15 KV) was a long-term prospect. Although, since that time, the development of SiC power devices have come a long way towards this goal. One of the recommendations of this report was to develop “high power, high voltage power electronics” [7]. SiC power devices may be able to provide the power electronics necessary in order to advance current shipboard power systems. Figure 7 shows more information on TRL’s [7] and Appendix A has a more detailed table of TRL levels [14].

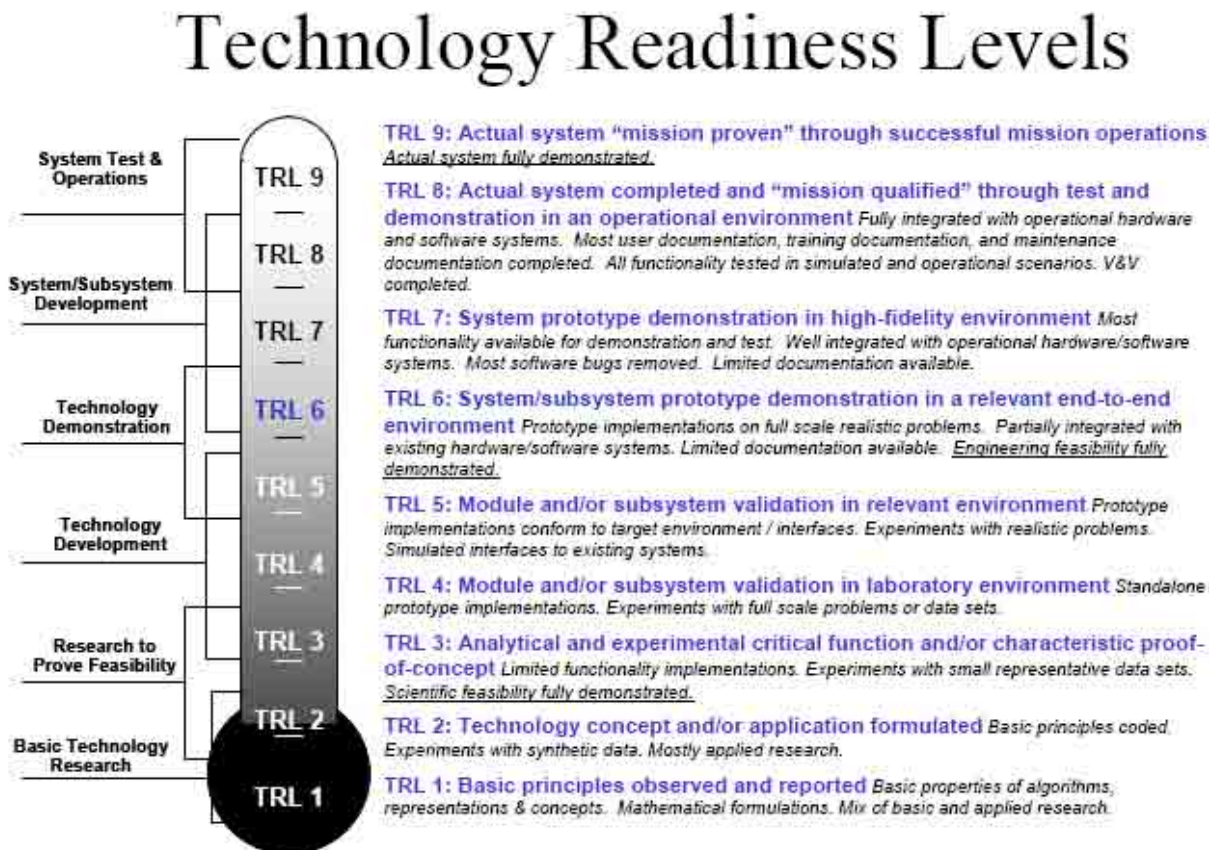


Figure 7: Technology Readiness Levels [7]

At the time of this report [7], the technology readiness level (TRL) [14] of a high voltage DC bus was three. By definition, a TRL of three means that the technology has a proof-of-concept with limited functionality and small data sets, but it has scientific feasibility fully demonstrated. The issues at the time with high voltage DC bus were with investments in the development of SiC and system integration [7]. With new, more advanced SiC diodes and switches becoming available on a continuing basis, the TRL level would most likely be in the range of five since technology demonstrations are ongoing with SiC devices. A TRL of five deals with module and/or subsystem validation in relevant environment, but the engineering feasibility is not yet fully demonstrated.

SiC Background

SiC is a wide bandgap semiconductor. “A wide bandgap semiconductor is a semiconductor with an energy band wider than about 2 electron volts (eV)” [15]. Other materials within the wide bandgap semiconductor area are gallium nitride (GaN) and aluminum nitride (AlN). In the past, it was thought that SiC would replace silicon entirely in the power electronic device field [10]. But, at least in the near term, SiC will not entirely replace silicon devices [9]. Although great advances have been made with regard to SiC properties, there are still technical difficulties with developing high power devices. Some of the common issues currently affecting SiC devices are “micropipes” in the wafer. These effectively are holes through the entire wafer. Some of the problems with SiC have made significant progress with higher quality substrates and better fabrication technologies [10]. SiC material also comes in different polytypes, depending on the chemical makeup of the material. These different polytypes have different energy bands. Some common polytypes of SiC are 3C, 4H, and 6H

with energy bands of 2.2 eV, 3.25 eV, and 3.0 eV [15], respectively. The most common SiC polytype currently being used in power electronic devices is 4H.

Even though there are numerous wide bandgap semiconductors, SiC semiconductors have advantages over other wide bandgap semiconductors. Some of these advantages include [11]:

- Indirect semiconductor (important for bipolar power electronics)
- Doping of both n- and p-type material
- Native thermal oxide Silicon Dioxide (SiO₂)
- High quality crystals available
- Broad range of applications

SiC Advantages

The benefits of SiC over traditional silicon are numerous. One of the advantages of SiC is the nearly one hundred percent compatibility with current silicon technology [9]. Some of the benefits include reduced dependence on temperature, faster switching times, smaller power electronic devices, lower on-resistance, and fewer components for a given power electronic circuit.

Another advantage of SiC over silicon is its ability to operate at much higher temperatures. Therefore, cooling will not be required or less cooling will be required for SiC. For example, if a SiC power electronic component can operate at junction temperature at 250°C, ambient cooling, without the use of a dedicated cooling system, may be able to cool this power electronic component. An example where less cooling would be required would be when the SiC power electronic component exceeded its junction temperature set point. For this example, the cooling system would only have to reduce the junction temperature to 250°C, unlike a typical silicon power electronic component which would have to reduce the junction temperature further to maintain proper operation of the circuit. As far the efficiency of cooling, since an IGBT has a

junction temperature limitation of 125°C, the difference in temperature (between circuit temperature and cooling medium temperature) with the cooling system is fairly small and the efficiency will be lower and the cooling requirements higher. SiC, unlike silicon, can operate, in theory, at a junction temperature of 300°C. This provides for a very large difference in temperature (from ambient or cooling medium temperature, depending on operating conditions) in order to provide a much more efficient cooling scheme compared to silicon [8].

SiC also has the advantage of being able to switch faster than silicon. This is mainly due to the diode having little or no reverse recovery charge. A SiC Schottky diode can switch in under 50 nanoseconds, which is a quarter of the time it takes a comparable PiN diode with one micro-coulomb (μC) of reverse recovery charge (200 ns) [8]. The advantage of having little or no reverse recovery charge makes the SiC diode very efficient due to a reduction of the switching losses. Also, with no reverse recovery charge, in some circuit types the snubber circuits can be removed, therefore resulting in a circuit with fewer components and a higher efficiency [12]. In addition to having little reverse recovery charge, this charge is independent of temperature. In contrast, silicon device reverse recovery charge increases significantly with temperature, thereby further stressing other elements within the power electronic circuit [8]. Therefore, with a higher operating temperature in silicon, the increase in reverse recovery charge causes the efficiency of the system to further degrade due to temperature increases.

SiC has ten times higher critical electrical field compared to silicon. For this reason, a 4H-SiC MOSFET has the thickness of only 10% and a doping concentration 100 times that compared to a silicon MOSFET with comparable blocking voltages [8]. This allows SiC to be ten times thinner [9] and greatly reduces the size of semiconductor circuits. This size reduction of SiC can be utilized in two ways. Smaller SiC devices can be used in order to reduce the size

of power electronic circuits, or similar sized devices (compared to silicon) can be used with higher device ratings thereby providing a similarly sized circuit with a much higher power rating. Because of the smaller size and higher doping concentration, the SiC majority carrier devices (for example, holes in p-type material and use only one type of charge carrier) on-resistance (R_{on}) can be up to 100 times less than comparable silicon diodes or MOSFETs [10]. For minority carrier devices (for example, electrons in p-type material), these advantages can result in a switching speed up to 100 times faster [10].

SiC Disadvantages

Cost is one of the major drivers of the current state of technology compared to silicon devices. SiC devices are currently more expensive and have not been fully developed to completely replace silicon devices. Some SiC technologies also have other disadvantages as compared to conventional power electronic devices. For example, SiC power bipolar junction transistors (BJT's) have limited current gain [8] compared to comparable silicon BJT's. These devices have ratings of 1400 V and 20 A, but have a current gain of only 14.

Current SiC Power Electronic Devices and applications

As stated earlier, one of the primary advantages of SiC devices is that they can replace silicon devices nearly 100% of the time due to the similar characteristics between the devices. Because of this, anywhere that silicon devices are today, SiC devices may be able to be utilized when the technology becomes available.

One of the devices that have been successfully utilized is the Schottky barrier diode (SBD). This diode is a unipolar device that can block voltages up to 1700 volts [11]. Since this diode has zero reverse recovery charge, losses can be reduced and the efficiency of circuits

increased. An application that can use this type of device is the power factor correction power electronics. Two disadvantages with Schottky barrier diodes currently are the cost of the diode compared to silicon and the restricted surge-current handling capability. In order to overcome the surge-current deficiency, a newer diode that has a bipolar part integrated into the device has improved the diodes performance [11]. This diode acts like a unipolar device in normal operation and is able to switch to bipolar operation under surge conditions [11].

Another device that has been successfully developed is a 180 A, 4.5 kV 4H-SiC PiN diode [13]. This diode had a forward voltage of 3.2 volts at 180 A and less than 0.4 μ A reverse leakage current at 4.5 kV. This device has an advantage over the SBD, which can only block voltages up to 2.5 kV due to an increase in resistance [13].

One application for SiC device is in the use of high voltage-high frequency conversion applications. Silicon's ability to be utilized in this application deteriorates as blocking voltage is increased, which causes on-resistance to increase and switching frequency to decrease [10]. The use of SiC devices allows for the conversion of medium voltage applications from 100 volts to 6.6 kilovolts. Utilizing SiC over silicon greatly reduces the losses, and thus greatly increases the efficiency of the system. Once SiC technology advances further, the use of these devices up to 25 kilovolts may be possible for high voltage-high frequency power conversion applications [10].

Another application that is directly applicable to an IPS ship is motor control. When SiC MOSFET's and SBD's replace silicon IGBTs and PiN diodes, a reduction of 80% in total losses (switching and conduction) is achieved when using a three phase pulse width modulated (PWM) motor controller [12]. This reduction in losses results in an efficiency increase of 4-6% [12]. Since SiC devices also require less cooling due to their ability to operate at higher temperatures,

the cooling demands of the systems are thus reduced. The most significant problem is the lack of the required 1200V / 100 A devices. These devices require an increase of die area of 10 times and a reduction of the density of micropipes in order to be able to obtain the current capacity of 100 A [12].

Future of SiC Devices

The major issue currently facing SiC devices is the cost compared to silicon devices. Although technological advances are happening continuously in the SiC field, they are not ready to replace silicon in all applications. SiC devices may be able to replace silicon in some applications and will be able to be used in applications where silicon cannot be used. The costs of the new SiC devices are compensated for by the fewer components required and the reduced size of power electronic circuits [9]. Although the costs of SiC devices are currently higher than silicon, with more development and the increased production and use of SiC devices, these costs will begin to become more affordable compared to silicon.

From 1993 until 2005, the status of the SiC wafers has improved from a 1 inch diameter with >1000 micropipes per cm^2 to a 3 inch diameter with <10 micropipes per cm^2 [9]. These great strides in the development of SiC wafers will likely increase for some time. Therefore, the use of SiC in applications like high voltage-high frequency power conversion and high power motor control will be possible in the not too distant future. These devices would make future shipboard power systems able to operate at several kilovolts and allow for more efficient operation. Eventually, SiC-based applications will become one of the applications with the highest power density and efficiency coupled with the lowest volume and weight [9].

SiC Conclusion

The primary benefit of SiC over silicon power electronic devices is their increased power density. If SiC and silicon devices are compared at the same power level, the SiC devices will be much smaller than the silicon devices at the same power level. Also reducing the size of SiC circuits is the reduced number of components required. For some silicon circuits to get the required blocking voltage, numerous power devices are required to be placed in series. For the SiC device, only one device may be necessary for the same circuit. Also reducing circuit size and complexity, if snubber circuits will not be required for SiC circuit, this further removes additional components from the circuit.

SiC power devices fit nicely into the future high voltage DC IPS distribution system. The future system will be able to reduce the size and increase the power density of the system. With SiC power electronic devices, the HV DC distribution system has the benefit of reducing the electromechanical components in the system and reducing the amount of cabling installed on the ship. The amount of cabling required for a DC system is only two-thirds compared to an AC system with similar power levels. This reduction is due to the DC system have two cables and the three phase AC system having three cables. SiC will not enable DC voltage systems, but will enable high voltage DC systems by being able to transform high voltage AC into high voltage DC without the use of electromechanical components.

In summary, the advantages that a SiC power electronic system have over the traditional silicon system are numerous. At the power and voltage level that future shipboard electrical distribution levels will be operating, SiC provides a power electronic device that will be unmatched compared to silicon. Therefore, the main benefit of utilizing SiC devices in the future shipboard power system is that they both seek to decrease the size of the system and provide a system that is much more power dense than what is currently available.

Page Intentionally Left Blank

CHAPTER 4: SYSTEM MODEL

Introduction

A model of a high voltage system was developed using Matlab and Simulink. The Sim Power Systems toolbox for Matlab/Simulink was also utilized in the development of this model. This system is a straight-line diagram from a three-phase synchronous generator power source to an induction motor. The induction motor is acting as the propulsion motor. The rectifier and inverter are power electronic devices composed of either ideal switches or simulated SiC devices.

Power Supply

The power supply for this model is a three-phase 20 MW synchronous generator. The voltage for the power supply is set at 6.0 kilovolts (KV) in order to get the required 10 KV on the DC bus. Figure 8 shows the system model power supply. Because of the downstream power electronic components, the power supply will be distorted due to the switching of the rectifier and the inverter. The implementation of a synchronous generator into the model allows for the interaction between the transients of the power electronic components and the synchronous generator.

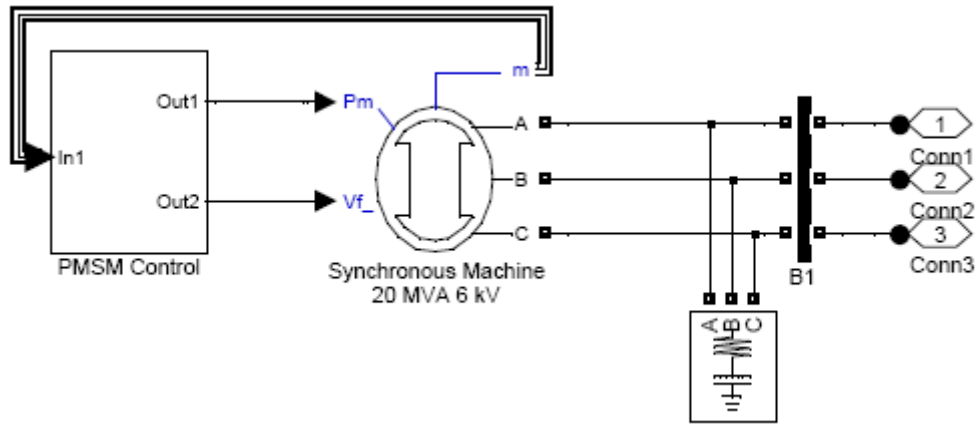


Figure 8: System Model Power Supply

Rectifier

The rectifier receives the 6.0 kV power from the synchronous generator. The universal bridge block in Simulink Sim Power Systems toolbox is utilized for the rectifier. Initially, the simulations were run with only ideal switches for the rectifier. Later simulations used IGBT devices that were simulated SiC power devices. It was attempted to idealize the rectifier in order for it to work like a future SiC power device, but some limitations within Simulink prevented some of the changes to make it more ideal. For example, as stated in chapter 3, the use of SiC power electronic components has allowed the removal of snubber circuits because of the zero reverse recovery charge associated with SiC power electronic devices. The snubber circuits in Simulink could not be removed because this would cause two current sources to be in series. Simulink models some components as current sources, therefore when the snubber circuit was removed from the rectifier, it appeared that there were two current sources in series and prevented the circuit from being simulated. The effect of the snubber circuit was minimized as much as possible, but it could not be removed entirely due to the Simulink limitations.

Figure 9 shows the rectifier and associated DC regulator. Because the rectifier is a controlled device, gating pulses must be produced by a DC regulator in order to regulate the DC voltage downstream from the rectifier. The DC voltage from the input of the inverter is supplied to the DC regulator in order to adjust the gate pulses and maintain the output of the rectifier at the desired voltage level. The control of the DC voltage is obtained by using two proportional-integral (PI) controllers [16].

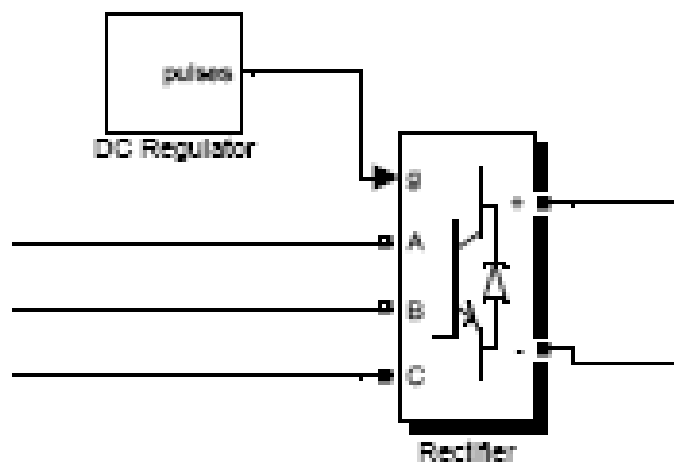


Figure 9: Rectifier and DC Regulator

DC Link Filter

In order to smooth the signal from the rectifier to the inverter, a filter is utilized to filter out the high frequency components in the signal. The purpose of this filter is to make the DC link voltage as near to ideal DC voltage as possible for the input to the inverter. This low pass filter consists of a series inductor and a parallel capacitor. There are also some measurements taken from this filter, which are the rectifier DC voltage and the inverter DC voltage. Figure 10 shows the DC link filter and associated measurements.

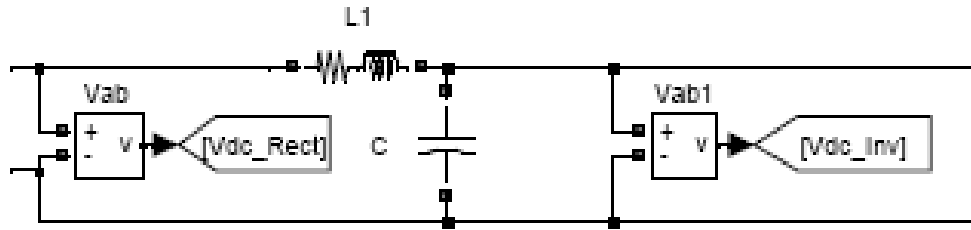


Figure 10: DC Link Filter

Inverter

In order to convert the DC link voltage to usable alternating current for the induction motor, an inverter was used. The inverter receives the DC link voltage at 10 KV and generates a pulse-width modulated (PWM) signal for the induction motor. The universal bridge block in Simulink Sim Power Systems toolbox was utilized for the inverter. Initially, the simulations were run with only ideal switches for the rectifier. Later simulations used IGBT devices that were simulated SiC power devices. Figure 11 shows the inverter and associated control system for this model.

The inverter is controlled by gate signals from the vector control block, which receives its inputs (speed and current) from the induction motor. The speed control loop in the vector control block uses a proportional-integral (PI) controller to produce the quadrature-axis current reference (i_q^*) in order to control motor torque by adjusting the gating signals to the inverter. The motor flux is controlled by the direct-axis current reference (i_d^*). A transformation block within the vector control transforms the D- and Q-currents into three-phase currents (i_a^* , i_b^* , and i_c^*) for the current regulator [16].

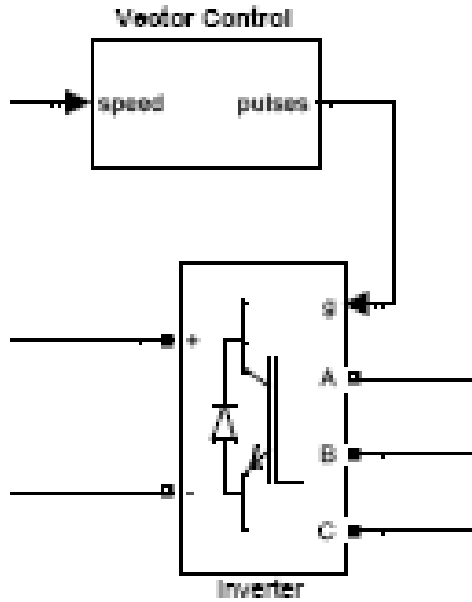


Figure 11: Inverter and Vector Control

Induction Motor

For the simulated propulsion motor in the system, an induction motor was utilized from the Sim Power Systems toolbox. This motor is a squirrel cage induction motor rated at 20 MW. This motor was used since it is somewhat similar to the current propulsion motor slated for the DDG-1000 ship, the Advanced Induction Motor (AIM). Although the AIM, with its 15-phase operation, has a more advanced control system than a typical induction machine, it is assumed that some of the issues with a simplified system would also be encountered by a system with an AIM installed. Figure 12 shows the induction motor with other associated inputs for the system model. The torque input allows the user to change the desired torque of the induction motor.

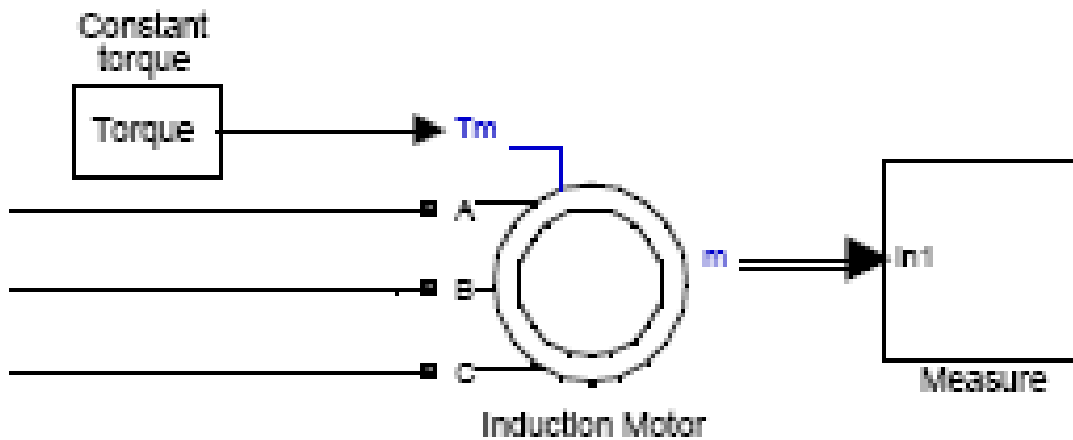


Figure 12: Induction Motor

One example where an AIM system may produce worse results is in the distortion of the main power bus. Since the AIM has 15 phases, with each set of five phases obtaining three-phase power from the main power bus, this could result in even more distortion than this current model. This would be due to each set of phases pulling power off the bus at different times. This configuration is shown in Figure 13 [17]. The AIM system must power three rectifier/inverter sets, whereas only one rectifier/inverter set for the current model. These three sets are phase shifted, which is why the power would be pulled off the main bus at three different times. This current model could also produce worse distortion as compared to the AIM. Since the AIM's total power is distributed across three sets of rectifier/inverters, the power that each set requires will be less than if all of the power was pulled off of the bus at the same time. Since the three sets will not be pulling power off the main bus at the same time, this could result in less distortion to the main bus.

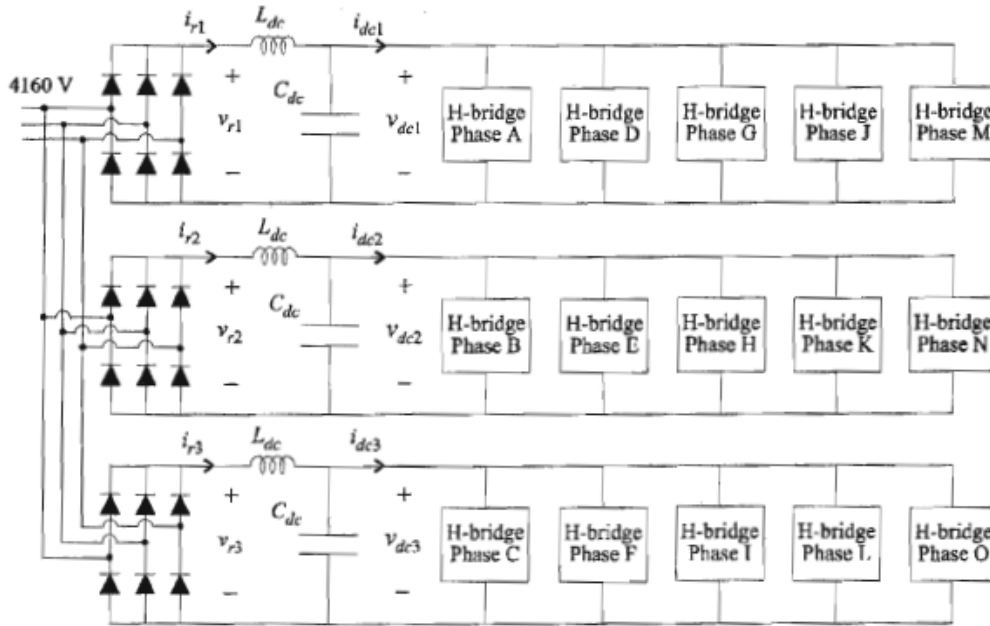


Figure 13: Advanced Induction Motor Configuration [17]

Measurements

Measurements are taken throughout the model in order to analyze the simulation results. The measure block consolidates numerous measurements for associated functions across the entire model. This block also has numerous scopes set up in order to capture the results of the simulations. This block also contains the measurement blocks for the Fourier transform in order to calculate the current and voltage individual harmonic distortions. These values are sent to the Matlab workspace for further analysis.

Miscellaneous Control Blocks

Figure 14 shows a set of simulink blocks that were used in the transient analysis of this model. There are two sets of these blocks, one for the speed control and another for the torque control. These blocks are simply timing blocks in order to increase the speed and torque of the

induction motor after a preset time. This allows for the system to reach steady state before transients are imposed on the system.

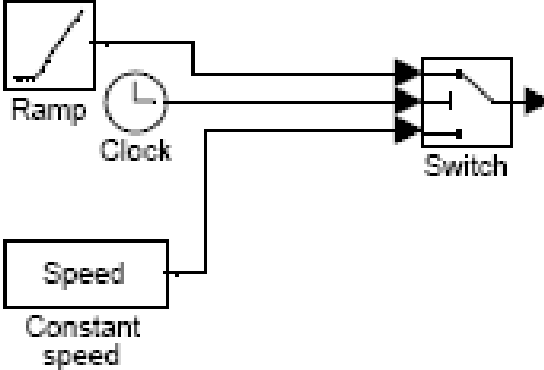


Figure 14: Transient Analysis Blocks

Validation

Since no system currently exists at this voltage level, coupled with the fact that current SiC devices cannot operate at this voltage and current level, this model cannot be compared to an existing model. Therefore, this model cannot be verified by analyzing it next to another model that is either already simulated or built. Every effort was made in order to ensure that a system that would utilized SiC power electronic components would closely resemble the system model in this thesis. Figure 15 shows the complete top-level model of this system.

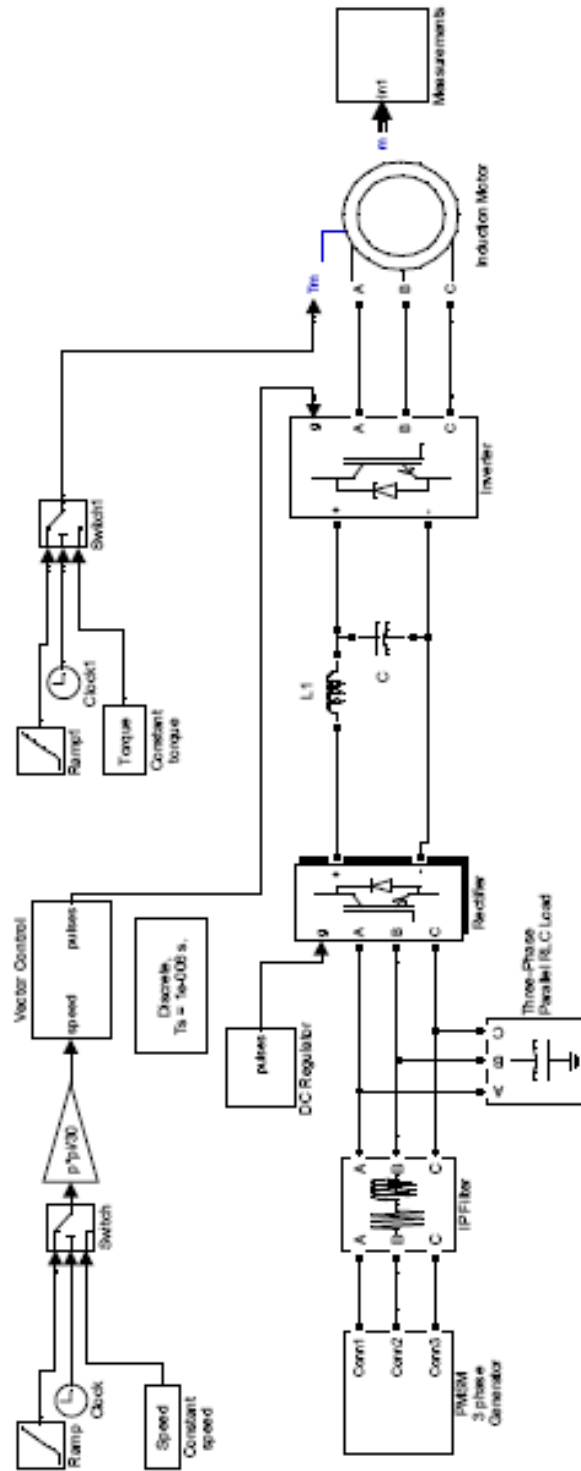


Figure 15: Complete System Model

Page Intentionally Left Blank

CHAPTER 5: SIMULATION RESULTS

Simulink Setup

The Matlab/Simulink model discussed in the previous chapter was utilized for the simulation. This model was adjusted in order to ascertain different operating conditions. The model was simulated with and without an input filter to the rectifier in order to assess the impact of the filter on the system. The model was also simulated during a transient from low power steady state to an increased power level.

The simulation was conducted in discrete time steps of 1 micro-second ($1 \mu\text{s}$). This time step was recommended in the software documentation [22]. This small time step allowed for increased precision of the output, although this resulted in increased computing times on a standard laptop. A 3 second run of this model took approximately 90 minutes. Due to the time intense operations of this simulation, a limited number of simulations were run.

The output that was obtained from these simulations was the current and voltage distortion on the main supply bus (60 Hz) to the rectifier. The individual harmonic distortion for the 0th, 5th, and 7th harmonics for the current and voltage were obtained. Also, the total harmonic distortion was also calculated with the simulink toolbox powergui. The figures in the proceeding sections differ in the analysis type. The plots with only the 0th, 5th, and 7th harmonics are plots that were generated by calculating the harmonics over a running window of one cycle of the fundamental frequency. The frequency plots that contain a range of frequencies (for example, 0 to 3000 hertz) are calculated over a specific period of time and number of cycles (normally 20 cycles). For this reason, these plots cover a wide range of frequencies compared to the aforementioned plots.

Distortion Limits

The requirements for the current and voltage individual harmonic and total harmonic distortion (THD) was investigated to determine the limits for an IPS system with SiC power electronic components. The following standards were examined for applicable setpoints: Military Standard 1399 (MIL STD 1399), IEEE Standard 519-1998, and IEEE Standard 45-2002. MIL STD 1399 is the interface standard for shipboard systems (Section 300A, electric power, alternating current) [23]. IEEE STD 519 is the IEEE Recommended Practices and Requirements for Harmonic Control in Electrical Power Systems [24]. IEEE Standard 45-2002 is the IEEE Recommended Practice for Electrical Installations on Shipboard [25].

MIL STD 1399

Limits for the input current waveform “shall have the minimum harmonic distortion effect on the electric system” [23]. The individual harmonic currents shall not be greater than 3%. This value is the ratio between the harmonic and the fundamental component. The total harmonic distortion for voltage shall be less than 5% and individual harmonic distortion <3%. These limits seem to imply that they are intended for extremely sensitive systems. Sensitive systems (communications, weapons control, radar) onboard ships are always separated from the main bus by either a separate power generation system or high fidelity conversion equipment to insure that main bus fluctuations do not interfere with vital operations on board the ship. Therefore, these limits may be too strict for a large electrical load similar to a propulsion motor being simulated here. The requirements as set forth in this standard are for systems of greater than 1 kVA and frequency of 60 hertz.

IEEE Standards

IEEE 519 requirements for the current and voltage individual harmonic distortion are the same as MIL STD 1399. These requirements are applicable to general systems. This standard also has a voltage THD limit of 10% for dedicated systems. For IEEE 519, a dedicated system is “exclusively dedicated to the converter load.” Therefore, the current Simulink model could be viewed as a dedicated system since it is dedicated to one converter load.

Since IEEE 45 has been recently updated, it specifically looks at IPS systems (integrated electrical propulsion plants). The requirements for voltage THD in IEEE 45 are 8% for a dedicated system. Non-dedicated buses should not exceed the same limits as set forth in the previous standards, 5% voltage THD and 3% for all individual harmonic distortions.

Limits Utilized

Since the standards had conflicting information, the requirements for the Land Based Engineering Site (LBES) in Philadelphia were obtained [26]. This site has the full set up for the next generation propulsion plant for the DDG-1000 ship class. This system is similar to the Simulink model here, with some differences. Although they are different, the harmonic limits utilized for the LBES can be used as limits for this analysis. For the LBES, the limits for the 5th and 7th individual current harmonic distortion were 9% and 8%, respectively. These values will be used in analyzing the simulated system here. Table 2 shows the limits used in this analysis.

Parameter	Limit
Voltage Individual Harmonic Distortion	3%
Voltage Total Harmonic Distortion	8%
5 th Harmonic Current Individual Harmonic Distortion	9%
7 th Harmonic Current Individual Harmonic Distortion	8%

Table 2: Harmonic Distortion Limits

Simulation Outputs

The simulations were conducted for 3 seconds with a time step of 1 microsecond. The fundamental, 0th (DC component), 5th, and 7th harmonics were calculated with the use of a Fourier block within Simulink. These results were sent to the Matlab workspace for further analysis after the completion of the simulation. The 0th, 5th, and 7th individual harmonic distortions were then calculated within Matlab. These results were plotted on a scale of percent of fundamental versus time. This shows the individual harmonic distortion of these components at all times during the simulation. These figures then allowed for quick analysis in determining if the individual harmonic distortion signals were within the above harmonic distortion limits.

Within Simulink, the main bus supply voltage and current were also analyzed with an FFT and the THD calculated. These outputs were also compared to the limits in order to determine the performance of the simulated system.

The simulations were run with and without a simple input filter to the rectifier. These were also run in steady state and transient conditions. The first four simulations were run using an ideal switch-based rectifier and inverter. The final simulations were run with an IGBT-based

rectifier and inverter. These IGBT's were used in order to simulate a SiC-based rectifier and inverter on the performance of the system.

Simulation 1: Ideal Steady State Unfiltered Results

The first simulation was an unfiltered steady state run using ideal switches in the rectifier and inverter. The 5th individual current harmonic distortion averaged 16% of the fundamental component, with numerous points above 20%. The 7th individual current harmonic distortion averaged 7% of the fundamental component, with numerous points above 10%. Figure 16 shows the plot of the individual current harmonic distortion percentage versus time. All plots obtained from Matlab/Simulink for this simulation are located in Appendix C.

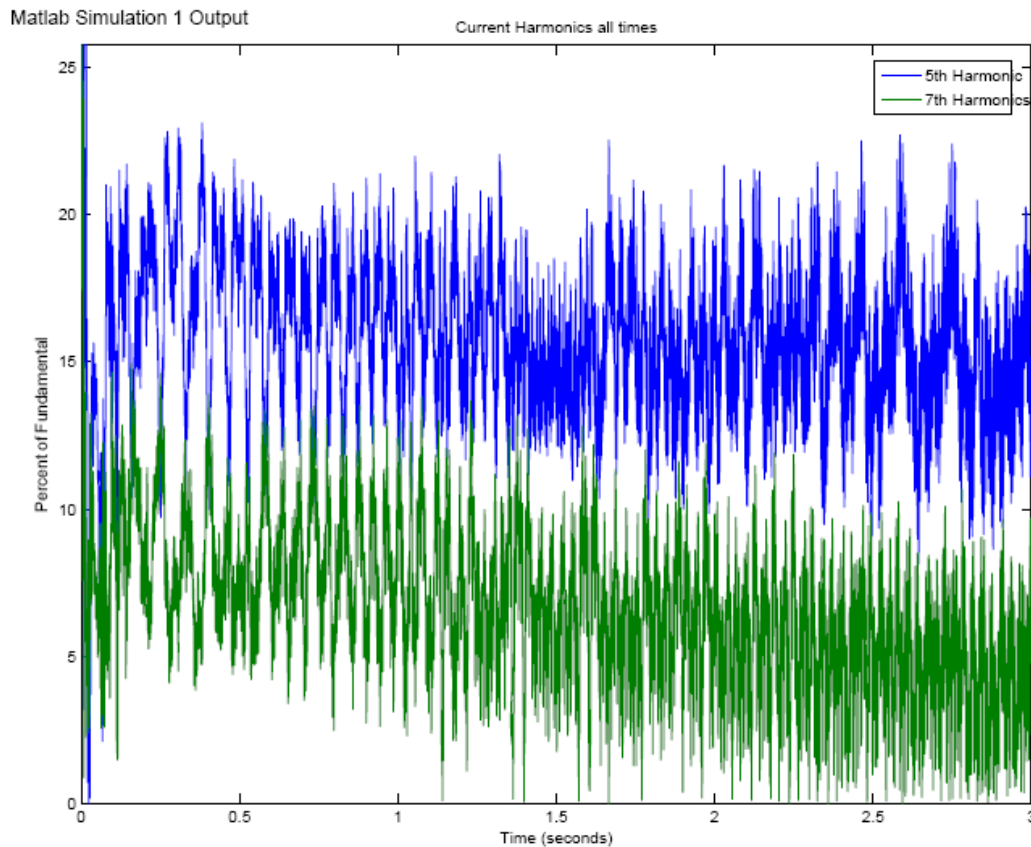


Figure 16: Simulation 1 Individual Current Harmonic Distortion

The individual voltage harmonic distortion was also analyzed for compliance with the above requirements. The 5th individual voltage harmonic distortion averaged 3% of the fundamental component, with numerous points above 6% during the starting transient. The 7th individual voltage harmonic distortion averaged 2% of the fundamental component, with numerous points above 5% during the starting transient. Figure 17 shows the plot of the individual voltage harmonic distortion percentage versus time.

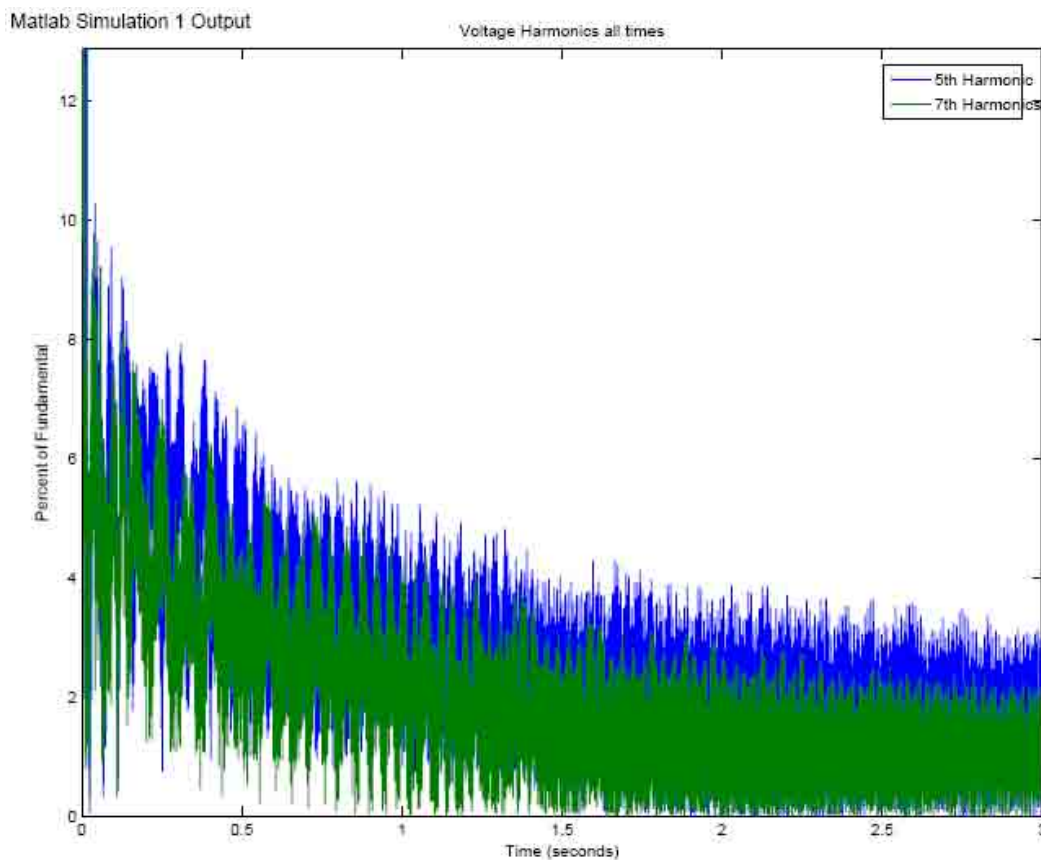


Figure 17: Simulation 1 Individual Voltage Harmonic Distortion

Next the FFT of the voltage and current waveforms were analyzed. The voltage THD was within the requirement of 8% for all calculations except for the analysis conducted between DC and 3000 Hz. The voltage THD for this calculation was 17%. Figure 18 shows the plot and FFT analysis of the voltage waveform. Figure 19 shows the plot and FFT of the current waveform. The THD of this current waveform is 28%. On these two plots, numerous harmonics are shown that are above the individual harmonic maximum limit of 3%.

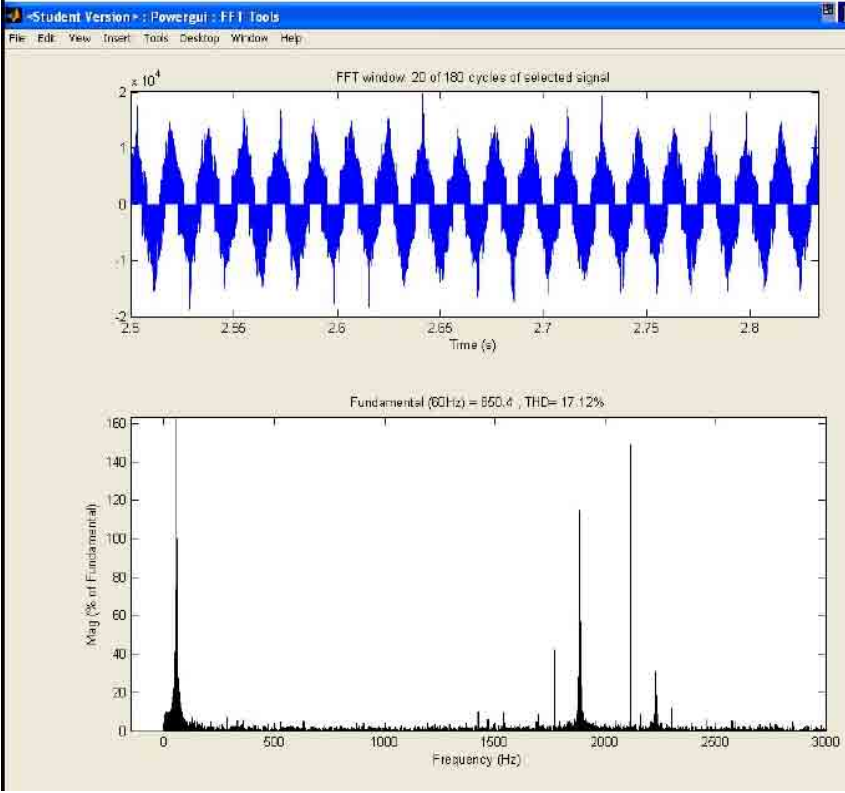


Figure 18: Simulation 1 Voltage Waveform and FFT

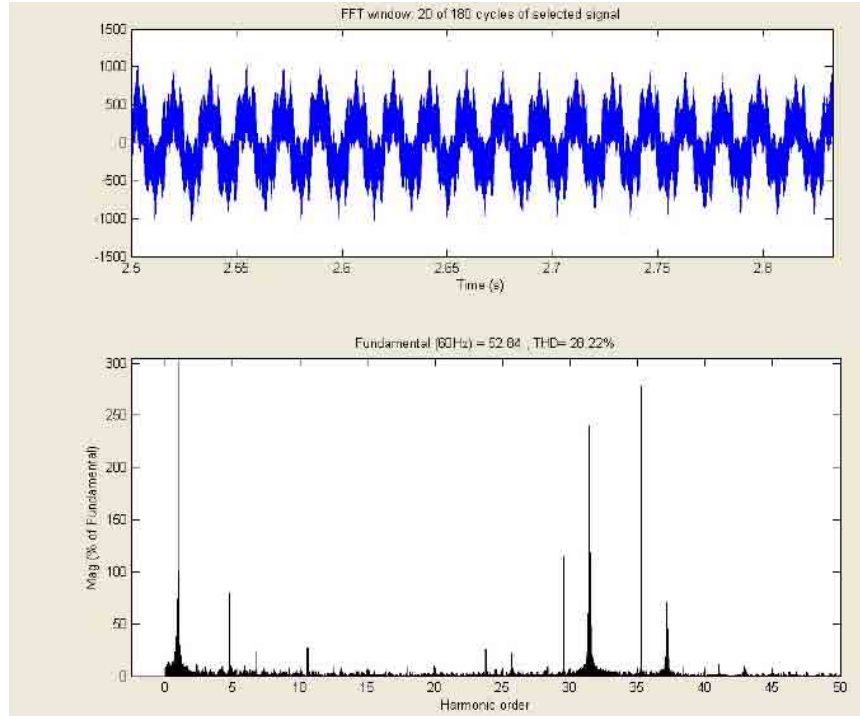


Figure 19: Simulation 1 Current Waveform and FFT

Simulation 2: Ideal Steady State Filtered Results

The next simulation conducted was with the same model as simulation 1, except for a simple input filter at the input of the rectifier. This was done in order to ascertain the effectiveness of a simple input filter on the operation of the model. The 5th individual current harmonic distortion averaged 11% of the fundamental component, with increasing distortion at the end of the simulation. This is an improvement of 5% over the unfiltered model. The 7th individual current harmonic distortion averaged 4% of the fundamental component. This is an improvement of 3% over the unfiltered model. Figure 20 shows the plot of the individual current harmonic distortion percentage versus time. All plots obtained from Matlab/Simulink for this simulation are located in Appendix D.

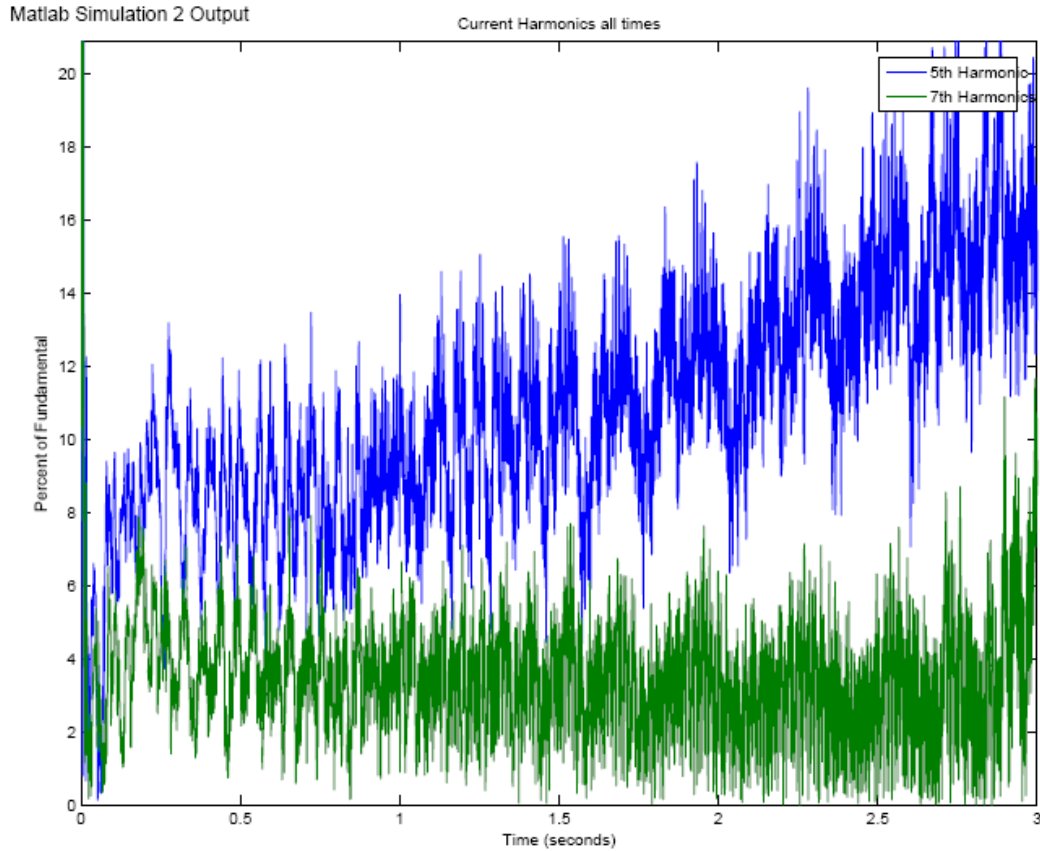


Figure 20: Simulation 2 Individual Current Harmonic Distortion

The improvement of the individual voltage harmonics were then analyzed. The 5th individual voltage harmonic distortion averaged 2% of the fundamental component. The 7th individual voltage harmonic distortion averaged 1% of the fundamental component. These two results showed a slight improvement over the un-filtered simulation. Figure 21 shows the plot of the individual voltage harmonic distortion percentage versus time.

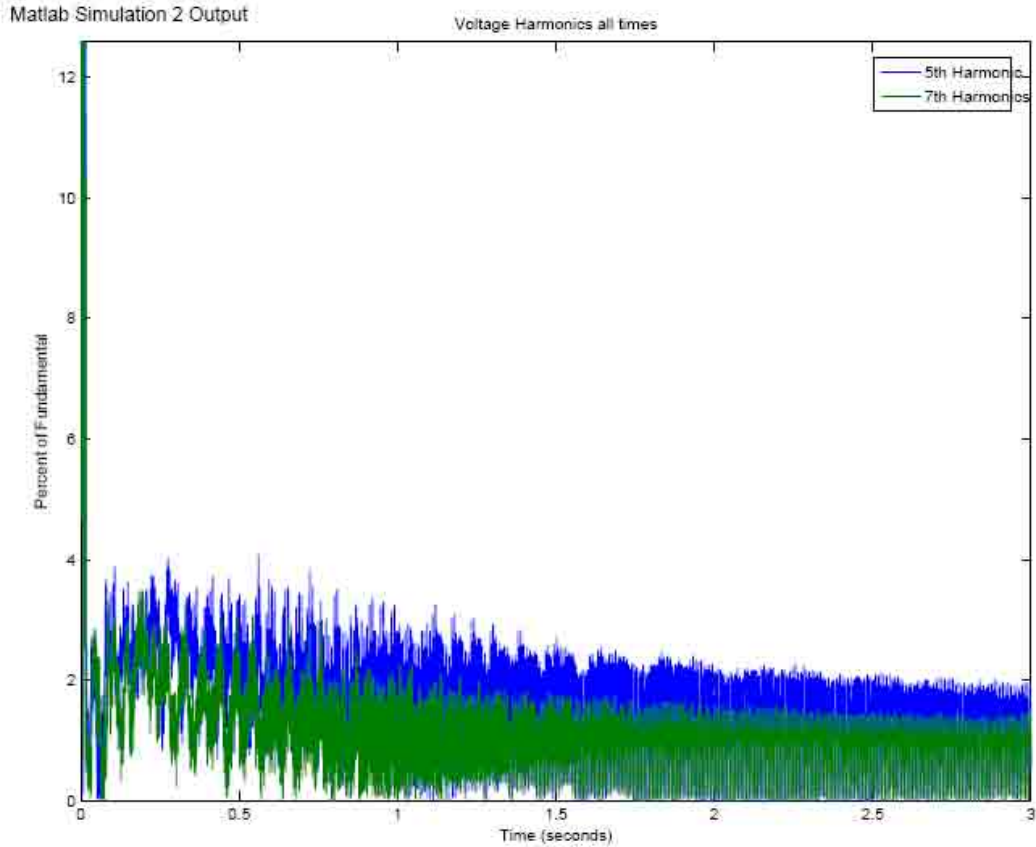


Figure 21: Simulation 2 Individual Voltage Harmonic Distortion

The FFT of the voltage and current waveforms were then analyzed and compared to the un-filtered results of simulation 1. The voltage THD was very near the requirement of 8% for all calculations. Figure 22 shows the plot and FFT analysis of the voltage waveform. Figure 23 shows the plot and FFT of the current waveform. The THD of this current waveform is 9%. On these two plots, numerous harmonics are shown that are above the individual harmonic maximum limit of 3%.

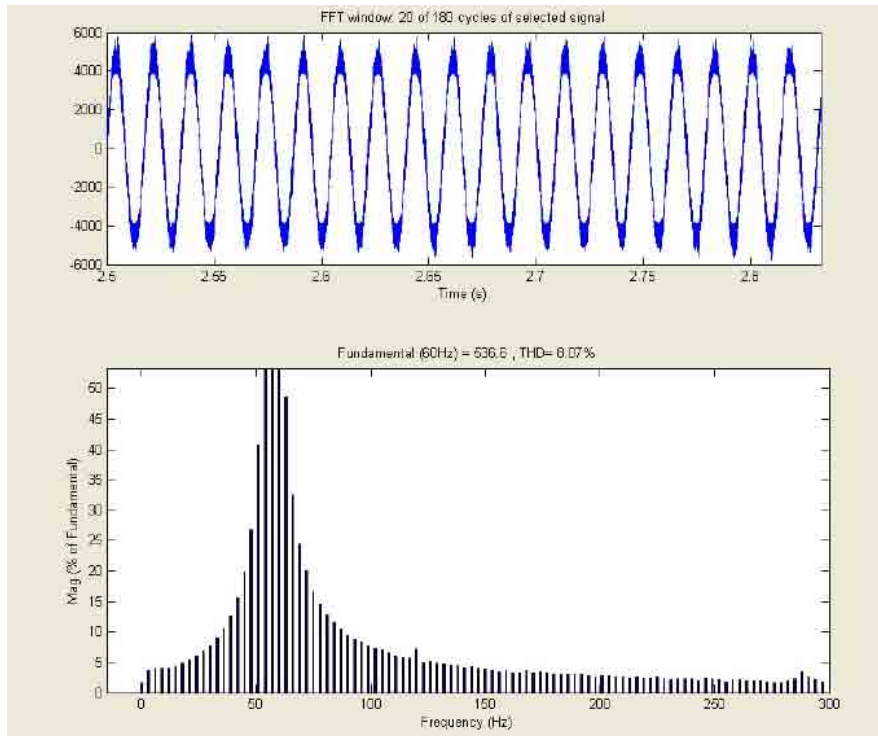


Figure 22: Simulation 2 Voltage Waveform and FFT

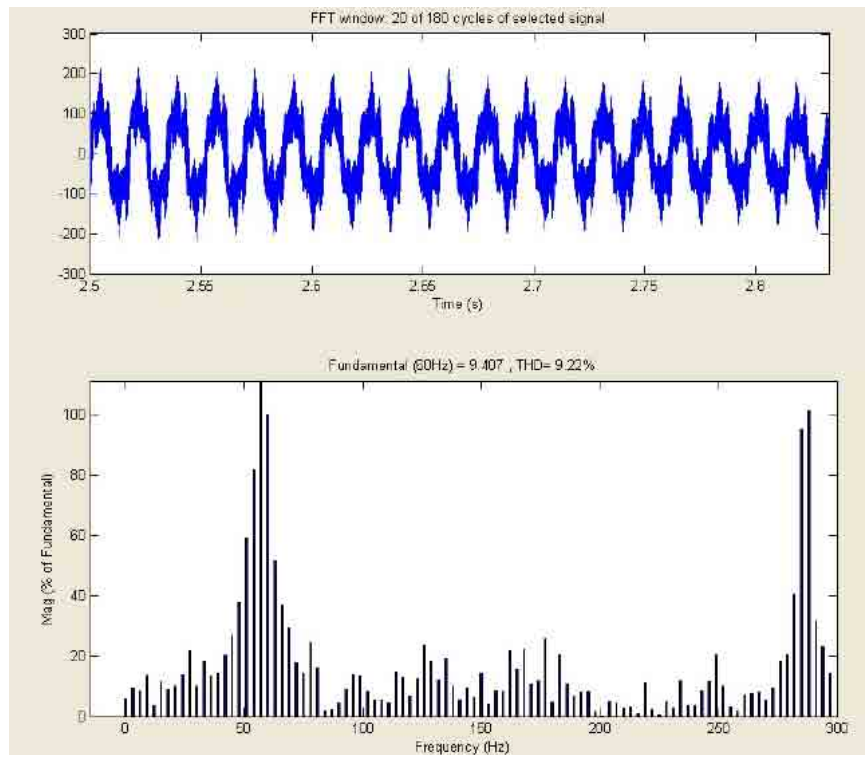


Figure 23: Simulation 2 Current Waveform and FFT

Simulation 3: Ideal Transient Unfiltered Results

The next simulation used the same unfiltered model of simulation 1. The simulation was conducted during a transient from low power steady state to a higher power level. The 5th individual current harmonic distortion averaged 20% of the fundamental component, slightly higher than the steady state results from simulation 1. The 7th individual current harmonic distortion averaged 6% of the fundamental component, the same level as simulation 1. Figure 24 shows the plot of the individual current harmonic distortion percentage versus time. This plot (and some future plots) has a different time range. This is due to allowing the model to come to steady state before initiating a transient on the system. All plots obtained from Matlab/Simulink for this simulation are located in Appendix E.

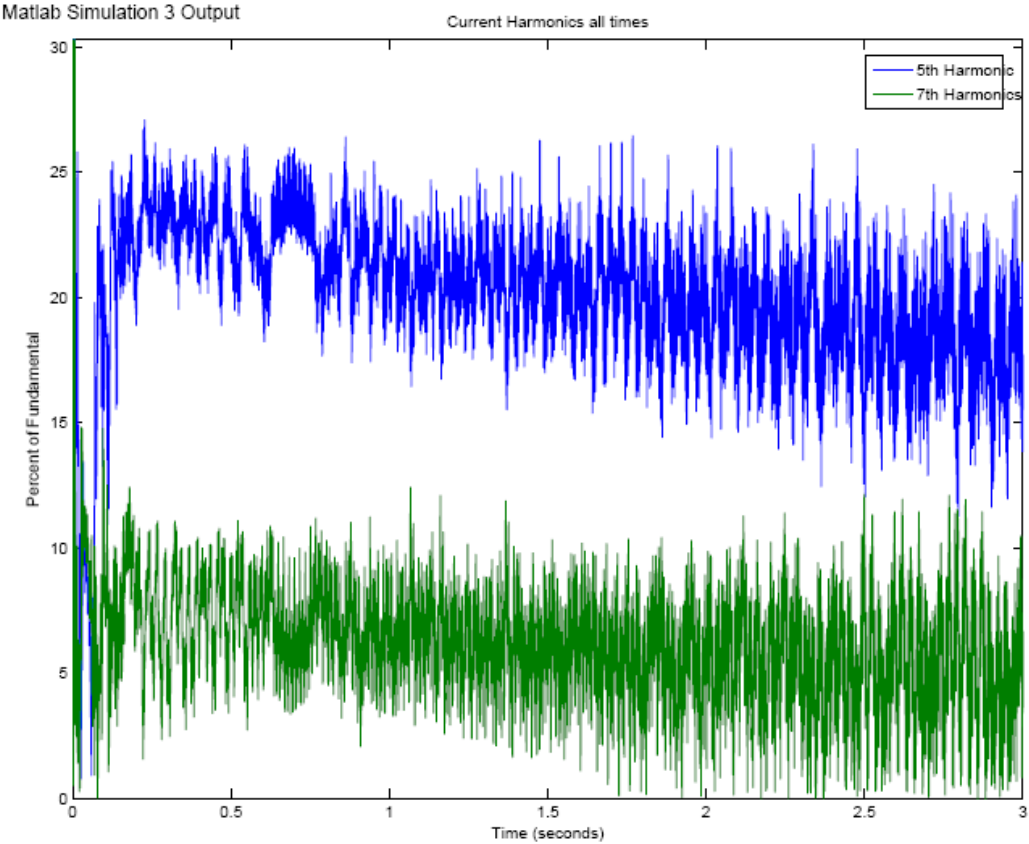


Figure 24: Simulation 3 Individual Current Harmonic Distortion

The individual voltage harmonic distortions were also compared to the results for simulation 1. The 5th individual voltage harmonic distortion averaged 4% of the fundamental component. The 7th individual voltage harmonic distortion averaged 2% of the fundamental component. These values were approximately the same as simulation 1. Figure 25 shows the plot of the individual voltage harmonic distortion percentage versus time.

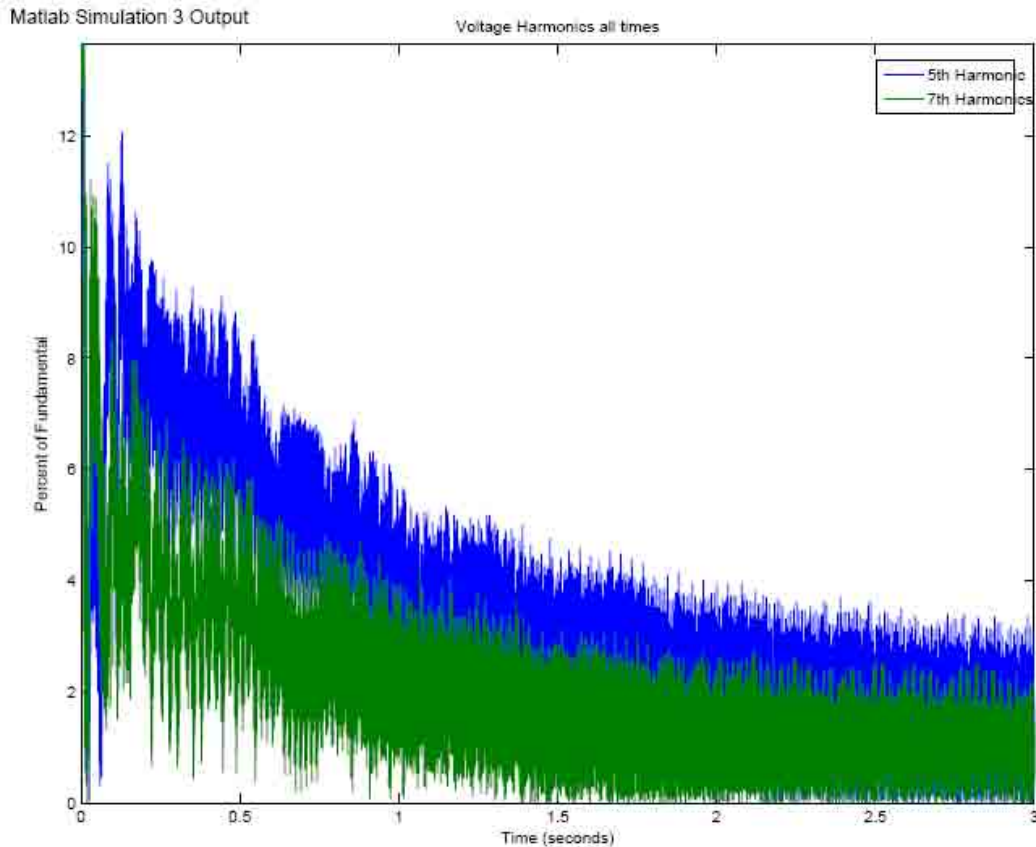


Figure 25: Simulation 3 Individual Voltage Harmonic Distortion

Next the voltage THD was compared to the steady state results. The voltage THD was less than 7%. Again, numerous individual voltage harmonics around the fundamental component were above the individual limit of 3%. Figure 26 shows the plot and FFT analysis of the voltage waveform.

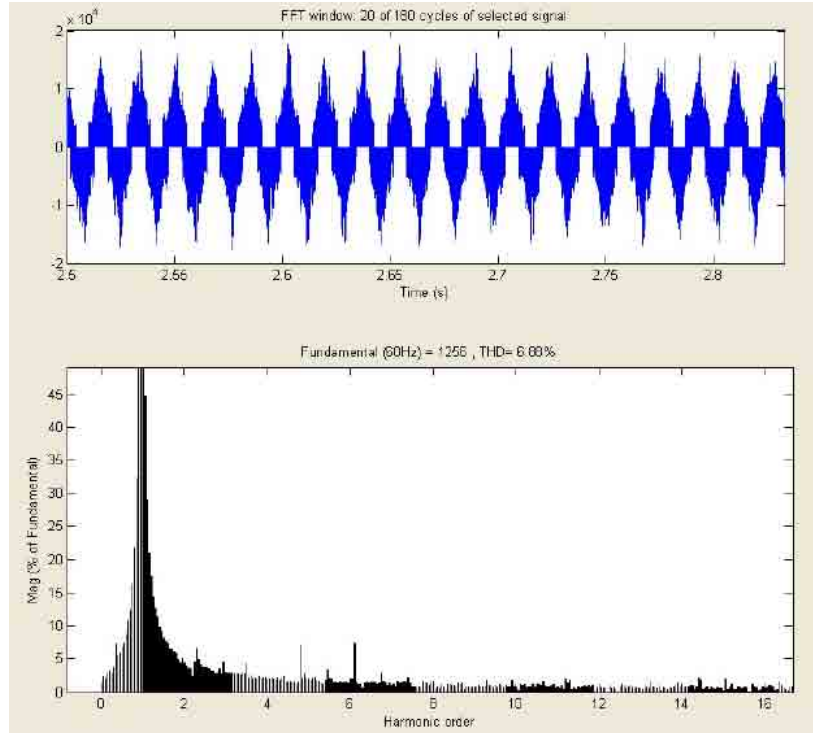


Figure 26: Simulation 3 Voltage Waveform and FFT

Simulation 4: Ideal Transient Filtered Results

For simulation 4, the same model was utilized with an input filter to the rectifier during a transient condition. The 5th individual current harmonic distortion averaged 4% of the fundamental component, 16% lower than the unfiltered transient response of simulation 3. The 7th individual current harmonic distortion averaged 2% of the fundamental component, 4% lower than the unfiltered transient response of simulation 3. Figure 24 shows the plot of the individual current harmonic distortion percentage versus time. All plots obtained from Matlab/Simulink for this simulation are located in Appendix F.

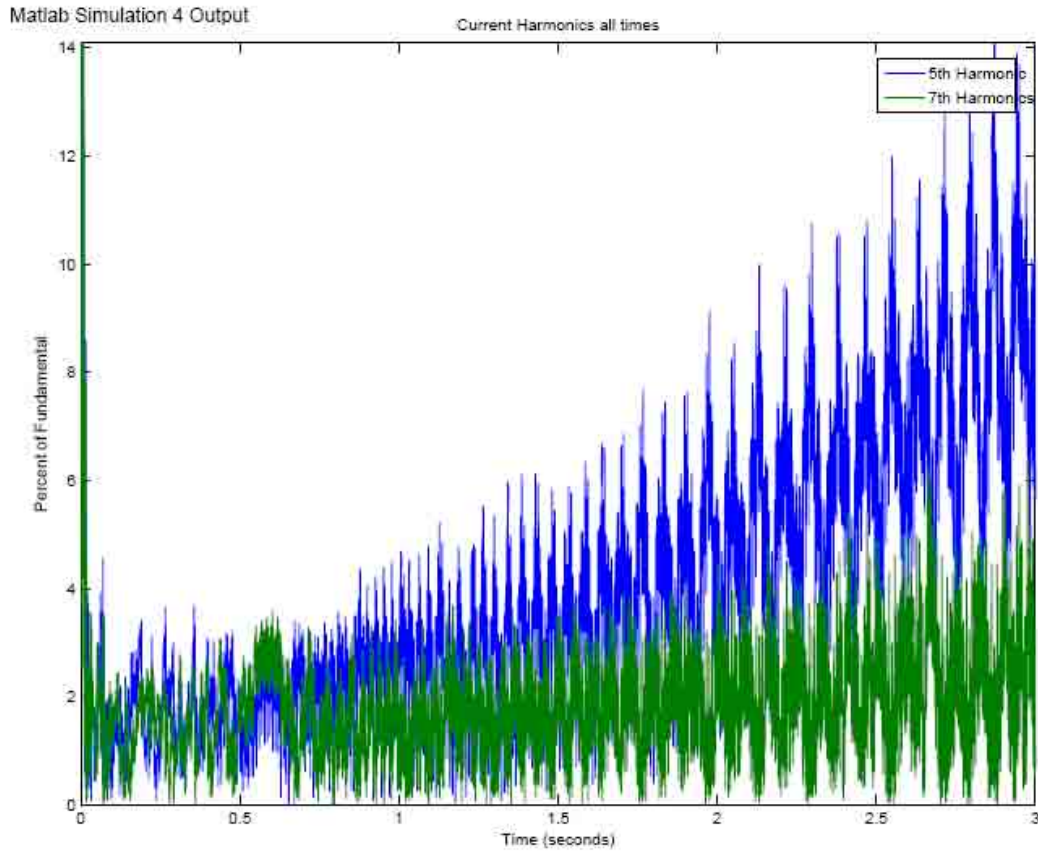


Figure 27: Simulation 4 Individual Current Harmonic Distortion

The 5th individual voltage harmonic distortion averaged 1% of the fundamental component. The 7th individual voltage harmonic distortion averaged <1% of the fundamental component. Figure 28 shows the plot of the individual voltage harmonic distortion percentage versus time.

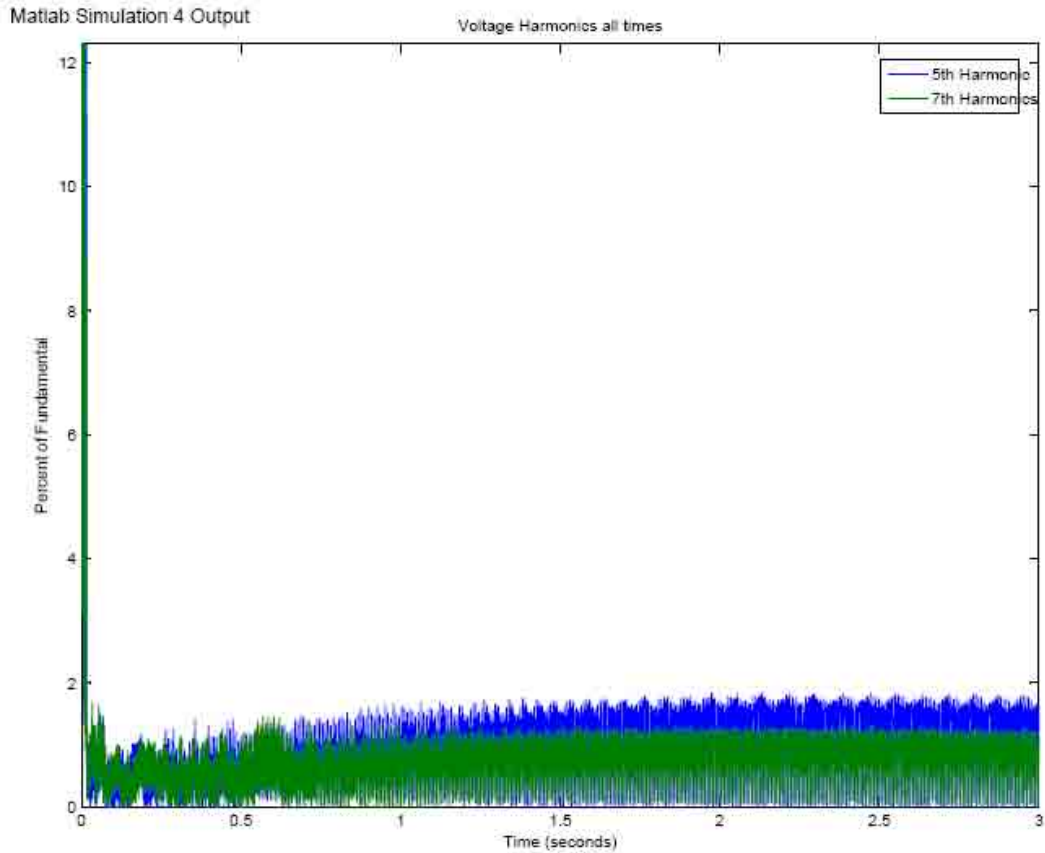


Figure 28: Simulation 4 Individual Voltage Harmonic Distortion

The voltage THD was less than 12%. Again, numerous individual voltage harmonics around the fundamental component were above the individual limit of 3%. Figure 26 shows the plot and FFT analysis of the voltage waveform.

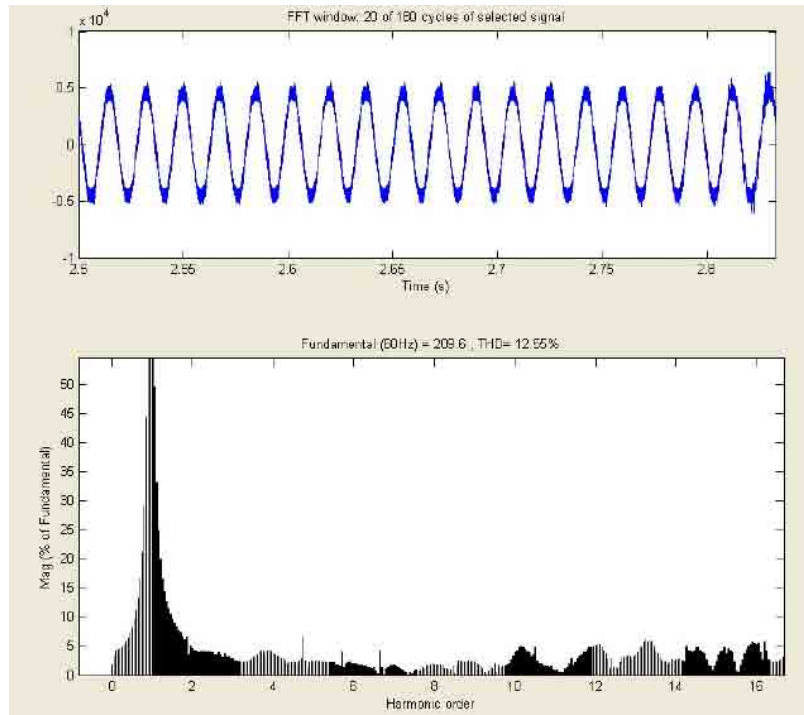


Figure 29: Simulation 4 Voltage Waveform and FFT

Recap of Simulations 1 – 4

The first four simulations utilized ideal switches in the rectifier and the inverter. This was completed in order to get results from a system with ideal switches operating at 10 kV. A summary of these results are shown in Table 3. As can be seen in Table 3, improvements to the individual current harmonic distortion were made with the input filter.

Simulation	Current Harmonic	Individual Current Harmonic Distortion	Voltage THD
1: Ideal Steady State Unfiltered	5 th	16%	8%
	7 th	7%	
2: Ideal Steady State Filtered	5 th	11%	8%
	7 th	4%	
3: Ideal Transient Unfiltered	5 th	20%	7%
	7 th	6%	
4: Ideal Transient Filtered	5 th	4%	12%
	7 th	2%	

Table 3: Recap of Simulations 1-4

Simulation 5: Simulated SiC Steady State Unfiltered Results

The following simulations were conducted with simulated SiC power electronic switches. The Simulink IGBT's were utilized to simulate a SiC device. Since the rise and fall times of SiC power devices are faster than silicon devices, the fall time of the simulated SiC device was adjusted in Simulink. The fall time was adjusted from the default value of 1 microsecond to 50 nanoseconds. Simulink does not allow the setting for rise time, therefore it was not adjusted.

The 5th individual current harmonic distortion averaged 33% of the fundamental component, with numerous points above 70%. The 7th individual current harmonic distortion averaged 13% of the fundamental component, with numerous points above 30%. Figure 30 shows the plot of the individual current harmonic distortion percentage versus time. The steady state values were taken from the plot between the time period of 1.5 seconds to 2 seconds. All plots obtained from Matlab/Simulink for this simulation are located in Appendix G.

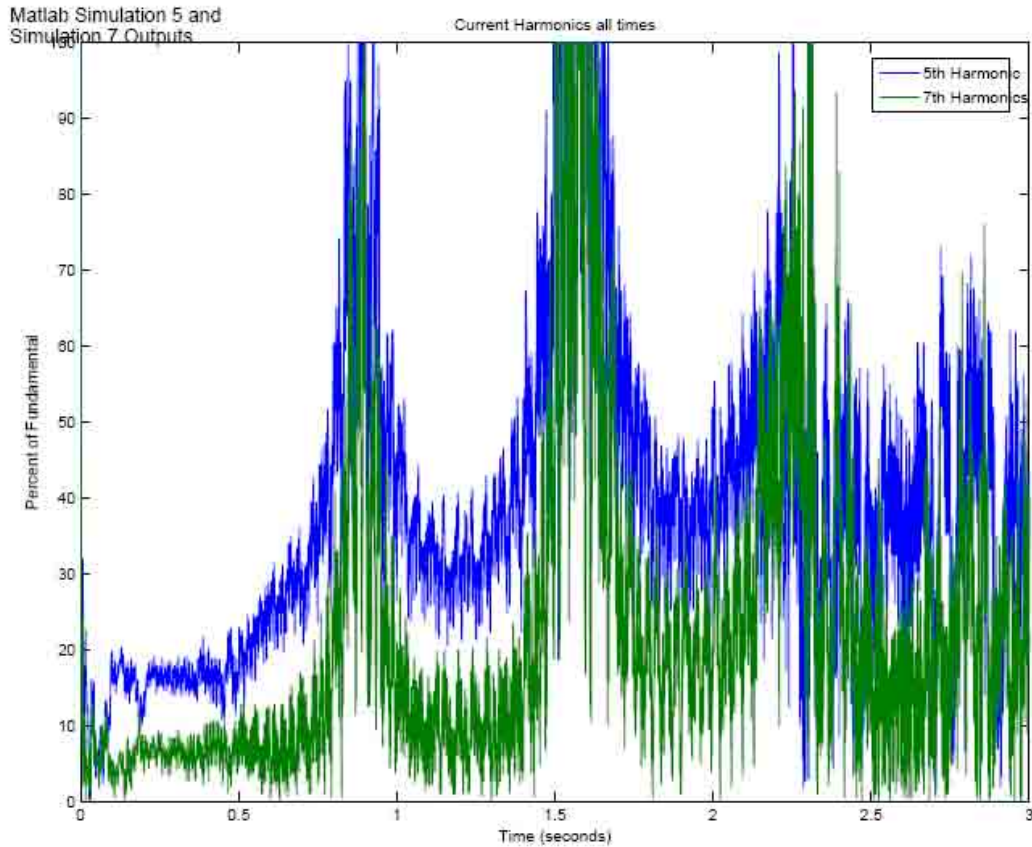


Figure 30: Simulation 5 Individual Current Harmonic Distortion

The 5th individual voltage harmonic distortion averaged 4% of the fundamental component. The 7th individual voltage harmonic distortion averaged 3% of the fundamental component. Figure 31 shows the plot of the individual voltage harmonic distortion percentage versus time. The steady state values were taken from the plot between the time period of 1.5 seconds to 2 seconds.

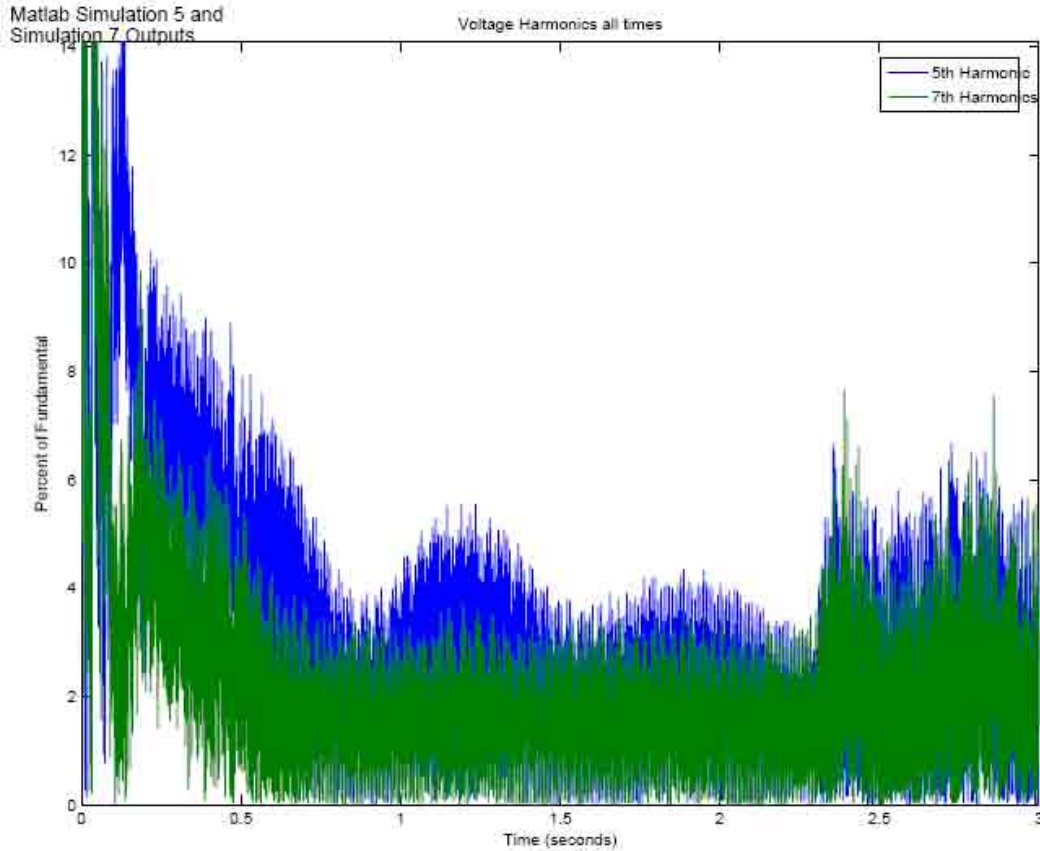


Figure 31: Simulation 5 Individual Voltage Harmonic Distortion

Next the FFT of the voltage and current waveforms were analyzed. The voltage THD was 5.7%. Figure 32 shows the plot and FFT analysis of the voltage waveform. Figure 33 shows the plot and FFT of the current waveform. The THD of this current waveform is 22%. On these two plots, numerous harmonics are shown that are above the individual harmonic maximum limit of 3%.

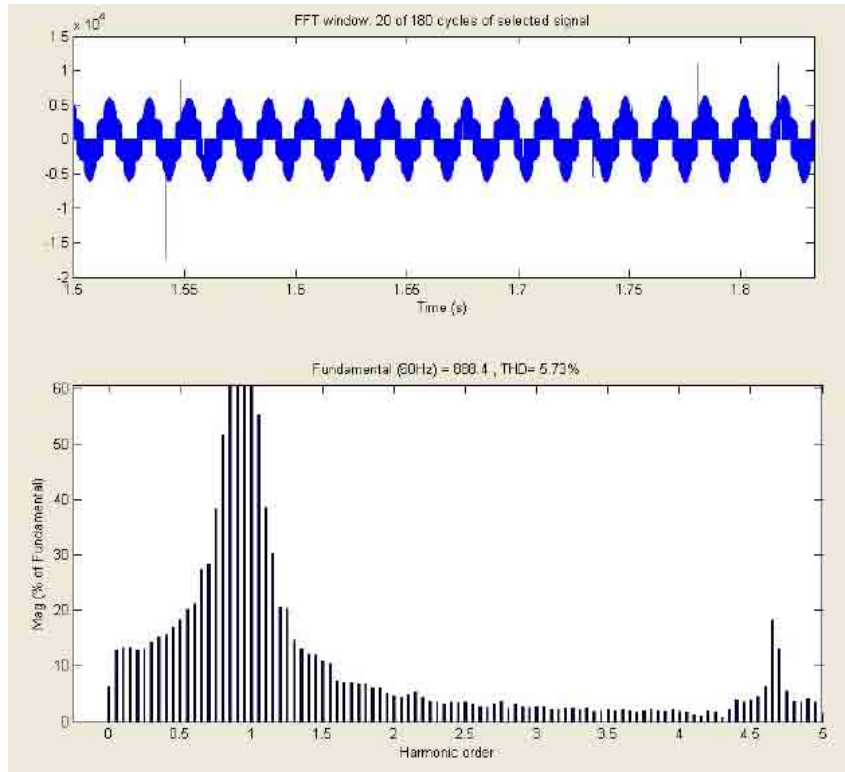


Figure 32: Simulation 5 Voltage Waveform and FFT

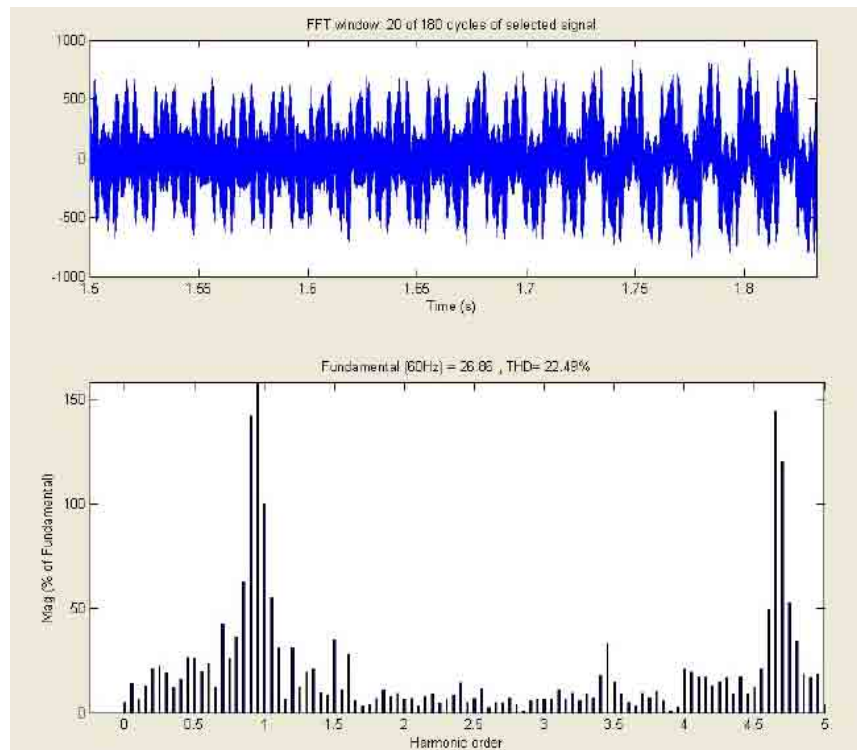


Figure 33: Simulation 5 Current Waveform and FFT

Simulation 6: Simulated SiC Steady State Filtered Results

The 5th individual current harmonic distortion averaged 23% of the fundamental component, with numerous points above 50%. The 7th individual current harmonic distortion averaged 17% of the fundamental component, with numerous points above 30%. Figure 34 shows the plot of the individual current harmonic distortion percentage versus time. The steady state values were taken from the plot between the time period of 1.5 seconds to 2 seconds. All plots obtained from Matlab/Simulink for this simulation are located in Appendix H.

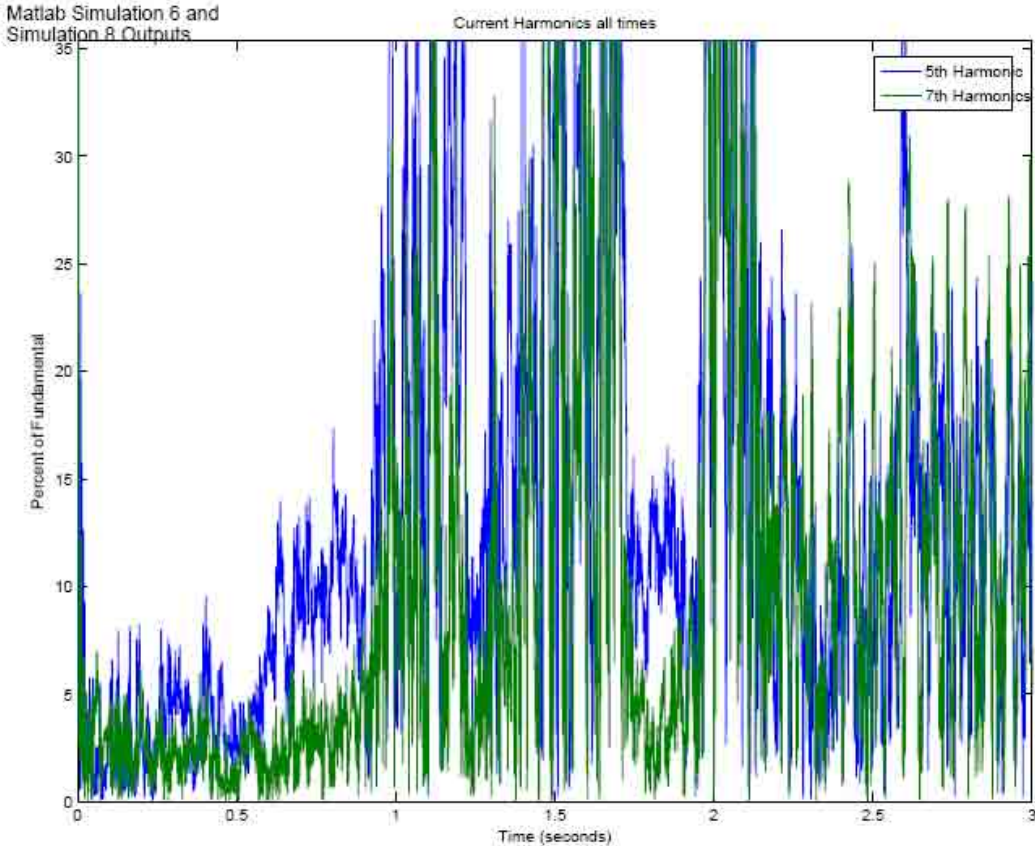


Figure 34: Simulation 6 Individual Current Harmonic Distortion

The 5th individual voltage harmonic distortion averaged 1% of the fundamental component. The 7th individual voltage harmonic distortion averaged <1% of the fundamental

component. Figure 35 shows the plot of the individual voltage harmonic distortion percentage versus time. The steady state values were taken from the plot between the time period of 1.5 seconds to 2 seconds.

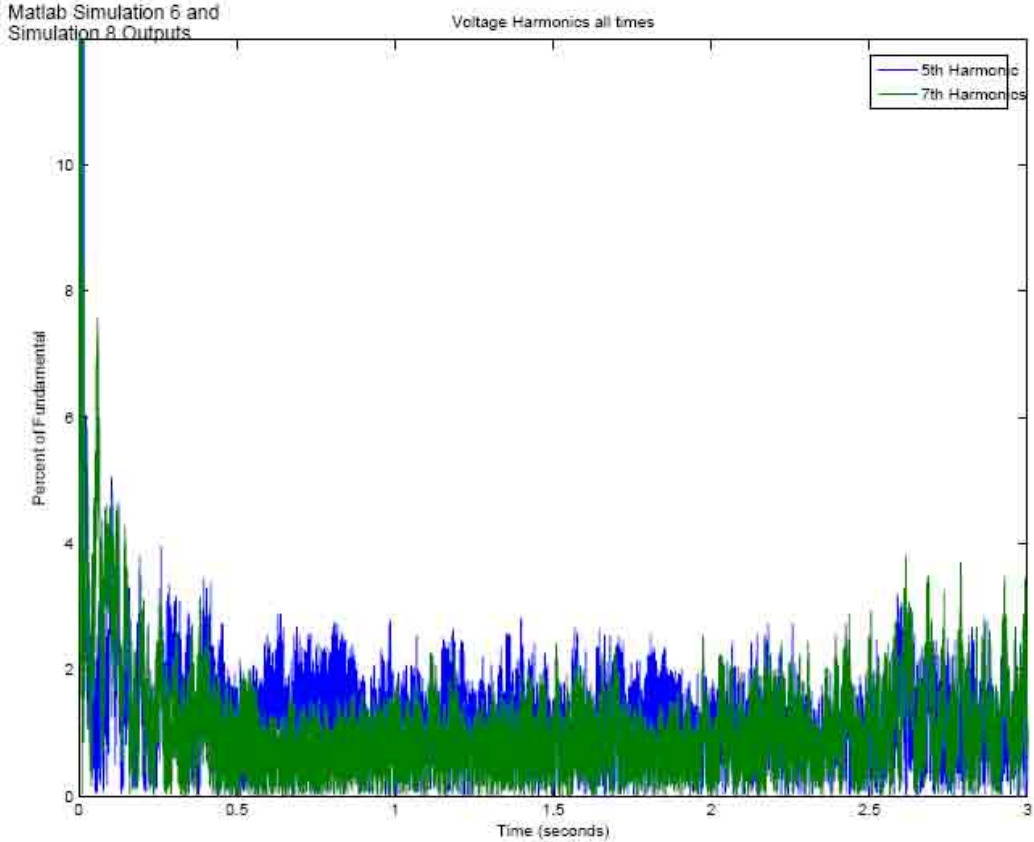


Figure 35: Simulation 6 Individual Voltage Harmonic Distortion

The FFT of the voltage and current waveforms were then analyzed. The voltage THD was 8.4%. Figure 36 shows the plot and FFT analysis of the voltage waveform. Figure 37 shows the plot and FFT of the current waveform. The THD of this current waveform is 7%. On these two plots, numerous harmonics are shown that are above the individual harmonic maximum limit of 3%.

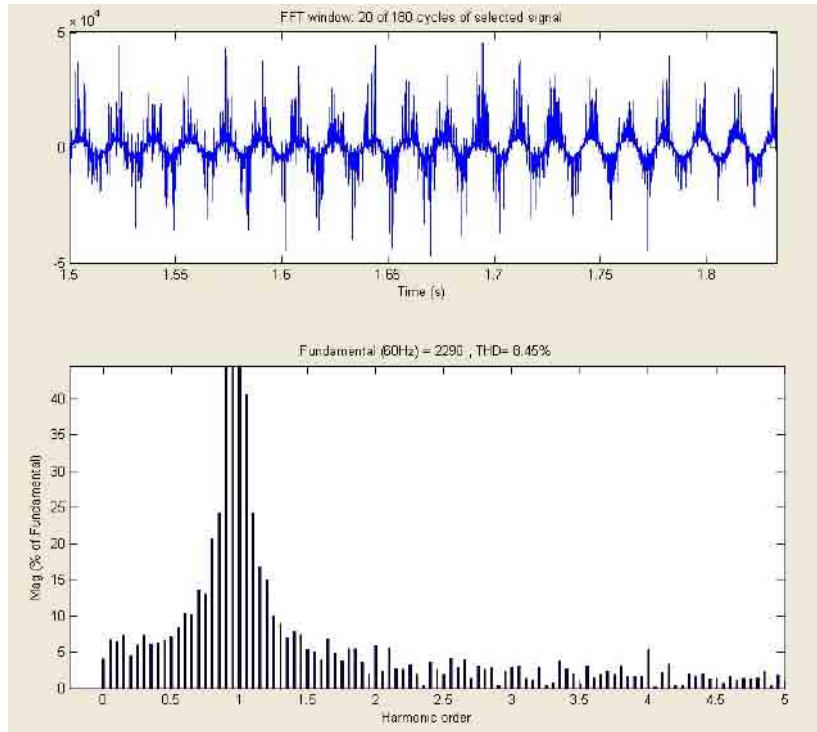


Figure 36: Simulation 6 Voltage Waveform and FFT

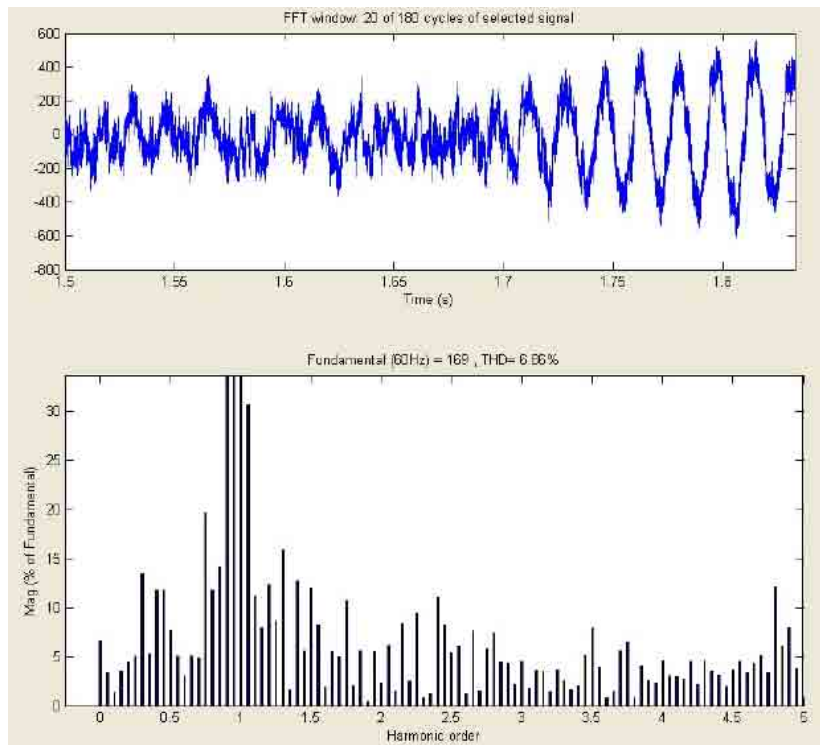


Figure 37: Simulation 6 Current Waveform and FFT

Simulation 7: Simulated SiC Transient Unfiltered Results

The 5th individual current harmonic distortion averaged 50% of the fundamental component, with numerous points above 70%. The 7th individual current harmonic distortion averaged 31% of the fundamental component, with numerous points above 30%. Figure 30 shows the plot of the individual current harmonic distortion percentage versus time. The transient values were taken from the plot between the time period of 2 seconds to 3 seconds. All plots obtained from Matlab/Simulink for this simulation are located in Appendix I.

The 5th individual voltage harmonic distortion averaged 3% of the fundamental component. The 7th individual voltage harmonic distortion averaged approximately 2% of the fundamental component. Figure 31 shows the plot of the individual voltage harmonic distortion percentage versus time. The transient values were taken from the plot between the time period of 2 seconds to 3 seconds.

Next the FFT of the voltage and current waveforms were analyzed. The voltage THD was 15%. Figure 40 shows the plot and FFT analysis of the voltage waveform. Figure 41 shows the plot and FFT of the current waveform. The THD of this current waveform is 106%. On these two plots, numerous harmonics are shown that are above the individual harmonic maximum limit of 3%.

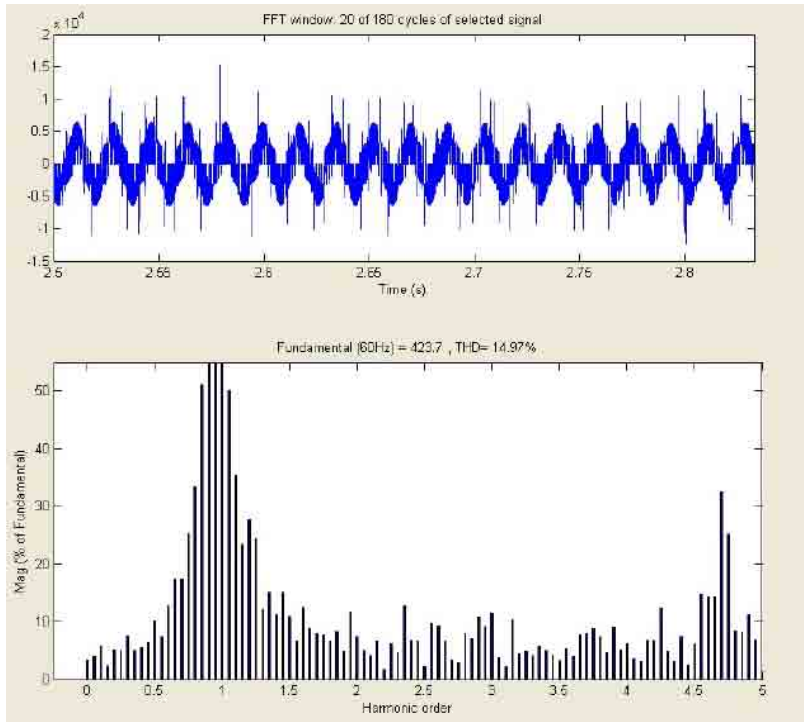


Figure 38: Simulation 7 Voltage Waveform and FFT

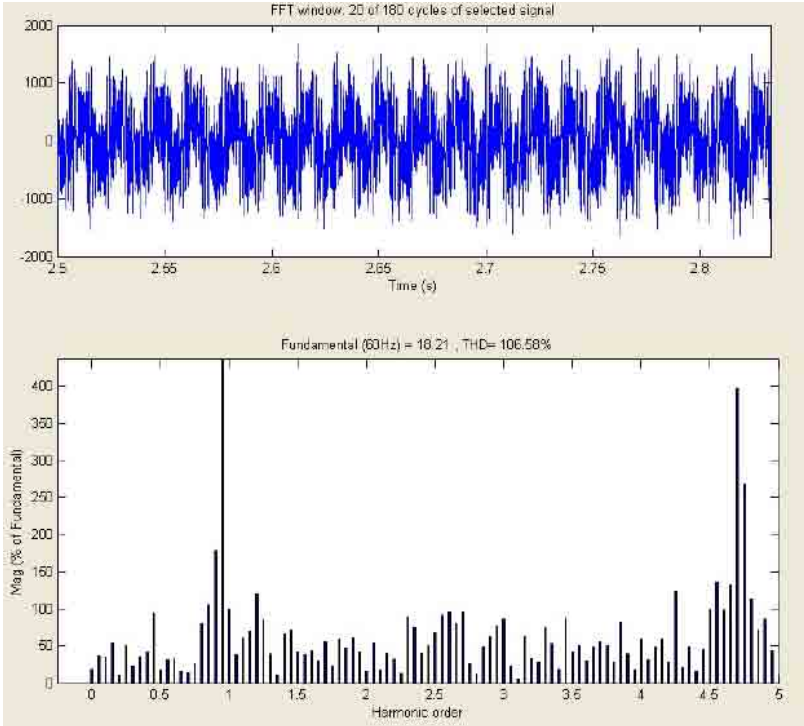


Figure 39: Simulation 7 Current Waveform and FFT

Simulation 8: Simulated SiC Transient Filtered Results

The 5th individual current harmonic distortion averaged 16% of the fundamental component. The 7th individual current harmonic distortion averaged 15% of the fundamental component. Figure 34 shows the plot of the individual current harmonic distortion percentage versus time. The transient values were taken from the plot between the time period of 2 seconds to 3 seconds. All plots obtained from Matlab/Simulink for this simulation are located in Appendix J.

The 5th individual voltage harmonic distortion averaged 1% of the fundamental component. The 7th individual voltage harmonic distortion averaged 1% of the fundamental component. Figure 35 shows the plot of the individual voltage harmonic distortion percentage versus time. The transient values were taken from the plot between the time period of 2 seconds to 3 seconds.

Next the FFT of the voltage and current waveforms were analyzed. The voltage THD was 4.3%. Figure 40 shows the plot and FFT analysis of the voltage waveform. Figure 41 shows the plot and FFT of the current waveform. The THD of this current waveform is 12%. On these two plots, numerous harmonics are shown that are above the individual harmonic maximum limit of 3%.

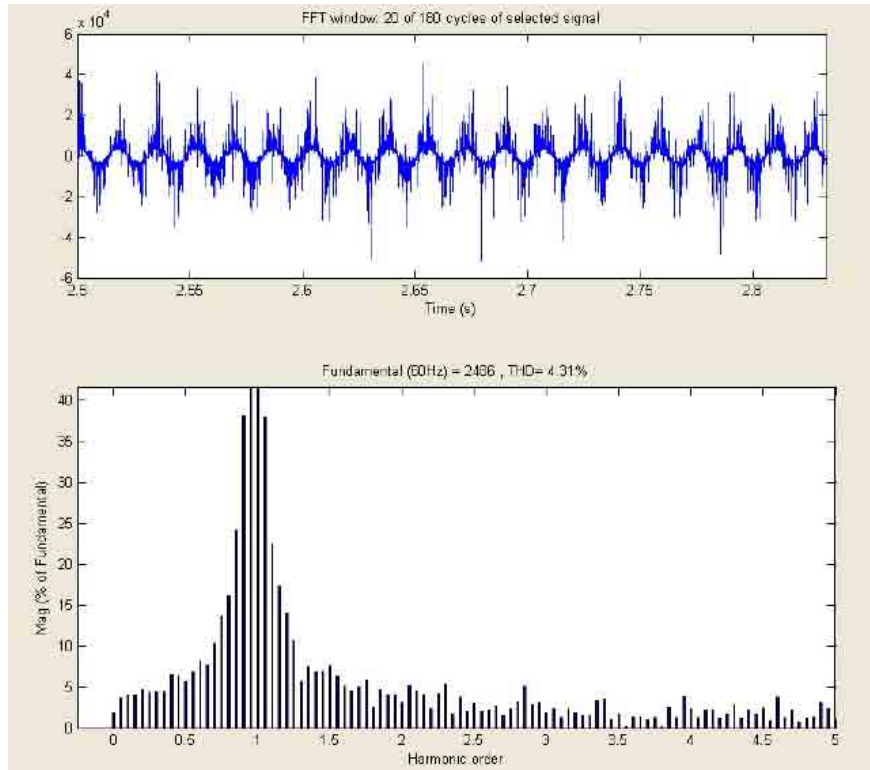


Figure 40: Simulation 8 Voltage Waveform and FFT

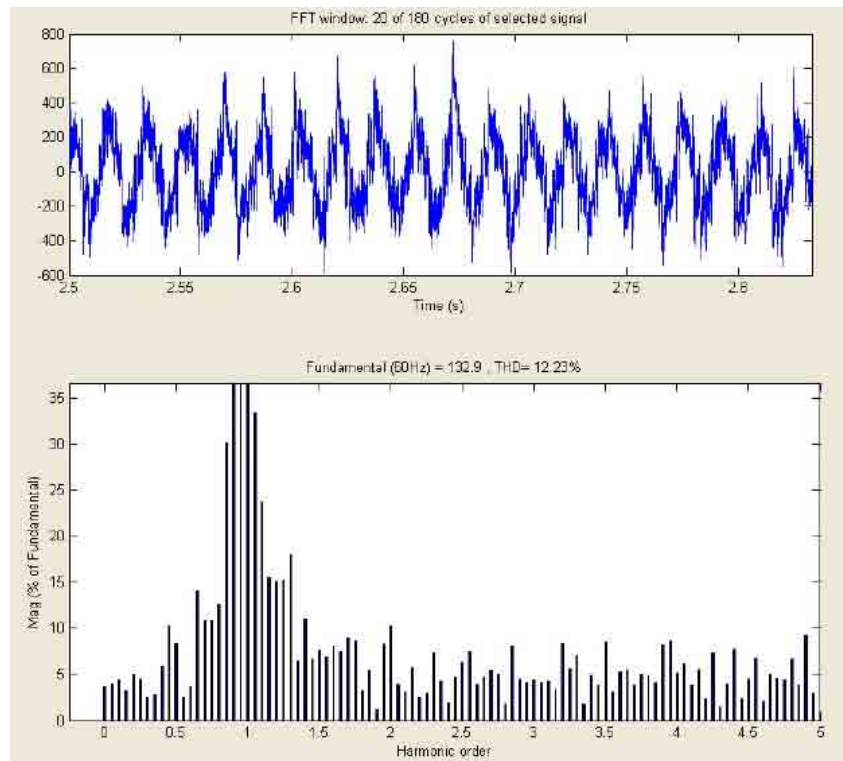


Figure 41: Simulation 8 Current Waveform and FFT

Recap of Simulations 5 – 8

The last four simulations utilized simulated SiC switches in the rectifier and the inverter. This was completed in order to get results from a system without ideal switches operating at 10 kV. A summary of these results are shown in Table 4. As can be seen in Table 4, the model with simulated SiC devices performed worse than the model with ideal switches. Although these simulations performed worse, the filter was effective at reducing the distortion in the voltage and current, albeit not improving the signal to within the harmonic distortion limits.

Simulation	Current Harmonic	Individual Current Harmonic Distortion	Voltage THD
5: SiC Steady State Unfiltered	5 th	33%	5.7%
	7 th	13%	
6: SiC Steady State Filtered	5 th	23%	8.4%
	7 th	17%	
7: SiC Transient Unfiltered	5 th	50%	15%
	7 th	31%	
8: SiC Transient Filtered	5 th	16%	4.3%
	7 th	15%	

Table 4: Recap of Simulations 5-8

Simulation 9: Simulated SiC Steady State and Transient Filtered Results

Simulation 9 was conducted as a kind of validation for some of the earlier results. The precision of the preceding simulations hinged on the value of the time step of the Simulink simulation. All of the previous simulations were set at 1 microsecond. The smaller the time step, the more accurate the results will be. Although the most accurate would be a continuous run, it was not possible. For simulation 9, the time step was reduced to 0.1 microseconds. This simulation took 20 hours on a standard laptop. In order to obtain approximately the same amount of data as the previous simulations, a decimation factor of 10 (only saves 1 of every 10 points) was utilized. This was to prevent the computer from running out of memory. The

computer did run out of memory, but this occurred at 2.8 seconds, therefore enough data was obtained to perform some analysis.

Simulation 9 was conducted with the same model as simulations 6 and 8 (Table 4) with the only exception being the time step. The results are shown in Table 5. These results show that simulation 9 was very close to the results from simulations 6 and 8. Therefore, the precision utilized in simulations 1 through 8 should not deviate too much from simulations with a more precise time step. Figure 42 shows the plot of the individual current harmonic distortion percentage versus time. Figure 43 shows the plot of the individual voltage harmonic distortion percentage versus time. Figure 44 shows the plot and FFT analysis of the voltage waveform. All plots obtained from Matlab/Simulink for this simulation are located in Appendix K.

Simulation	Current Harmonic	Individual Current Harmonic Distortion	Voltage THD
9: SiC Steady State Filtered	5 th	15%	3.4%
	7 th	12%	
9: SiC Transient Filtered	5 th	12%	4.0%
	7 th	10%	

Table 5: Simulation 9 Results

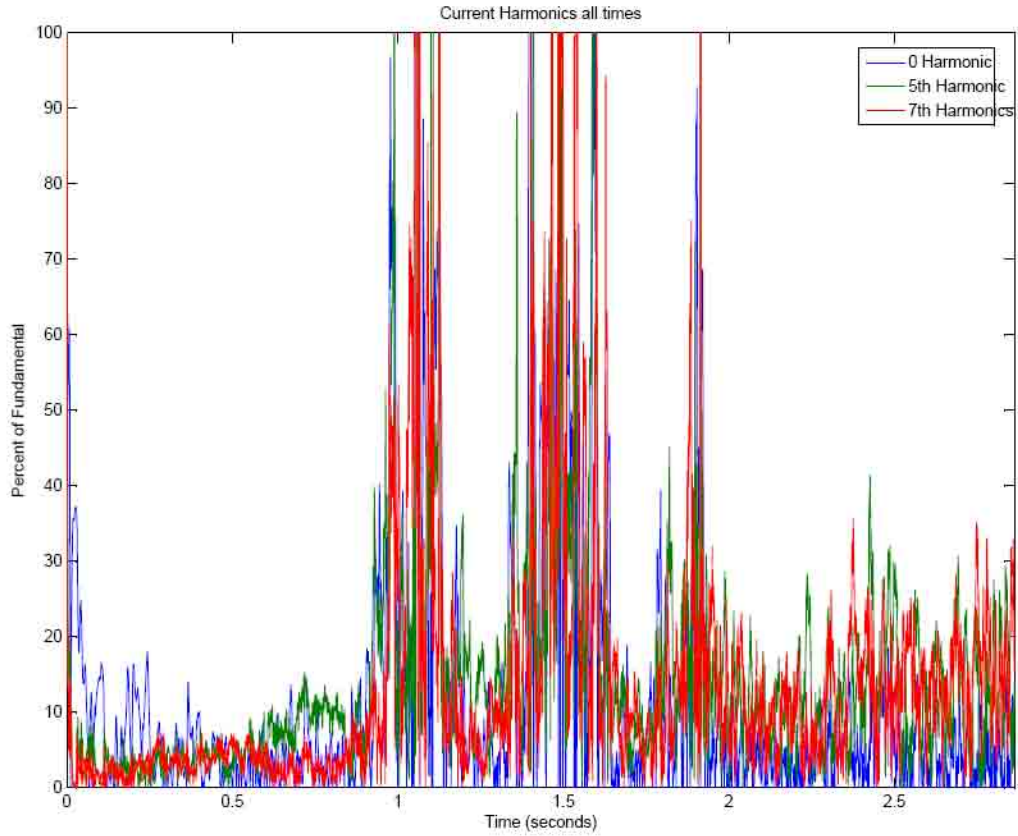


Figure 42: Simulation 9 Individual Current Harmonic Distortion

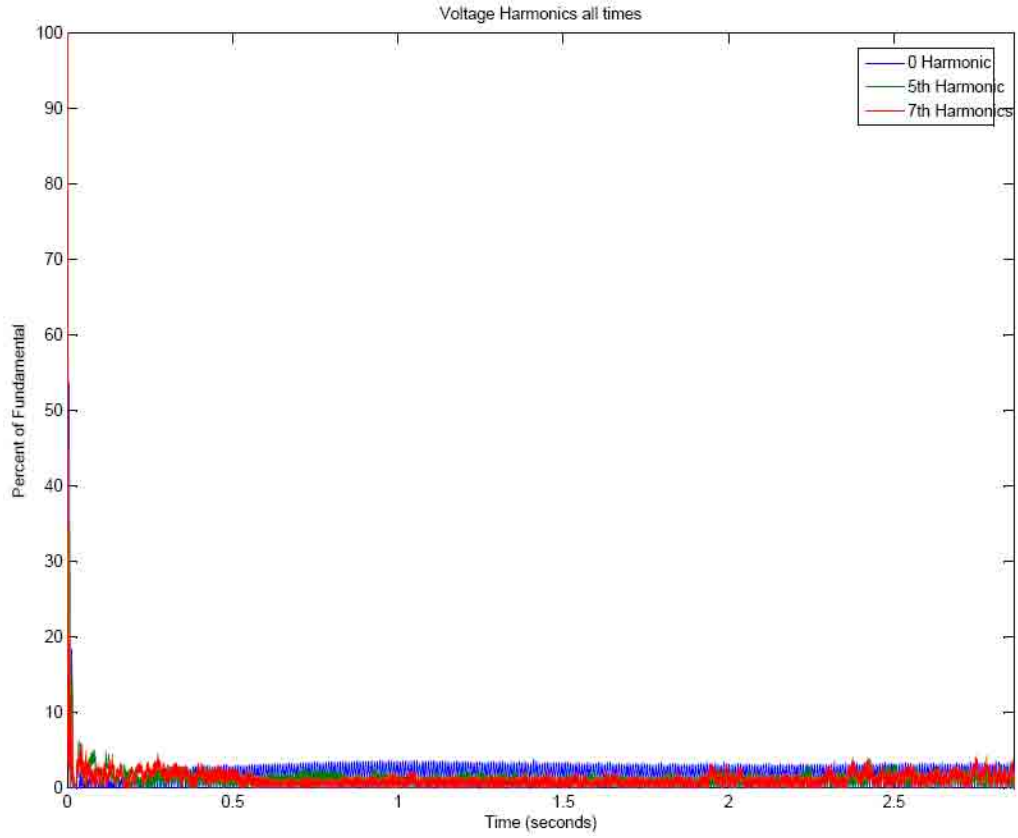


Figure 43: Simulation 9 Individual Voltage Harmonic Distortion

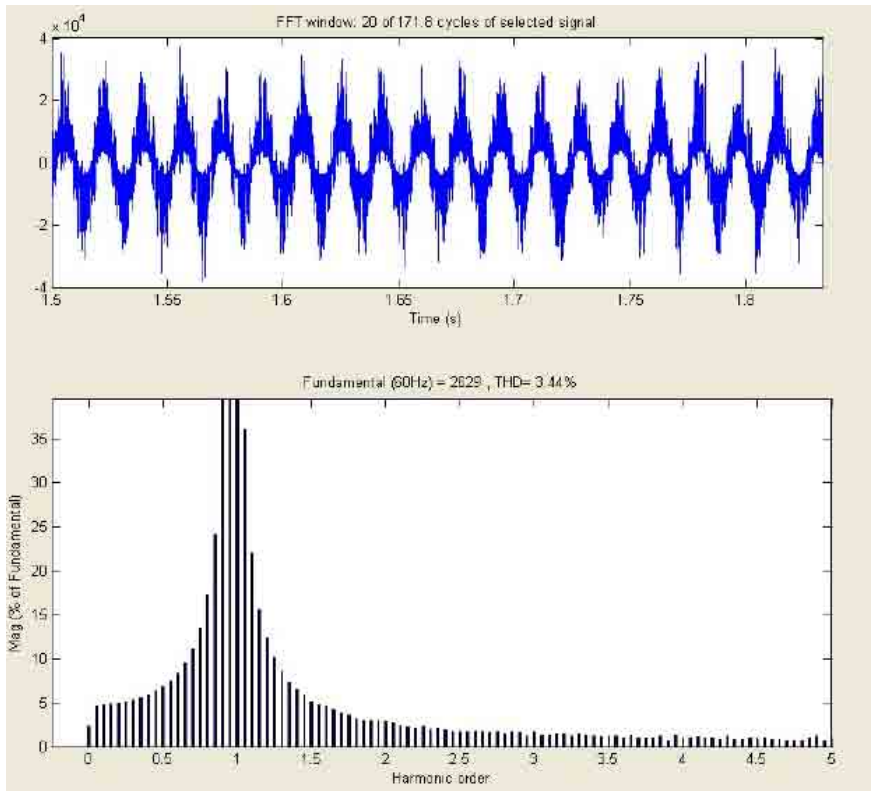


Figure 44: Simulation 9 Voltage Waveform and FFT

Page Intentionally Left Blank

CHAPTER 6: CONCLUSIONS AND FUTURE WORK

As the U. S. Navy continues toward ships with IPS systems installed, the requirement for more power dense ships will continue to increase. The requirement to maintain the lowest possible distortion necessary will require that systems have harmonic mitigation systems installed in order to prevent distortion from impacting the ship's systems negatively. When SiC power electronic technology becomes available for use in high power applications, the need for high power mitigation techniques will also grow.

Model Testing

The need for accurate model testing is required to accurately simulate these high power systems prior to large scale developmental testing. The results herein have shown that more accurate models of SiC power electronic devices need to be developed for use in simulation programs. This research used ideal switches and modified silicon IGBT's in order to evaluate the impact of SiC on an IPS system. The difference between the ideal and IGBT system performance in harmonic distortion was significant. Also, the IGBT model was a simple approximation of a SiC IGBT, therefore if a reliable model of a SiC IGBT was available, the results may have been more accurate. The use of Simulink in this model was a very slow process. Most simulation runs lasting upwards of three hours, with a more accurate simulation requiring 20 hours. Other software programs designed specifically for power systems analysis may allow for more simulations to be completed in a more expeditious manner.

Mitigation Techniques

Even though this analysis examined only one very simple method of reducing the voltage total harmonic distortion and the individual current harmonics, it was successful in reducing these harmonic distortions. Although it was successful, the amount of distortion when utilizing a

simulated SiC device was very large. New mitigation techniques may have to be developed in order to handle distortion at this power level and within the requirements for use onboard U. S. Navy ships. Since these systems deliver power to very sensitive equipment, even though they may be fairly well insulated from the main power bus, the effects of large distortion on the supply bus may impact these sensitive systems.

Future Work

More complex, accurate, and dynamic simulations need to be pursued in order to fully understand the impact of operating SiC power devices at voltages upward of 10 kV DC. In addition to this testing, more advanced mitigation techniques may be required in order to reduce the distortion in order to prevent disruptions to vital shipboard systems.

Although this research only analyzed the impact of SiC devices on the distortion of the main supply bus, the impact on the downstream loads also needs to be taken into account. For example, the effects of utilizing SiC devices on the insulation of the propulsion motor need to be investigated in order to insure that the propulsion motor will not be damaged due to the transients of the rectifier and inverter.

Conclusions

The importance of SiC power electronic devices compared to silicon can be shown for a power converter introduced in chapter 4 (Figure 13). This silicon-based power converter requires 512 silicon IGBT's for each H-bridge in order to meet the blocking voltage and current carrying capacity. If SiC power electronic devices continue to advance, this silicon H-bridge would be able to be replaced with 4 SiC devices. Therefore, for a 15 phase motor converter (Figure 13), 60 SiC IGBT's would be able to replace 7,680 silicon IGBT's.

Although it is a relatively new technology, silicon carbide power electronic components may be able to replace standard silicon power electronic components in the near future. If this comes to fruition, then high voltage DC buses at or above 10 kV will become possible onboard U. S. Navy ships. This may allow for the removal of transformers onboard ship, which will result in a large savings with respect to weight and volume. The ability to transform high voltage AC power directly to high voltage DC power for use with the propulsion system will have numerous advantages for the U. S. Navy ships of the future.

Page Intentionally Left Blank

REFERENCE LIST

- [1] J. M. Prousalidis, I K Hatzilau, S Perros, "Harmonic Electric Power Quality Concepts for the Electrified Ships", Proceedings of All Electric Ship (AES 2003), pp. 279-290, Edinburg (2003)
- [2] Fas.org, <http://www.fas.org/main/home.jsp>
- [3] Commander Timothy J. McCoy, "Class Notes: Electrical Systems Lecture", Course 2.703 Principles of Naval Ship Design, Massachusetts Institute of Technology, Department of Mechanical Engineering, Fall 2005
- [4] Captain Norbert Doerry, Electric Warship Design I, PowerPoint presentation, August 3, 2005.
- [5] Henry Hegner, Bipin Desai, "Integrated Fight Through Power", IEEE Power Engineering Society Summer Meeting, 2002
- [6] Captain Norbert Doerry, Electric Warship Design II, PowerPoint presentation, August 3, 2005.
- [7] R.C. Smith, L. T. Dunnington, G.F.Grater, "Future Shipboard Power System Architecture Analysis Interim Report, Shipboard Electrical Distribution Characteristics," Anteon Corporation, MSD-50-TR-2001/13 December 2001.
- [8] Anant Agarwal, Mrinal Das, Sumithra Krishnaswami, John Palmour, James Richmond, and Sei-Hyung Ryu, SiC Power Devices – An Overview, Materials Research Society Symposium Proceedings Volume 815, 2004.
- [9] Friedrichs, P., SiC Power Devices – Recent and upcoming developments, IEEE International Symposium on Industrial Electronics, Volume 2, July 2006, Pages 993 - 997
- [10] A. Hefner, Sei-Hyung Ryu, B. Hull, D. Berning, C. Hood, J.M. Ortiz-Rodriguez, A. Rivera-Lopez, Tam Duong, A. Akuffo, M. Hernandez-Mora, Recent advances in high-voltage, high frequency silicon carbide power devices, The 2006 IEEE Industry Applications Conference, Forty-First IAS Annual Meeting, Volume 1, October 2006
- [11] P. Friedrichs, Unipolar SiC Devices – Latest Achievements on the way to a new generation of high voltage power semiconductors, Power Electronics and Motion Control Conference, CES/IEEE 5th International, Volume 1, August 2006
- [12] Anant Agarwal and Sei-Hyung Ryu, Status of SiC Power Devices and Manufacturing Issues, CS MANTECH Conference, April 24-27, 2006

- [13] Brett A. Hulla, Mrinal K. Dasa, James T. Richmond, Joseph J. Sumakerisa, Robert Leonard, John W. Palmoura, and Scoff Leslieb, A 180 Amp/4.5 kV 411-SiC PiN Diode for High Current Power Modules, Proceedings of the 18th International Symposium on Power Semiconductor Devices & IC's June 4-8, 2006 Naples, Italy
- [14] Deputy Under Secretary of Defense for Science and Technology, Technology Readiness Assessment (TRA) Deskbook, May 2005
- [15] <http://www.ecn.purdue.edu/WBG/Introduction/>, Purdue University's Wide Band Gap Semiconductor Device Research Program
- [16] Mathworks, Matlab and Simulink, version R14.
- [17] K. A. Corzine, S. D. Sudhoff, E. A. Lewis, D. H. Schmucher, R. A. Youngs, and H. J. Hegner, Use of Multi-level Converters in Ship Propulsion Drives, All Electric Ship Conference, 1998
- [18] James L. Kirtley Jr, "Class Notes," Course 6.685 Electric Machines, Massachusetts Institute of Technology, Department of Electrical Engineering and Computer Science, Fall 2005
- [19] A.E. Fitzgerald, C. Kingsley Jr., S.D. Umans, Electric Machinery, McGraw Hill Inc., New York, 1990.
- [20] J. G. Kassakian, M. F. Schlecht, G.C. Verghese, Principles of Power Electronics, Addison-Wesley Publishing Company, Reading, MA, 1991
- [21] Thomas L. Floyd, Electronic Devices, Merrill Publishing Company, Columbus, OH, 1988.
- [22] SimPowerSystems 4 for Matlab / Simulink, The Mathworks Company, 2007.
- [23] Military Standard 1399 Section 300A, Interface Standards for Shipboard Systems, Electric Power and Alternating Current, 13 October, 1987.
- [24] IEEE Recommended Practices and Requirements for Harmonic Control in Electrical Power Systems, IEEE STD 519-1992, IEEE, 1992
- [25] IEEE Recommended Practice for Electrical Installations on Shipboard, IEEE STD 45-2002, IEEE, 2002
- [26] Edward G. West, Analysis of Harmonic Distortion in an Integrated Power System for Naval Applications, Master's Thesis, Departments of Ocean and Electrical Engineering, Massachusetts Institute of Technology, 2005

APPENDICES

APPENDIX A: HARDWARE TRL DEFINITIONS [14]

Table 3-1. Hardware TRL Definitions, Descriptions, and Supporting Information
(Source: *Defense Acquisition Guidebook*)

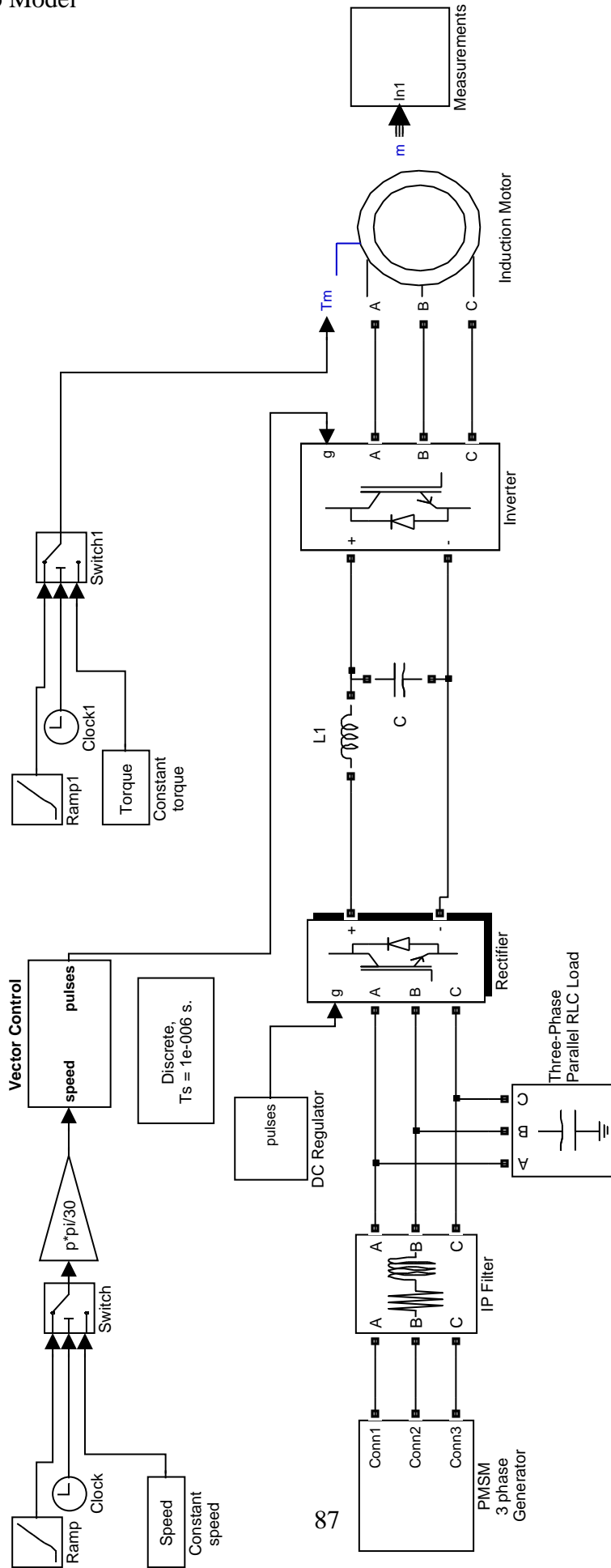
TRL	Definition	Description	Supporting Information
1	Basic principles observed and reported.	Lowest level of technology readiness. Scientific research begins to be translated into applied research and development (R&D). Examples might include paper studies of a technology's basic properties.	Published research that identifies the principles that underlie this technology. References to who, where, when.
2	Technology concept and/or application formulated.	Invention begins. Once basic principles are observed, practical applications can be invented. Applications are speculative, and there may be no proof or detailed analysis to support the assumptions. Examples are limited to analytic studies.	Publications or other references that outline the application being considered and that provide analysis to support the concept.
3	Analytical and experimental critical function and/or characteristic proof of concept.	Active R&D is initiated. This includes analytical studies and laboratory studies to physically validate the analytical predictions of separate elements of the technology. Examples include components that are not yet integrated or representative.	Results of laboratory tests performed to measure parameters of interest and comparison to analytical predictions for critical subsystems. References to who, where, and when these tests and comparisons were performed.
4	Component and/or breadboard validation in a laboratory environment.	Basic technological components are integrated to establish that they will work together. This is relatively "low fidelity" compared with the eventual system. Examples include integration of "ad hoc" hardware in the laboratory.	System concepts that have been considered and results from testing laboratory-scale breadboard(s). References to who did this work and when. Provide an estimate of how breadboard hardware and test results differ from the expected system goals.
5	Component and/or breadboard validation in a relevant environment.	Fidelity of breadboard technology increases significantly. The basic technological components are integrated with reasonably realistic supporting elements so they can be tested in a simulated environment. Examples include "high-fidelity" laboratory integration of components.	Results from testing a laboratory breadboard system are integrated with other supporting elements in a simulated operational environment. How does the "relevant environment" differ from the expected operational environment? How do the test results compare with expectations? What problems, if any, were encountered? Was the breadboard system refined to more nearly match the expected system goals?

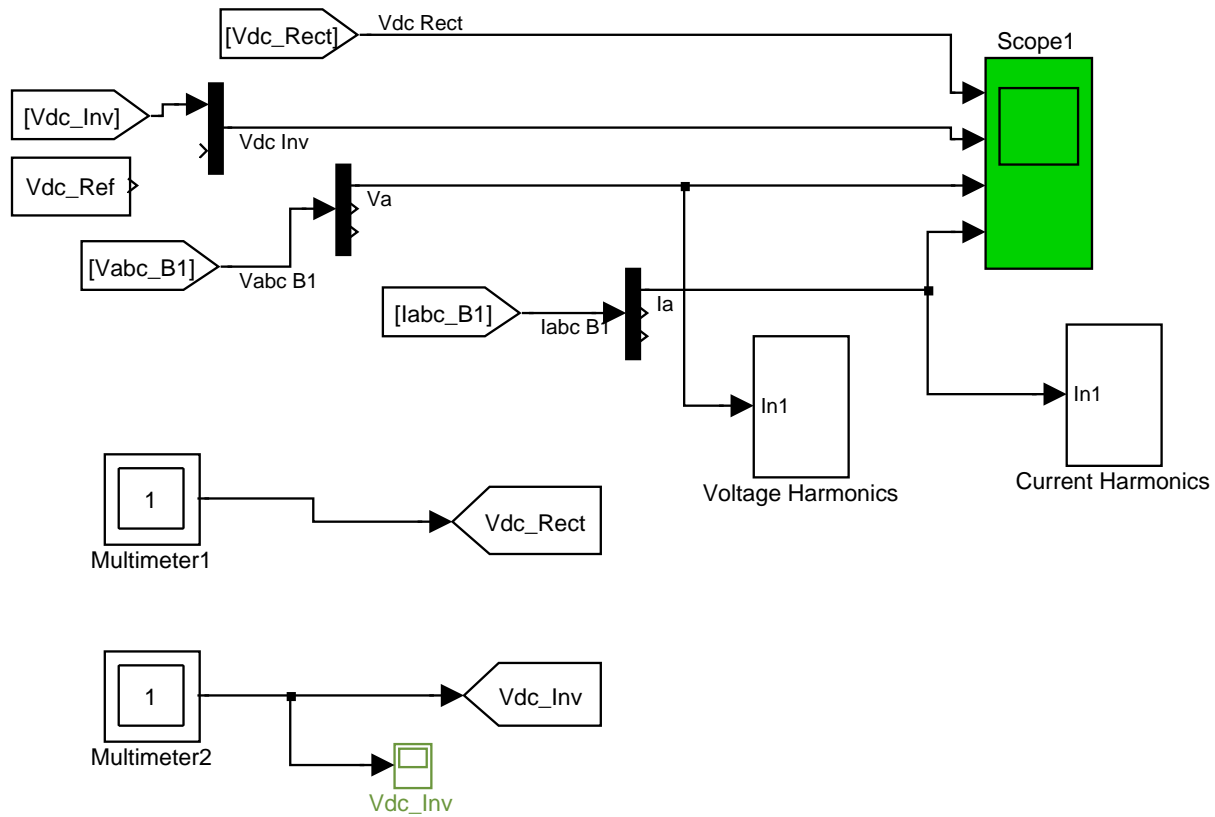
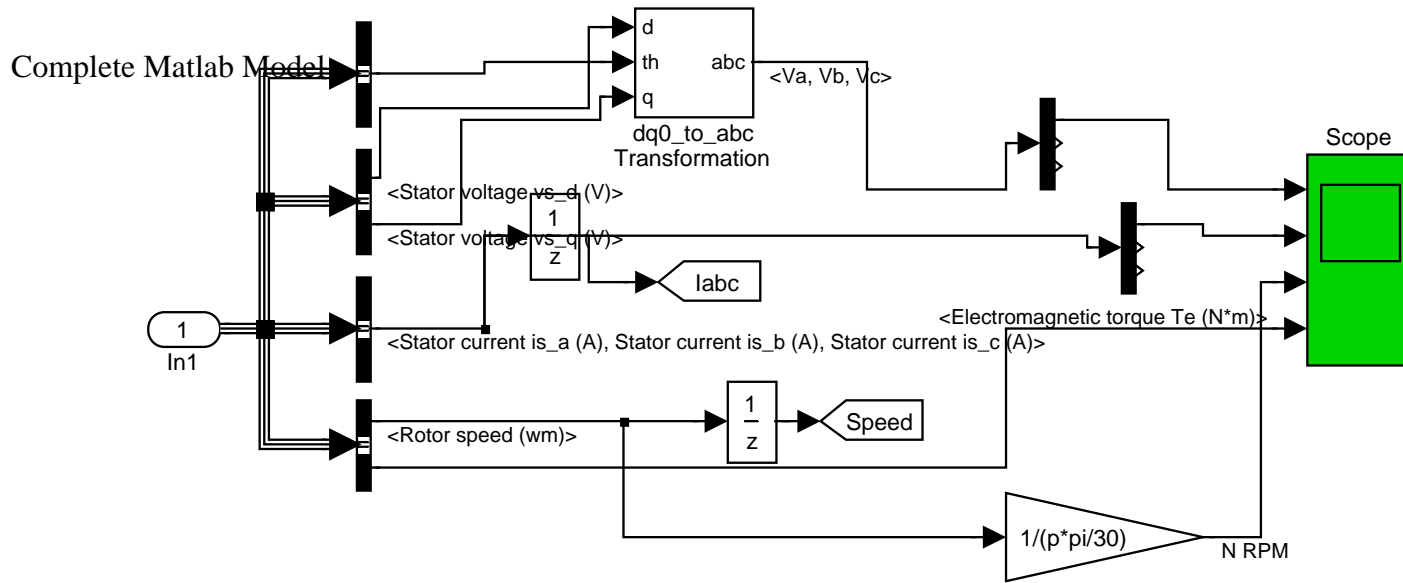
Table 3-1. Hardware TRL Definitions, Descriptions, and Supporting Information
 (Source: *Defense Acquisition Guidebook*) (Continued)

TRL	Definition	Description	Supporting Information
6	System/subsystem model or prototype demonstration in a relevant environment.	Representative model or prototype system, which is well beyond that of TRL 5, is tested in a relevant environment. Represents a major step up in a technology's demonstrated readiness. Examples include testing a prototype in a high-fidelity laboratory environment or in a simulated operational environment.	Results from laboratory testing of a prototype system that is near the desired configuration in terms of performance, weight, and volume. How did the test environment differ from the operational environment? Who performed the tests? How did the test compare with expectations? What problems, if any, were encountered? What are/were the plans, options, or actions to resolve problems before moving to the next level?
7	System prototype demonstration in an operational environment.	Prototype near or at planned operational system. Represents a major step up from TRL 6 by requiring demonstration of an actual system prototype in an operational environment (e.g., in an aircraft, in a vehicle, or in space). Examples include testing the prototype in a test bed aircraft.	Results from testing a prototype system in an operational environment. Who performed the tests? How did the test compare with expectations? What problems, if any, were encountered? What are/were the plans, options, or actions to resolve problems before moving to the next level?
8	Actual system completed and qualified through test and demonstration.	Technology has been proven to work in its final form and under expected conditions. In almost all cases, this TRL represents the end of true system development. Examples include developmental test and evaluation of the system in its intended weapon system to determine if it meets design specifications.	Results of testing the system in its final configuration under the expected range of environmental conditions in which it will be expected to operate. Assessment of whether it will meet its operational requirements. What problems, if any, were encountered? What are/were the plans, options, or actions to resolve problems before finalizing the design?
9	Actual system proven through successful mission operations.	Actual application of the technology in its final form and under mission conditions, such as those encountered in operational test and evaluation (OT&E). Examples include using the system under operational mission conditions.	OT&E reports.

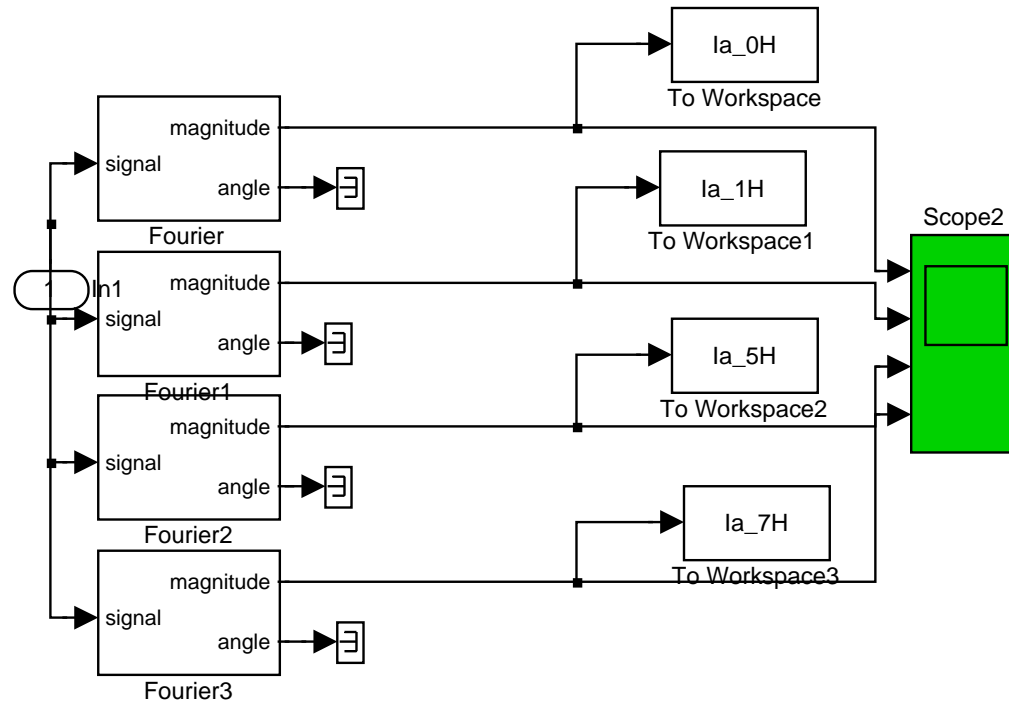
APPENDIX B: MATLAB SYSTEM MODEL

Complete Matlab Model

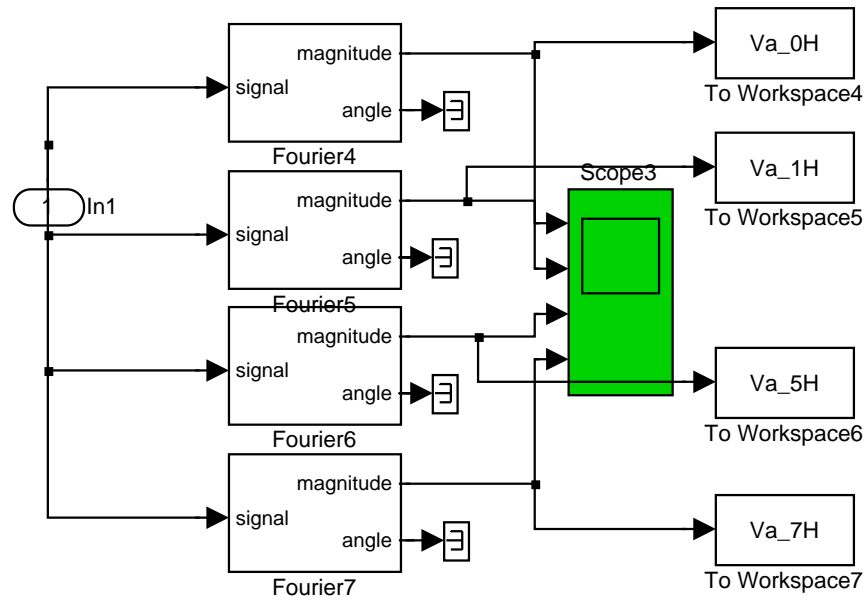




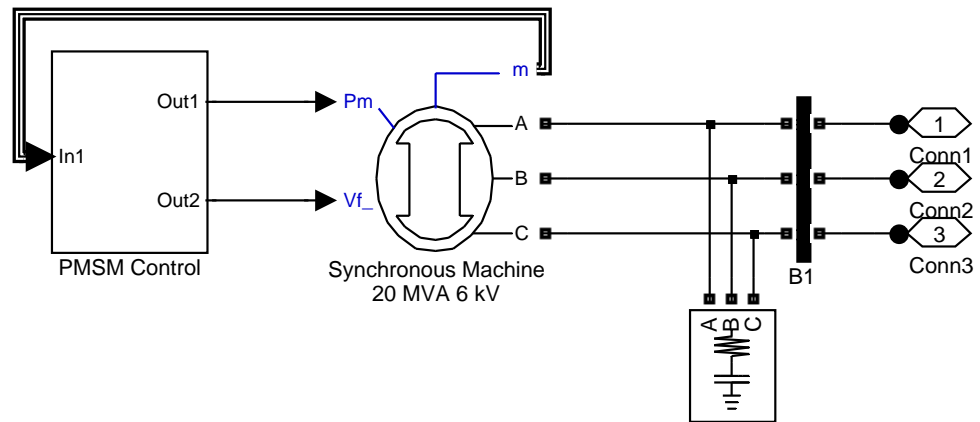
Complete Matlab Model



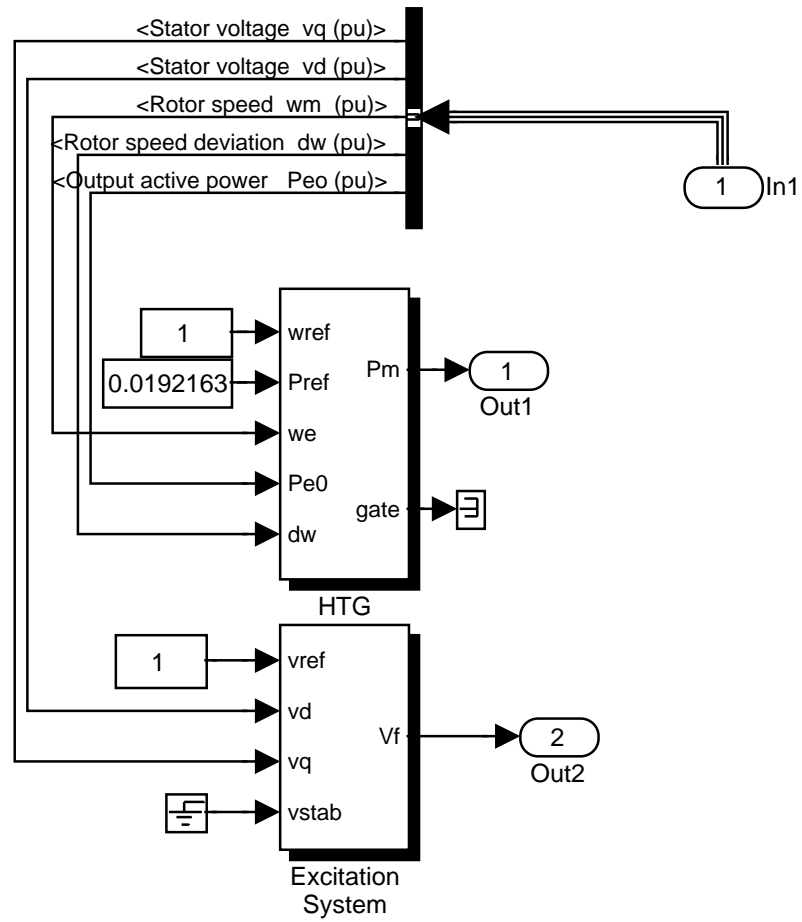
Complete Matlab Model



Complete Matlab Model

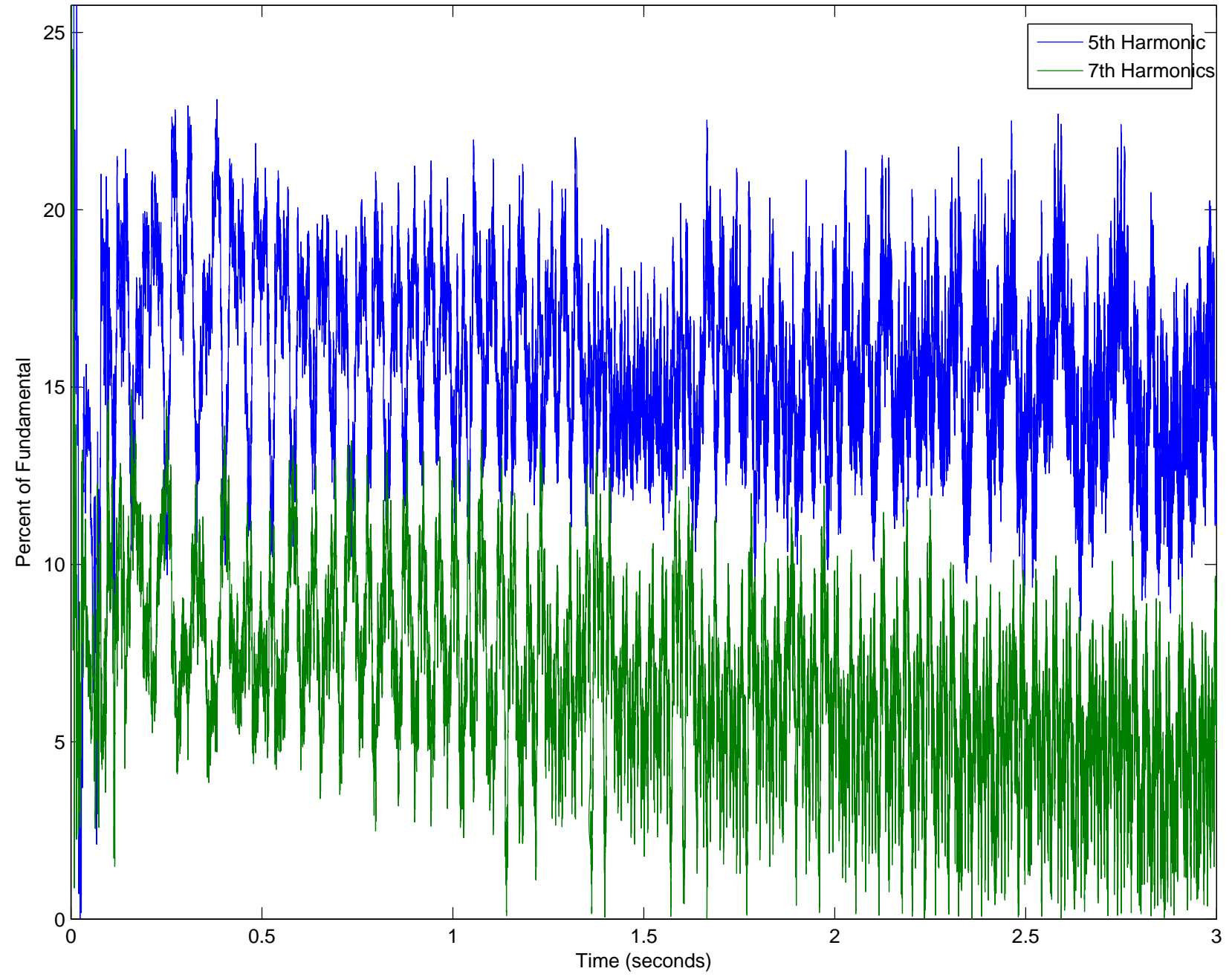


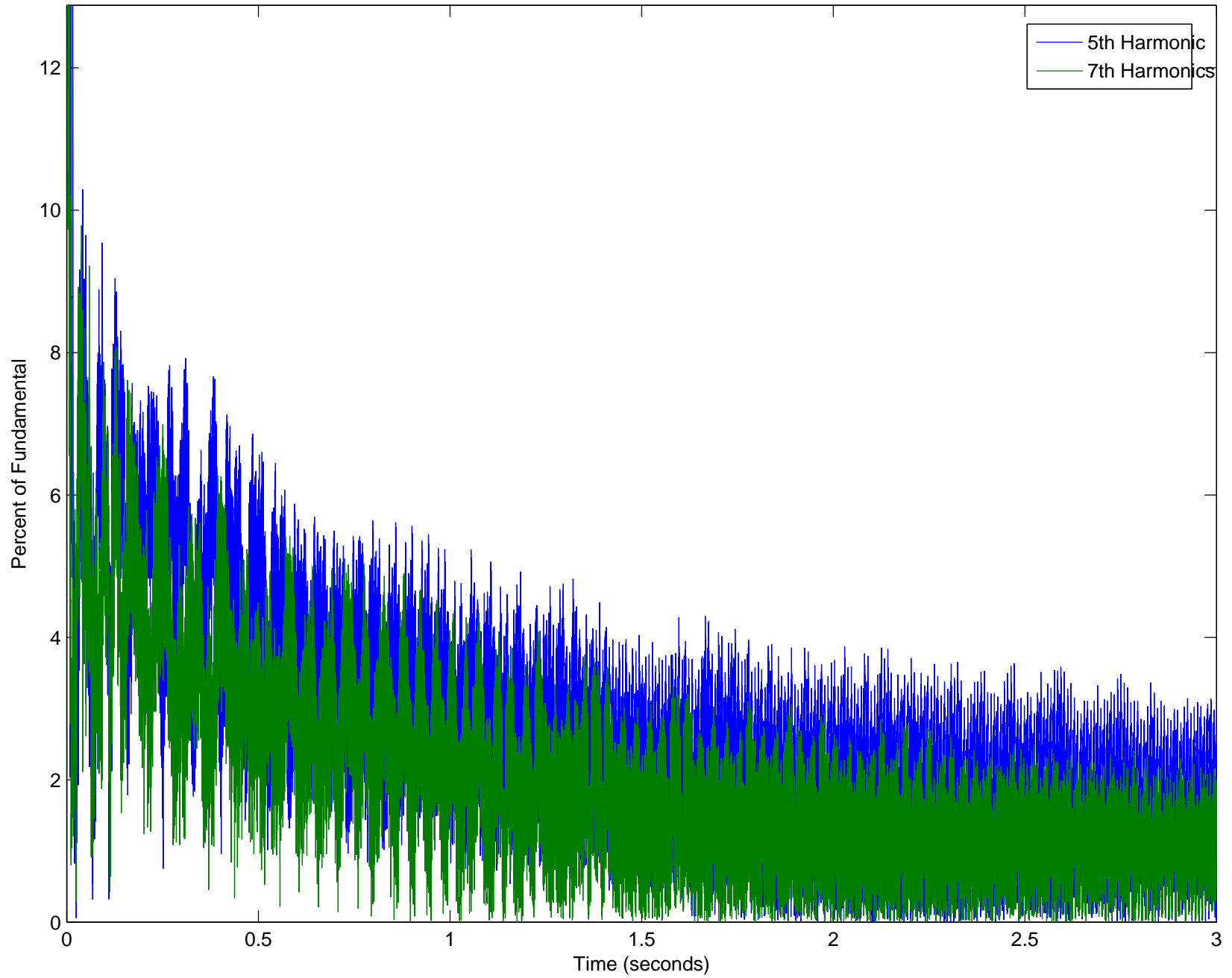
Complete Matlab Model



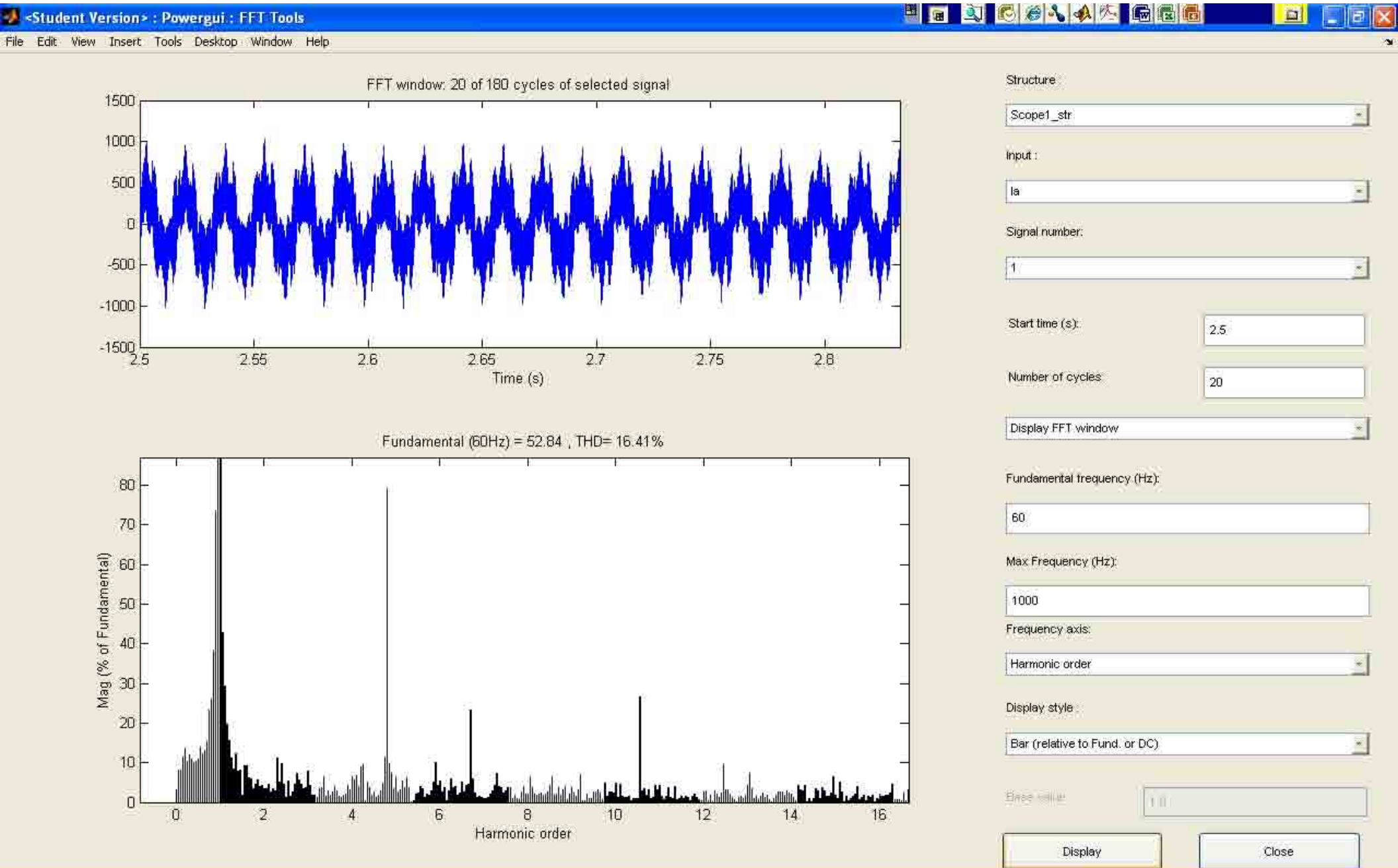
APPENDIX C: MATLAB SIMULATION 1 OUTPUT

Current Harmonics all times

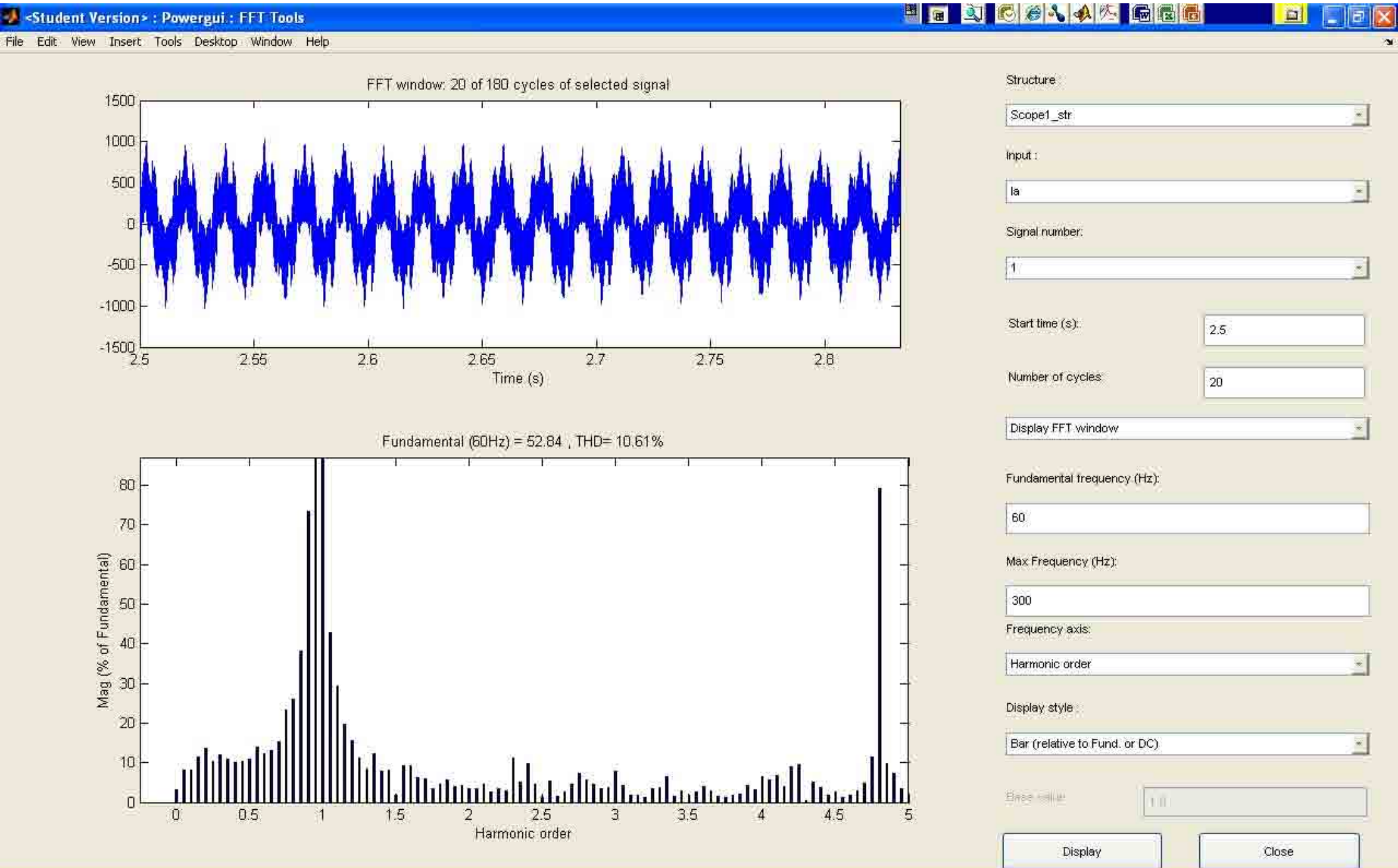




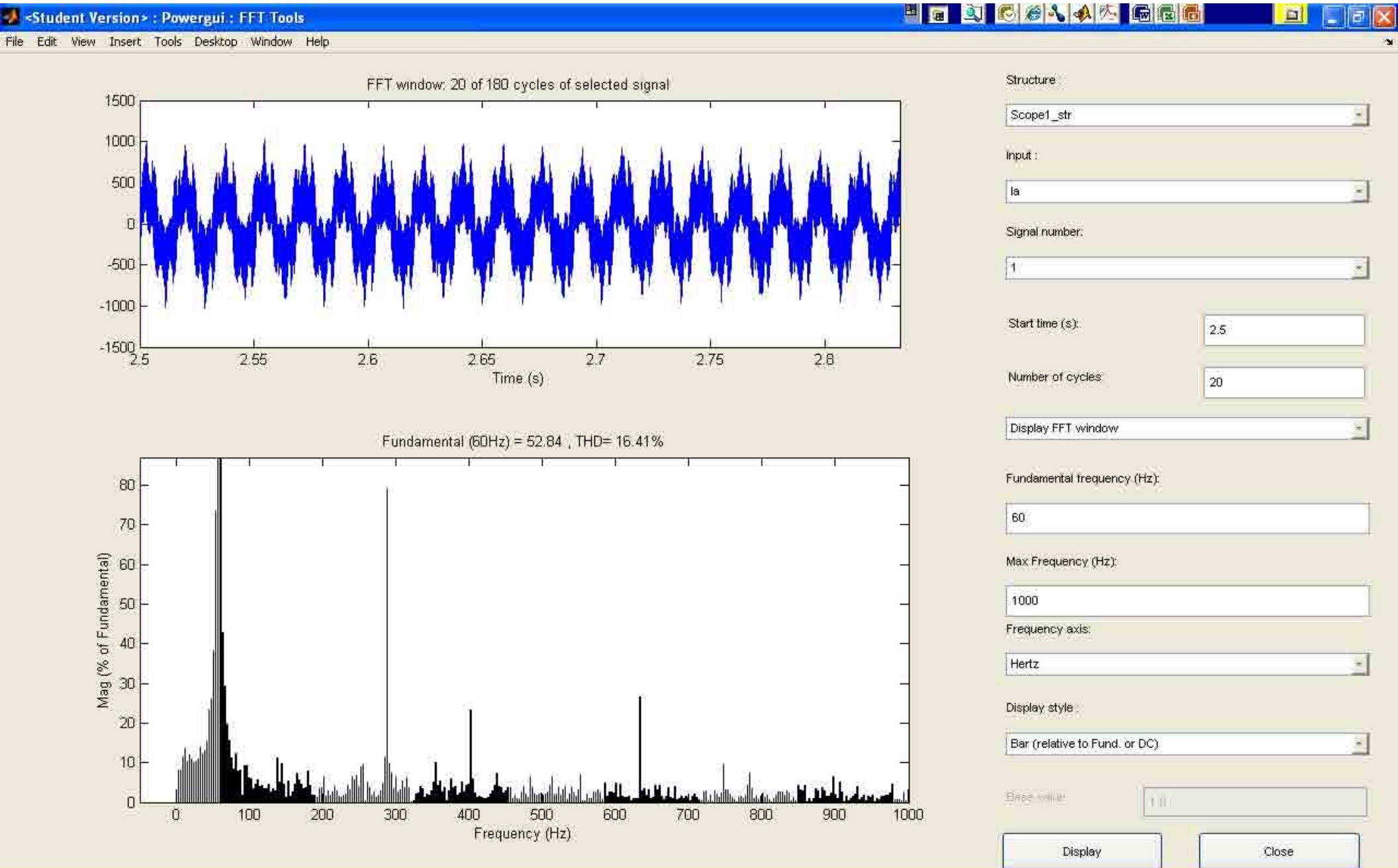
Matlab Simulation 1 Output



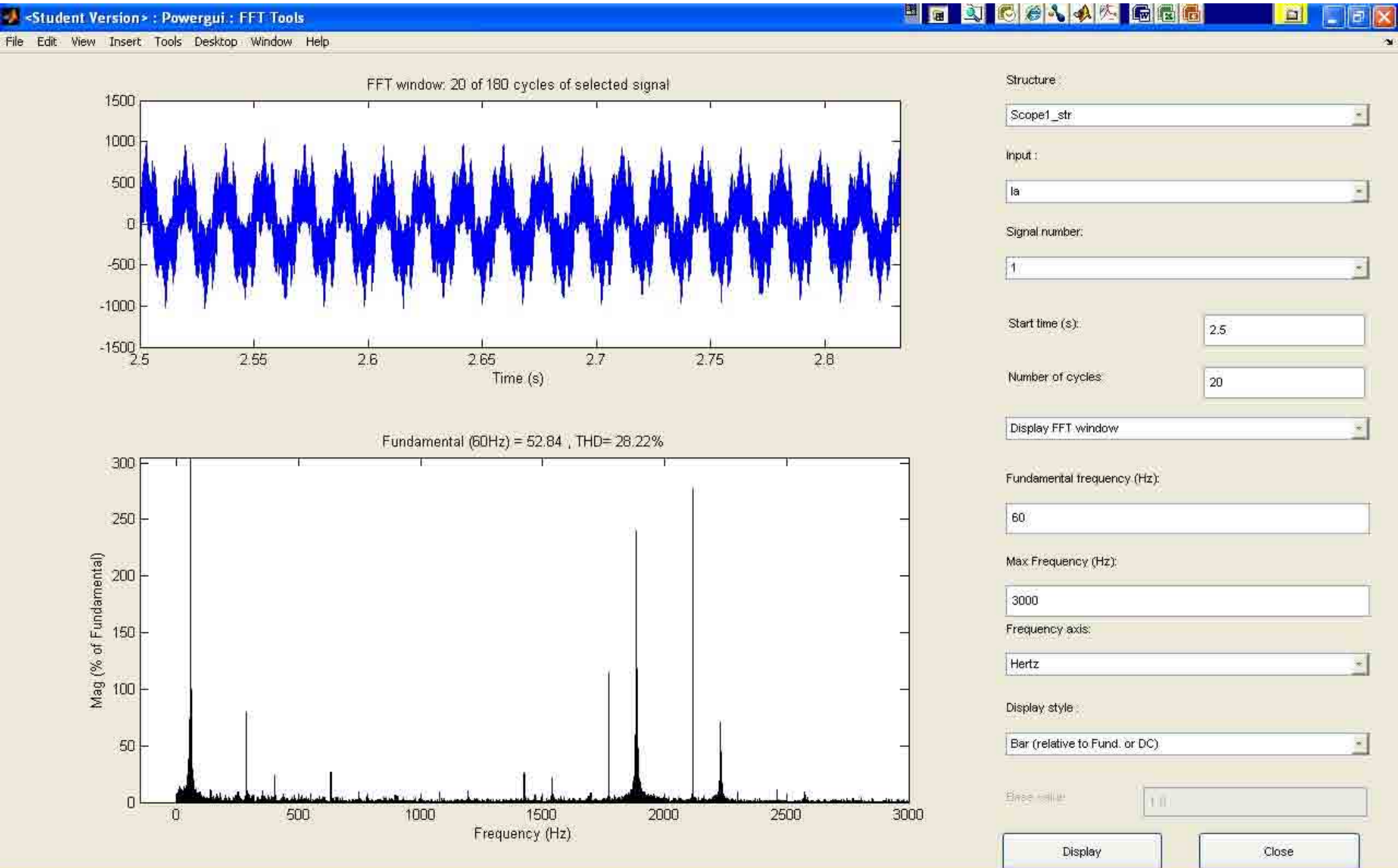
Matlab Simulation 1 Output



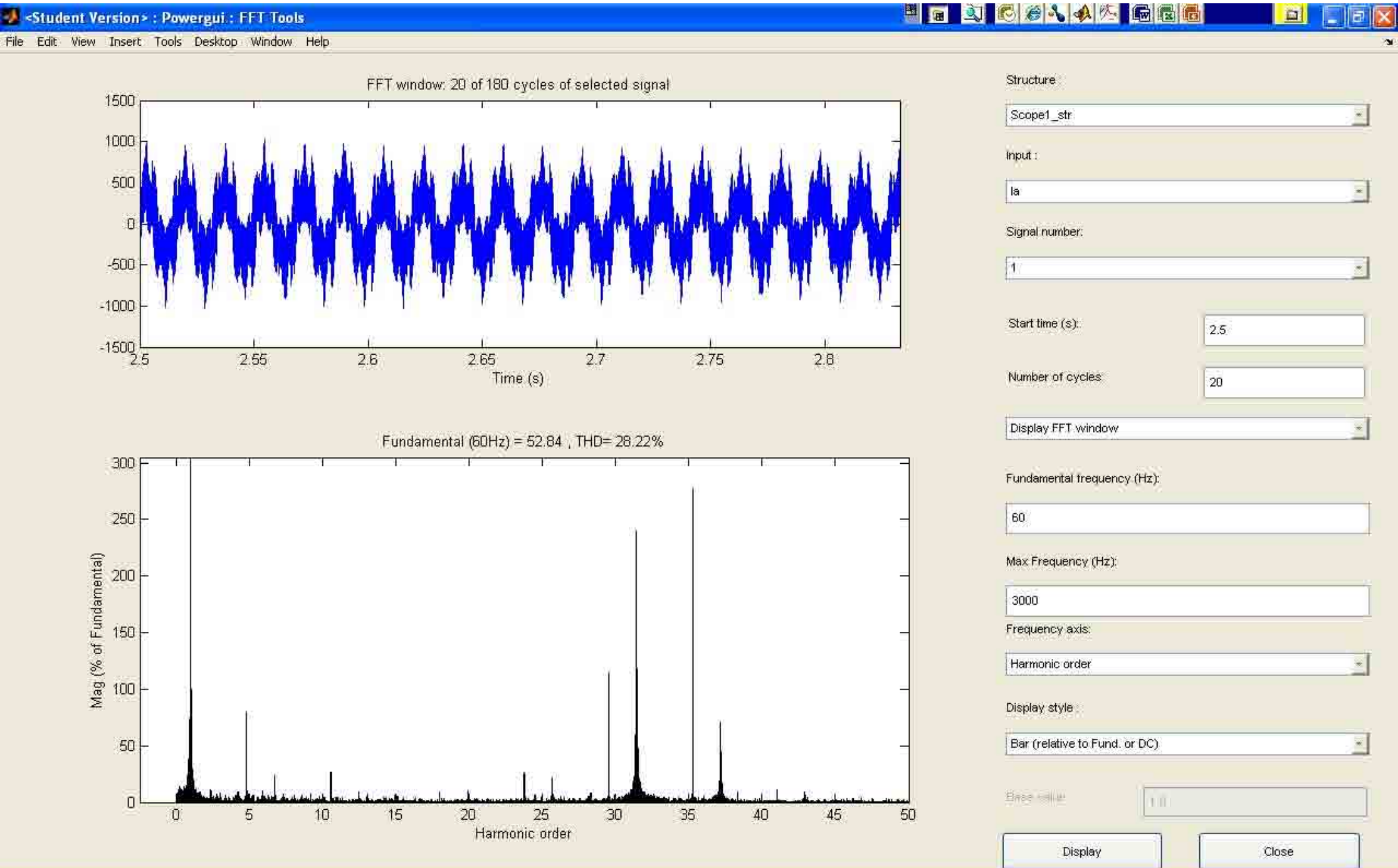
Matlab Simulation 1 Output



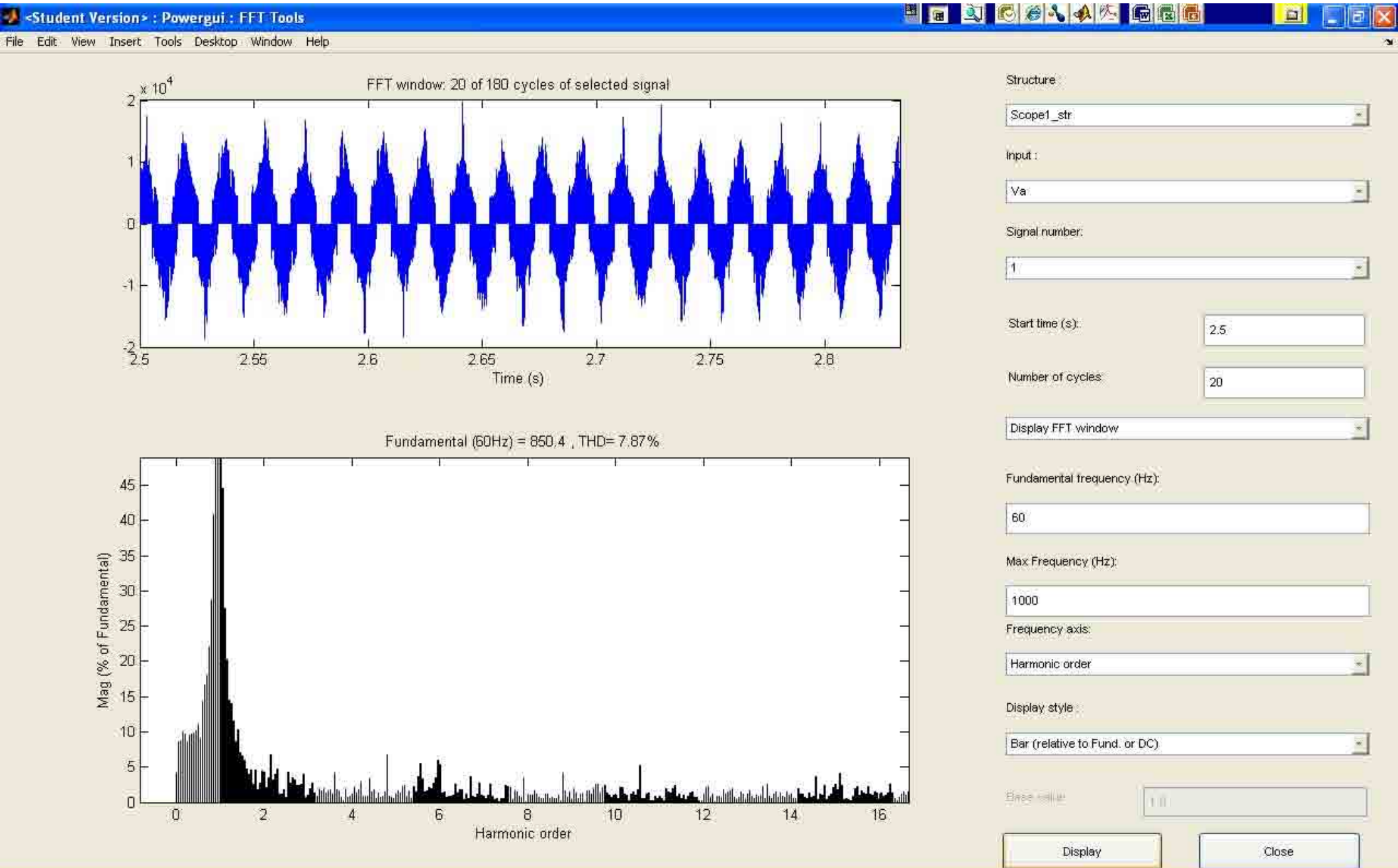
Matlab Simulation 1 Output



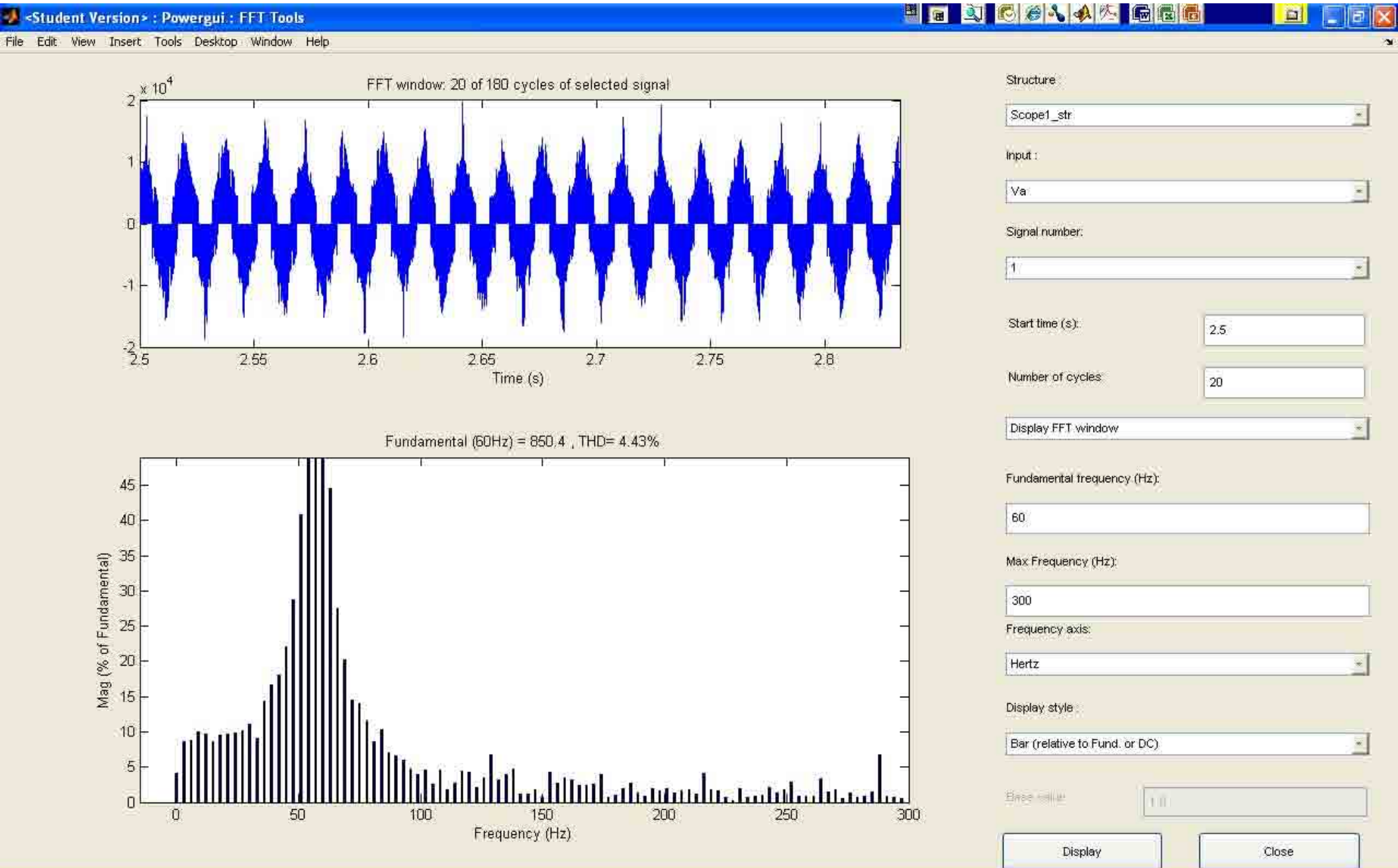
Matlab Simulation 1 Output



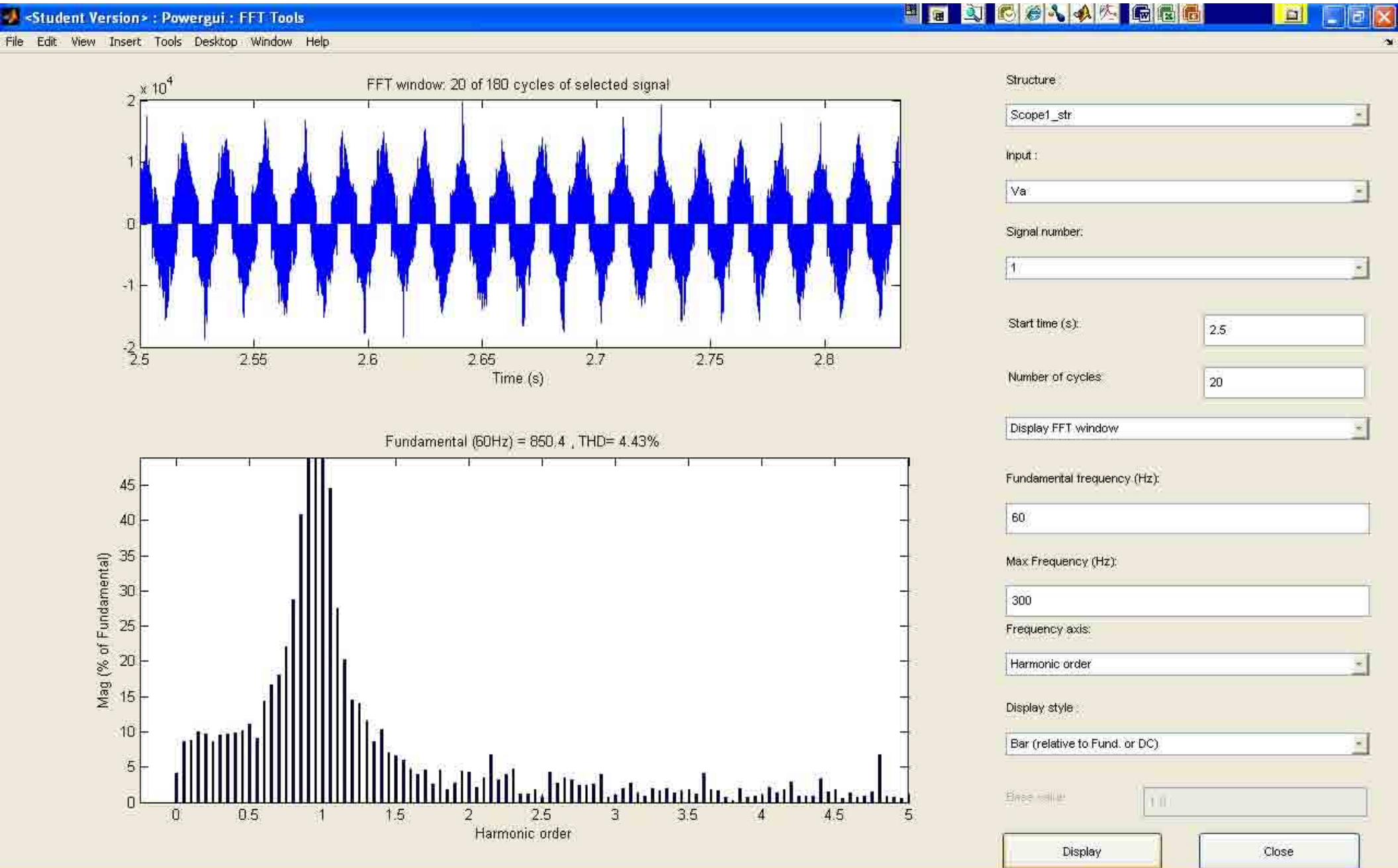
Matlab Simulation 1 Output



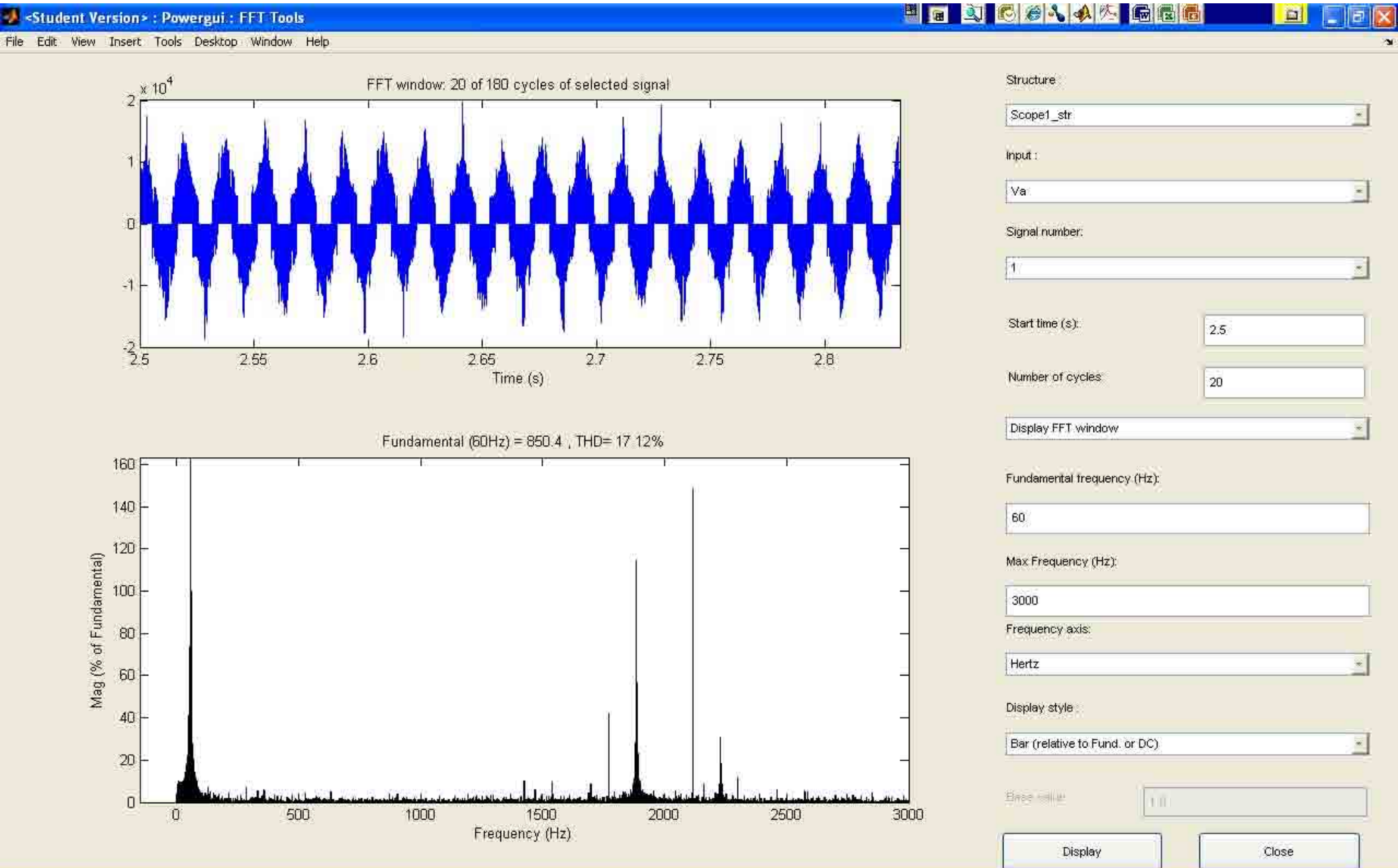
Matlab Simulation 1 Output



Matlab Simulation 1 Output

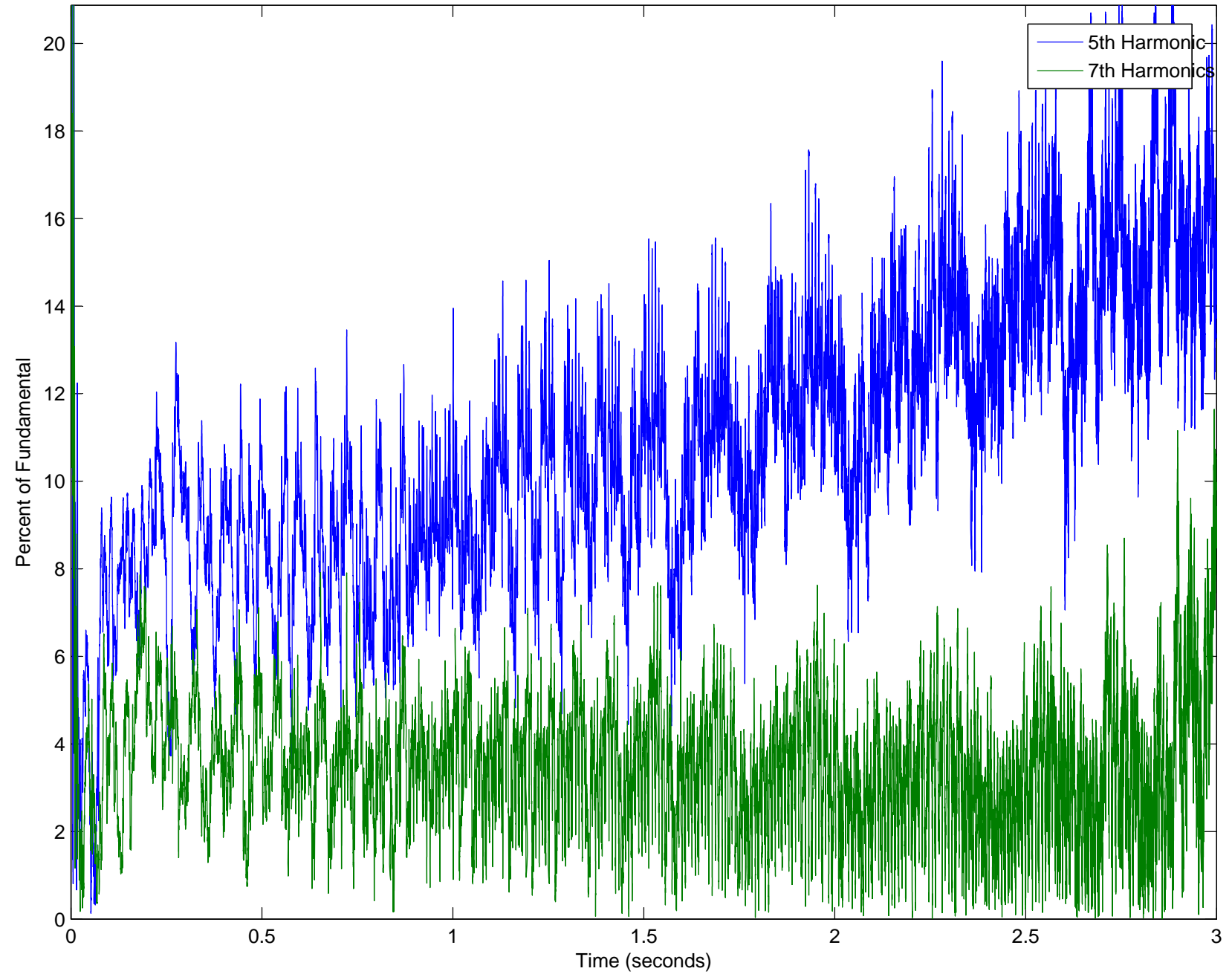


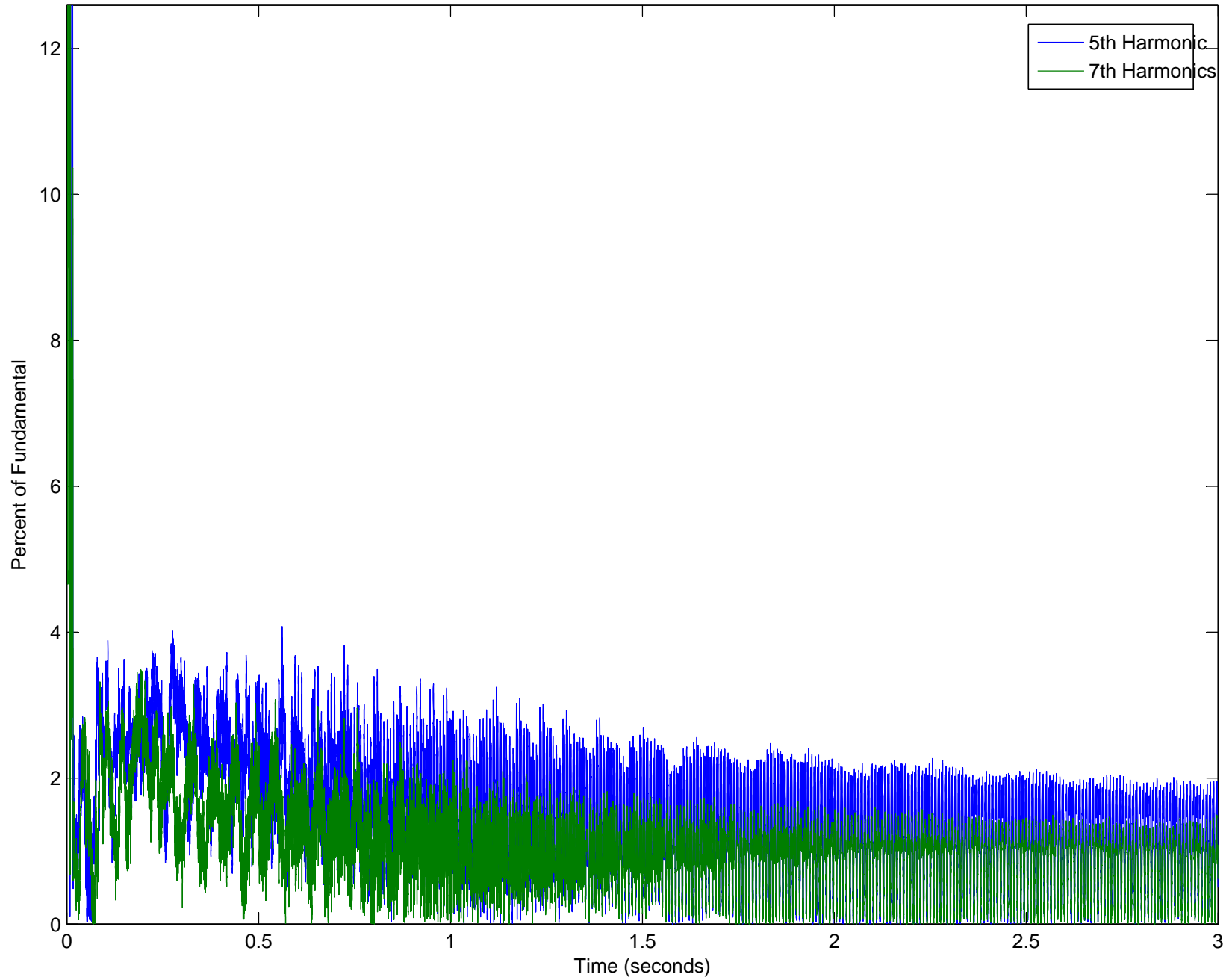
Matlab Simulation 1 Output



APPENDIX D: MATLAB SIMULATION 2 OUTPUT

Current Harmonics all times



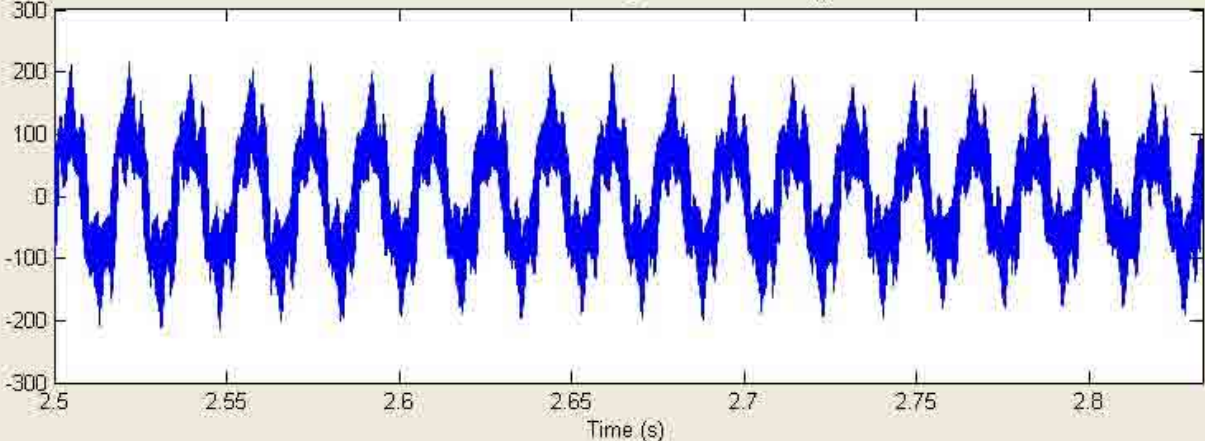


Matlab Simulation 2 Output

<Student Version> : Powergui : FFT Tools

File Edit View Insert Tools Desktop Window Help

FFT window: 20 of 180 cycles of selected signal



Time (s)

Structure: Scope1_str

Input: Ia

Signal number: 1

Start time (s): 2.5

Number of cycles: 20

Display FFT window

Fundamental frequency (Hz): 60

Max Frequency (Hz): 1000

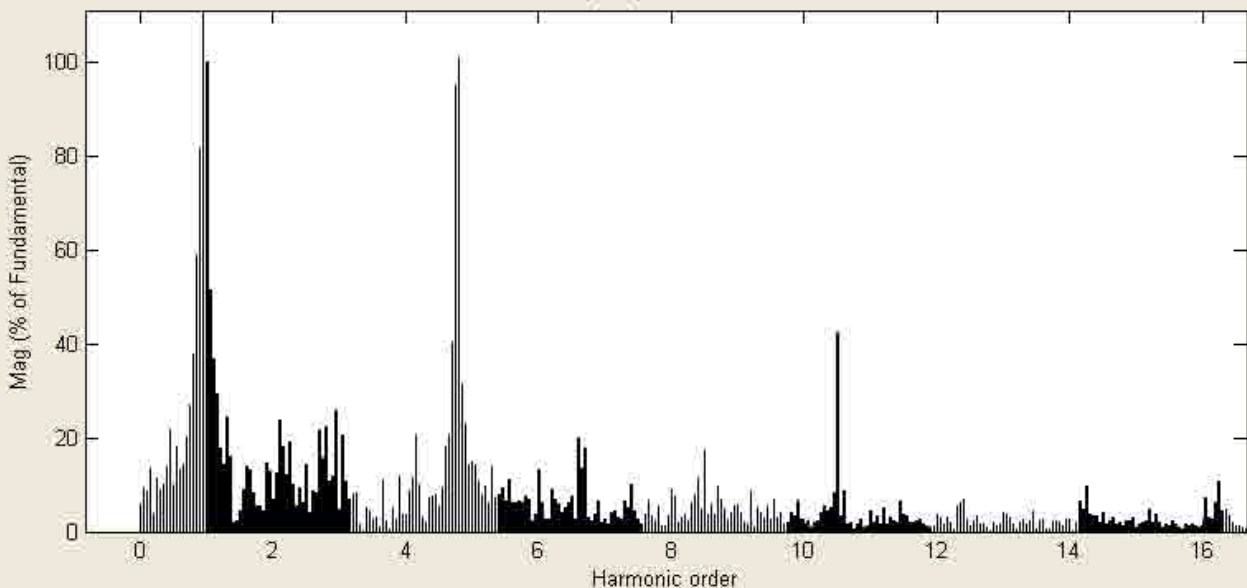
Frequency axis: Harmonic order

Display style: Bar (relative to Fund. or DC)

Base value: 1.0

Display Close

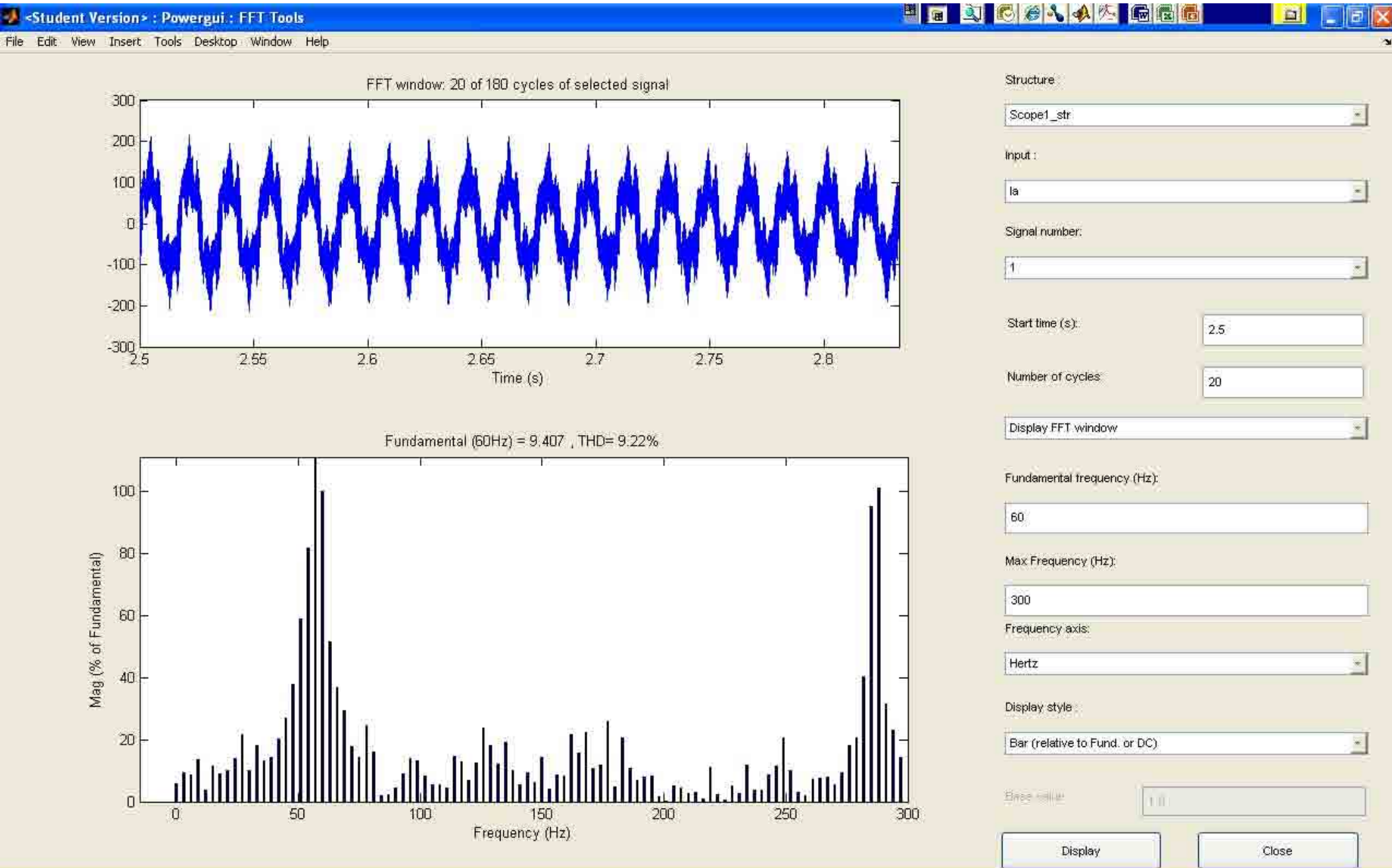
Fundamental (60Hz) = 9.407 , THD= 25.60%



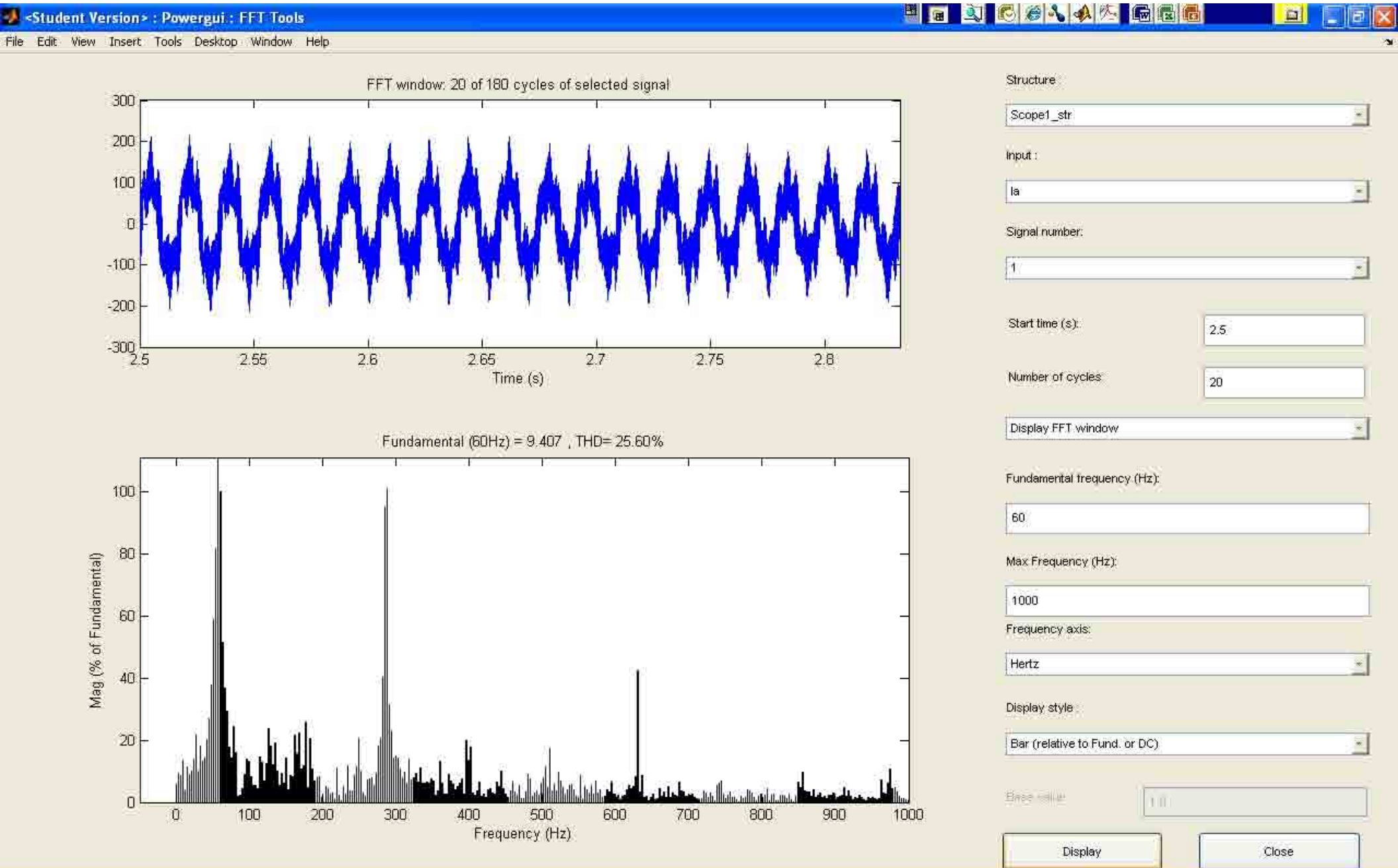
Mag (% of Fundamental)

Harmonic order

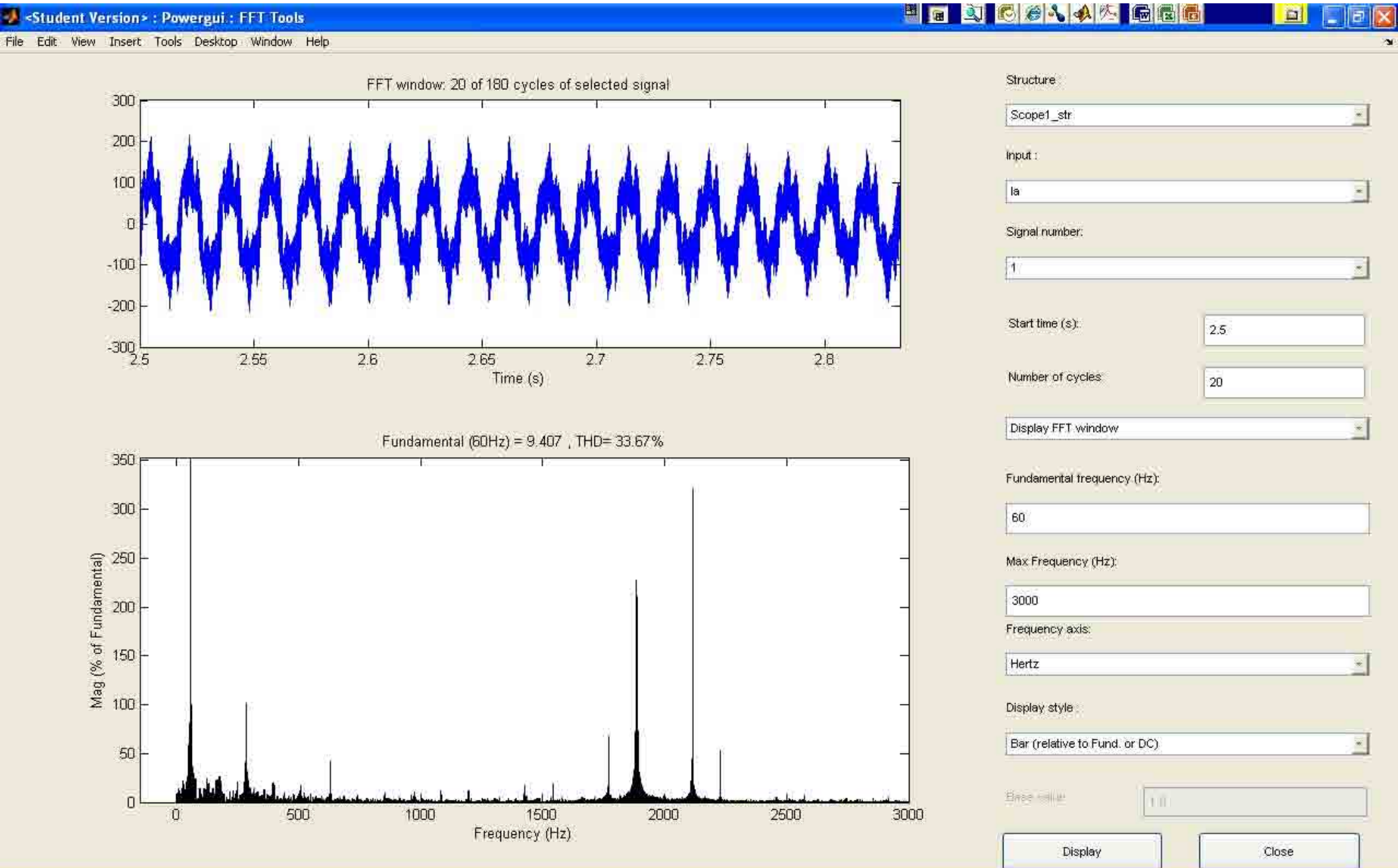
Matlab Simulation 2 Output



Matlab Simulation 2 Output



Matlab Simulation 2 Output

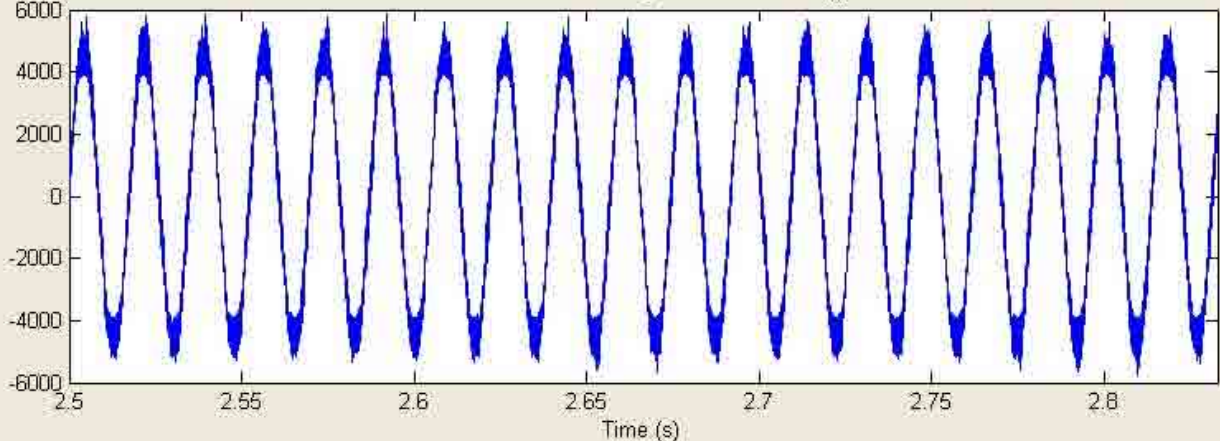


Matlab Simulation 2 Output

<Student Version> : Powergui : FFT Tools

File Edit View Insert Tools Desktop Window Help

FFT window: 20 of 180 cycles of selected signal



Time (s)

Structure: Scope1_str

Input: Va

Signal number: 1

Start time (s): 2.5

Number of cycles: 20

Display FFT window

Fundamental frequency (Hz): 60

Max Frequency (Hz): 1000

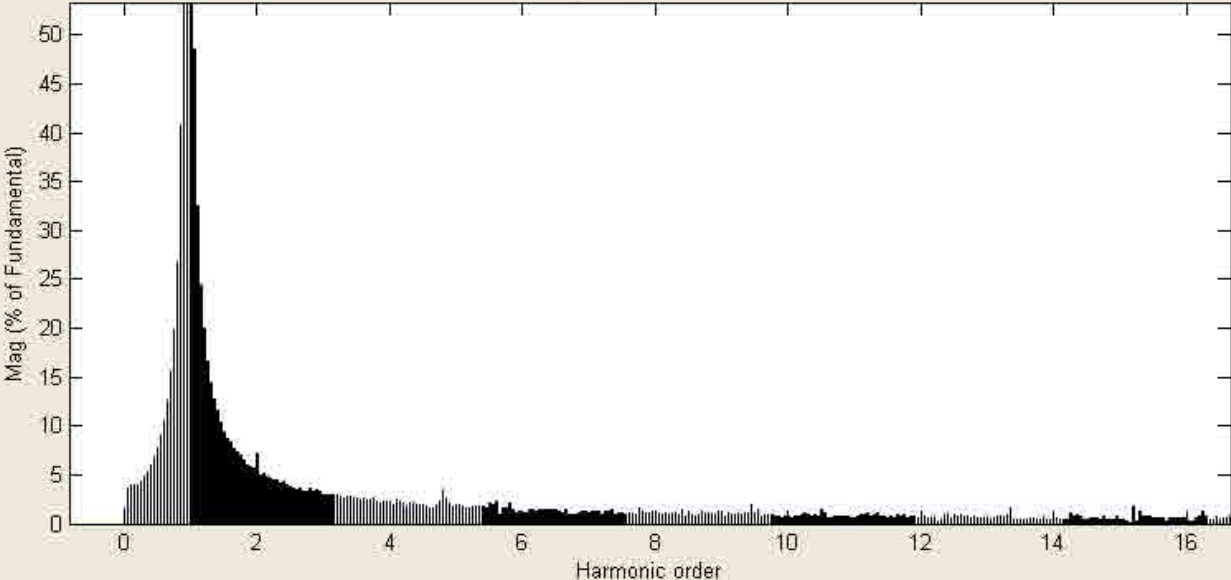
Frequency axis: Harmonic order

Display style: Bar (relative to Fund. or DC)

Base value: 1.0

Display Close

Fundamental (60Hz) = 536.6 , THD= 8.79%

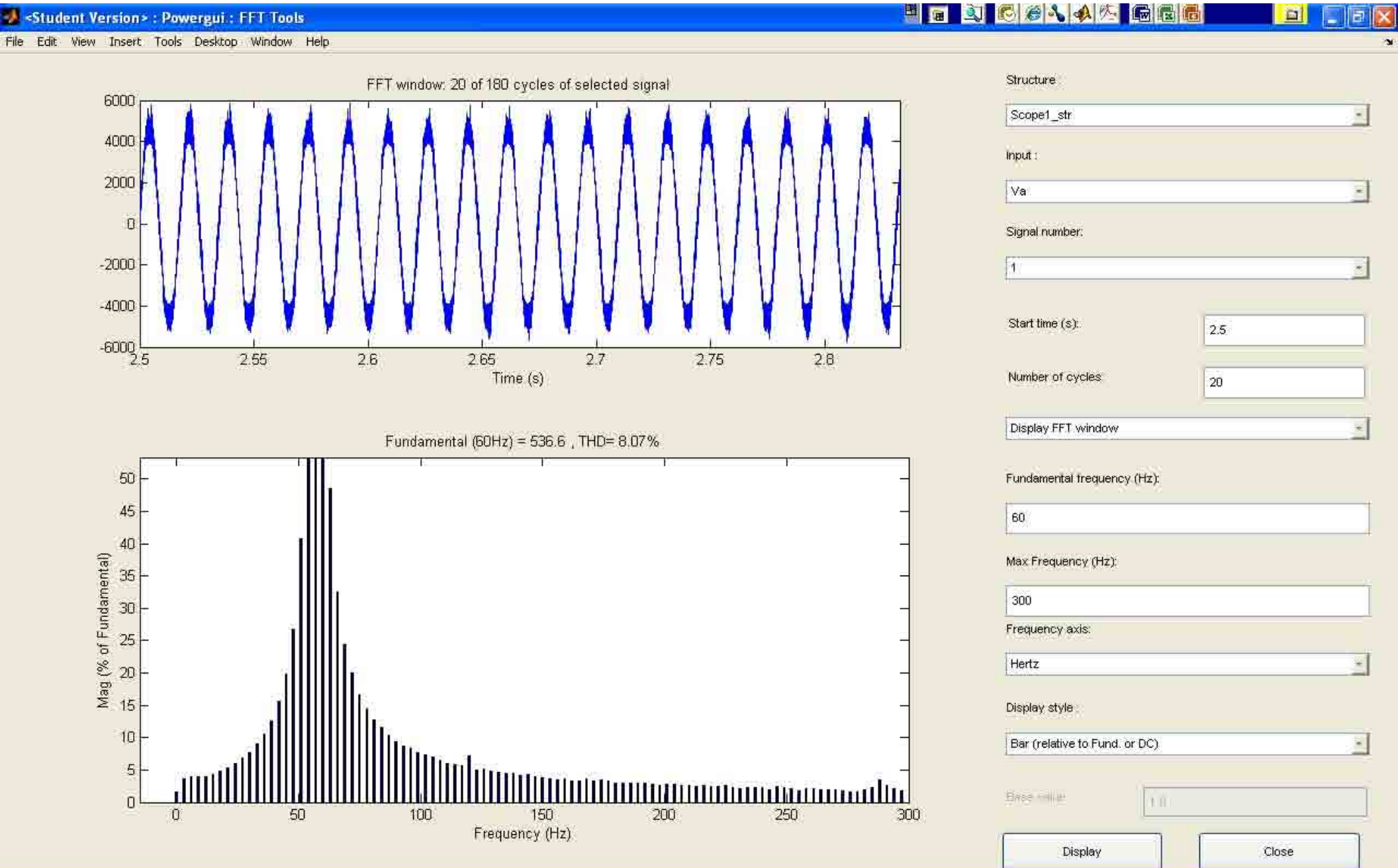


Mag (% of Fundamental)

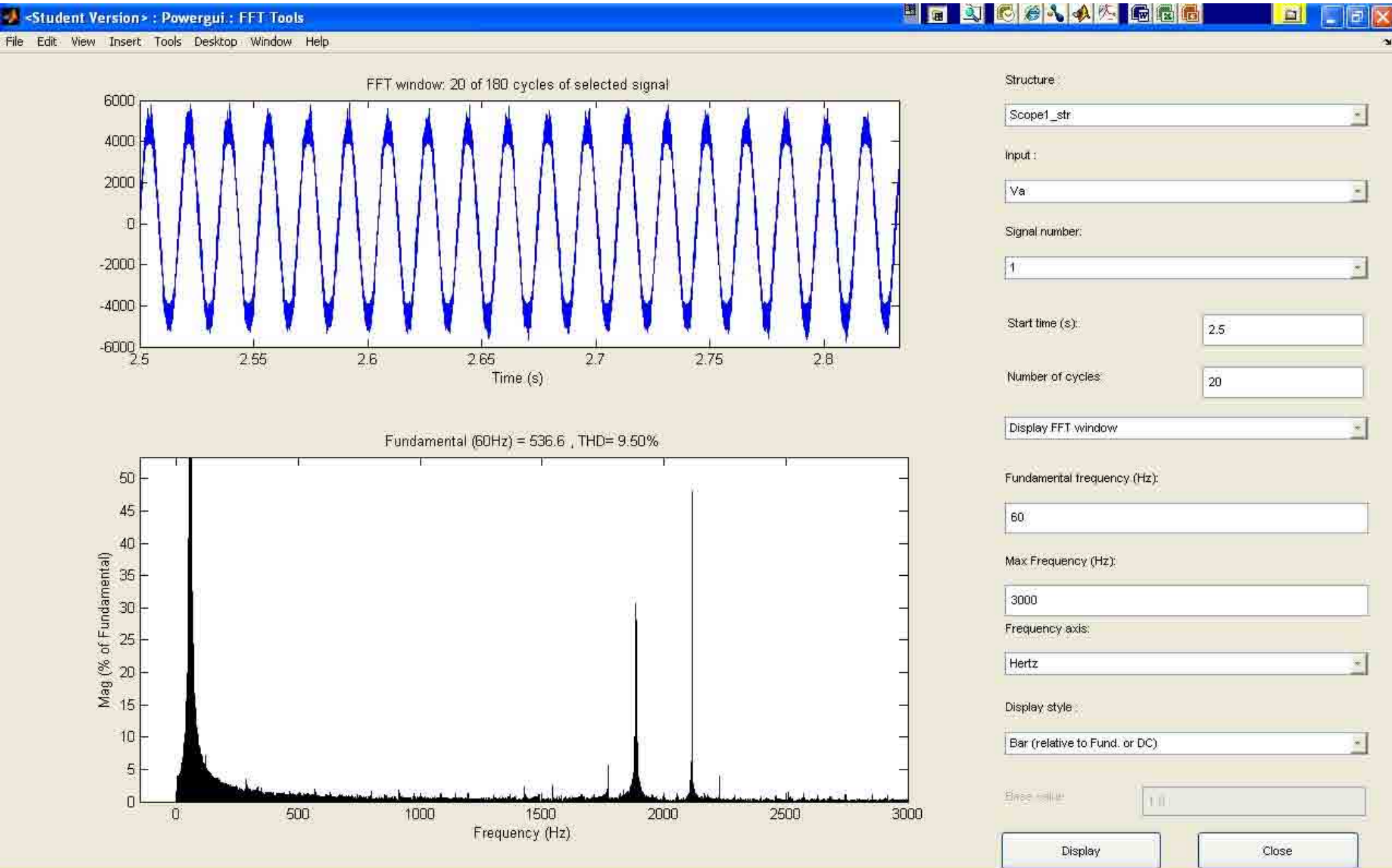
Harmonic order

Harmonic order	Mag (% of Fundamental)
1	536.6
2	~10
3	~5
4	~3
5	~2
6	~1.5
7	~1
8	~0.8
9	~0.6
10	~0.5
11	~0.4
12	~0.3
13	~0.25
14	~0.2
15	~0.15
16	~0.1

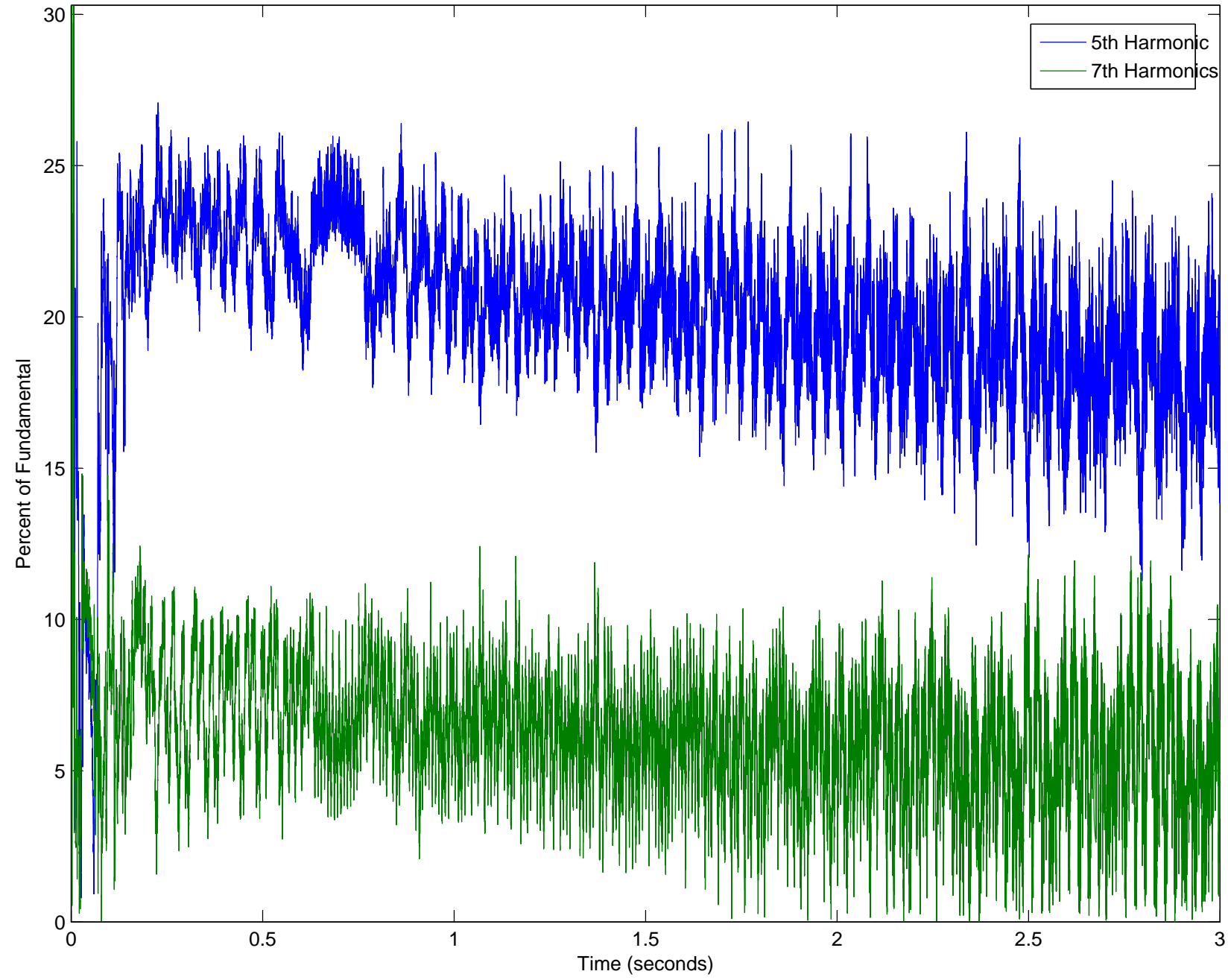
Matlab Simulation 2 Output

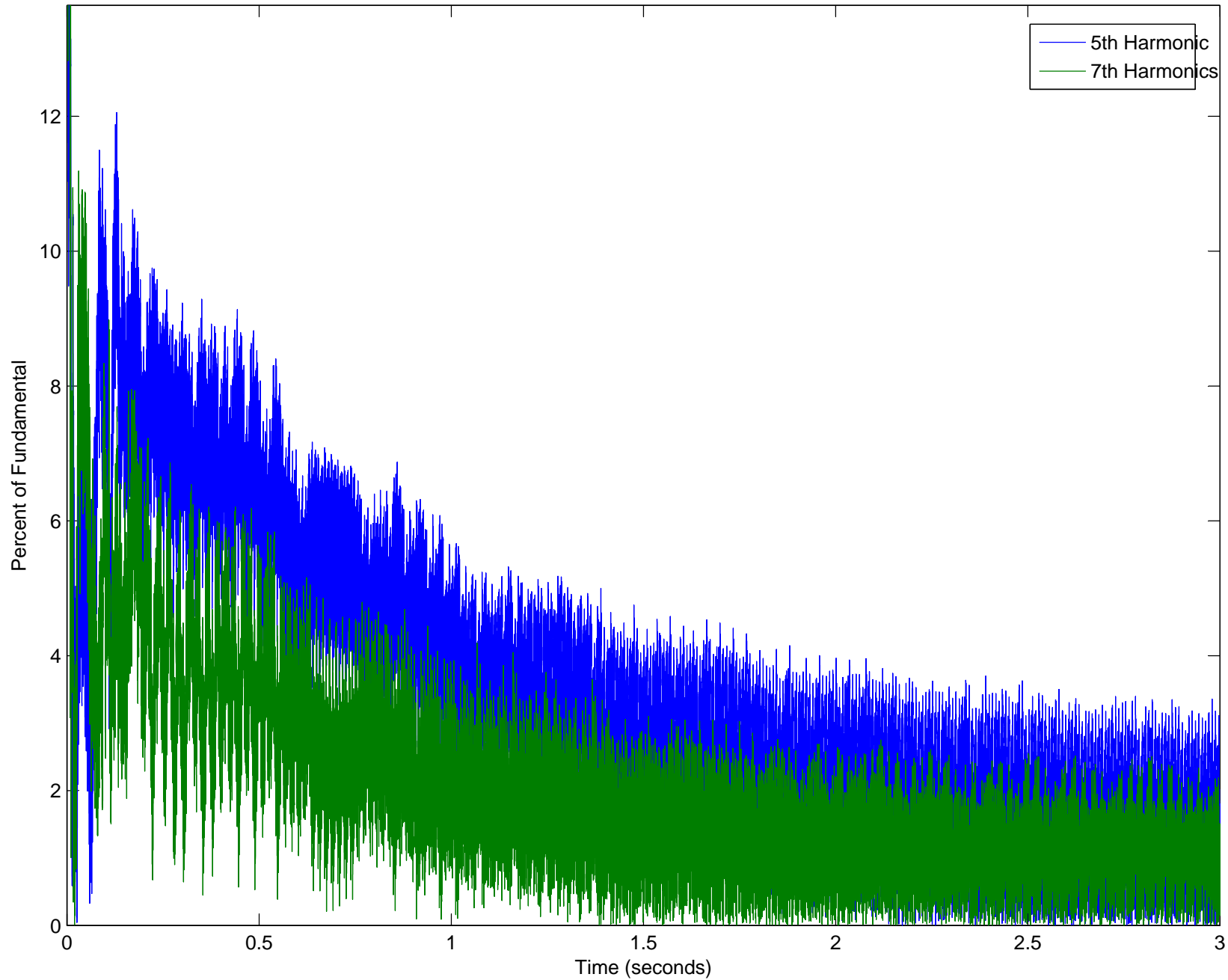


Matlab Simulation 2 Output

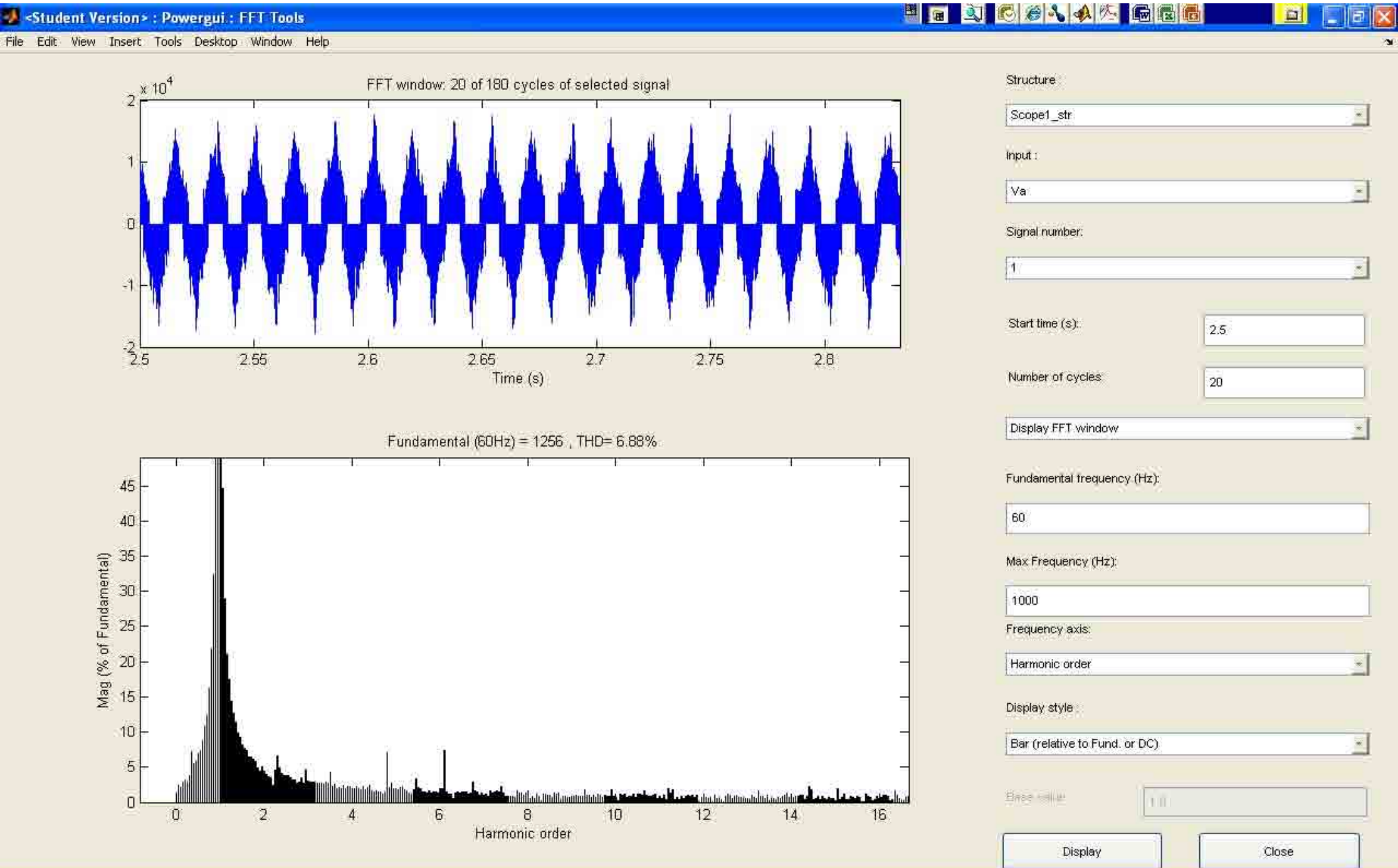


APPENDIX E: MATLAB SIMULATION 3 OUTPUT

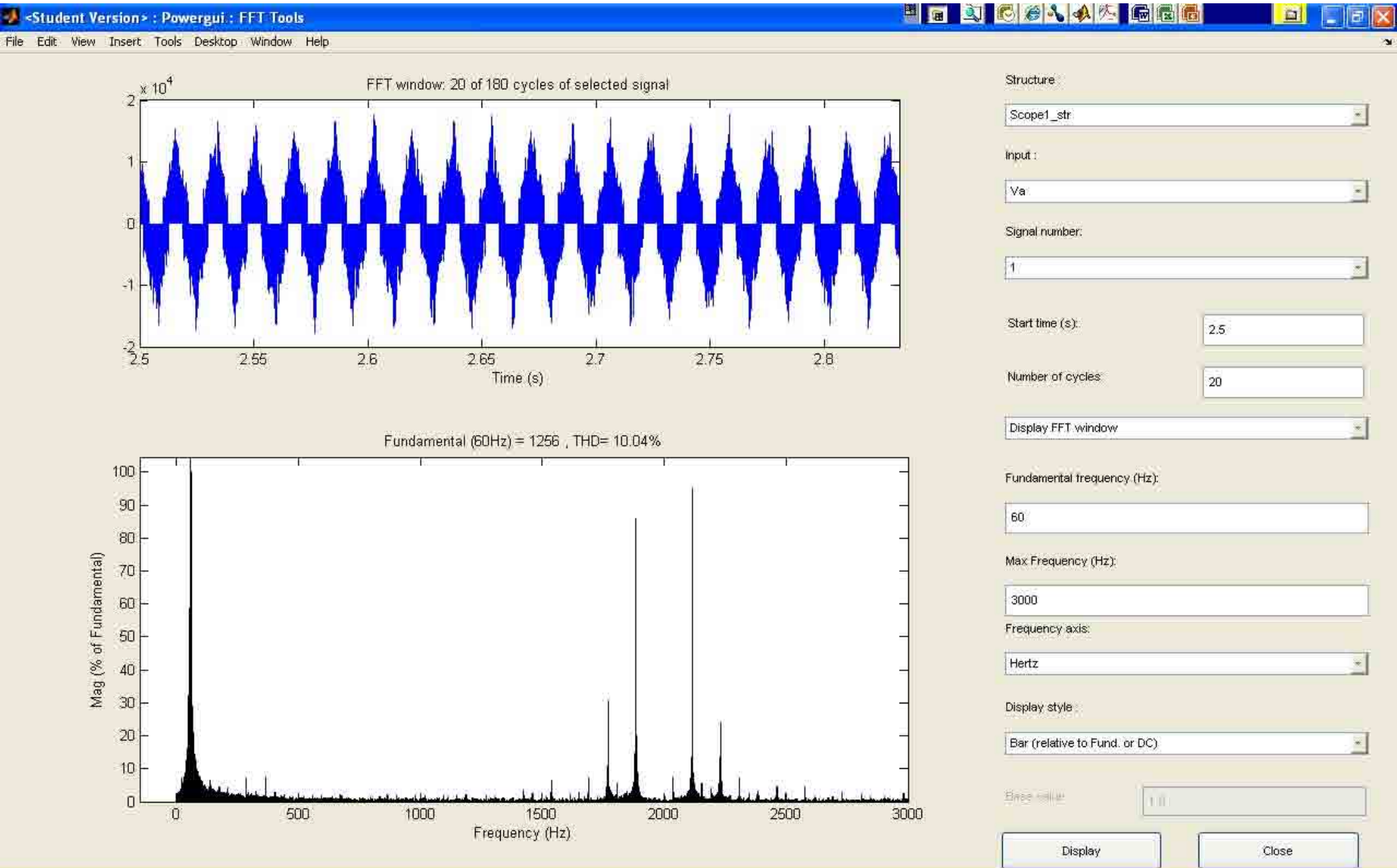




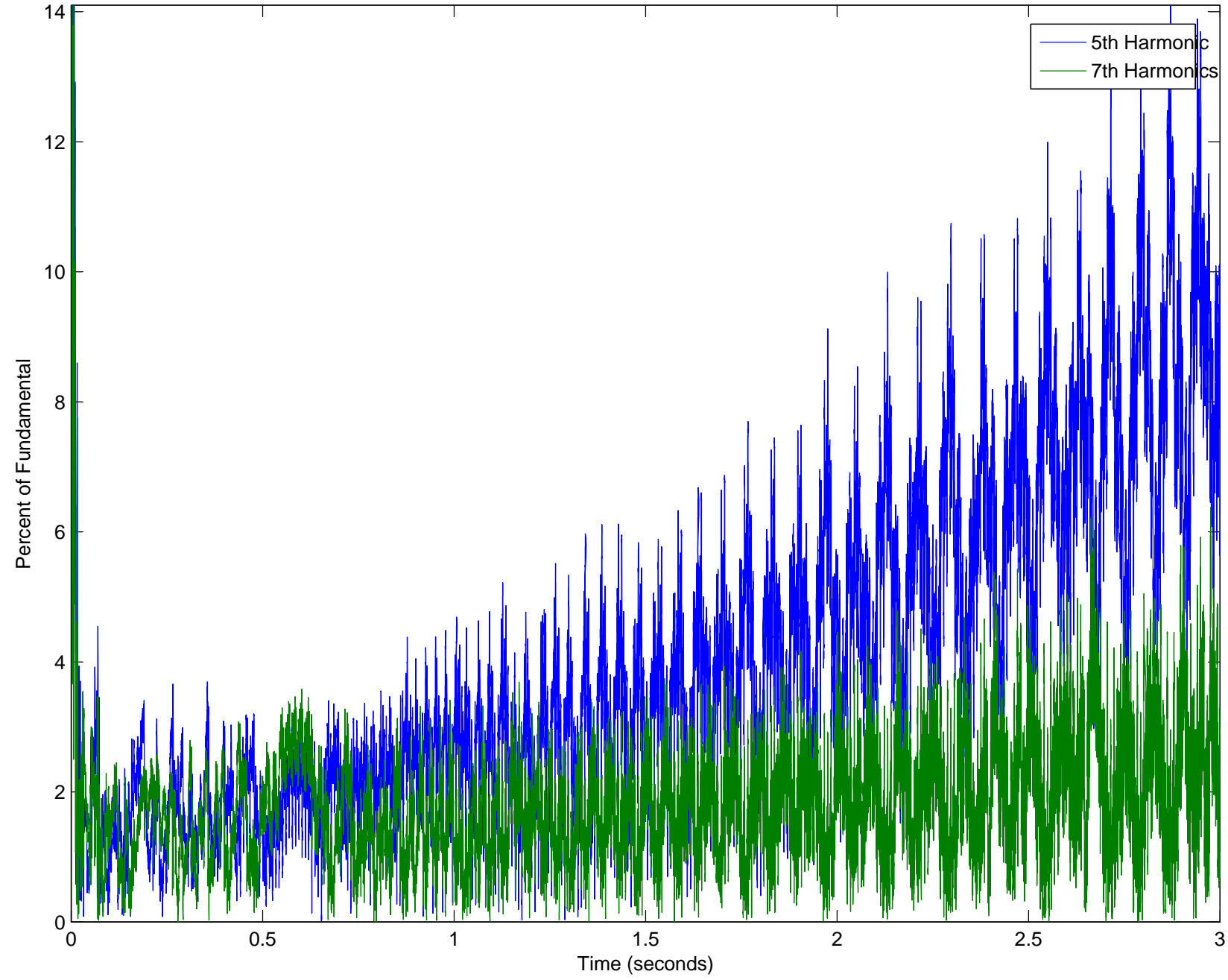
Matlab Simulation 3 Output

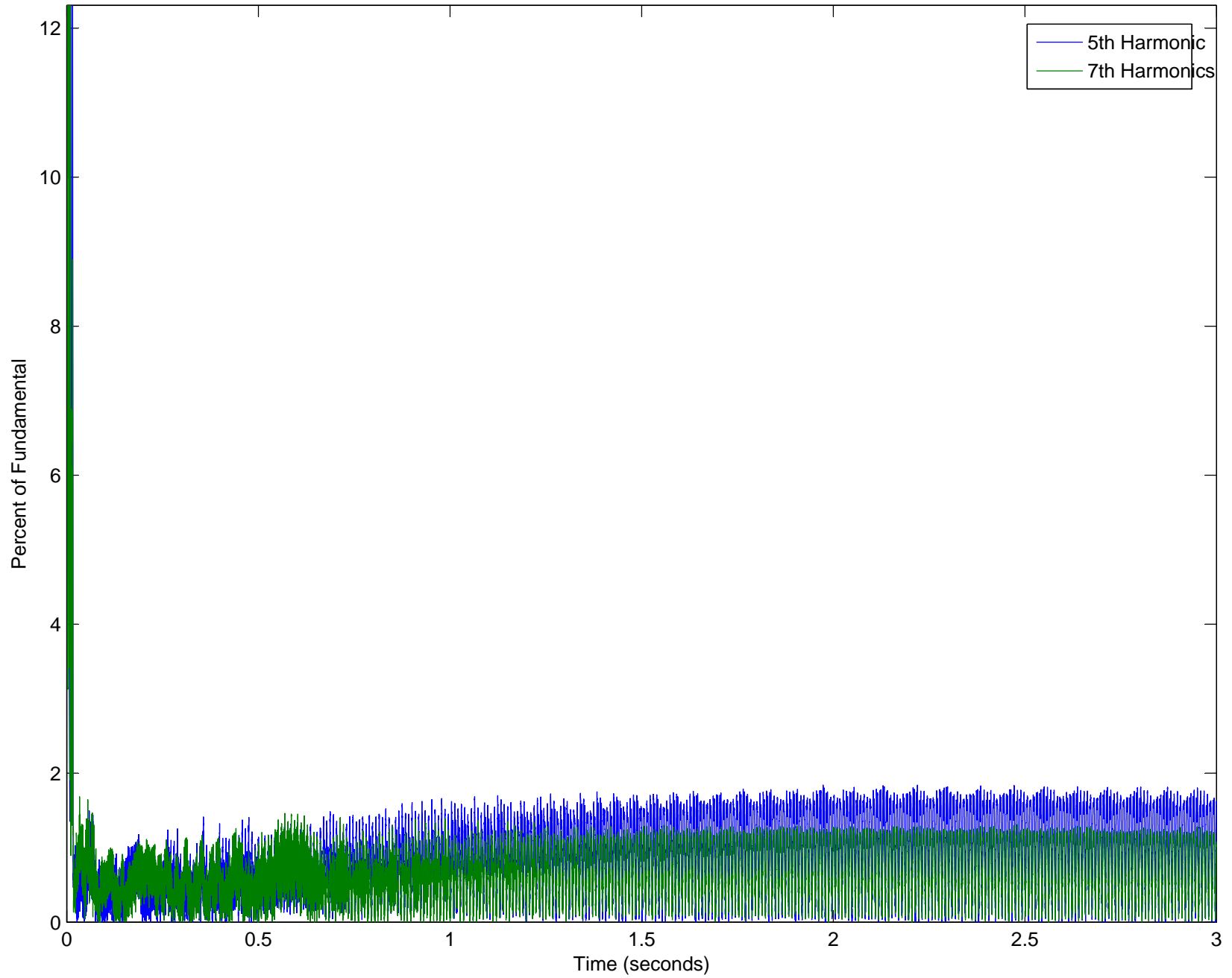


Matlab Simulation 3 Output

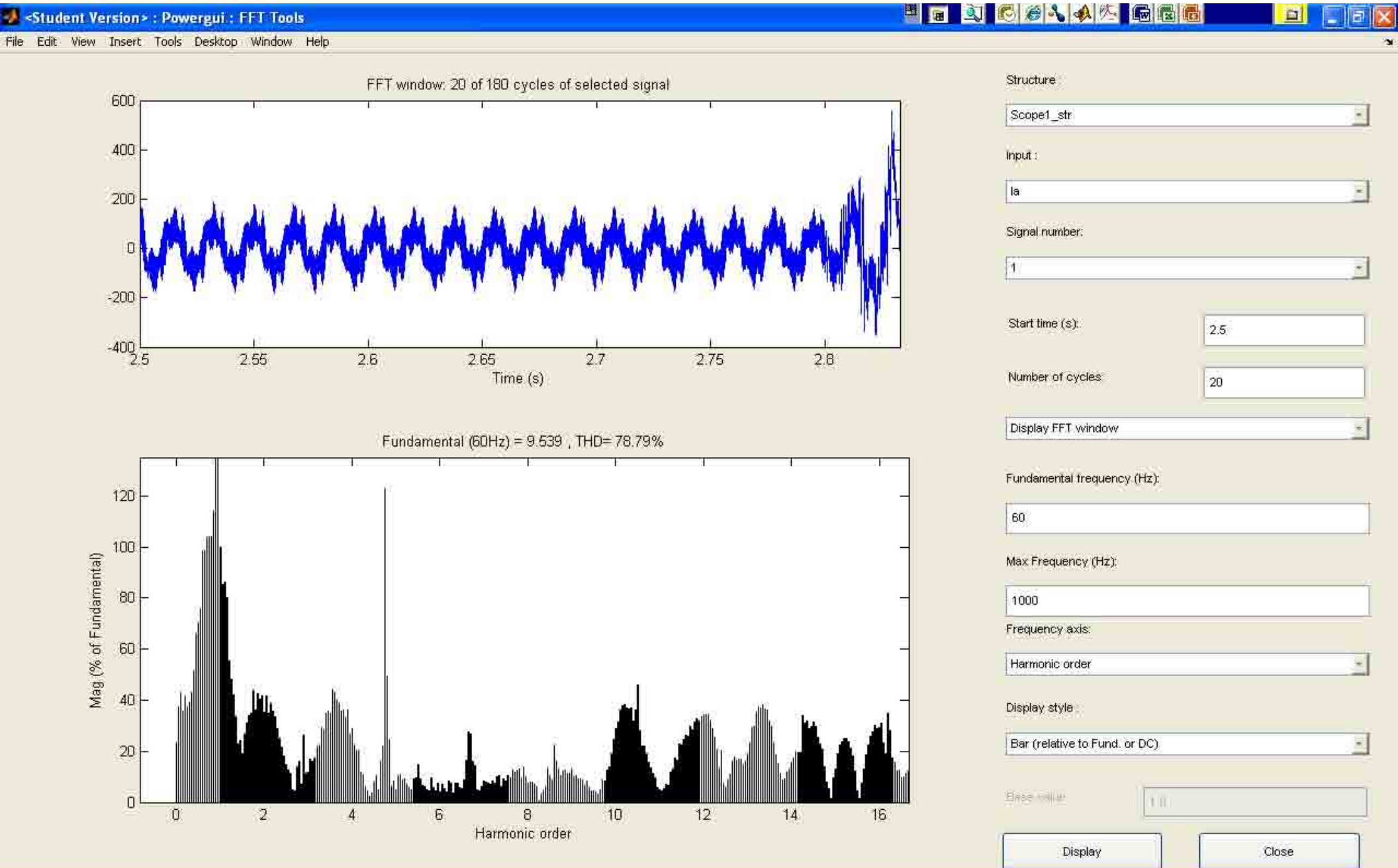


APPENDIX F: MATLAB SIMULATION 4 OUTPUT

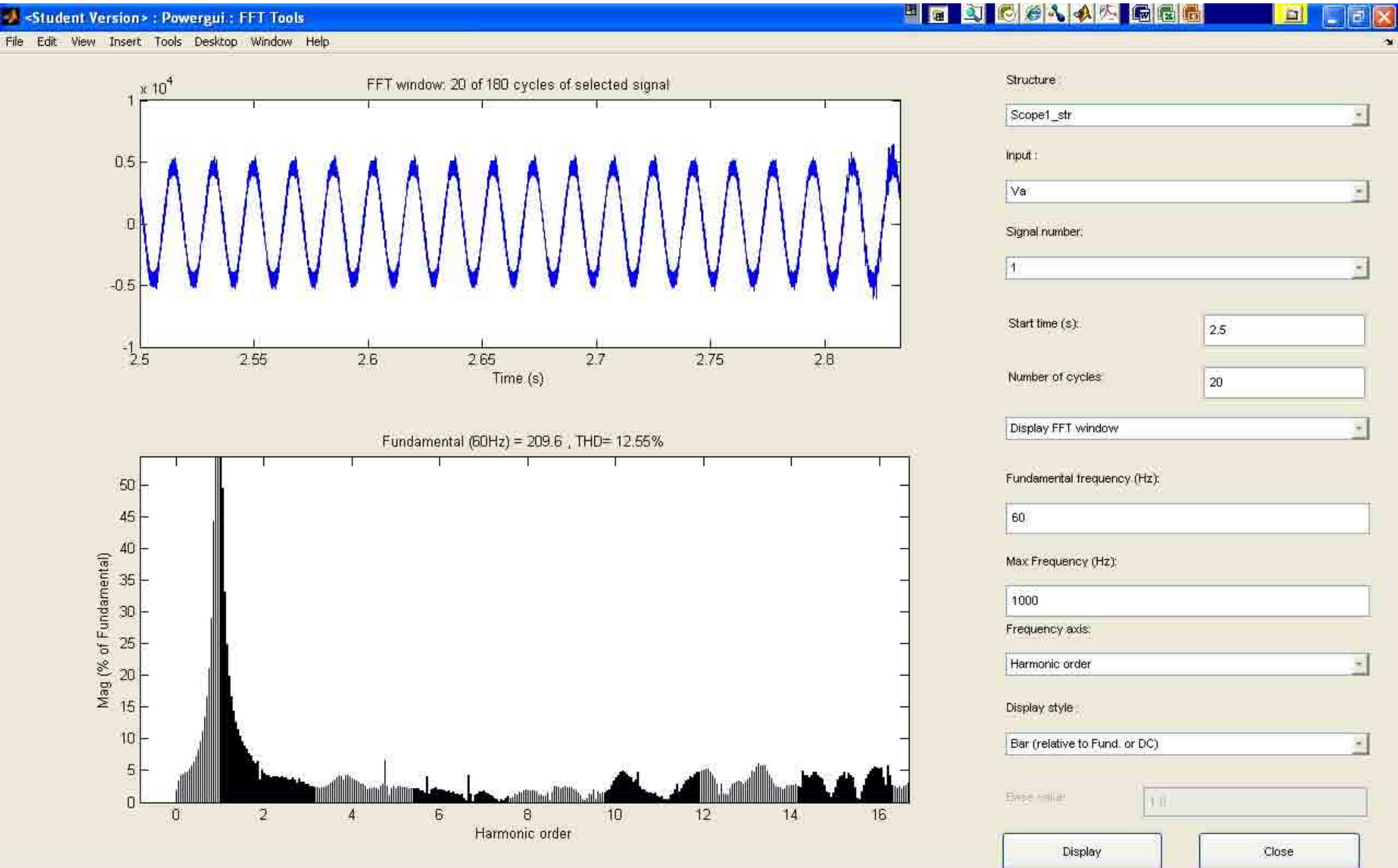




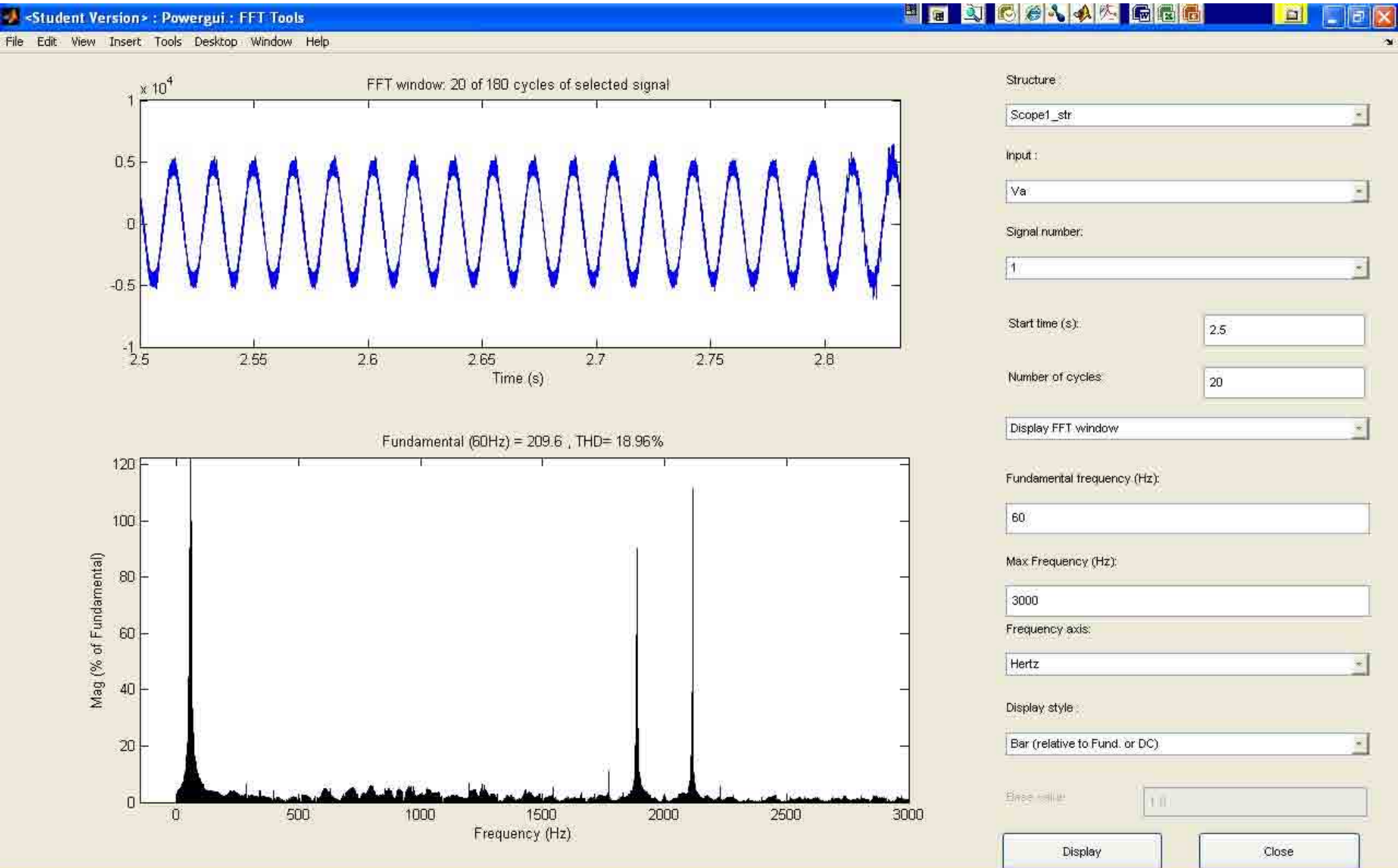
Matlab Simulation 4 Output



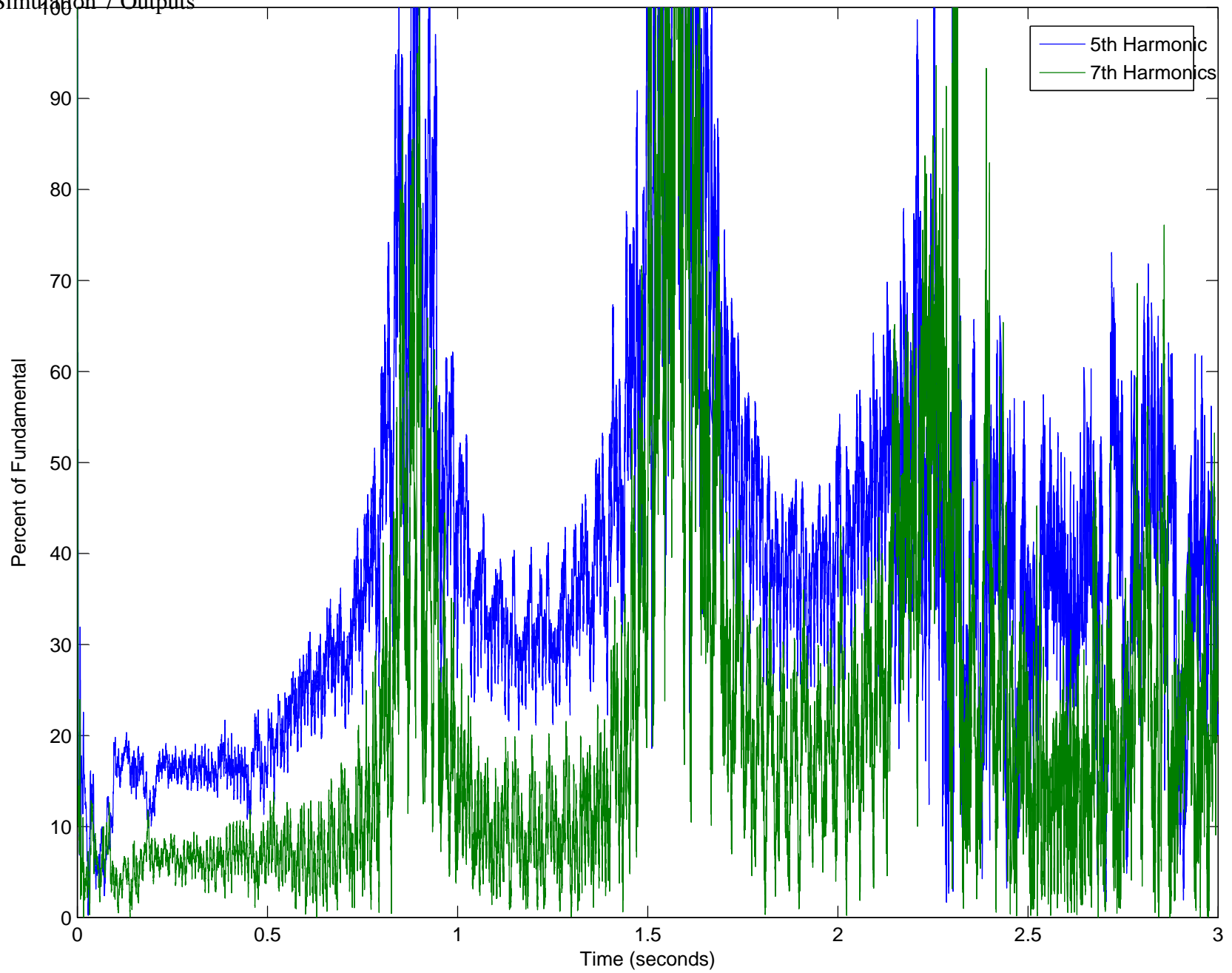
Matlab Simulation 4 Output

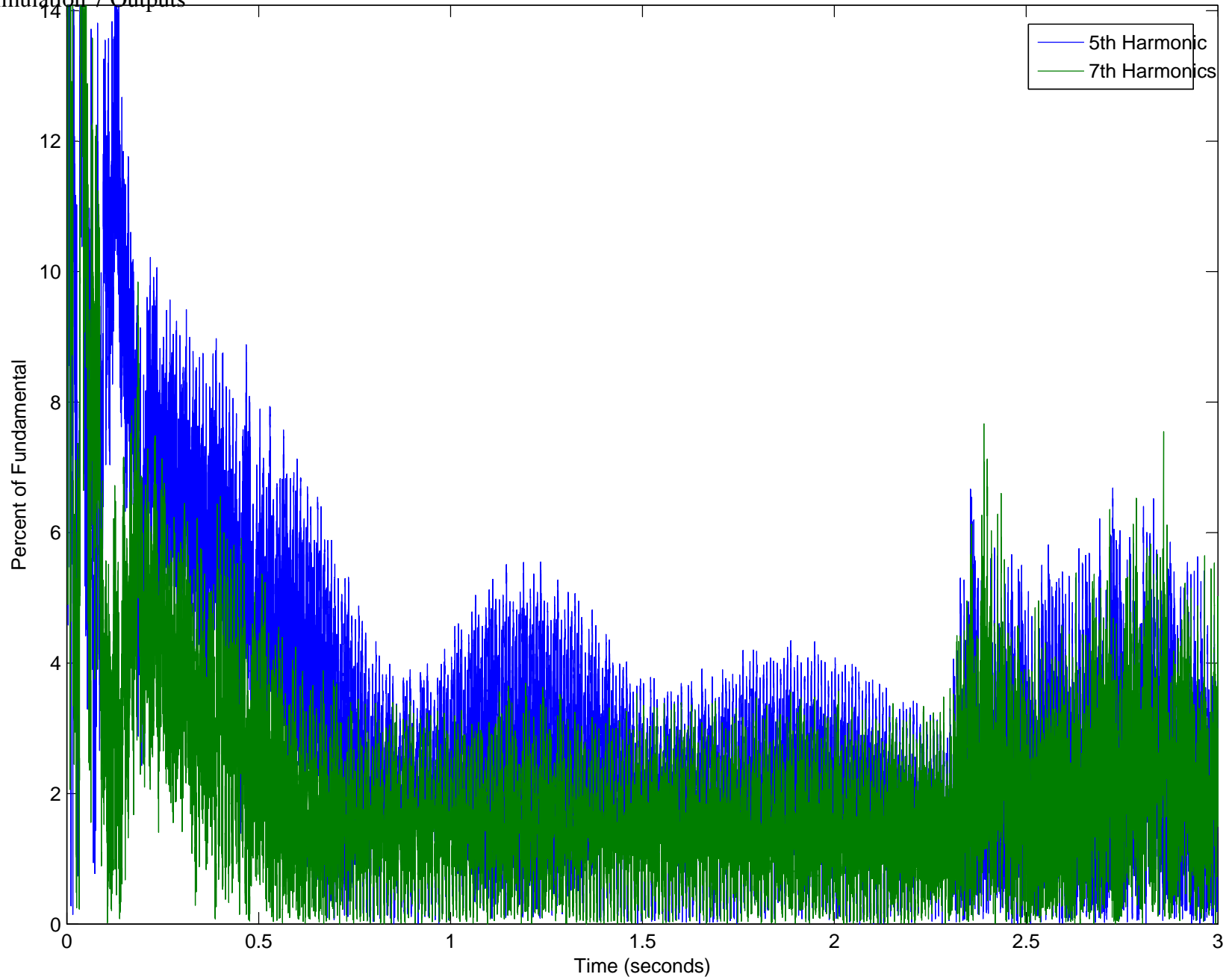


Matlab Simulation 4 Output



APPENDIX G: MATLAB SIMULATION 5 OUTPUT



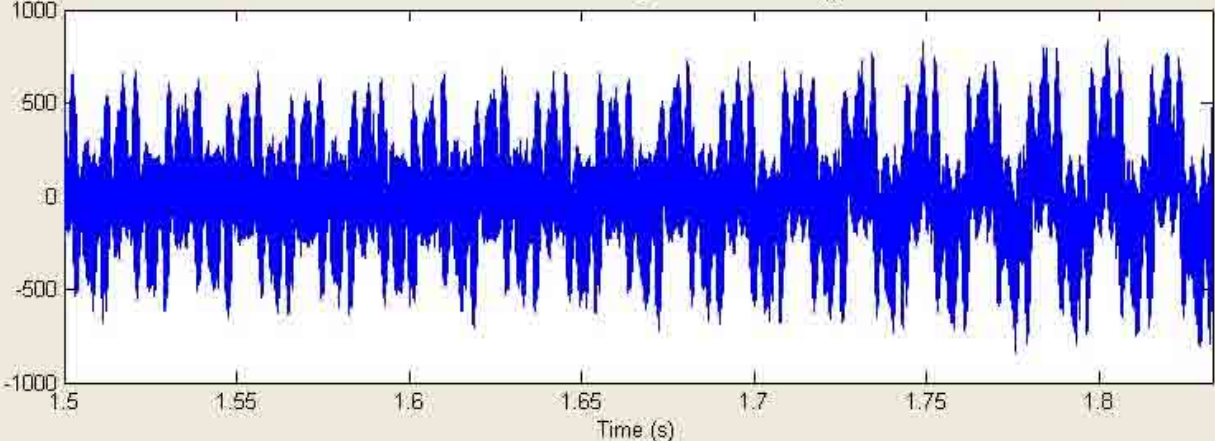


Matlab Simulation 5 Outputs

<Student Version> : Powergui : FFT Tools

File Edit View Insert Tools Desktop Window Help

FFT window: 20 of 180 cycles of selected signal



Time (s)

Structure: Scope1_str

Input: Ia

Signal number: 1

Start time (s): 1.5

Number of cycles: 20

Display FFT window

Fundamental frequency (Hz): 60

Max Frequency (Hz): 300

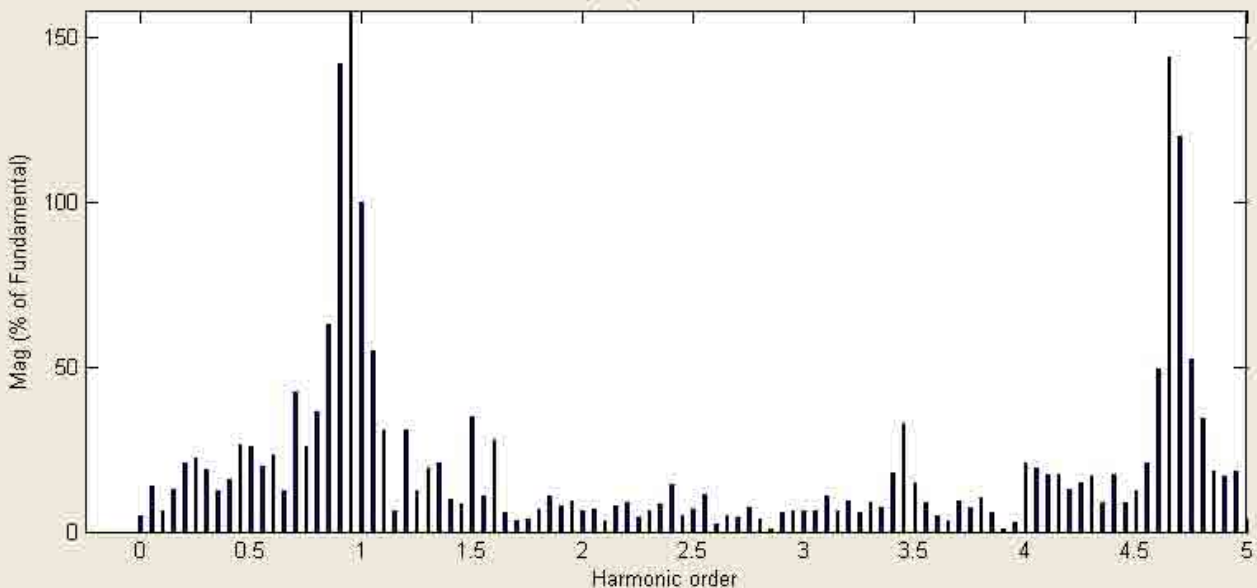
Frequency axis: Harmonic order

Display style: Bar (relative to Fund. or DC)

Base value: 1.0

Display Close

Fundamental (60Hz) = 26.86 , THD= 22.49%



Mag (% of Fundamental)

Harmonic order

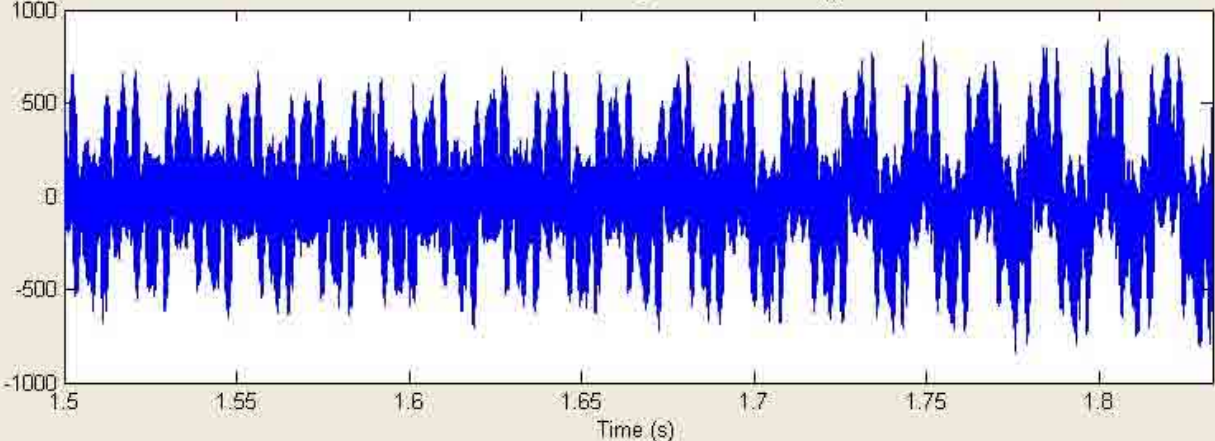
Detailed description: The image shows a screenshot of the MATLAB 'FFT Tools' interface. The top plot is a time-domain waveform of a signal, labeled 'FFT window: 20 of 180 cycles of selected signal'. The x-axis is 'Time (s)' ranging from 1.5 to 1.8, and the y-axis ranges from -1000 to 1000. The signal is a complex periodic waveform. The bottom plot is a harmonic spectrum plot showing 'Mag (% of Fundamental)' on the y-axis (0 to 150) and 'Harmonic order' on the x-axis (0 to 5). The plot shows a dominant peak at the 1st harmonic (60 Hz) and several other significant peaks at higher harmonic orders. The text above the plot indicates 'Fundamental (60Hz) = 26.86 , THD= 22.49%'. On the right side, there is a control panel with various settings: 'Structure' (Scope1_str), 'Input' (Ia), 'Signal number' (1), 'Start time (s)' (1.5), 'Number of cycles' (20), 'Display FFT window' (checked), 'Fundamental frequency (Hz)' (60), 'Max Frequency (Hz)' (300), 'Frequency axis' (Harmonic order), 'Display style' (Bar (relative to Fund. or DC)), and 'Base value' (1.0). At the bottom right are 'Display' and 'Close' buttons.

Matlab Simulation 5 Outputs

<Student Version> : Powergui : FFT Tools

File Edit View Insert Tools Desktop Window Help

FFT window: 20 of 180 cycles of selected signal



The top plot shows a time-domain signal. The x-axis is labeled 'Time (s)' and ranges from 1.5 to 1.8. The y-axis ranges from -1000 to 1000. The signal is a complex, periodic waveform with a period of approximately 0.05 seconds. The amplitude varies between approximately -800 and 800.

Structure: Scope1_str

Input: Ia

Signal number: 1

Start time (s): 1.5

Number of cycles: 20

Display FFT window

Fundamental frequency (Hz): 60

Max Frequency (Hz): 1000

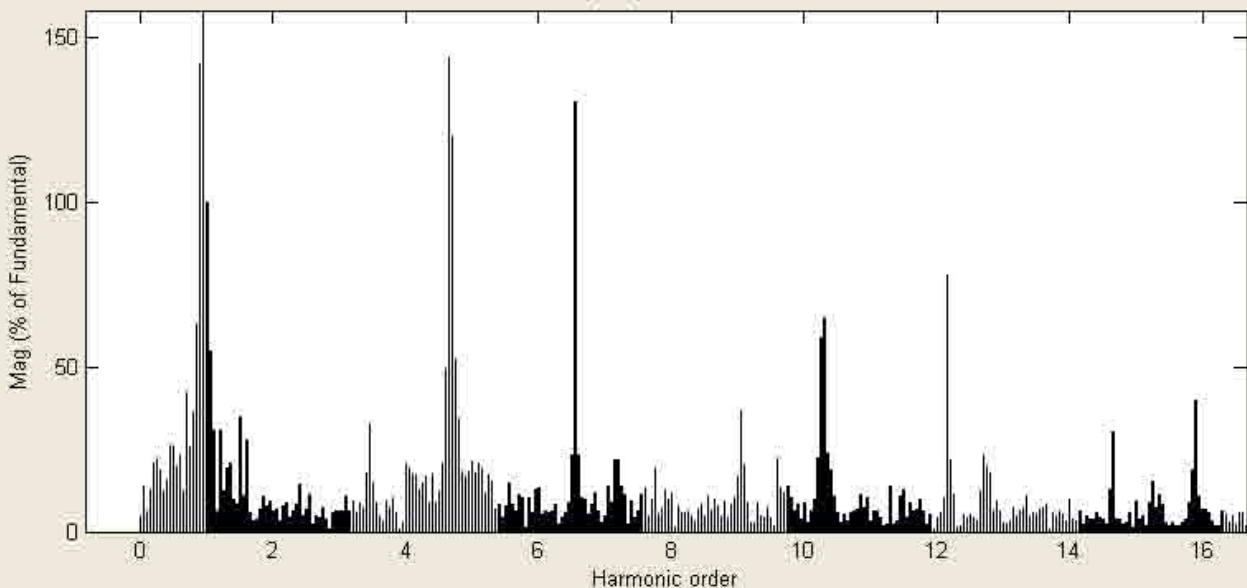
Frequency axis: Harmonic order

Display style: Bar (relative to Fund. or DC)

Base value: 1.0

Display Close

Fundamental (60Hz) = 26.86 , THD= 43.78%



The bottom plot shows the harmonic spectrum. The x-axis is labeled 'Harmonic order' and ranges from 0 to 16. The y-axis is labeled 'Mag (% of Fundamental)' and ranges from 0 to 150. The plot shows a series of peaks representing harmonics. The fundamental frequency (60 Hz) is the highest peak at approximately 150%. The total harmonic distortion (THD) is 43.78%.

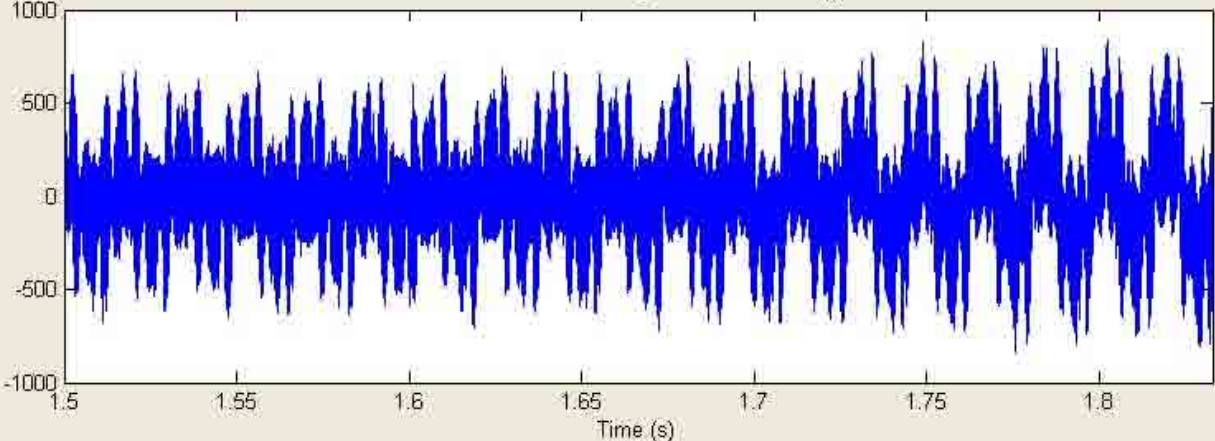
Harmonic order	Mag (% of Fundamental)
1	150
2	~20
3	~40
4	~140
5	~20
6	~130
7	~20
8	~20
9	~35
10	~65
11	~20
12	~75
13	~20
14	~20
15	~30
16	~40

Matlab Simulation 5 Outputs

<Student Version> : Powergui : FFT Tools

File Edit View Insert Tools Desktop Window Help

FFT window: 20 of 180 cycles of selected signal



The top plot shows a time-domain signal. The x-axis is labeled 'Time (s)' and ranges from 1.5 to 1.8. The y-axis ranges from -1000 to 1000. The signal is a complex, periodic waveform with a period of approximately 0.05 seconds. The amplitude varies between approximately -800 and 800.

Structure: Scope1_str

Input: Ia

Signal number: 1

Start time (s): 1.5

Number of cycles: 20

Display FFT window

Fundamental frequency (Hz): 60

Max Frequency (Hz): 3000

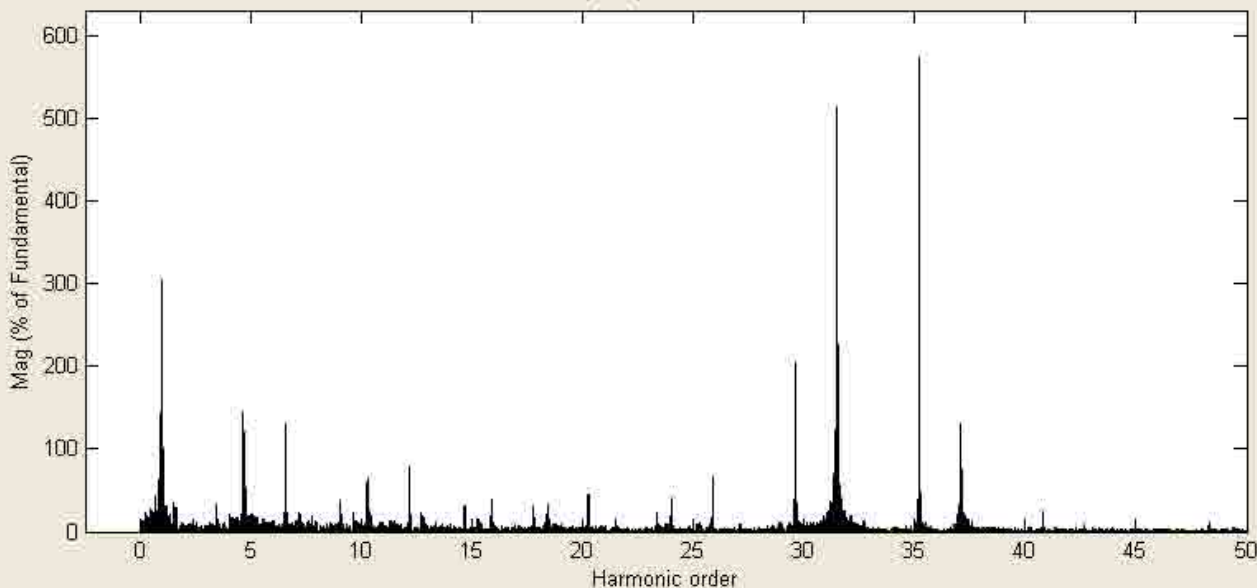
Frequency axis: Harmonic order

Display style: Bar (relative to Fund. or DC)

Base value: 1.0

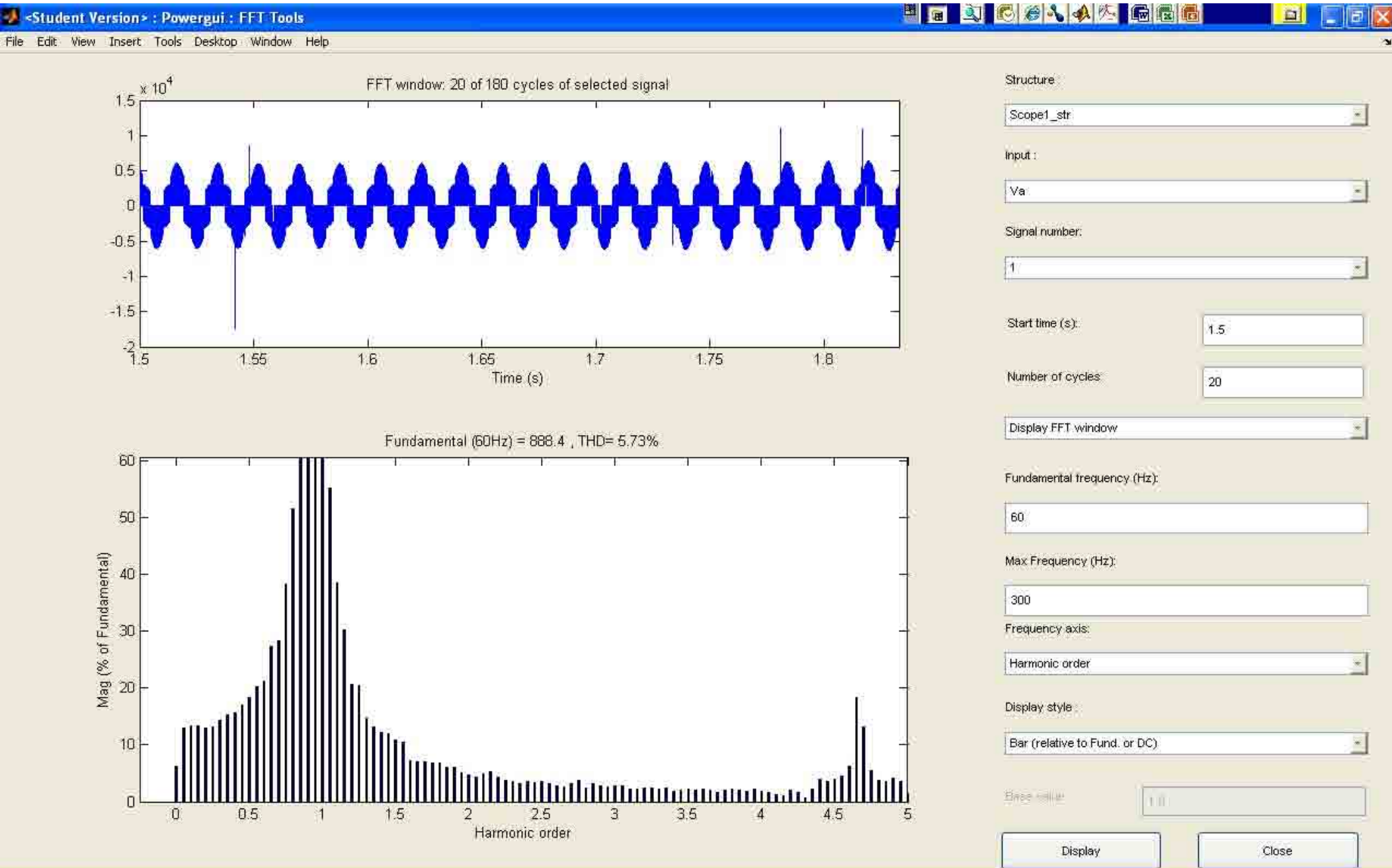
Display Close

Fundamental (60Hz) = 26.86 , THD= 76.88%

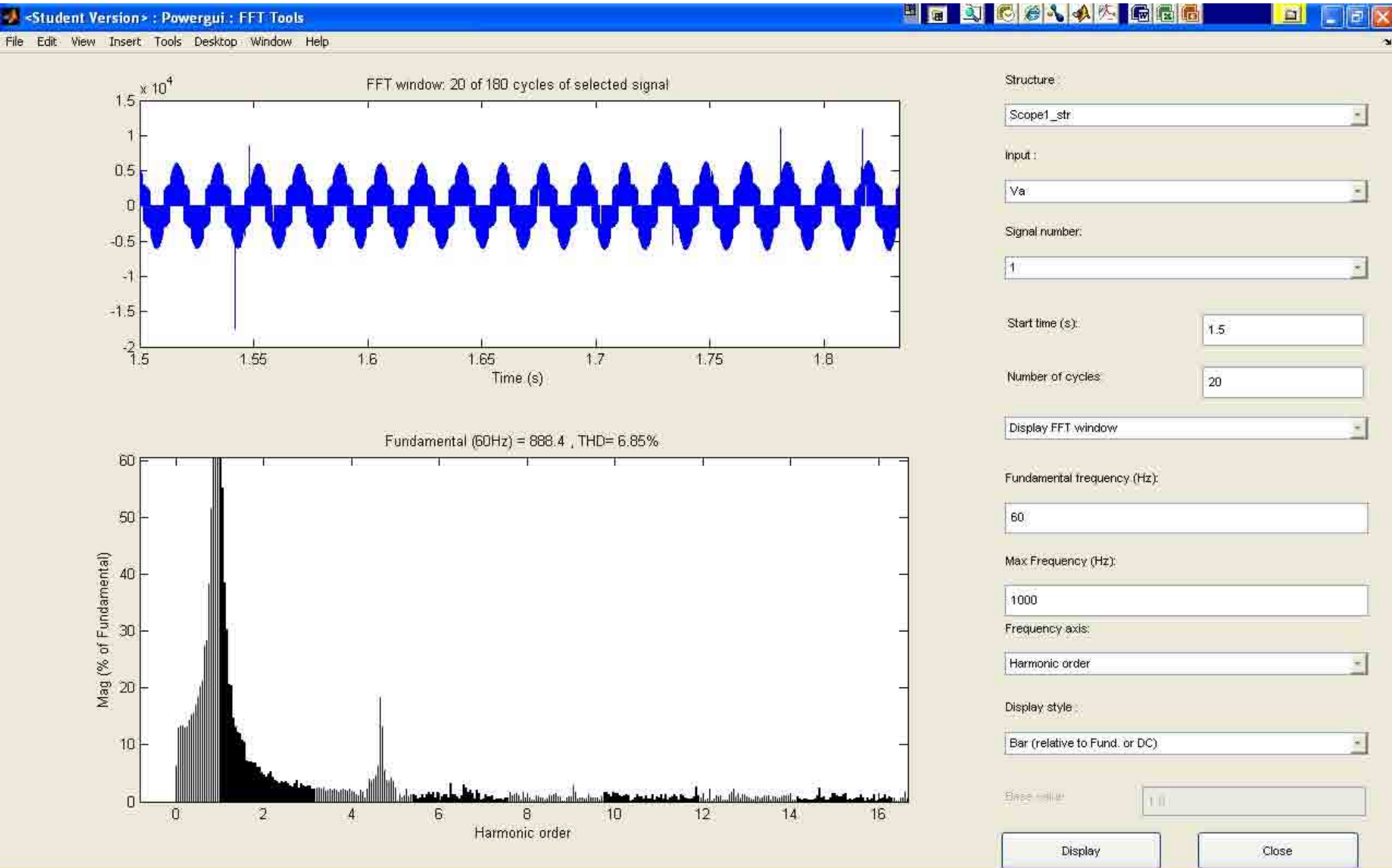


The bottom plot shows the harmonic spectrum. The x-axis is labeled 'Harmonic order' and ranges from 0 to 50. The y-axis is labeled 'Mag (% of Fundamental)' and ranges from 0 to 600. The plot shows a series of discrete peaks representing harmonics. The fundamental frequency (60 Hz) is the most prominent peak, with a magnitude of approximately 580%. The total harmonic distortion (THD) is 76.88%. The plot title indicates 'Fundamental (60Hz) = 26.86 , THD= 76.88%'.

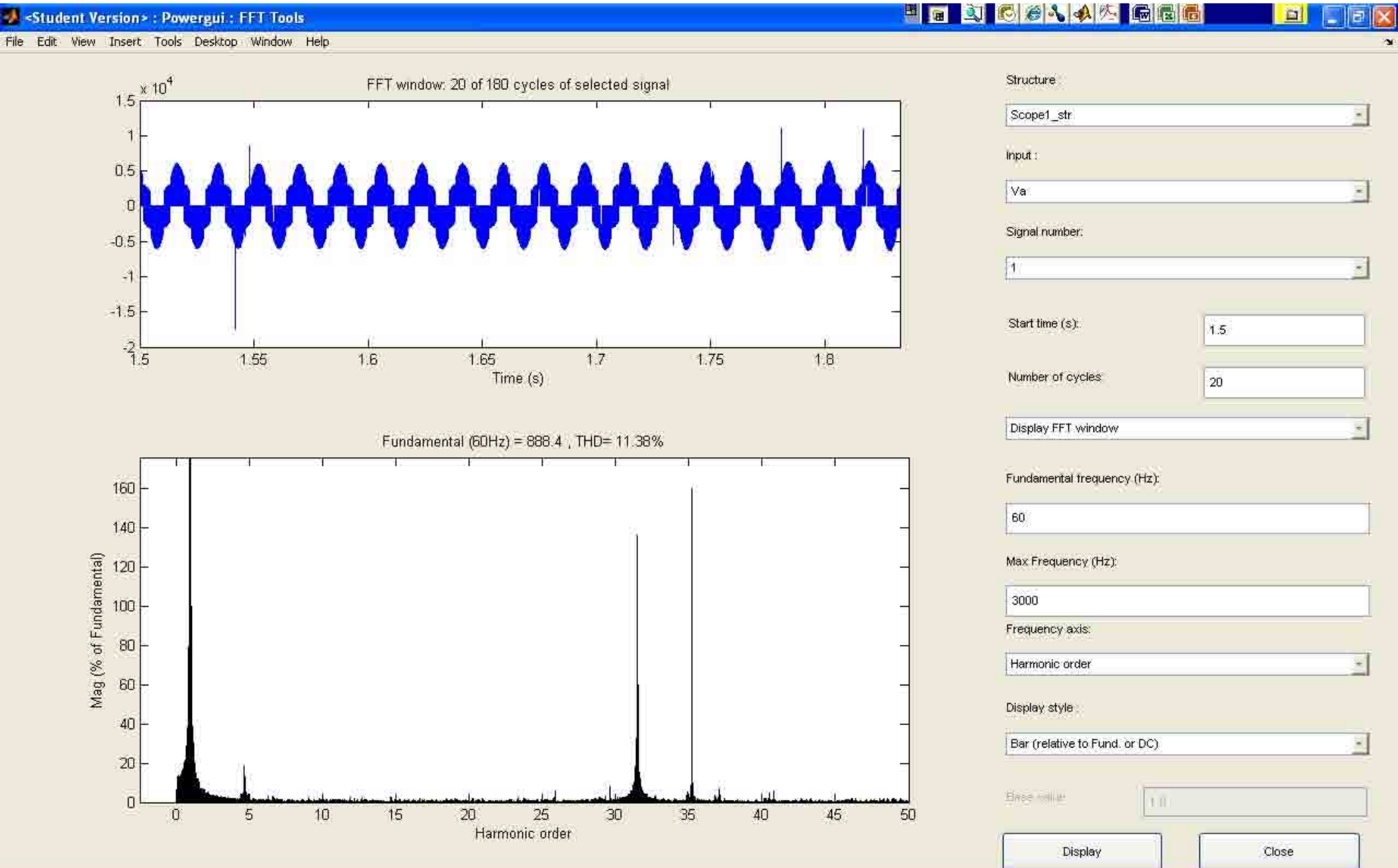
Matlab Simulation 5 Outputs



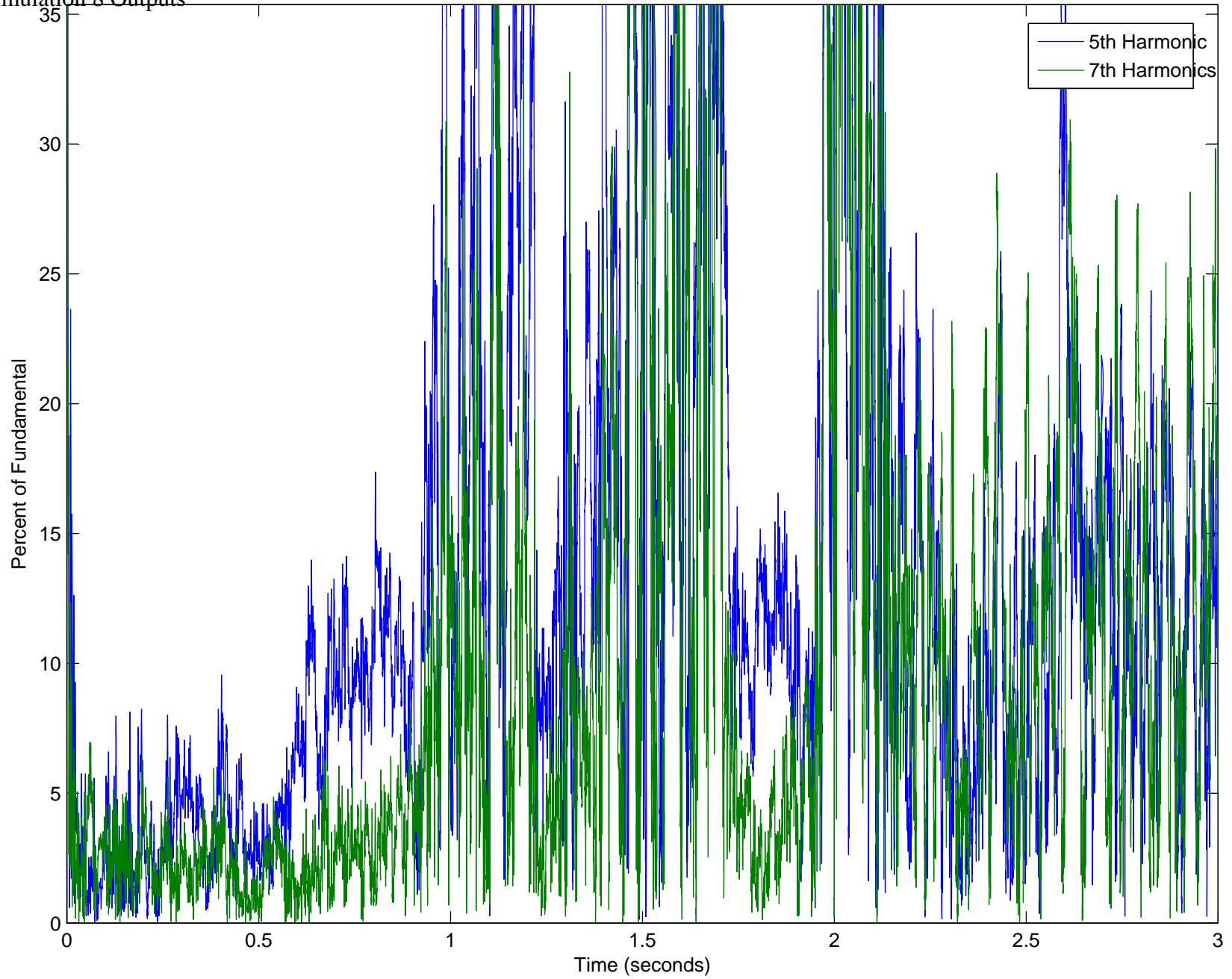
Matlab Simulation 5 Outputs

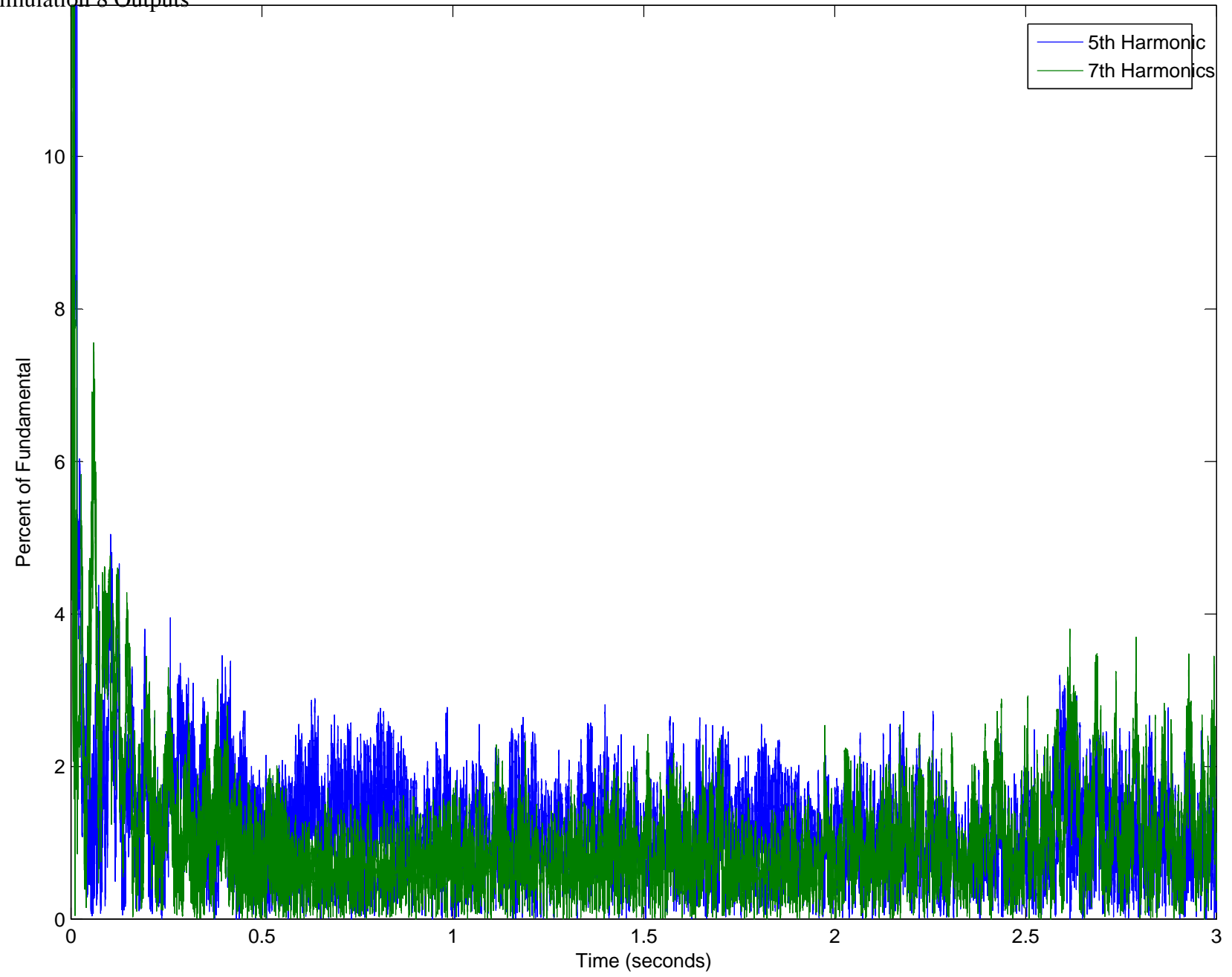


Matlab Simulation 5 Outputs

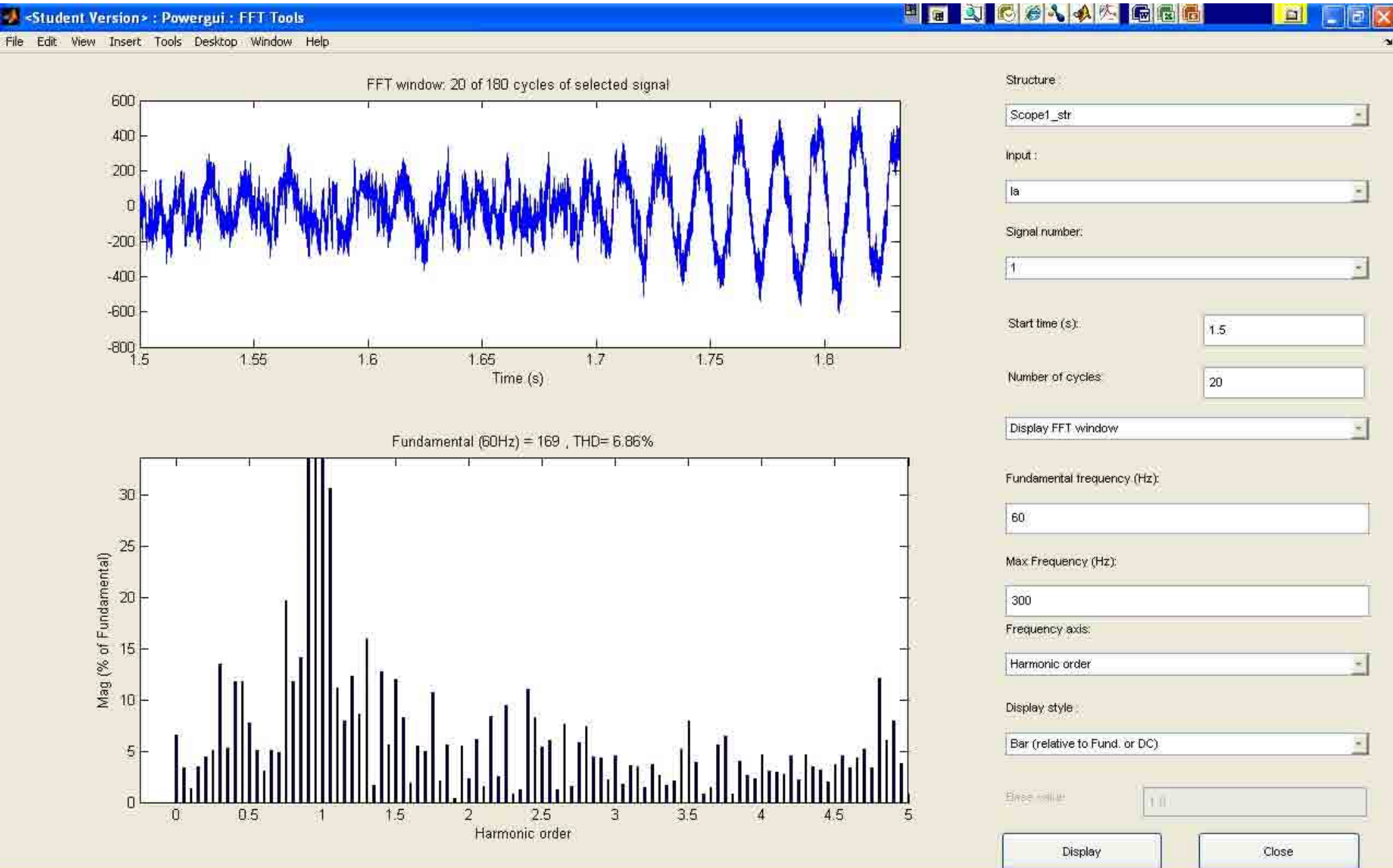


APPENDIX H: MATLAB SIMULATION 6 OUTPUT

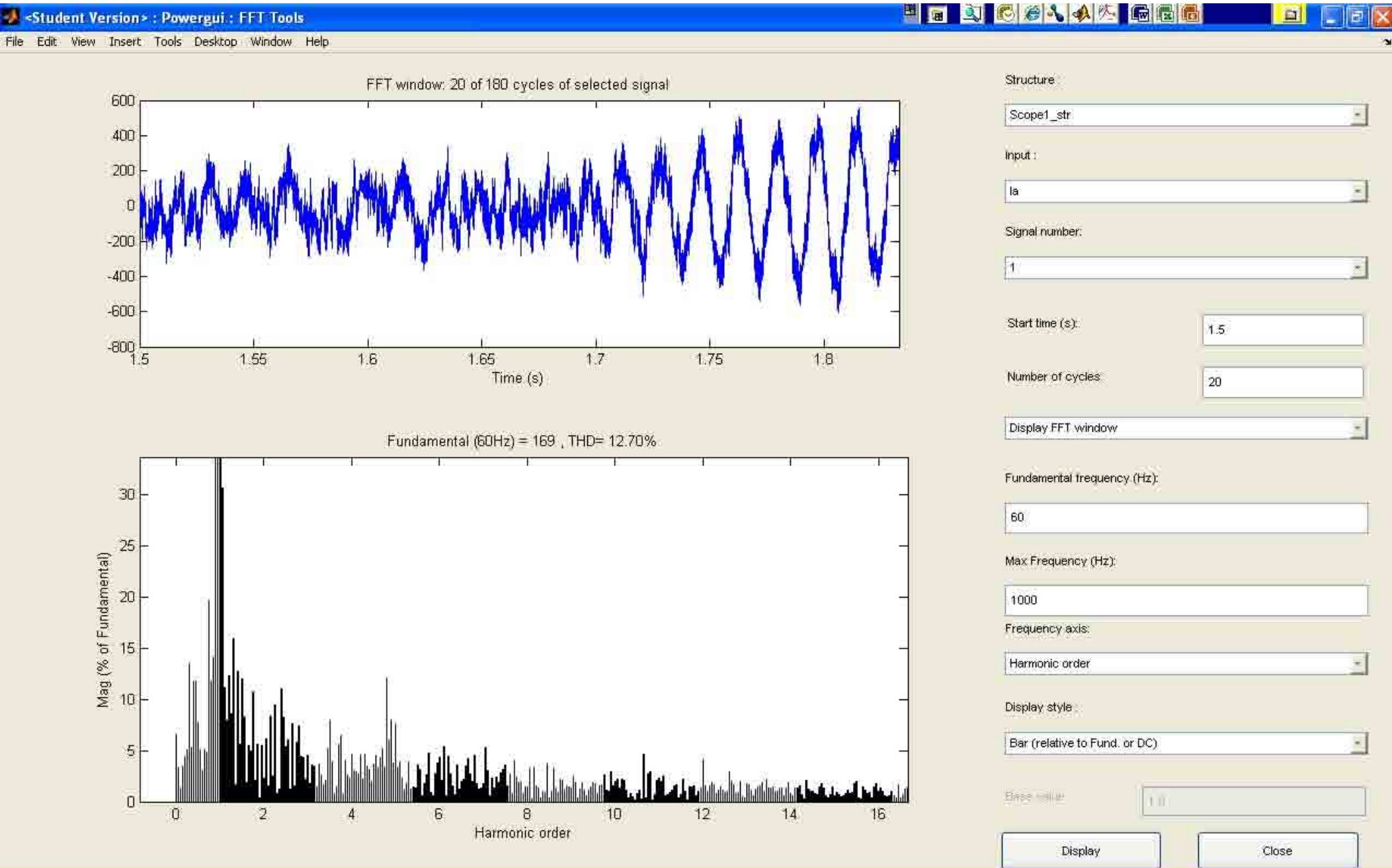




Matlab Simulation 6 Outputs



Matlab Simulation 6 Outputs

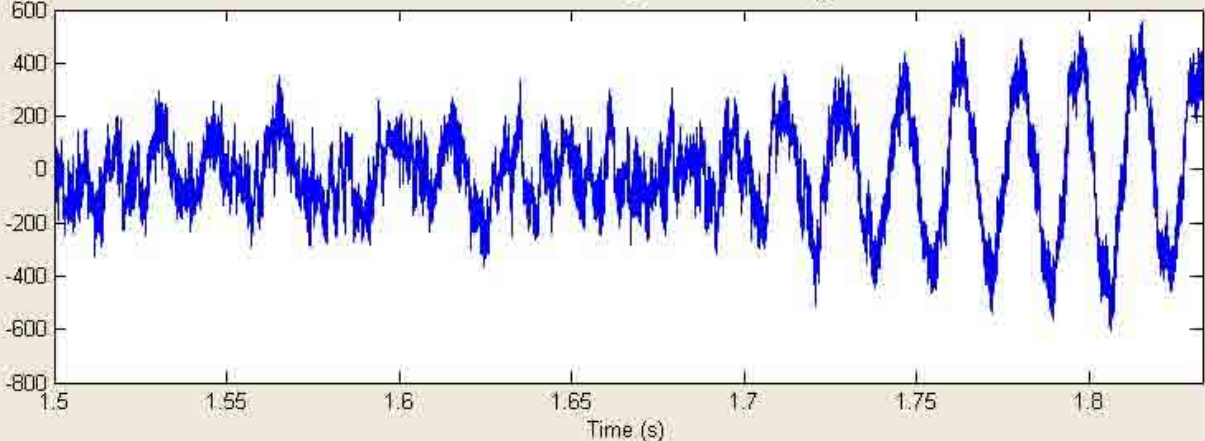


Matlab Simulation 6 Outputs

<Student Version> : Powergui : FFT Tools

File Edit View Insert Tools Desktop Window Help

FFT window: 20 of 180 cycles of selected signal



Time (s)

Structure: Scope1_str

Input: Ia

Signal number: 1

Start time (s): 1.5

Number of cycles: 20

Display FFT window

Fundamental frequency (Hz): 60

Max Frequency (Hz): 3000

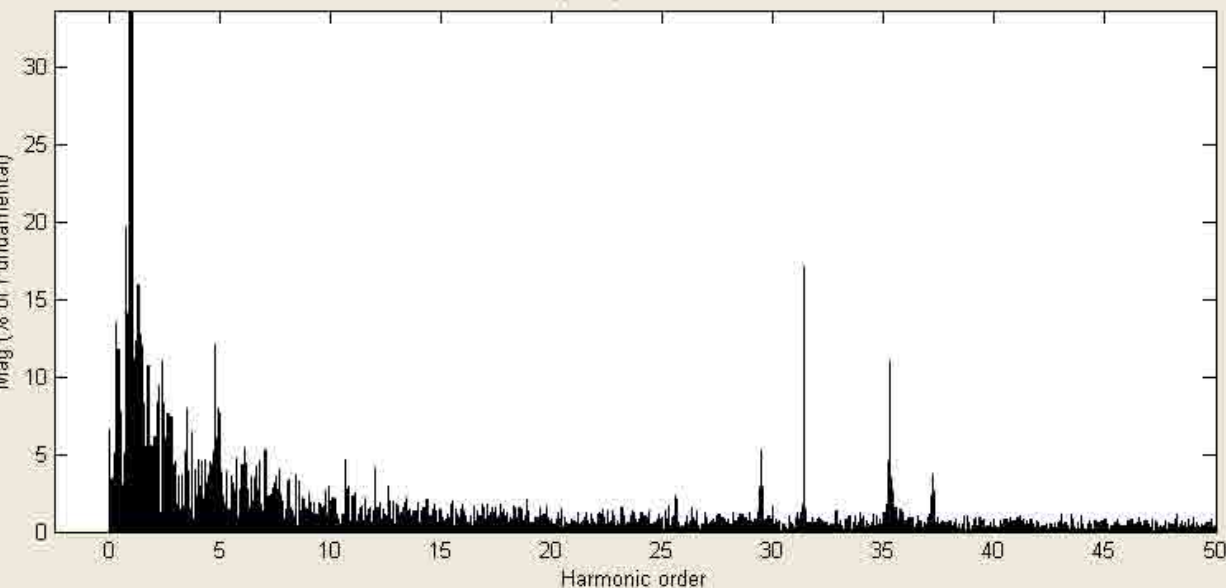
Frequency axis: Harmonic order

Display style: Bar (relative to Fund. or DC)

Base value: 1.0

Display Close

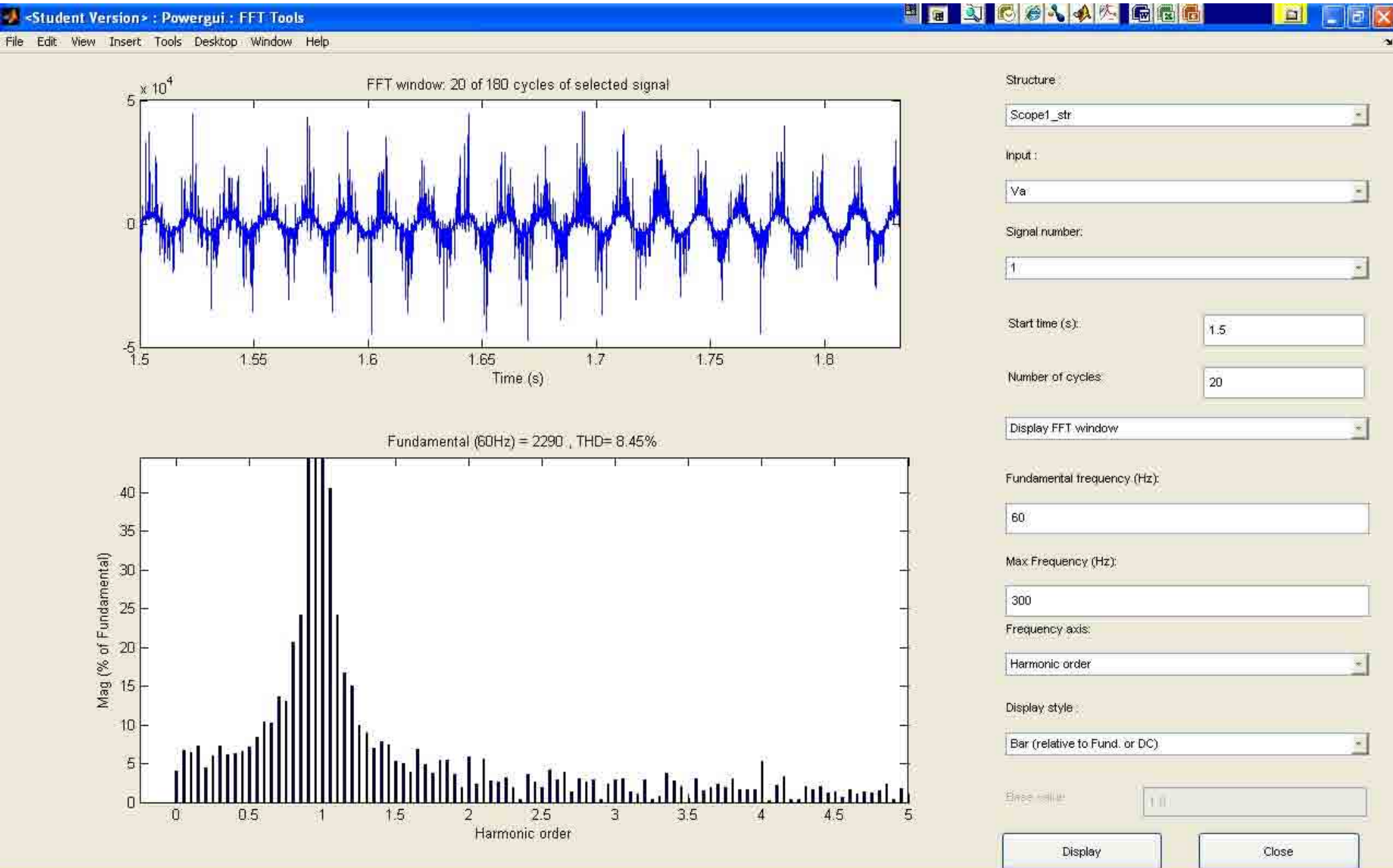
Fundamental (60Hz) = 169 , THD= 13.23%



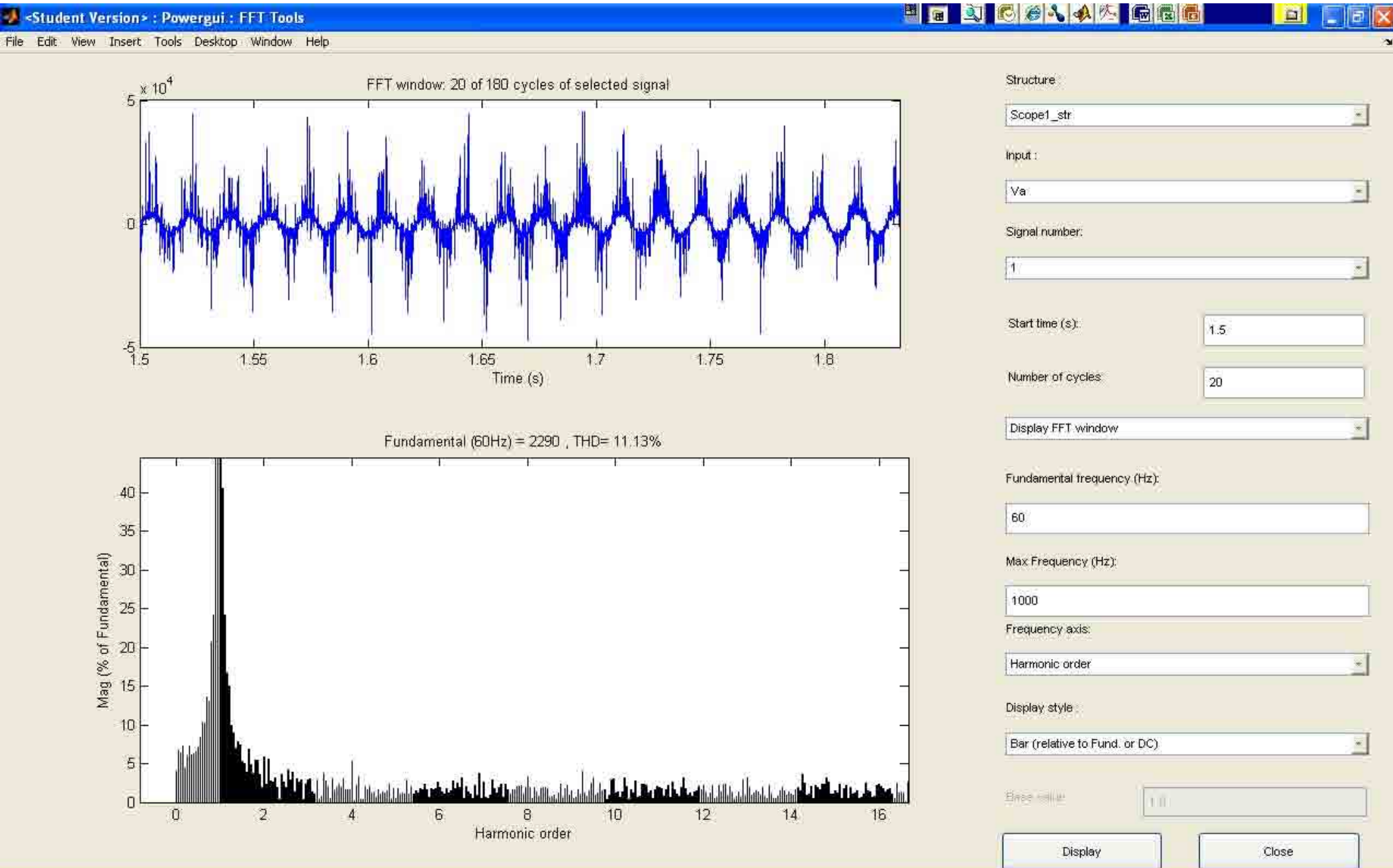
Mag (% of Fundamental)

Harmonic order

Matlab Simulation 6 Outputs



Matlab Simulation 6 Outputs

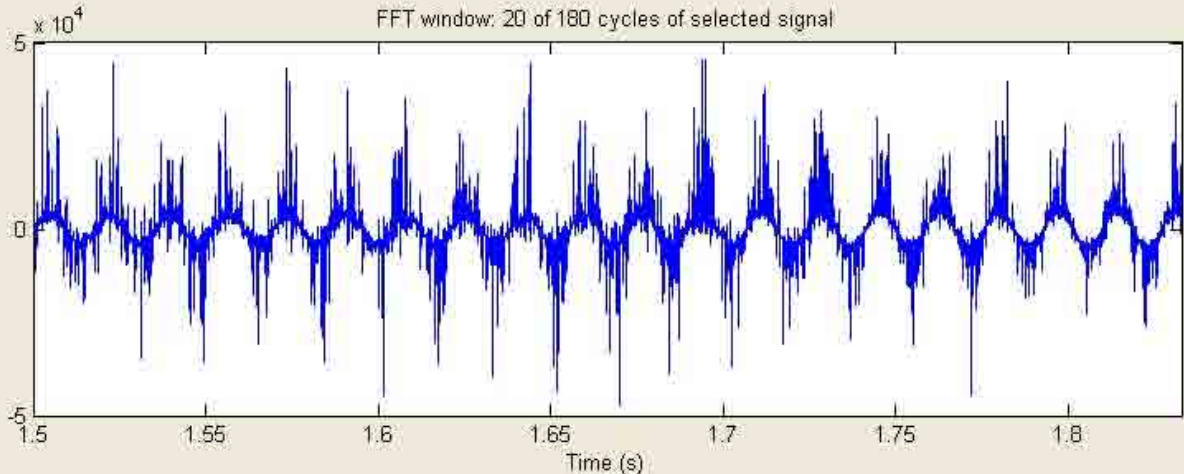


Matlab Simulation 6 Outputs

<Student Version> : Powergui : FFT Tools

File Edit View Insert Tools Desktop Window Help

FFT window: 20 of 180 cycles of selected signal



Structure: Scope1_str

Input: Va

Signal number: 1

Start time (s): 1.5

Number of cycles: 20

Display FFT window

Fundamental frequency (Hz): 60

Max Frequency (Hz): 3000

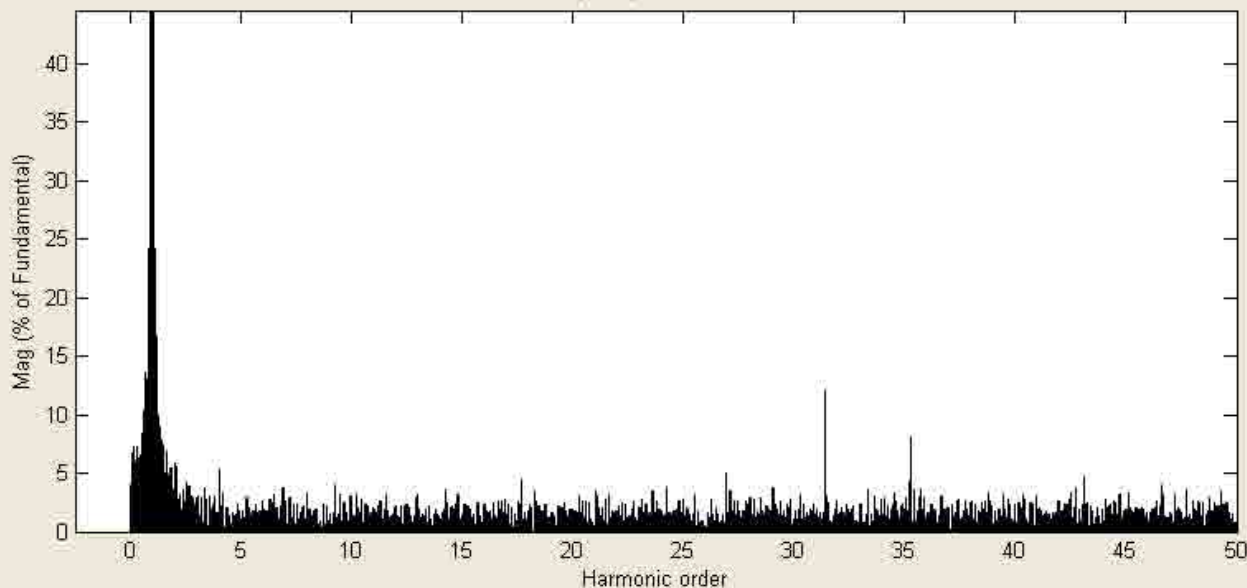
Frequency axis: Harmonic order

Display style: Bar (relative to Fund. or DC)

Base value: 1.0

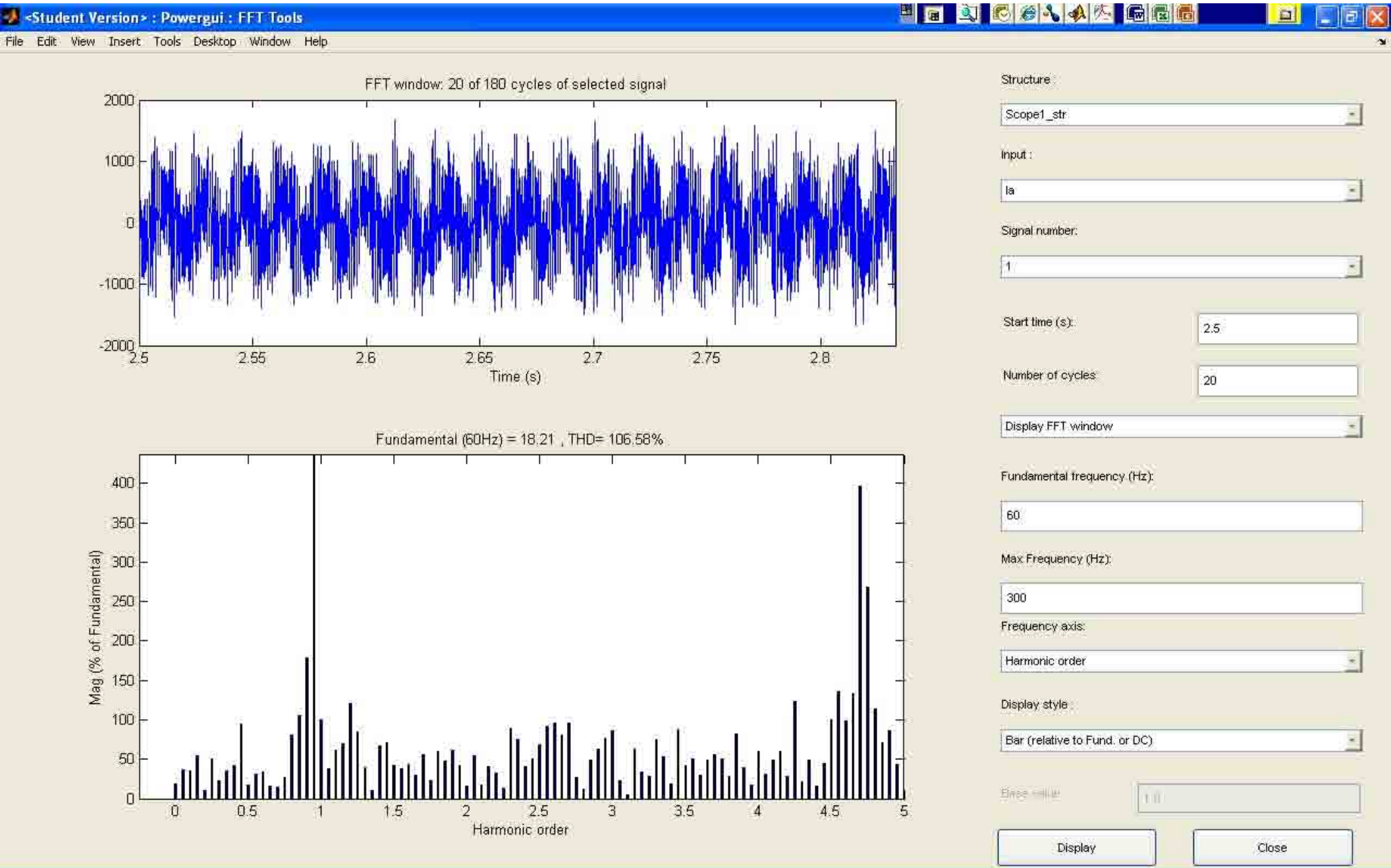
Display Close

Fundamental (60Hz) = 2290 , THD= 14.66%

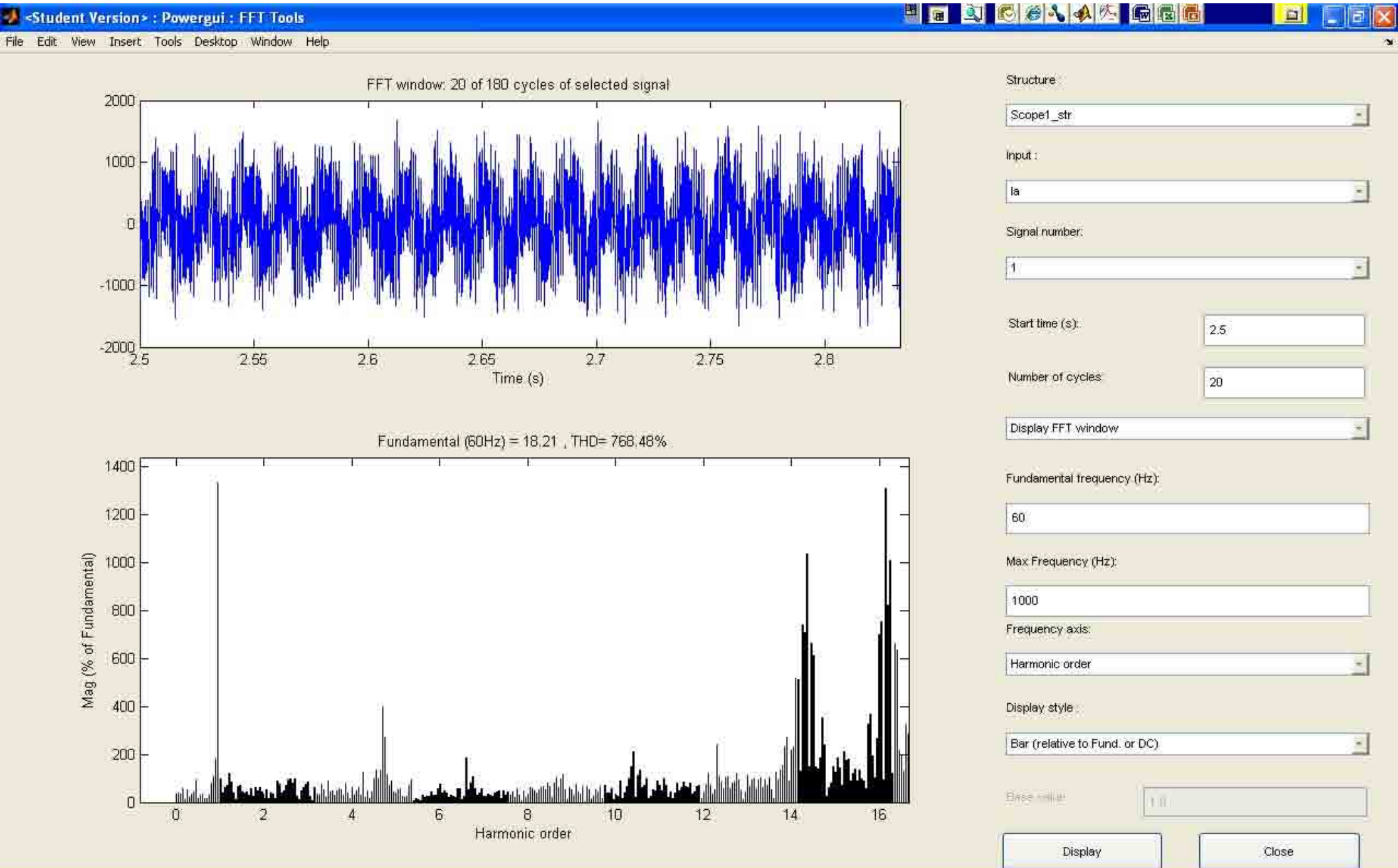


APPENDIX I: MATLAB SIMULATION 7 OUTPUT

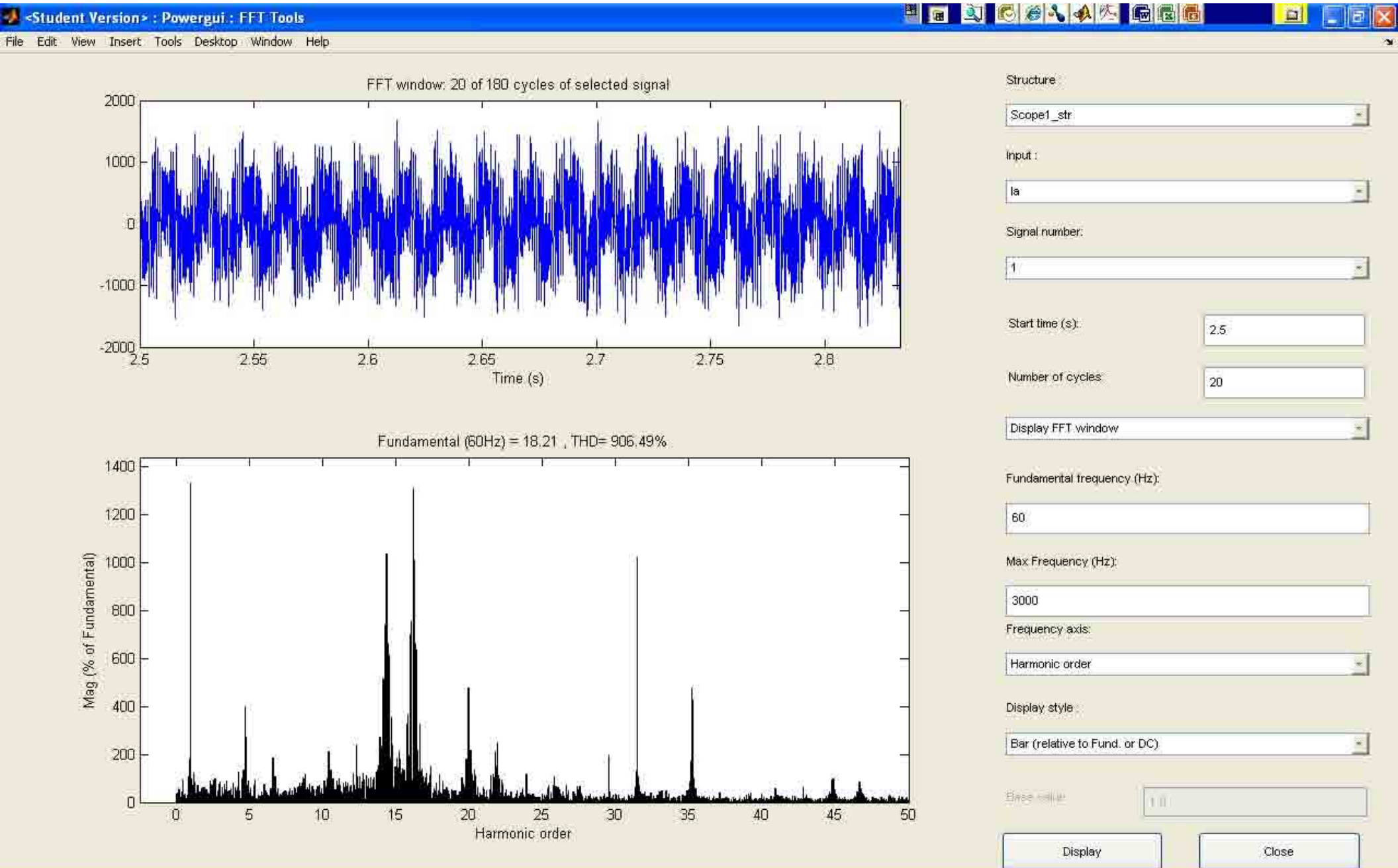
Matlab Simulation 7 Output



Matlab Simulation 7 Output



Matlab Simulation 7 Output

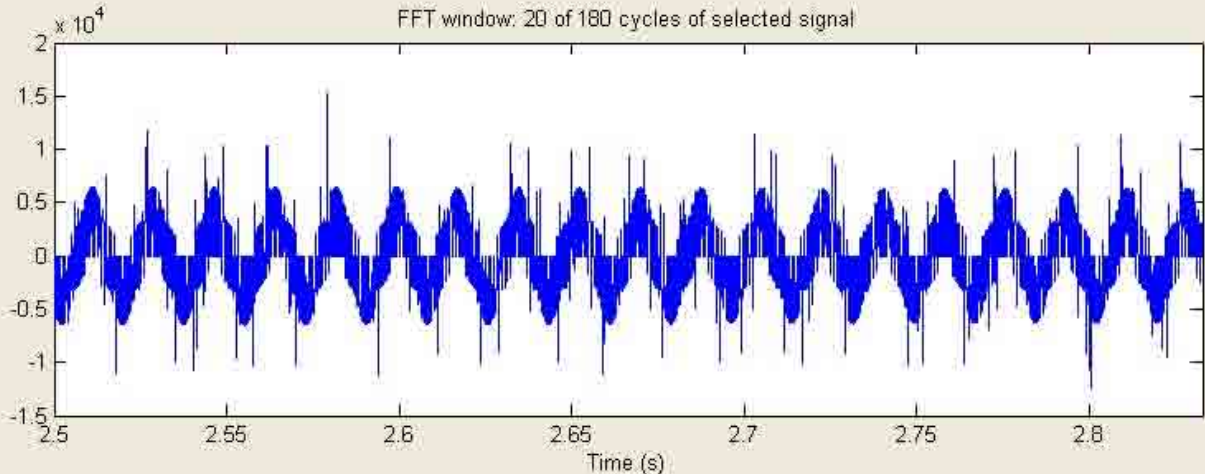


Matlab Simulation 7 Output

<Student Version> : Powergui : FFT Tools

File Edit View Insert Tools Desktop Window Help

FFT window: 20 of 180 cycles of selected signal



Structure: Scope1_str

Input: Va

Signal number: 1

Start time (s): 2.5

Number of cycles: 20

Display FFT window

Fundamental frequency (Hz): 60

Max Frequency (Hz): 300

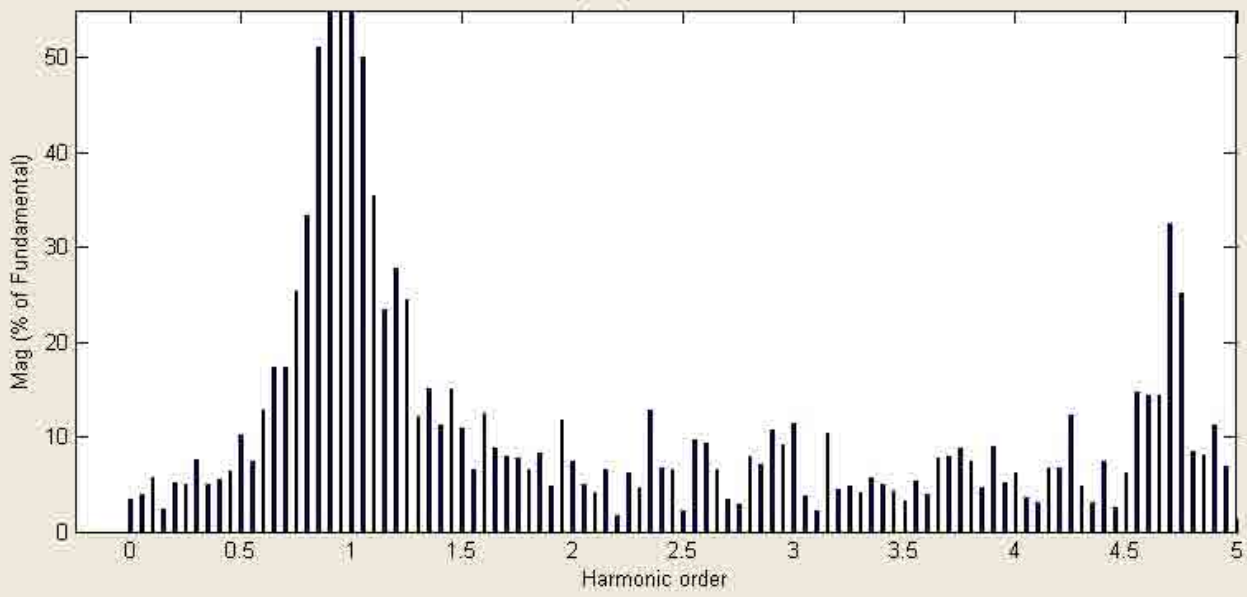
Frequency axis: Harmonic order

Display style: Bar (relative to Fund. or DC)

Base value: 1.0

Display Close

Fundamental (60Hz) = 423.7 , THD= 14.97%

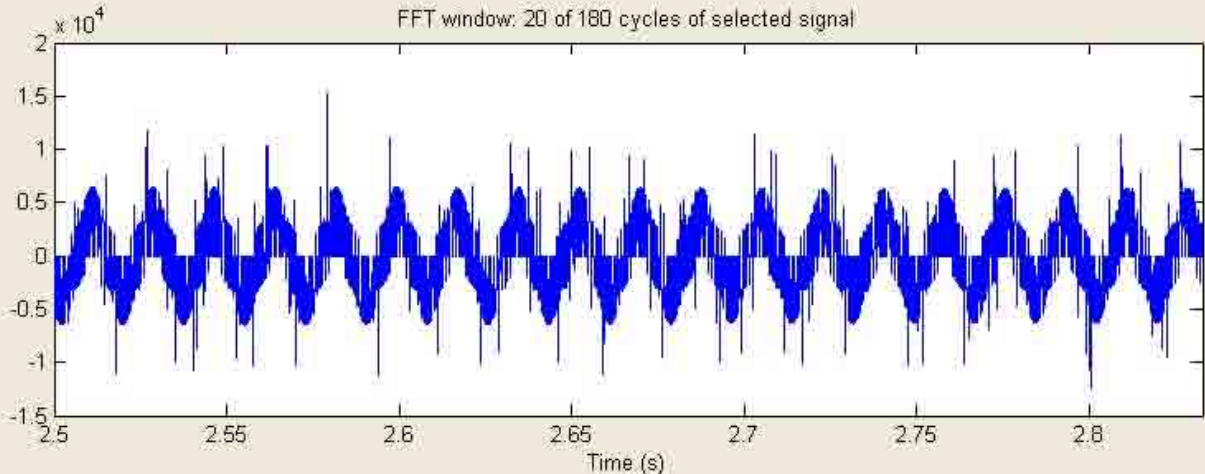


Matlab Simulation 7 Output

<Student Version> : Powergui : FFT Tools

File Edit View Insert Tools Desktop Window Help

FFT window: 20 of 180 cycles of selected signal



Structure: Scope1_str

Input: Va

Signal number: 1

Start time (s): 2.5

Number of cycles: 20

Display FFT window

Fundamental frequency (Hz): 60

Max Frequency (Hz): 1000

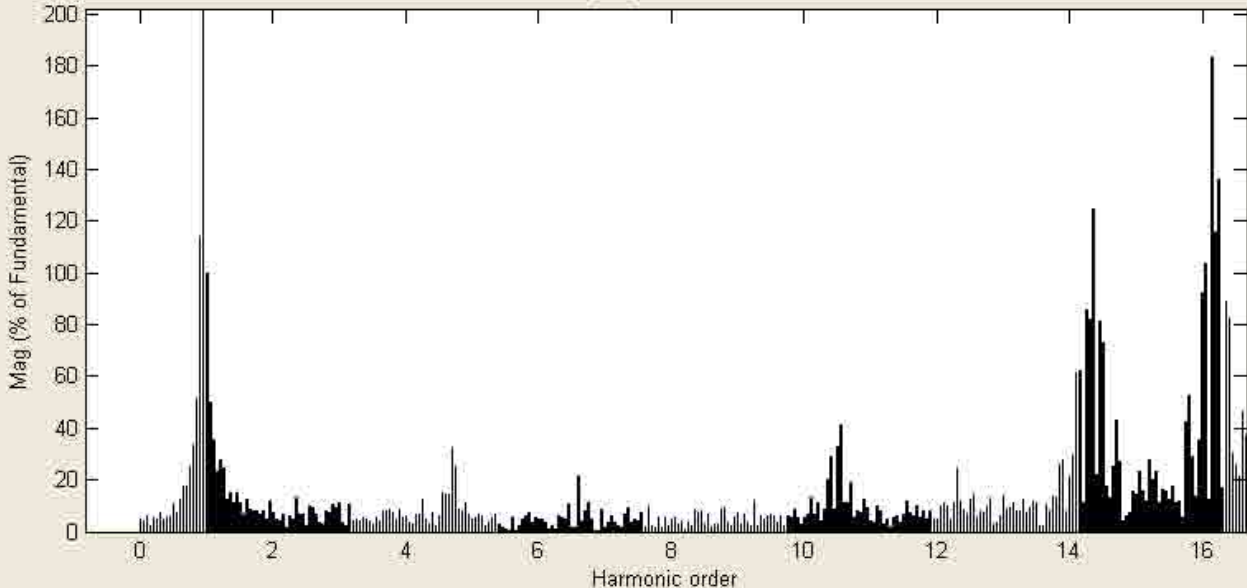
Frequency axis: Harmonic order

Display style: Bar (relative to Fund. or DC)

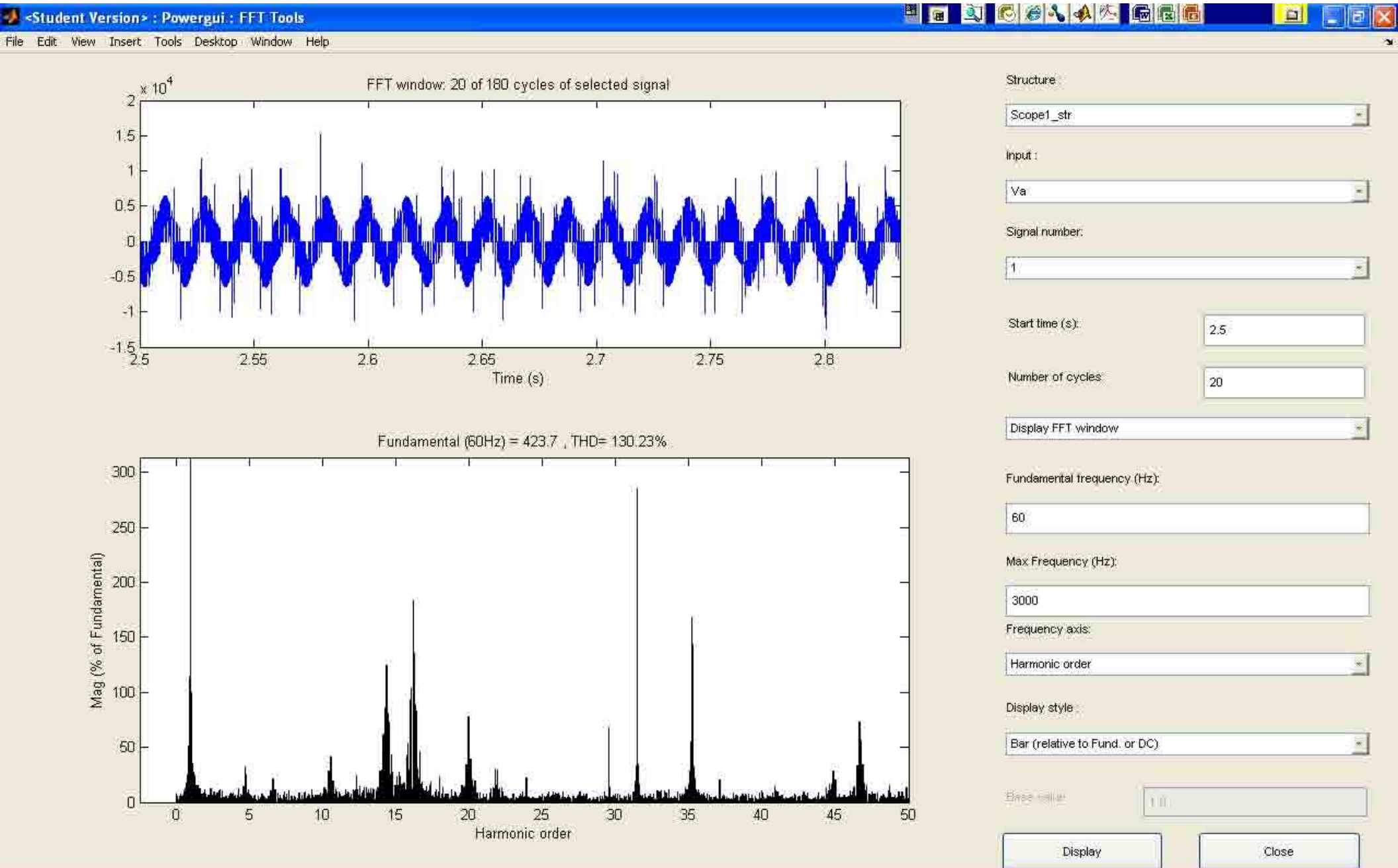
Base value: 1

Display Close

Fundamental (60Hz) = 423.7 , THD= 98.80%

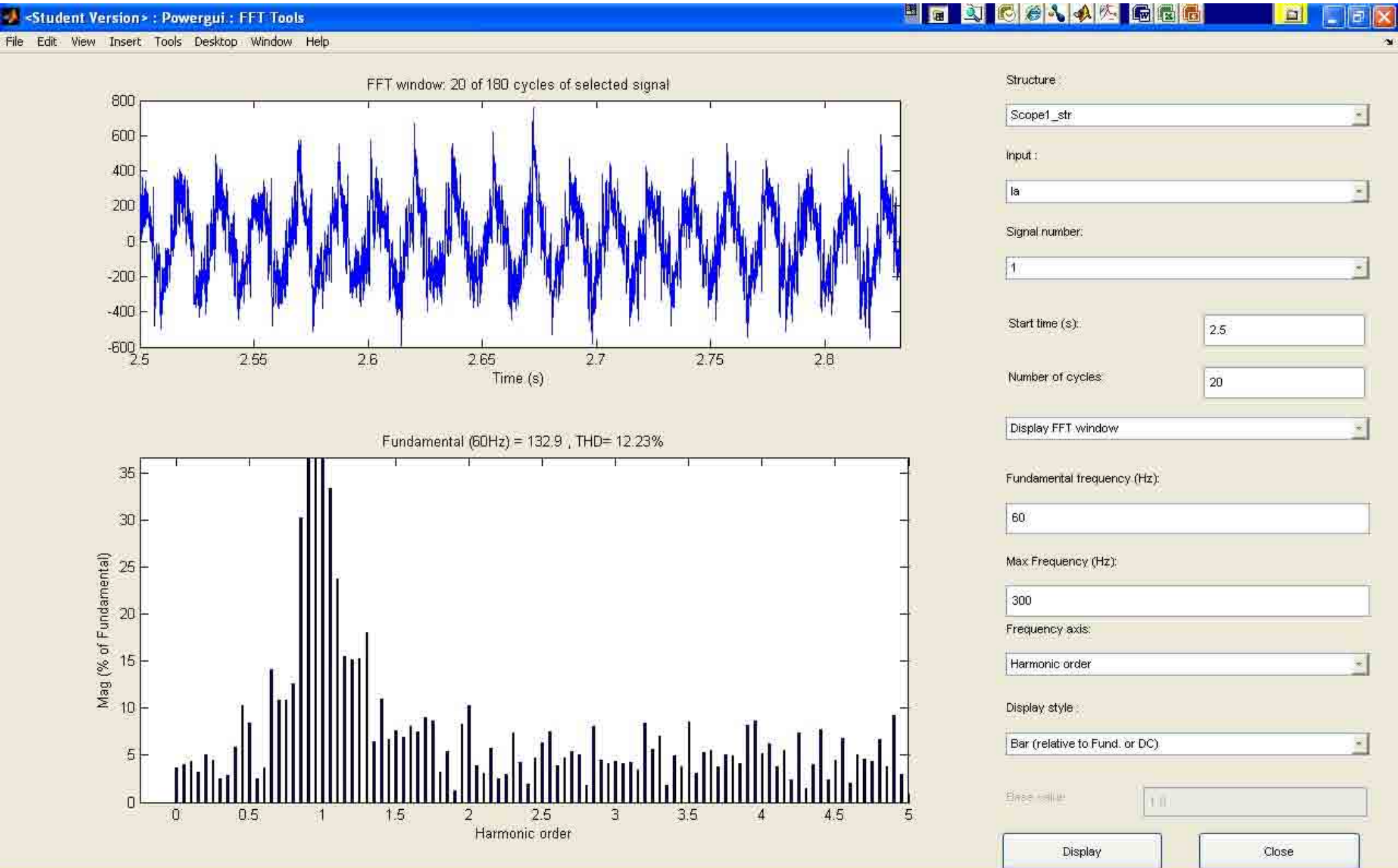


Matlab Simulation 7 Output



APPENDIX J: MATLAB SIMULATION 8 OUTPUT

Matlab Simulation 8 Output

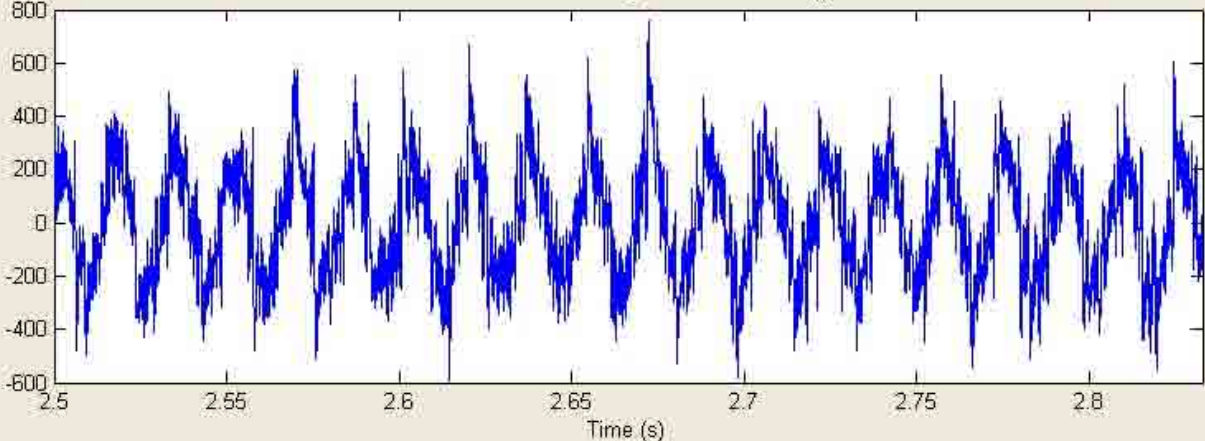


Matlab Simulation 8 Output

<Student Version> : Powergui : FFT Tools

File Edit View Insert Tools Desktop Window Help

FFT window: 20 of 180 cycles of selected signal



Time (s)

Structure: Scope1_str

Input: Ia

Signal number: 1

Start time (s): 2.5

Number of cycles: 20

Display FFT window

Fundamental frequency (Hz): 60

Max Frequency (Hz): 1000

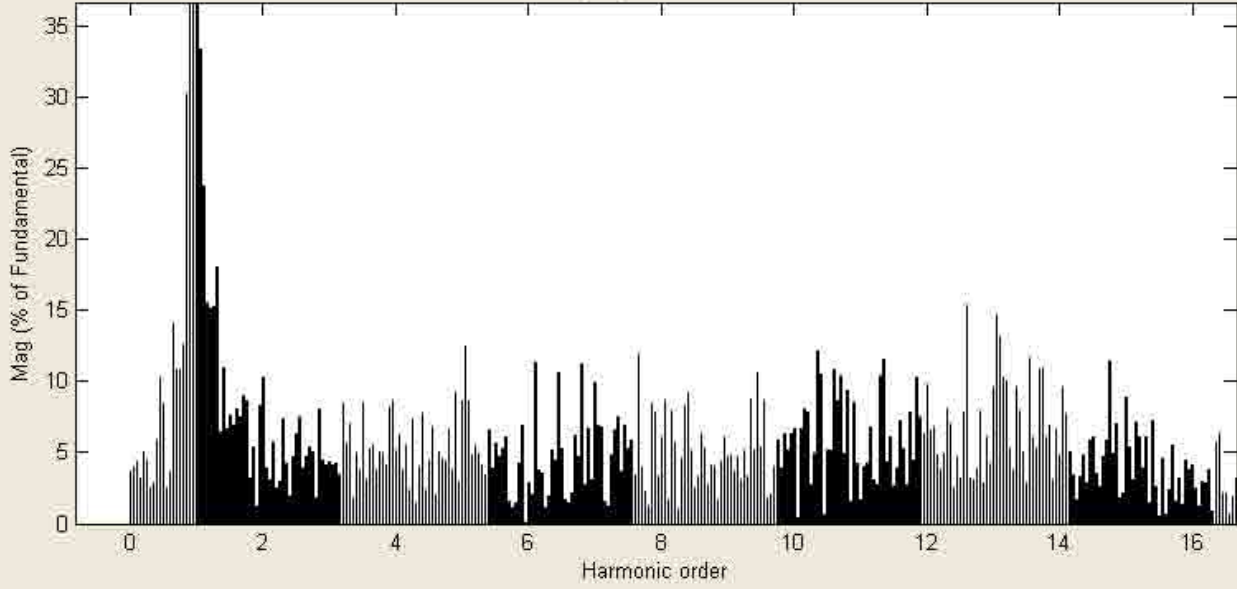
Frequency axis: Harmonic order

Display style: Bar (relative to Fund. or DC)

Base value: 1.0

Display Close

Fundamental (60Hz) = 132.9 , THD= 27.33%

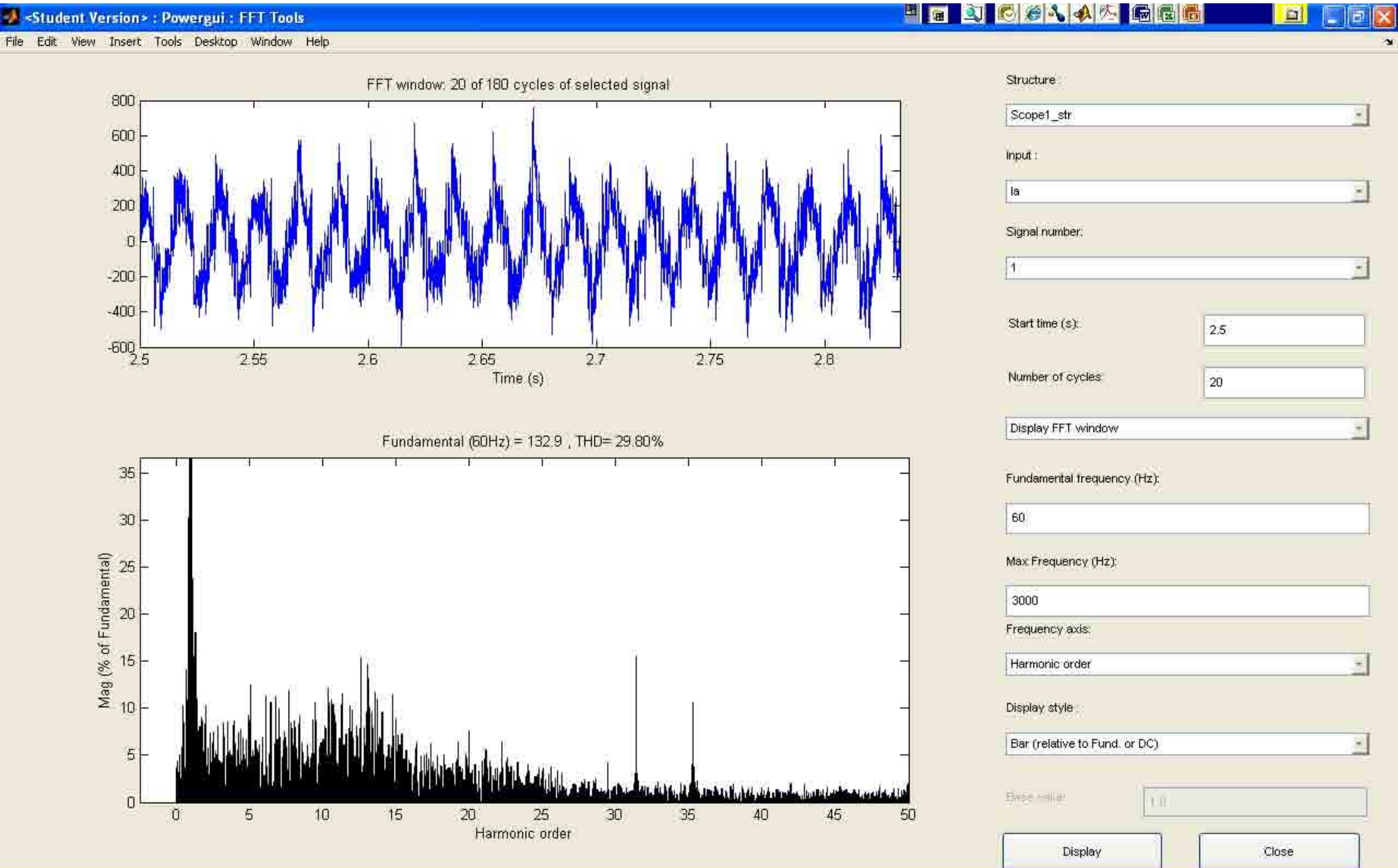


Mag (% of Fundamental)

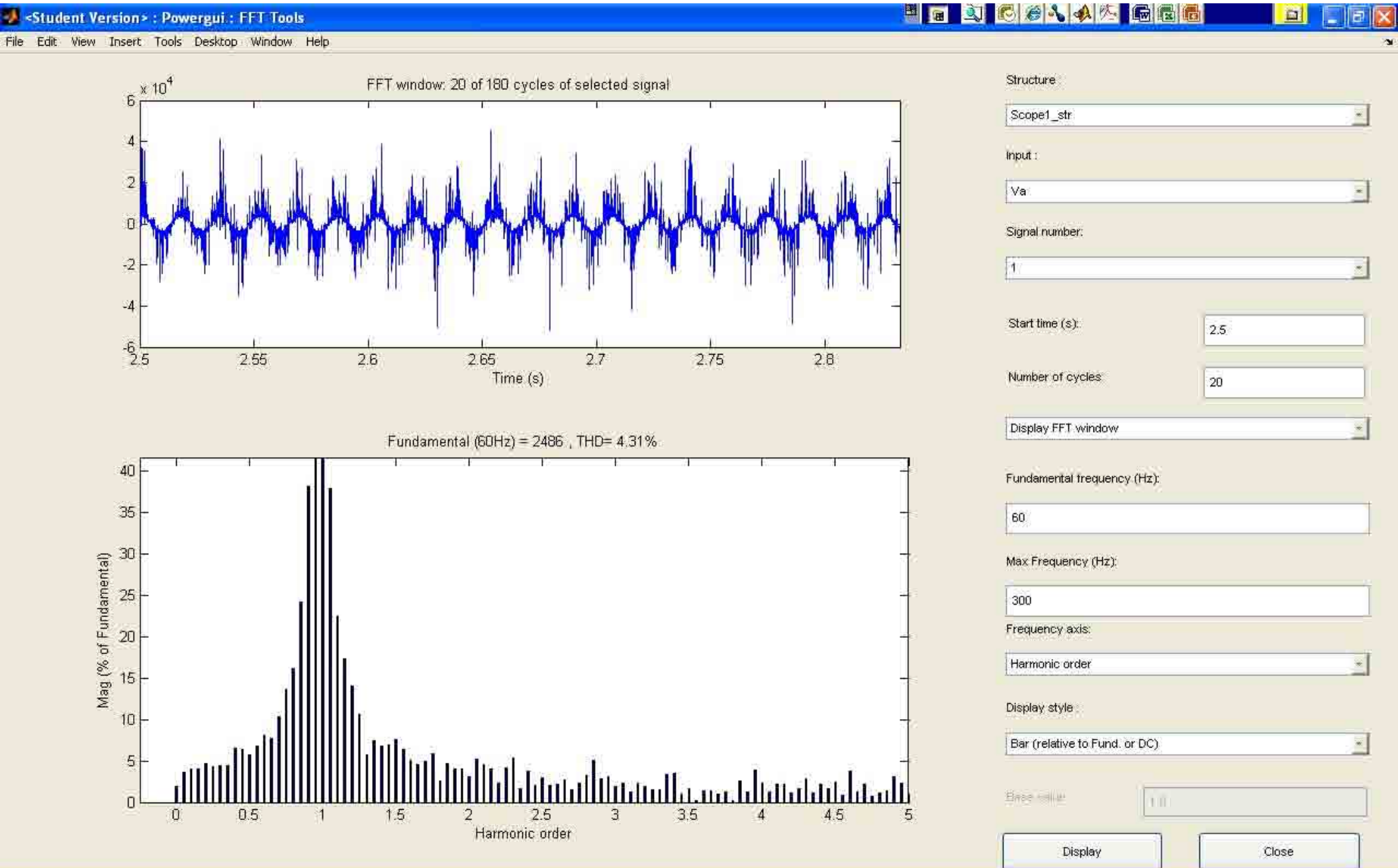
Harmonic order

Detailed description: The image shows a screenshot of the MATLAB FFT Tools interface. The top plot is a time-domain waveform of a signal, labeled 'FFT window: 20 of 180 cycles of selected signal'. The x-axis is 'Time (s)' ranging from 2.5 to 2.8, and the y-axis ranges from -600 to 800. The bottom plot is a harmonic spectrum plot titled 'Fundamental (60Hz) = 132.9 , THD= 27.33%'. The x-axis is 'Harmonic order' from 0 to 16, and the y-axis is 'Mag (% of Fundamental)' from 0 to 35. The right-hand side contains a control panel with various settings: 'Structure' (Scope1_str), 'Input' (Ia), 'Signal number' (1), 'Start time (s)' (2.5), 'Number of cycles' (20), 'Display FFT window' (checked), 'Fundamental frequency (Hz)' (60), 'Max Frequency (Hz)' (1000), 'Frequency axis' (Harmonic order), 'Display style' (Bar (relative to Fund. or DC)), and 'Base value' (1.0). 'Display' and 'Close' buttons are at the bottom right.

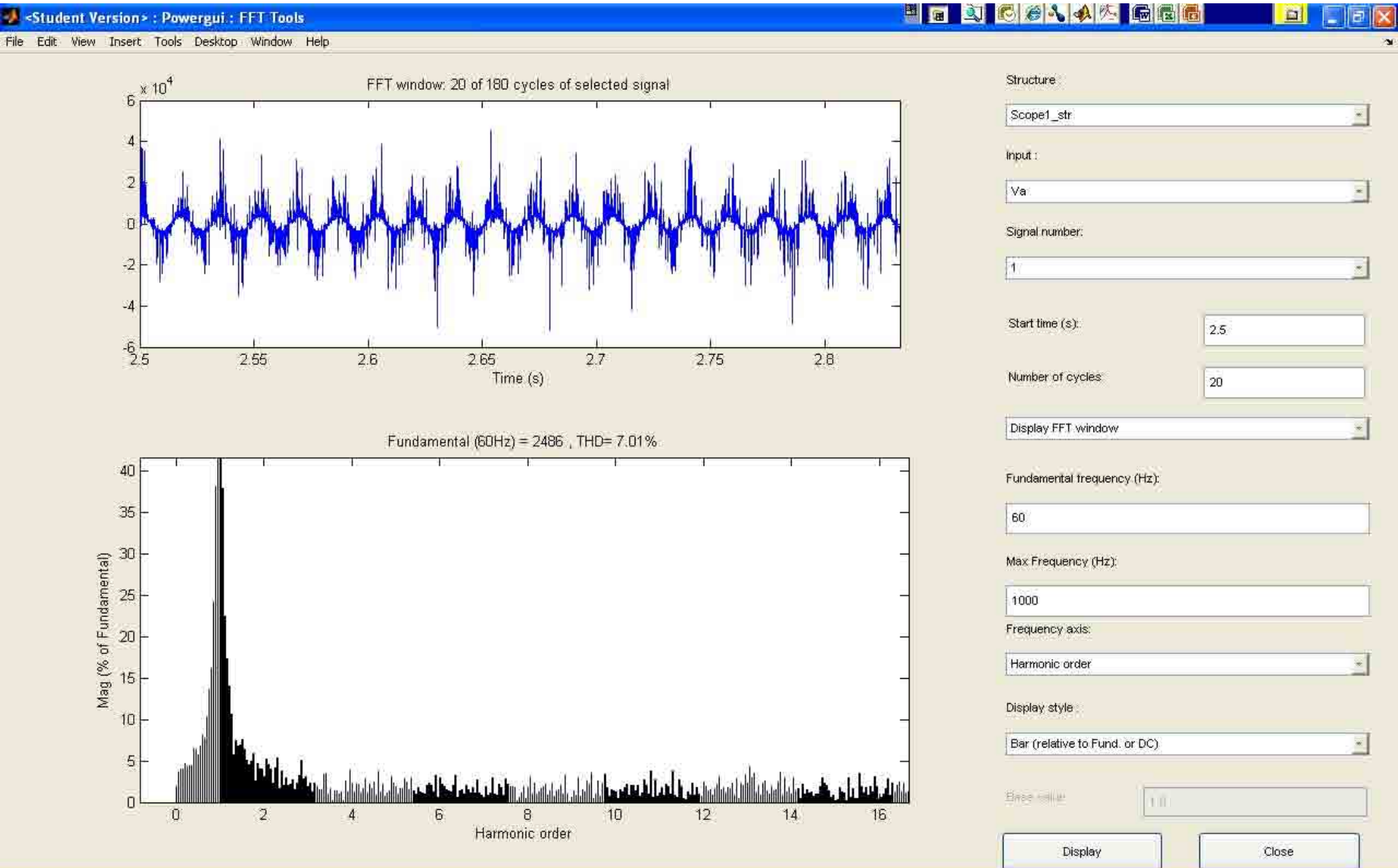
Matlab Simulation 8 Output



Matlab Simulation 8 Output



Matlab Simulation 8 Output

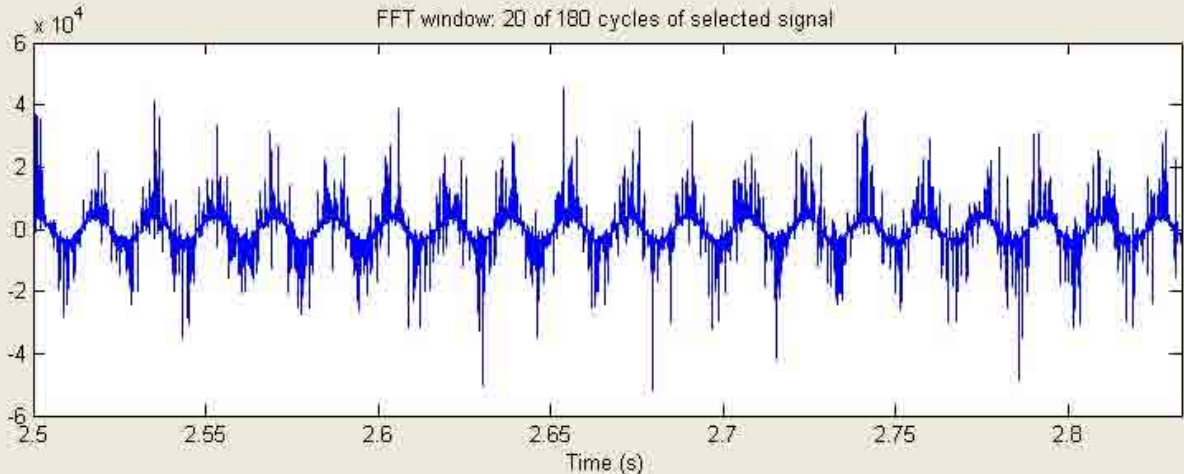


Matlab Simulation 8 Output

<Student Version> : Powergui : FFT Tools

File Edit View Insert Tools Desktop Window Help

FFT window: 20 of 180 cycles of selected signal



Structure: Scope1_str

Input: Va

Signal number: 1

Start time (s): 2.5

Number of cycles: 20

Display FFT window

Fundamental frequency (Hz): 60

Max Frequency (Hz): 3000

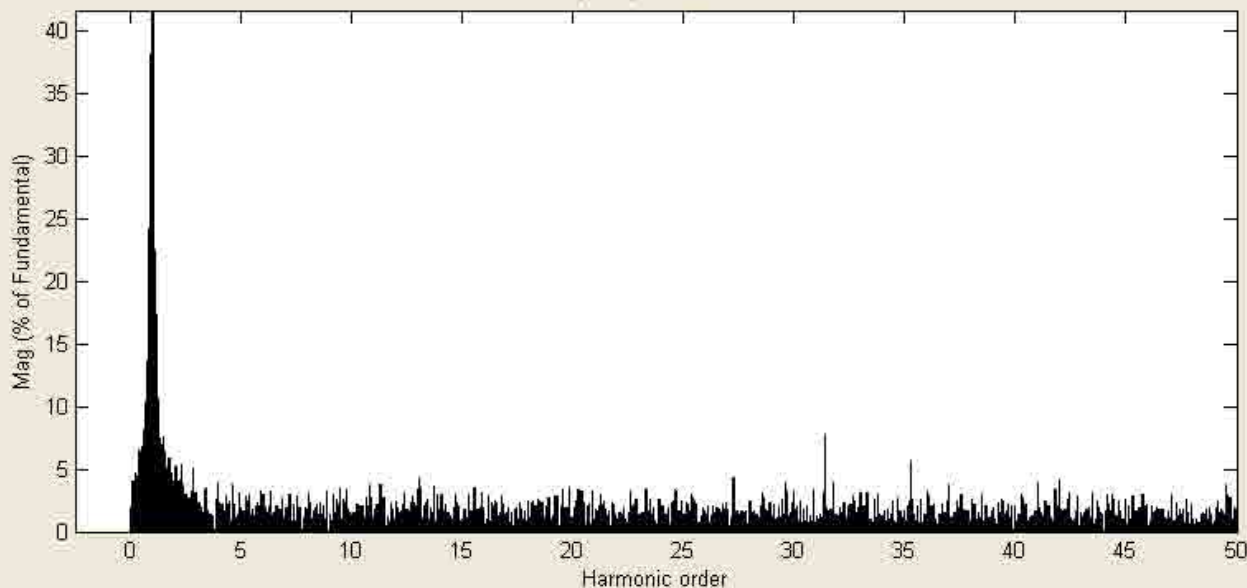
Frequency axis: Harmonic order

Display style: Bar (relative to Fund. or DC)

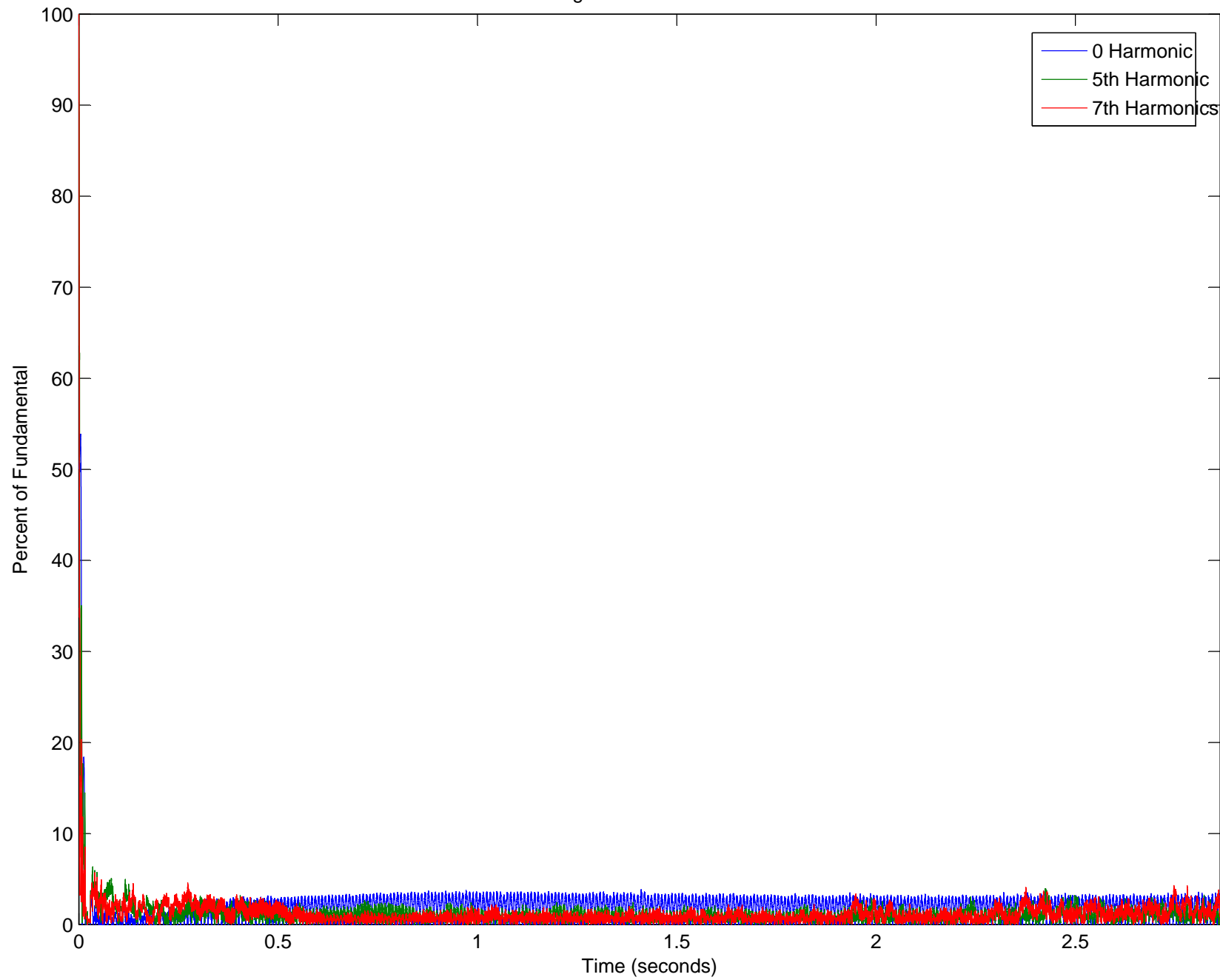
Base value: 1.0

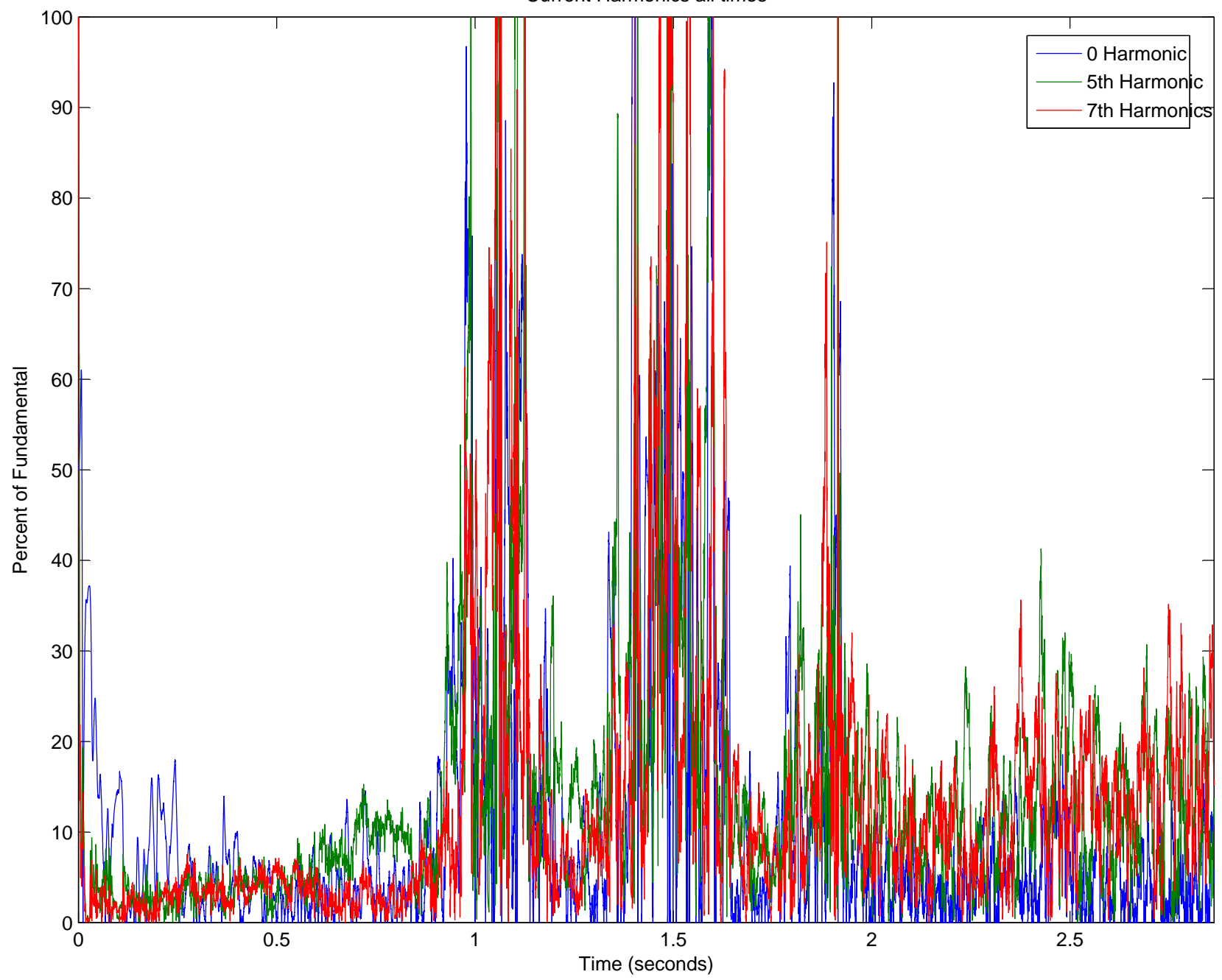
Display Close

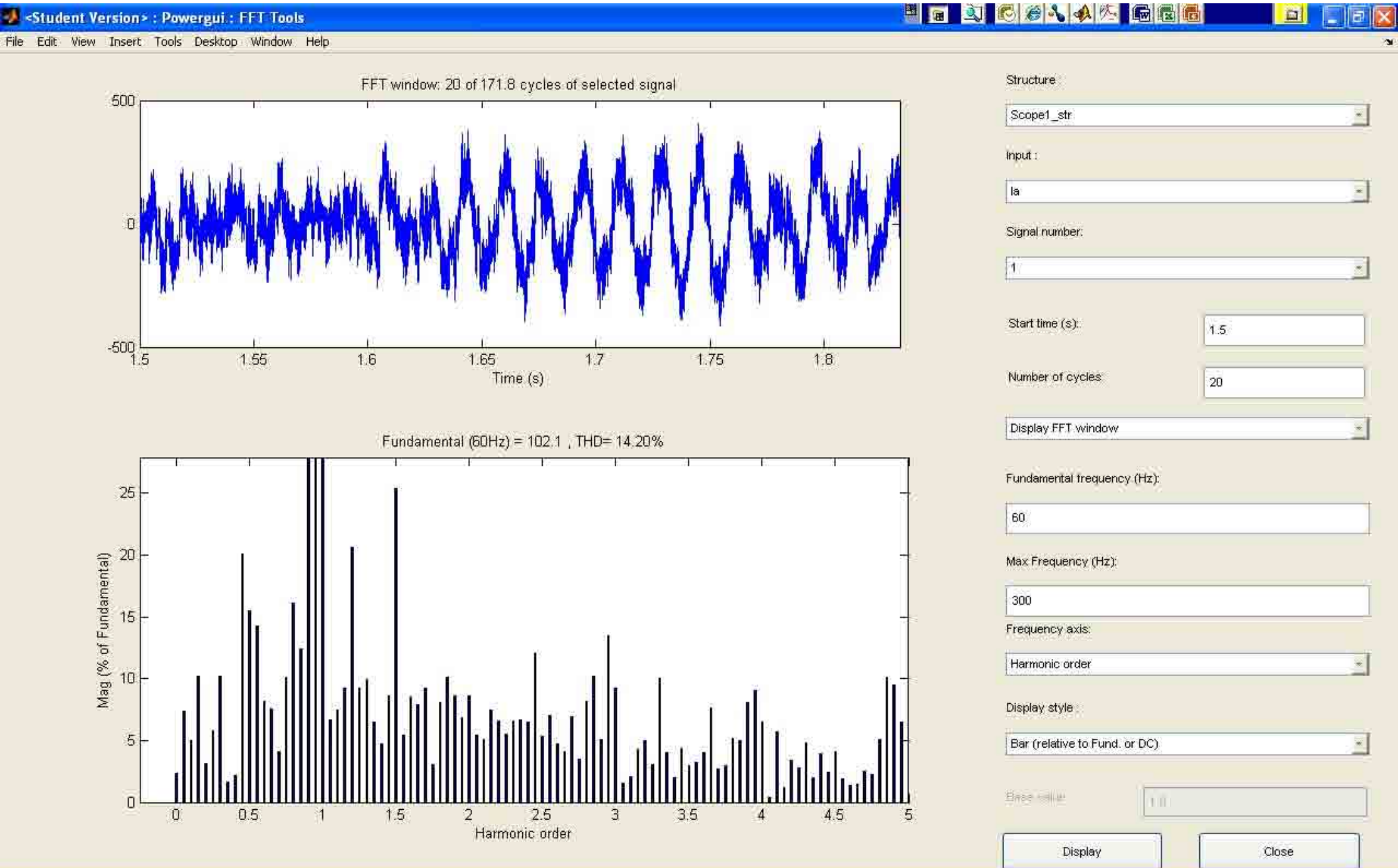
Fundamental (60Hz) = 2486 , THD= 12.90%

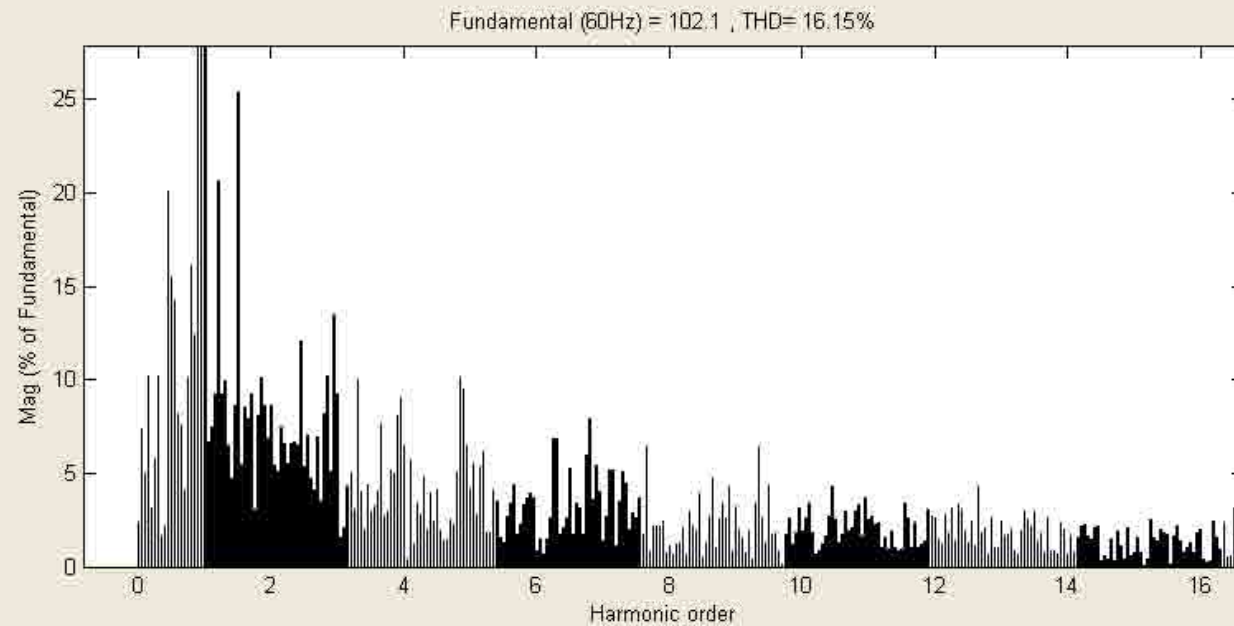
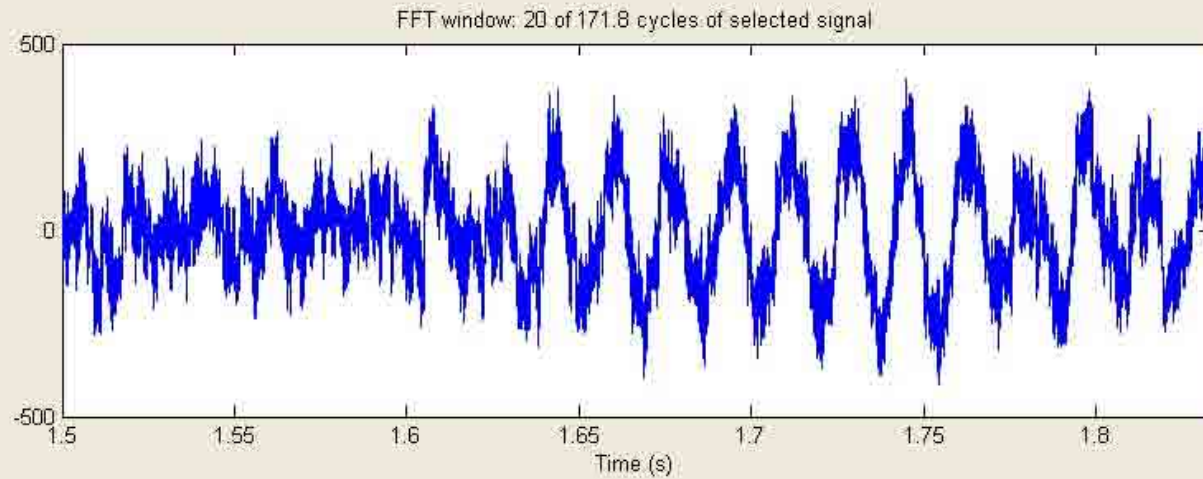
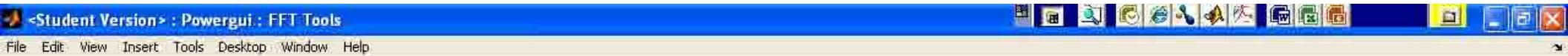


APPENDIX K: MATLAB SIMULATION 9 OUTPUT









Structure: Scope1_str

Input: Ia

Signal number: 1

Start time (s): 1.5

Number of cycles: 20

Display FFT window

Fundamental frequency (Hz): 60

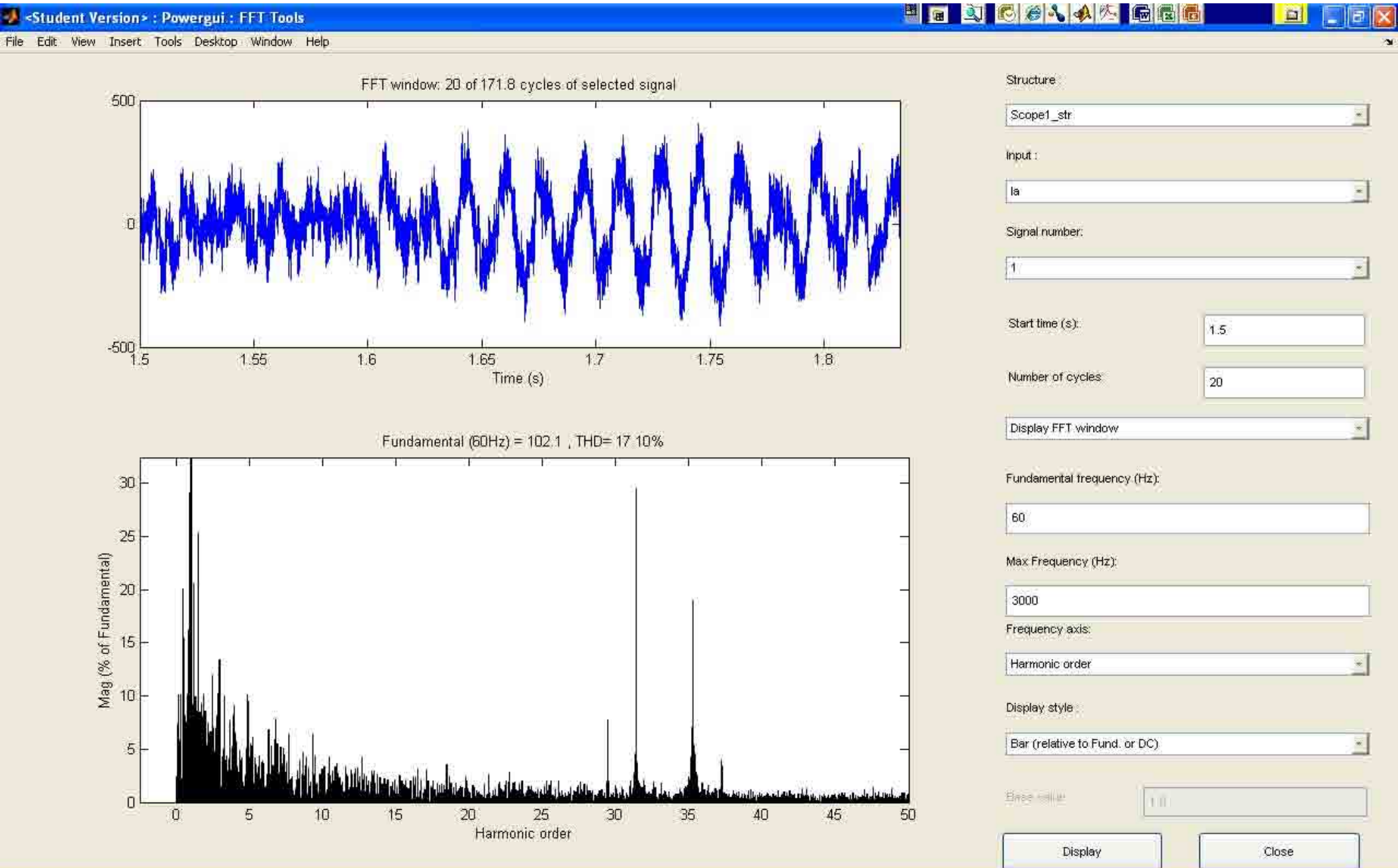
Max Frequency (Hz): 1000

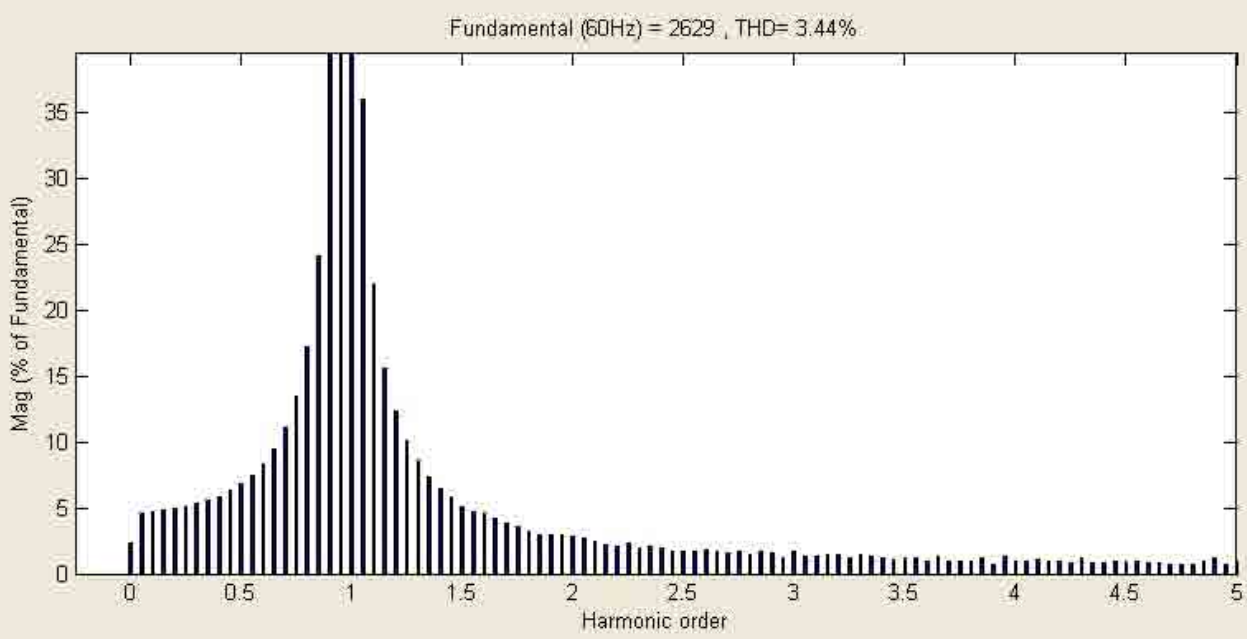
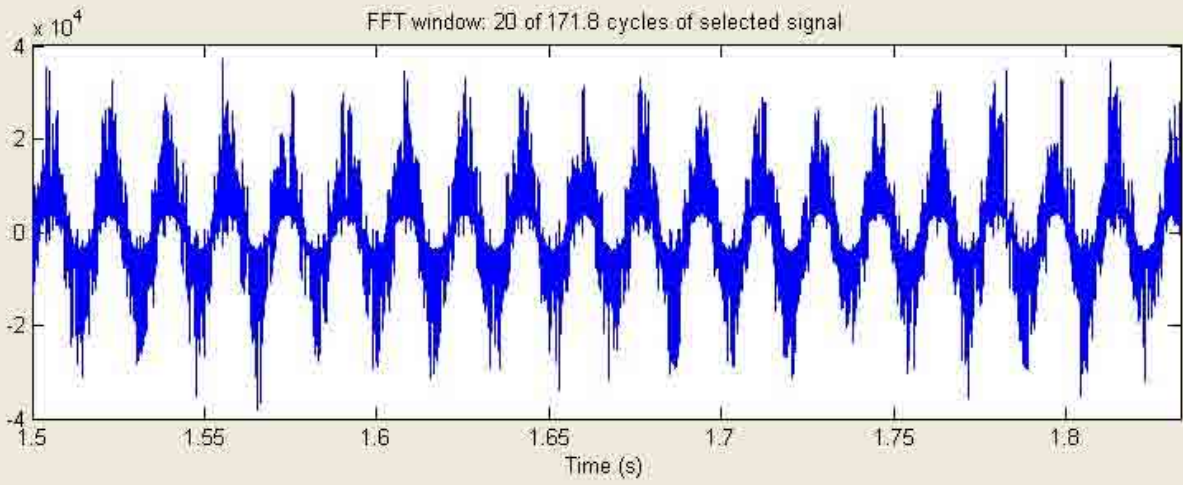
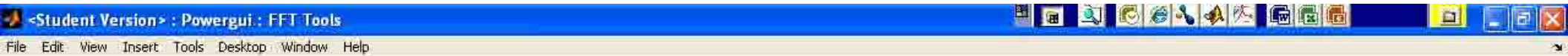
Frequency axis: Harmonic order

Display style: Bar (relative to Fund. or DC)

Base value: 100

Display Close





Structure: Scope1_str

Input: Va

Signal number: 1

Start time (s): 1.5

Number of cycles: 20

Display FFT window

Fundamental frequency (Hz): 60

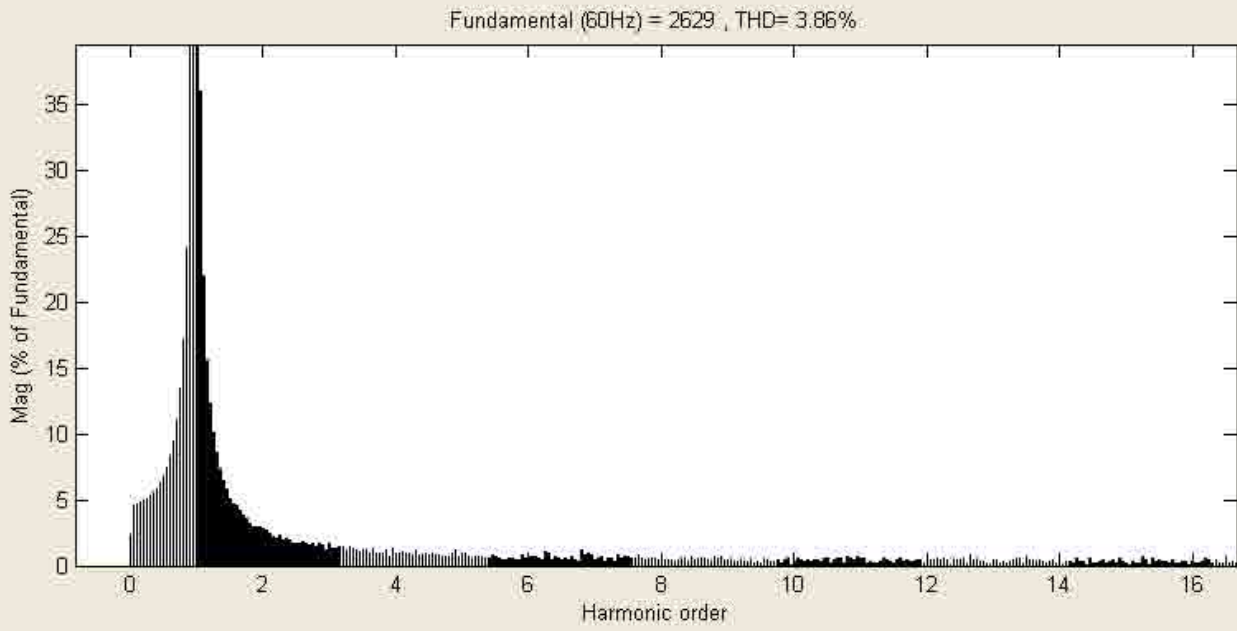
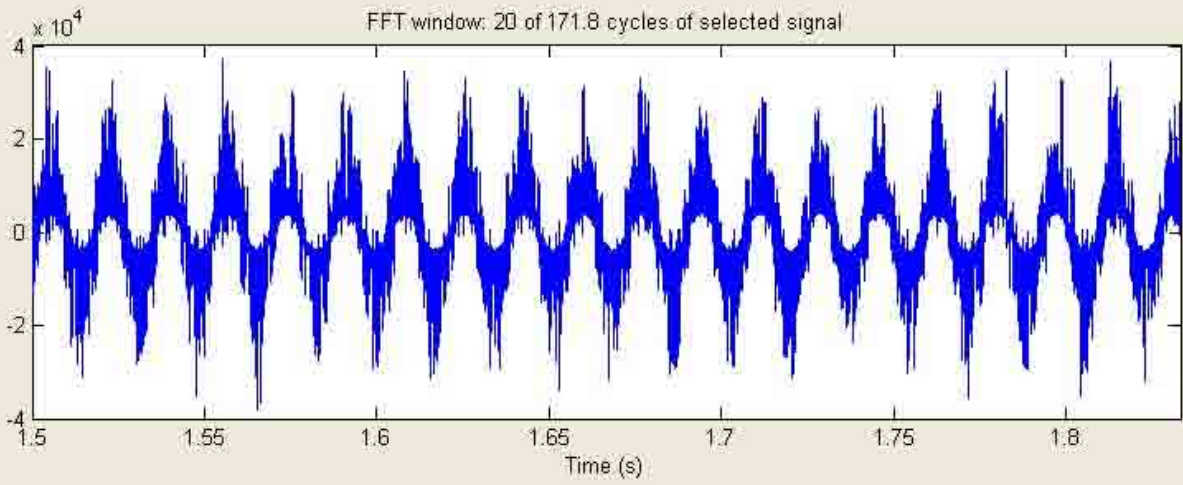
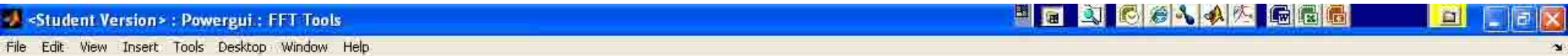
Max Frequency (Hz): 300

Frequency axis: Harmonic order

Display style: Bar (relative to Fund. or DC)

Base value: 1.0

Display Close



Structure: Scope1_str

Input: Va

Signal number: 1

Start time (s): 1.5

Number of cycles: 20

Display FFT window

Fundamental frequency (Hz): 60

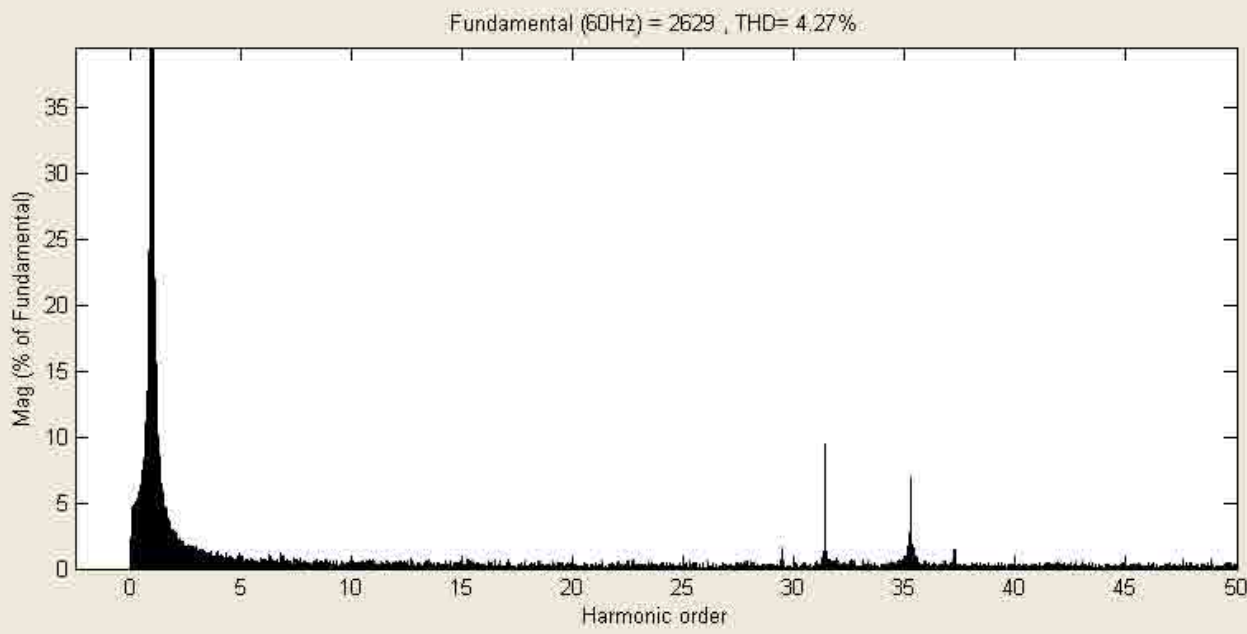
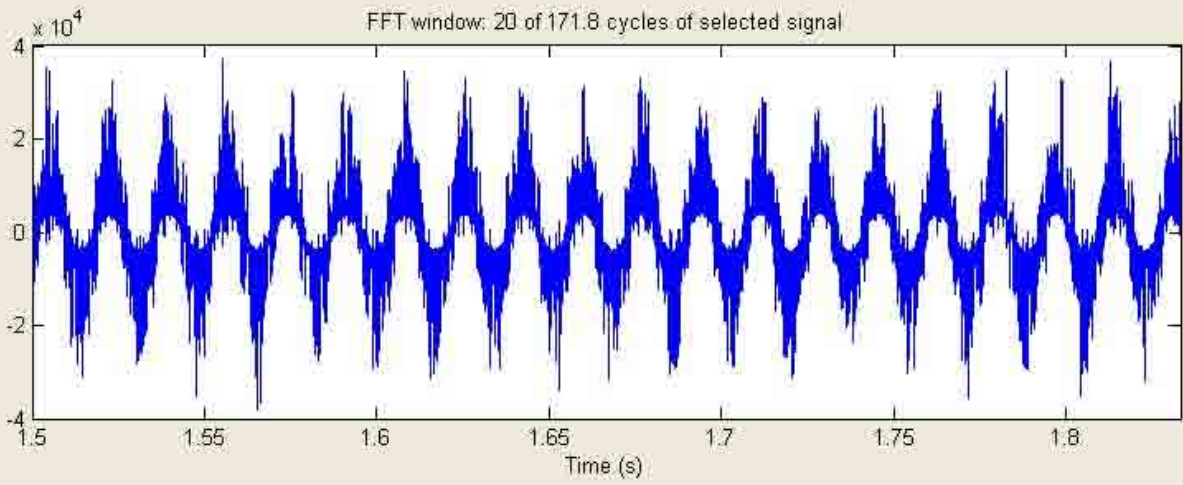
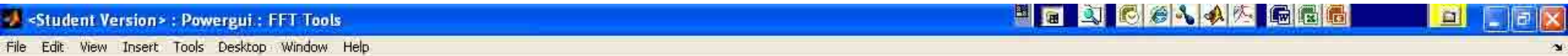
Max Frequency (Hz): 1000

Frequency axis: Harmonic order

Display style: Bar (relative to Fund. or DC)

Base value: 1

Display Close



Structure: Scope1_str

Input: Va

Signal number: 1

Start time (s): 1.5

Number of cycles: 20

Display FFT window

Fundamental frequency (Hz): 60

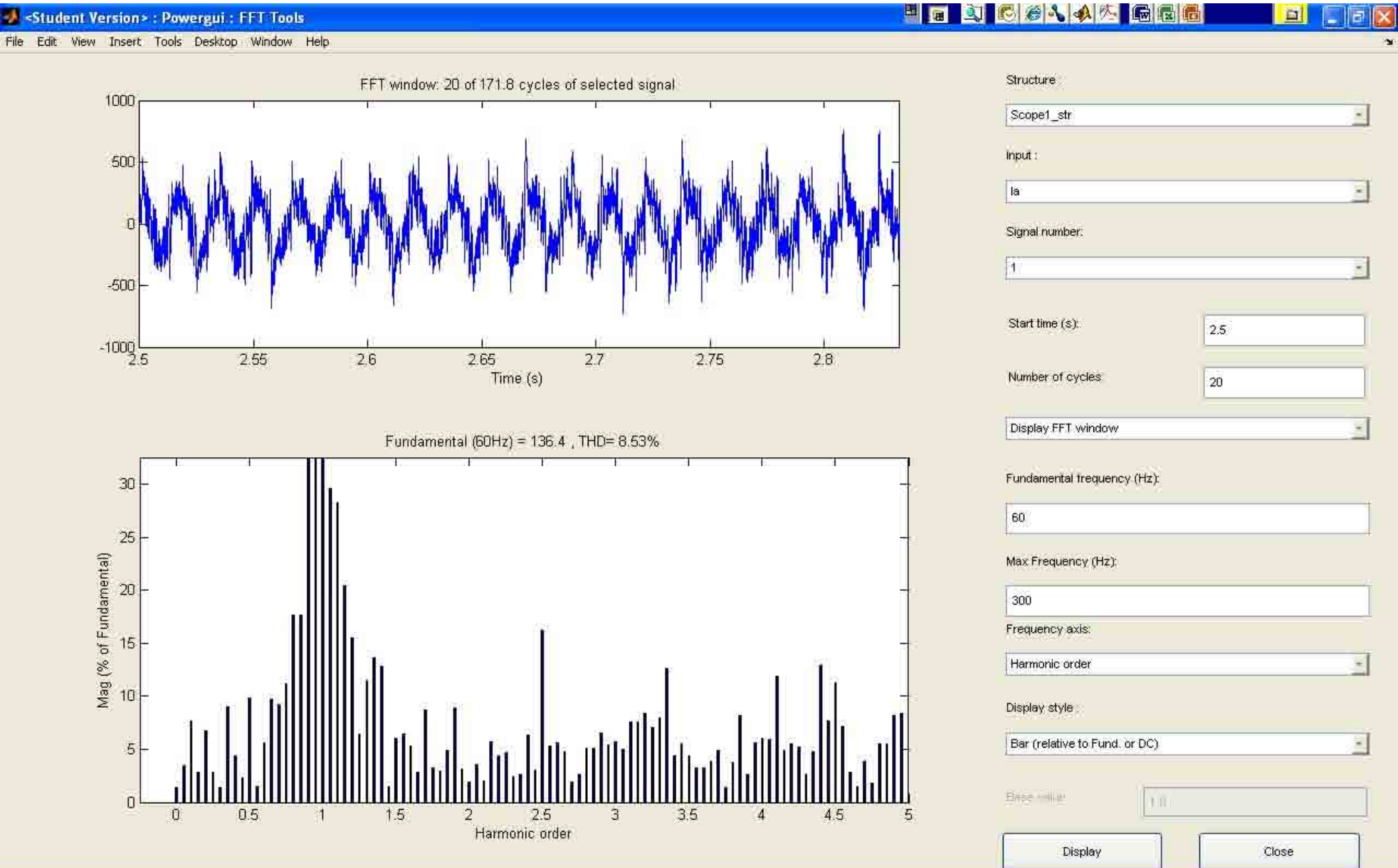
Max Frequency (Hz): 3000

Frequency axis: Harmonic order

Display style: Bar (relative to Fund. or DC)

Base value: 1.0

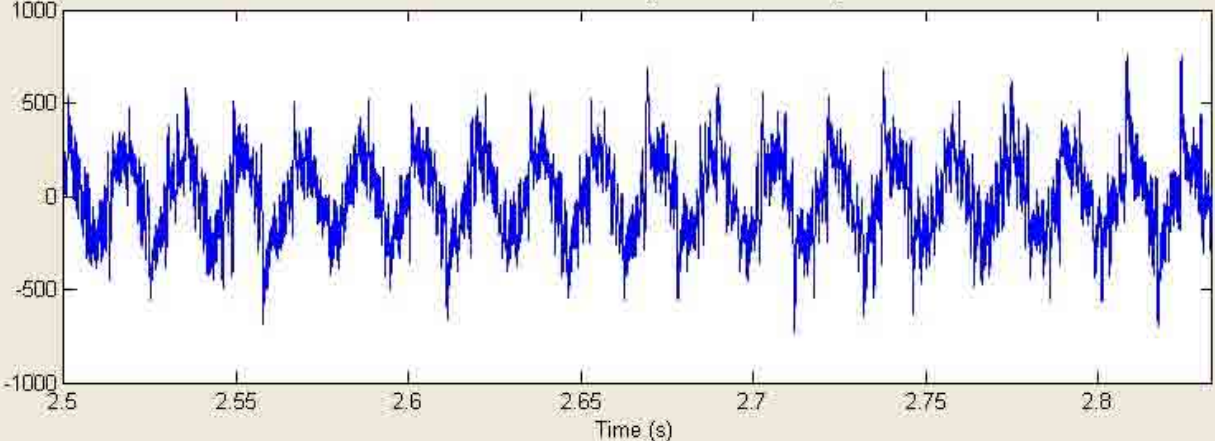
Display Close



<Student Version> : Powergui : FFT Tools

File Edit View Insert Tools Desktop Window Help

FFT window: 20 of 171.8 cycles of selected signal



Structure: Scope1_str

Input: Ia

Signal number: 1

Start time (s): 2.5

Number of cycles: 20

Display FFT window

Fundamental frequency (Hz): 60

Max Frequency (Hz): 1000

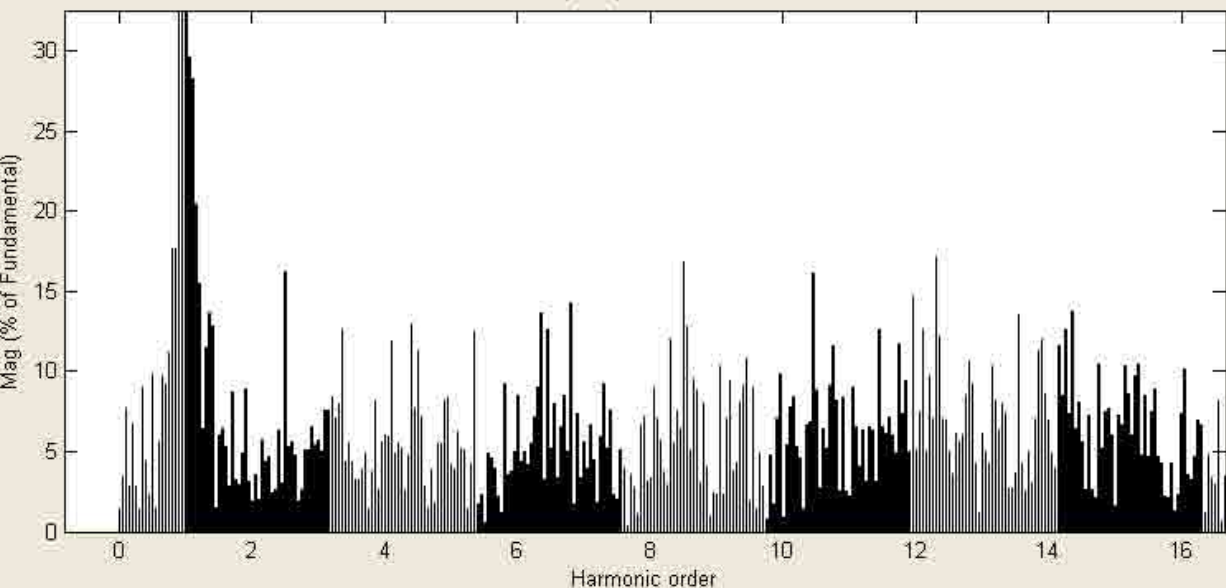
Frequency axis: Harmonic order

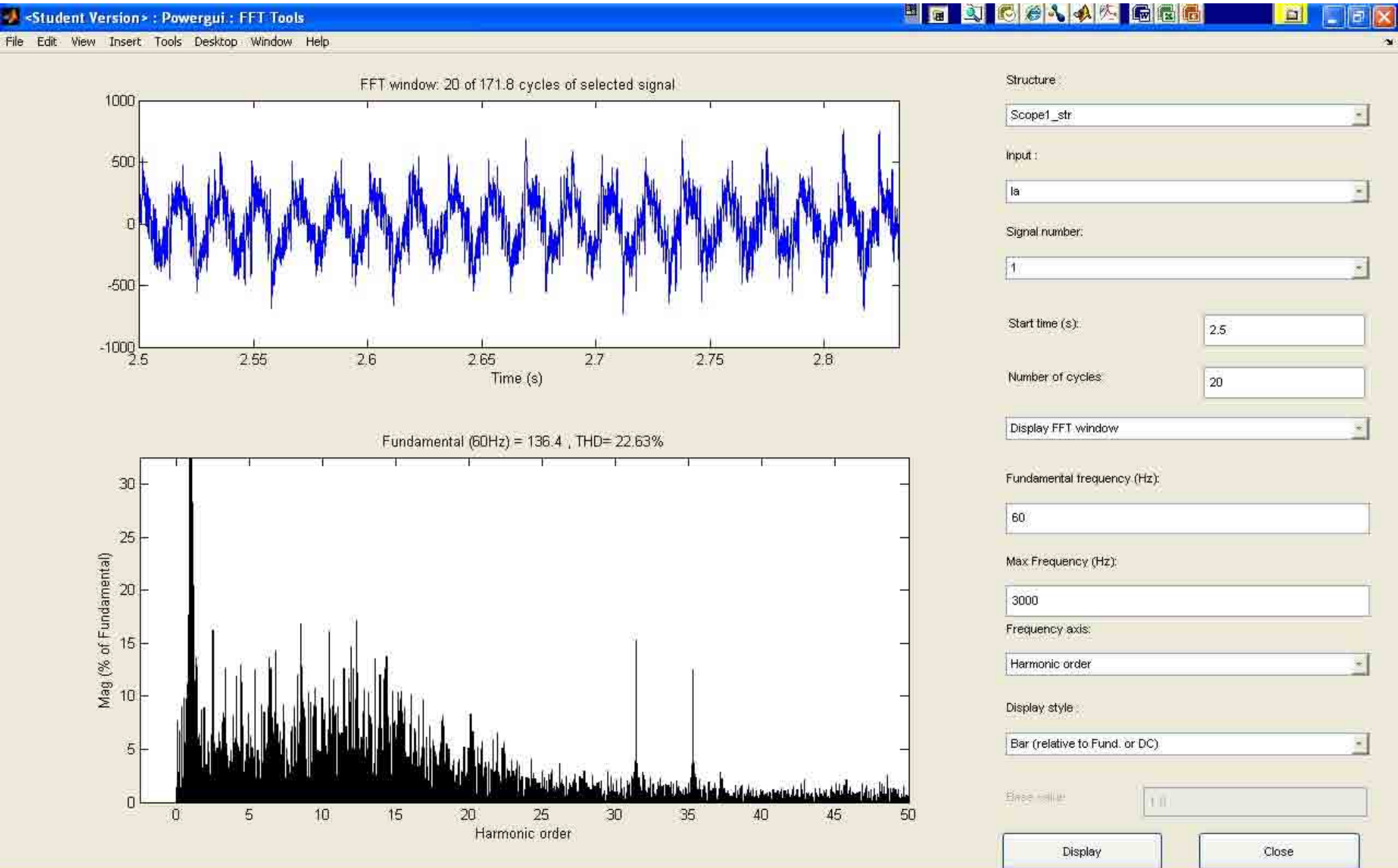
Display style: Bar (relative to Fund. or DC)

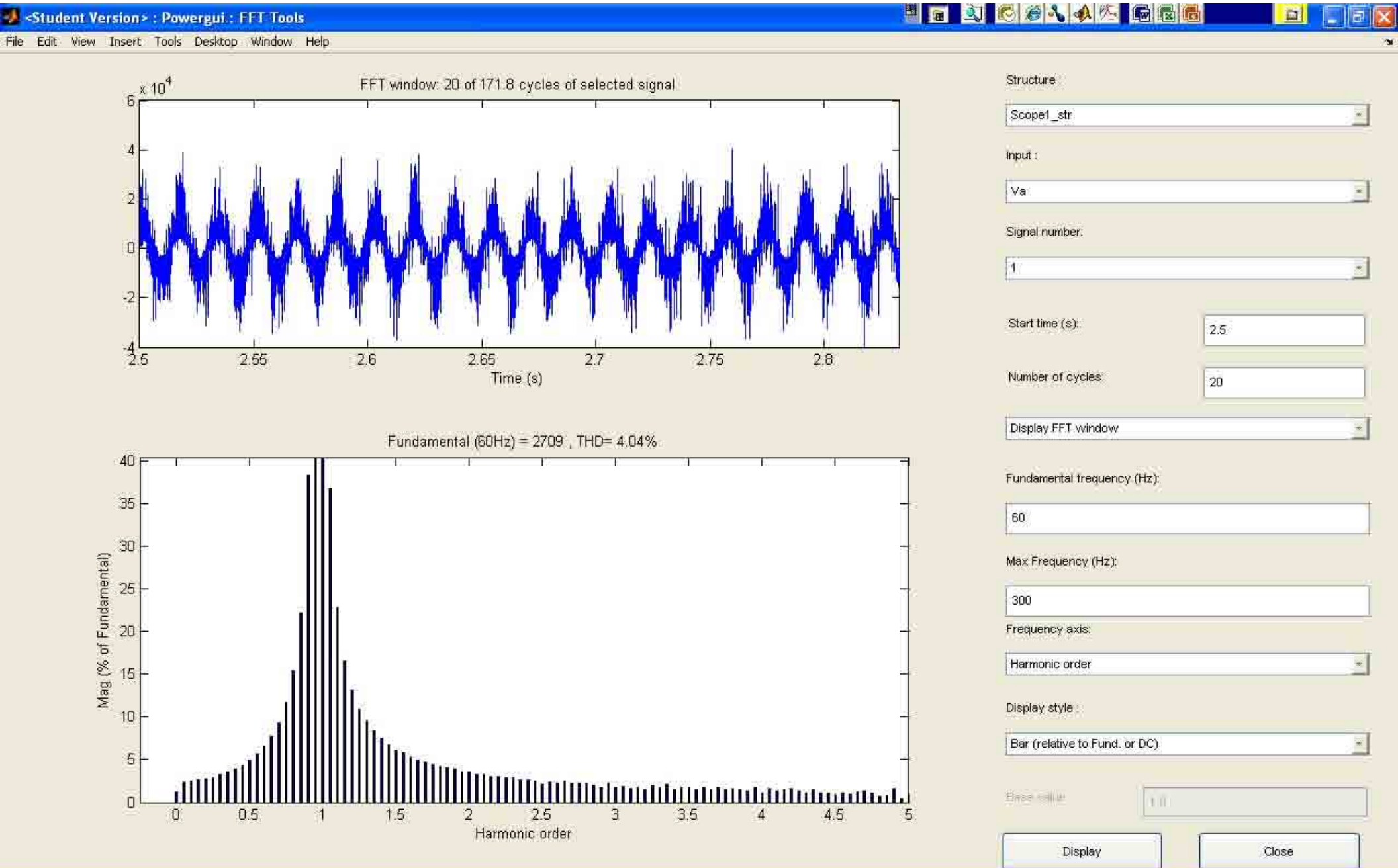
Base value: 1.0

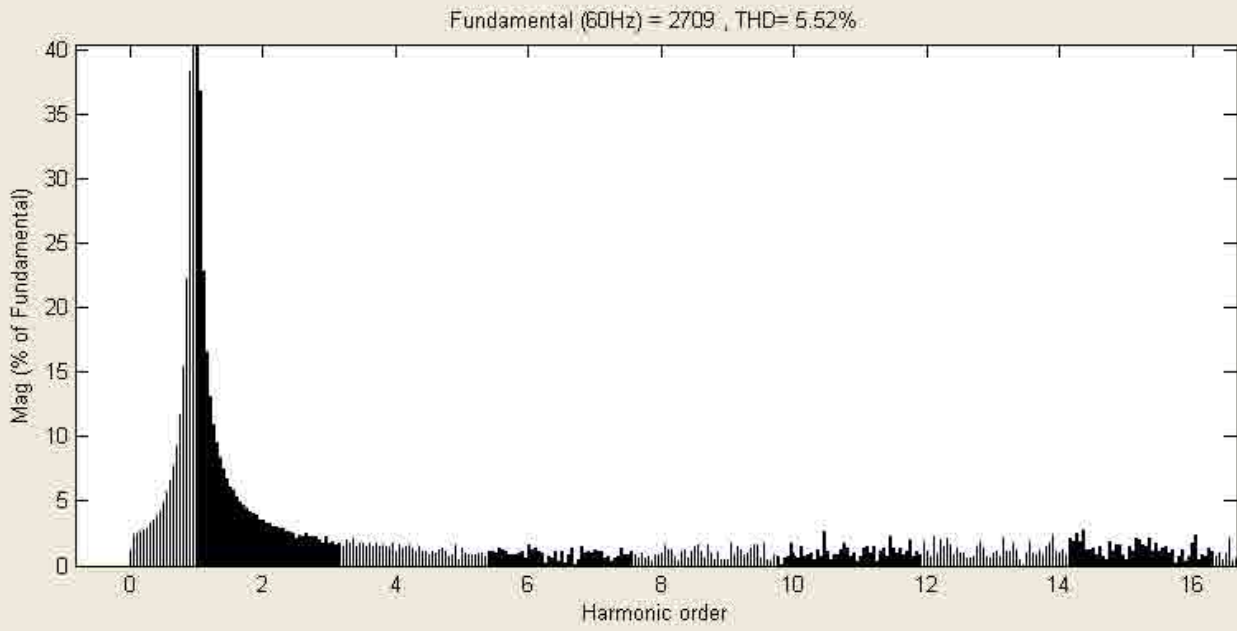
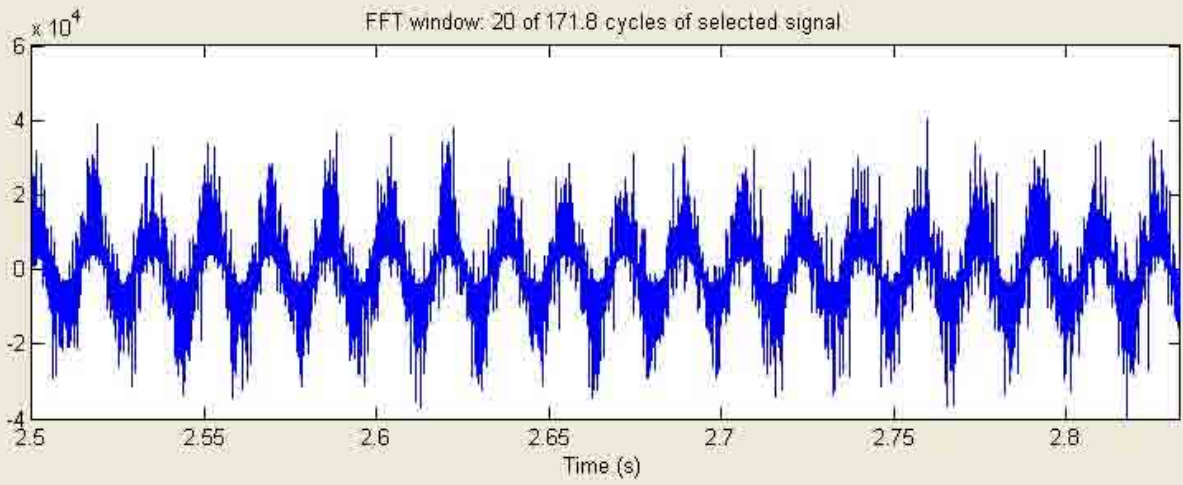
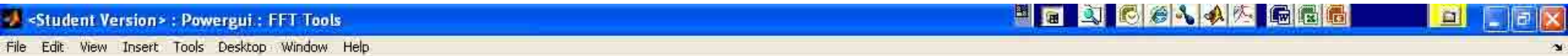
Display Close

Fundamental (60Hz) = 136.4 , THD= 19.65%









Structure: Scope1_str

Input: Va

Signal number: 1

Start time (s): 2.5

Number of cycles: 20

Display FFT window

Fundamental frequency (Hz): 60

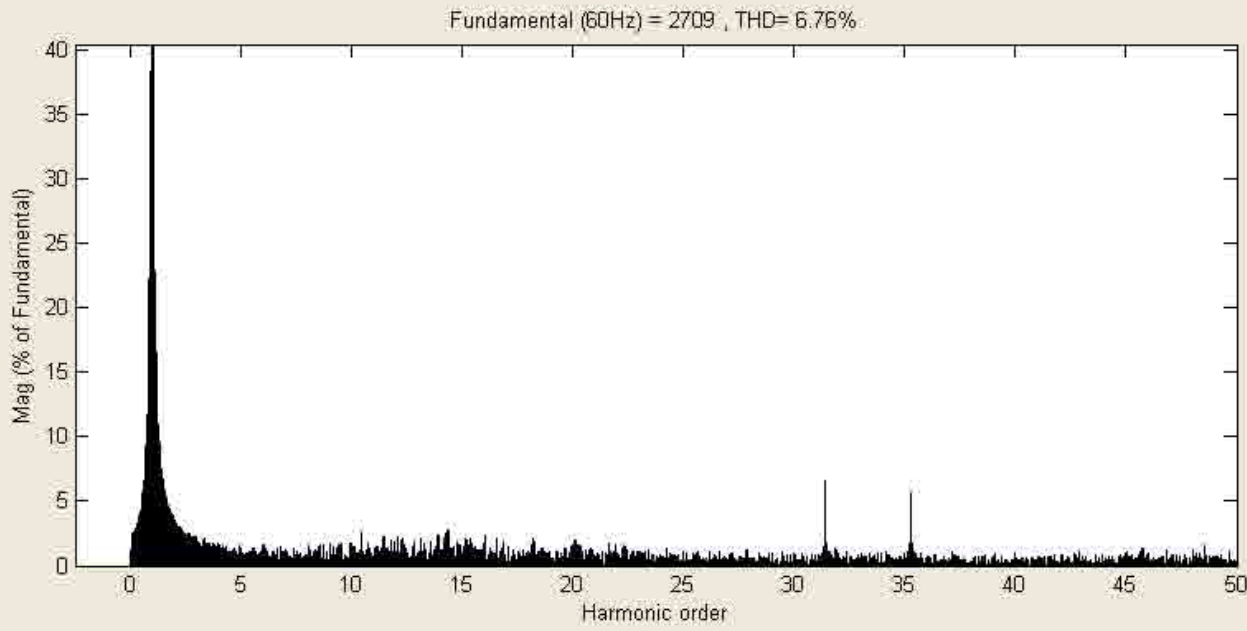
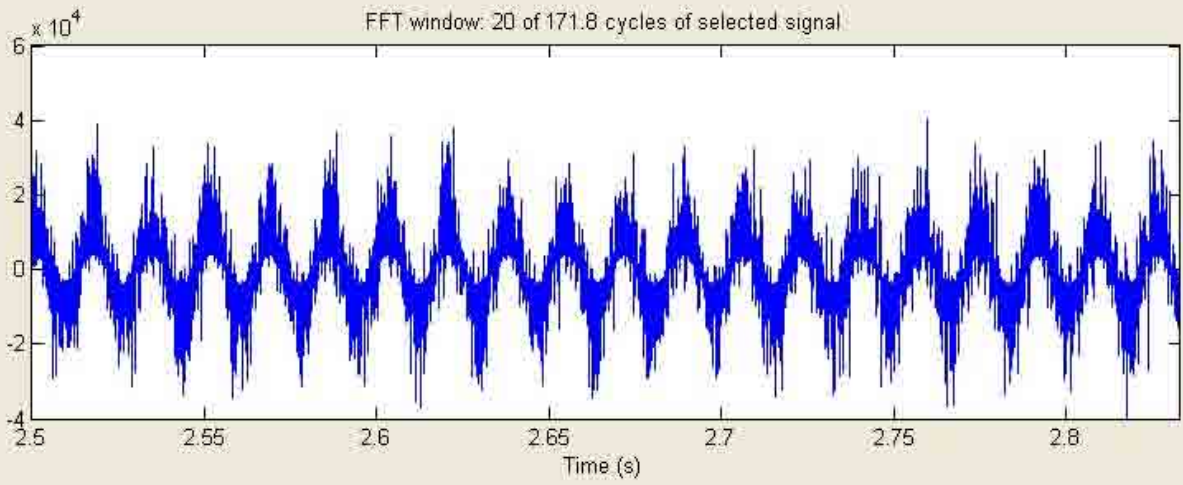
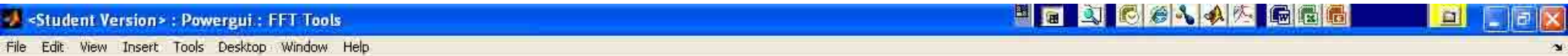
Max Frequency (Hz): 1000

Frequency axis: Harmonic order

Display style: Bar (relative to Fund. or DC)

Base value: 1

Display Close



Structure: Scope1_str

Input: Va

Signal number: 1

Start time (s): 2.5

Number of cycles: 20

Display FFT window

Fundamental frequency (Hz): 60

Max Frequency (Hz): 3000

Frequency axis: Harmonic order

Display style: Bar (relative to Fund. or DC)

Base value: 1.0

Display Close